

Role of the Purinergic Signaling in Healing Processes of the Heart and the Kidney after Ischemia/ Reperfusion Injury

Inaugural dissertation

for the attainment of the title of doctor
in the Faculty of Mathematics and Natural Sciences
at the Heinrich Heine University Düsseldorf

presented by

Nicole Görltdt

from Pirna, Germany

Düsseldorf, May 2017

From the Institute of Molecular Cardiology at the Heinrich Heine University Düsseldorf

Published by permission of the Faculty of Mathematics and Natural Sciences at Heinrich Heine University Düsseldorf

Supervisor: Prof. Dr. Jürgen Schrader

Co-supervisor: Prof. Dr. Thomas Klein

Date of the oral examination: 1st September 2017

Table of content

I. List of abbreviations	V
1. Summary	1
2. Zusammenfassung	2
3. Introduction	3
3.1. Ischemia/ reperfusion injury	3
3.1.1. Vascular leakage	4
3.1.2. Innate and adaptive immune activation	4
3.1.3. Autoimmunity	5
3.1.4. Transcriptional reprogramming	6
3.1.5. Cell death programs	7
3.2. Myocardial Infarction.....	8
3.2.1. Wound healing after myocardial infarction	9
3.2.1.1. Ischemia-induced cell death of cardiomyocytes.....	9
3.2.1.2. Activation of the inflammatory system	11
3.2.1.3. Proliferation of fibroblasts and endothelial cells	12
3.3. Acute kidney injury.....	13
3.3.1. Wound healing after acute kidney injury	15
3.3.1.1. Ischemia-induced alterations in tubule cell metabolism and structure	15
3.3.1.2. Initiation of the cellular immune response	16
3.3.1.3. Fibrosis formation and tissue recovery.....	16
3.4. Regulation of tissue healing processes and maladaptive repair mechanism	17
3.5. Purinergic signaling	20
3.5.1. Release of nucleotides.....	21
3.5.2. Signaling via P2 receptors	21
3.5.3. Extracellular degradation of nucleotides by ectoenzymes	22
3.5.4. CD73 – a key enzyme for generating extracellular adenosine.....	24
3.5.5. Signaling via P1 receptors (adenosine receptors)	25
3.5.6. Adenosine degradation and internalization.....	28
3.6. Aims of the study	29
4. Material	31
4.1. Laboratory equipment	31

Table of content

4.2. Chemicals and enzymes	32
4.3. Cell culture material, medium, buffer and substances	32
4.4. Buffer and solutions	33
4.5. Antibodies	34
4.6. TaqMan assays	35
4.7. Gene-specific primers	35
5. Methods.....	36
5.1. Mouse models	36
5.1.1. Mouse studies in the heart including <i>ex vivo</i> T cell culture	36
5.1.2. Mouse studies in the kidney including <i>ex vivo</i> fibroblast culture	37
5.2. <i>In vivo</i> methods	38
5.2.1. Myocardial infarction in mice.....	38
5.2.2. Acute kidney injury in mice.....	39
5.2.3. Measurement of body and kidney weight	40
5.3. <i>In vitro</i> methods	40
5.3.1. Isolation of cells from different tissues.....	40
5.3.1.1. Lymphoid T cell isolation.....	41
5.3.1.2. Cardiac T cell isolation	42
5.3.1.3. Renal fibroblast isolation.....	43
5.3.3. HPLC analysis of T cell nucleotide metabolism.....	44
5.3.4. Re-stimulation of cardiac T cells for cytokine secretion	46
5.3.5. Adenosine receptors activation of stimulated lymphoid T cells	46
5.3.6. <i>Ex vivo</i> fibroblast cell culture.....	47
5.3.7. Fibroblast proliferation assay.....	47
5.4. Molecular biological methods.....	48
5.4.1. RNA isolation	48
5.4.2. Reverse transcription	50
5.4.3. qPCR analysis	53
5.5. Biochemical methods.....	55
5.5.1. Analysis of T cell cytokine secretion.....	55
5.5.2. Flow cytometry analysis of immune cells.....	57
5.5.3. Analysis of kidney function by measurement of plasma creatinine levels	58
5.5.4. Quantification of renal collagen content by hydroxyproline assay.....	59
5.6. Histochemical methods	60

Table of content

5.6.1. Detection of renal tissue fibrosis and matrix deposition by Masson's trichrome staining.....	60
5.6.2. Immunofluorescence analysis of renal tissue sections and confocal microscopy.....	60
5.7. Statistics	61
6. Results	62
6.1. Extracellular nucleotide metabolism after T cell activation.....	62
6.2. Cytokine profile of isolated cardiac T cells lacking CD73	65
6.3. Expression of the various adenosine receptors in T cells infiltrating the heart after myocardial infarction	67
6.4. Function of the A _{2A} R and the A _{2B} R on activated CD4 ⁺ T cells	68
6.5. Purinergic signaling in a chronic cardiac disease model.....	70
6.6. Characterization of Foxd1 ^{Cre/+} /CD73 ^{fl/fl} mice.....	72
6.6.1. Kidney function of Foxd1 ^{Cre/+} /CD73 ^{fl/fl} mice after acute kidney injury	72
6.6.2. Collagen formation and matrix deposition in Foxd1 ^{Cre/+} /CD73 ^{fl/fl} mice after acute kidney injury.....	73
6.6.3. Myofibroblast transformation in Foxd1 ^{Cre/+} /CD73 ^{fl/fl} mice after acute kidney injury	75
6.6.4. Immune cell infiltration in Foxd1 ^{Cre/+} /CD73 ^{fl/fl} mice after acute kidney injury	76
6.6.5. 5'NT treatment of Foxd1 ^{Cre/+} /CD73 ^{fl/fl} mice after acute kidney injury	78
6.7. <i>Ex vivo</i> fibroblast cell culture.....	81
6.7.1. Cell proliferation of <i>ex vivo</i> wildtype and CD73 ^{-/-} kidney fibroblasts	81
6.8. Characterization of Pepck ^{Cre/+} /CD73 ^{fl/fl} mice.....	82
6.8.1. Kidney function and collagen formation of Pepck ^{Cre/+} /CD73 ^{fl/fl} mice after acute kidney injury.....	82
6.9. Initial injury in Foxd1 ^{Cre/+} /CD73 ^{fl/fl} and Pepck ^{Cre/+} /CD73 ^{fl/fl} mice after acute kidney injury	84
7. Discussion.....	86
7.1. Myocardial infarction – the medical dimension.....	86
7.2. Purinergic signaling and its contribution to healing processes in the heart	86
7.3. The destructive and protective role of T cells in myocardial infarction	87
7.3.1. Role of T cells in mediating healing processes and tissue recovery after myocardial infarction	88
7.3.2. Metabolic reprogramming in T cells after infiltrating into the infarcted heart	88
7.3.3. Role of CD73 on T cells in mediating cytokine production	91
7.3.4. Contribution of the A _{2A} R and the A _{2B} R to wound healing and immune response.....	92
7.4. Purinergic signaling in chronic inflammation of the heart.....	94
7.5. Acute kidney injury – the medical dimension.....	95

Table of content

7.6. CD73 expression in renal tissue and its contribution to injury	95
7.6.1. Role of CD73 on fibroblasts/ pericytes in promoting matrix deposition due to myofibroblast transformation and immune cell resolution	96
7.6.2. Treatment of mice lacking CD73 on fibroblast/ pericytes with soluble CD73 restored kidney function after acute kidney injury	98
7.6.3. Role of CD73 on tubular cells in healing processes of the kidney	99
7.6.4. Potential interaction between fibroblasts/ pericytes and tubular cells in orchestrating cellular processes injury	101
8. Conclusion.....	102
8.1. Purinergic signaling in myocardial infarction and acute kidney injury	102
9. Publications.....	106
10. References	107
Statutory declaration	141
Danksagung	142

I. List of abbreviations

A

A ₁ R	Adenosine A ₁ receptor
A _{2A} R	Adenosine A _{2A} receptor
A _{2B} R	Adenosine A _{2B} receptor
A ₃ R	Adenosine A ₃ receptor
AR	Adenosine receptor
ACK	Acetate kinase
ACPP	Prostatic acid phosphatase
ADA	adenosine deaminase
AdoR	Adenosine receptor
ADP	Adenosine diphosphate
ADPR	Adenosine diphosphate -ribose
AKI	Acute kidney injury
ALP	Alkaline phosphatase
ALPI	Alkaline phosphatase – intestinal
ALPL	Alkaline phosphatase – liver/bone/kidney
ALPP	Alkaline phosphatase – placental
ALPP2	Alkaline phosphatase – placental like 2
AMP	Adenosine monophosphate
AMPase	Adenosine monophosphatase
AMPCP	α,β -methyleneadenosine 5'-diphosphate
APAF1	Apoptotic protease activating factor 1
APCs	Antigen presenting cells
Arg	Arginase
ART	ADP-ribosyltransferase
ATP	Adenosine triphosphate
ATPase	Adenosine triphosphatase

B

BSA	Bovine serum albumin
-----	----------------------

I. List of abbreviations

C

CAM	Cell adhesion molecules
cAMP	Cyclic adenosine monophosphate
CCR2	Chemokine receptor type 2
CD	Cluster differentiation
cDNA	Complementary DNA
Chil	Chitinase-like
CKD	Chronic kidney disease
CNT	Concentrative nucleoside transporter
cTnl	Cardiac troponin I
Cx	connexin

D

d	day
DAMP	Damage-associated molecular pattern
DAPI	4',6-diamidino-2-phenylindole
DMEM	Dulbecco's Modified Eagle's Medium
DMSO	Dimethyl sulfoxide
DNA	Deoxyribonucleic acid

E

ECG	Electrocardiogram
EDTA	Ethylenediaminetetraacetic acid
EMC	Extracellular matrix
ENPP	Ectonucleotide pyrophosphatase/ phosphodiesterase
ENT	Equilibrative nucleoside transporter
ENTPD	Ectonucleoside triphosphate diphosphohydrolase
EPO	Erythropoietin
ETGA	ethylene glycol-bis(β -aminoethyl ether)-N,N,N',N'-tetraacetic acid

F

FGF	Fibroblast growth factor
Fig.	Figure

I. List of abbreviations

FMO	Fluorescence-minus-one
Foxd1	Forkhead box D1
G	
GPI	glycosyl phosphatidylinositol
H	
h	hour
HIF	Hypoxia-inducible transcription factor
HMGb1	High-mobility group box 1
HPLC	High-performance liquid chromatography
HSP	Heat shock proteins
I	
IFN- γ	Interferon
IL	Interleukin
IP3	Inositol-trisphosphate
IRI	Ischemia reperfusion injury
L	
LAD	Left anterior descending
LANUV	Landesamt für Natur-, Umwelt- und Verbraucherschutz
LPS	Lipopolysaccharide
M	
MACS	Magnetic-activated cell sorting
MAP2	Microtubule-associated protein 2
MCP1	Monocyte chemotactic protein-1
MFI	Median fluorescence intensity
MHC	Major histocompatibility complex
MI	Myocardial infarction
min	Minute
MMP-9	Matrix metalloproteinases-9

I. List of abbreviations

Mrc	Mannose receptor C
Msr	Macrophage scavenger receptors
MTT	3-(4,5-dimethylthiazol-2-yl)-2,5-diphenyltetrazolium bromide
N	
NAD	Nicotinamide adenine dinucleotide
n.d.	not detectable
NFL	Neurofilament protein light
Nos	Nitric oxide synthases
NT	Nucleotidase
NTPDases	Nucleoside triphosphate diphosphohydrolase
O	
OCT	Optimum-cutting-temperature
P	
Panx	Pannexin
PDGFR	Platelet-derived growth factor receptor
PEPCK	Phosphoenolpyruvate carboxykinase
PHD	Prolylhydroxylase
PKA	Protein kinase A
PKC	Protein kinase C
PLC	Phospholipase C
pVHL	von Hippel-Lindau tumour suppressor protein
Q	
qPCR	Quantitative polymerase chain reaction
R	
REPCs	Renal EPO-producing cells
ROS	Reactive oxygen species
RPMI	Cell culture medium developed at the Roswell Park Memorial Institute (RPMI)
RT	Reverse Transcription

S

SMA Smooth muscle actin

T

Tab. Table

Tbp TATA-box binding protein

TGF Transforming growth factor

TIMP-1 Tissue inhibitor of metalloproteinases-1

TLR Toll-like receptors

Tnf Tumor necrosis factor-alpha

TRAIL Tumor necrosis factor-related apoptosis-inducing ligand

TRAP Tartrate-resistant acid phosphatase

U

UDP Uridine diphosphate

UTP Uridine triphosphate

V

VEGF Vascular endothelial growth factor

W

wo without

WT Wildtype

1. Summary

Despite advances in preventive strategies in the treatment of ischemia/reperfusion injury (IRI), IRI continues to be associated with high morbidity and mortality. Further improvement of therapeutic strategies requires a deeper understanding of the cellular and molecular mechanisms, that occur after myocardial infarction (MI) and acute kidney injury (AKI). A key event in the early phase after injury is ATP release into the tissue microenvironment by apoptotic/ necrotic cells promoting pro-inflammatory responses, while its breakdown-product, adenosine, formed by CD39 and CD73, signals via adenosine receptors (A_1R , $A_{2A}R$, $A_{2B}R$ or A_3R) and promotes healing processes. The present study explored the role of the purinergic signaling and adenosine in two experimental models: the heart and the kidney after IRI using various tissue-specific CD73 mouse mutants.

In the heart, we demonstrated that cardiac infiltrating T cells upregulated the expression of CD73 after MI. Stimulation of T cells resulted in increased ATP hydrolysis and adenosine formation underlining the role of T cells in nucleotide breakdown. Moreover, we showed that extracellular ATP catabolism aside of CD39 importantly involves pyrophosphatases. Infiltrating and blood circulating $CD4^+$ T cells express $A_{2A}R$, but more interestingly the $A_{2B}R$ became upregulated only on cardiac infiltrating $CD4^+$ T cells after MI. In functional studies we demonstrated that $A_{2A}R$ as well as $A_{2B}R$ stimulation reduced the overall cytokine secretion profile (e.g., $IFN-\gamma$ and IL-17). FACS sorted cardiac T cells lacking CD73 showed increased secretion of pro-inflammatory cytokines indicating an important role of $A_{2A}R$ and $A_{2B}R$ signaling for the healing process after MI. In the kidney, we found that loss of CD73 on fibroblasts/ pericytes led to reduced kidney function, increased collagen formation and matrix deposition due to increased myofibroblast transformation as well as impaired immune cell infiltration after 14d, while initial injury was the same compared to control littermates. This phenotype could be fully reversed after treatment with soluble CD73. Moreover, fibroblasts isolated from $CD73^{-/-}$ mouse kidneys and cultured *in vitro* displayed a hyperproliferative phenotype compared to fibroblasts isolated from wildtype kidneys. In contrast, lack of CD73 on tubular cells resulted in increased tissue damage in the initial phase after injury leading to impaired kidney function and increased fibrosis formation after 14d.

Taking together, our findings suggest that CD73 activity on T cells infiltrating the infarcted myocardium plays an important role in tissue recovery and healing, which is mediated by $A_{2A}R$ and $A_{2B}R$ signaling by inhibition of pro-inflammatory cytokines. In the kidney, we found that CD73 on fibroblasts/ pericytes and tubular cells importantly contributes to fibrosis formation and resolution of inflammation after AKI. In summary, we showed the importance of CD73 and adenosine signaling in orchestrating wound healing and immune response, which may lead to novel therapeutic concepts for treatment of MI or AKI.

2. Zusammenfassung

Trotz Fortschritte bei der Behandlung von Ischämie/ Reperfusionsschäden (I/R) an Herz und Niere, bleibt der resultierende Krankheitsprozess mit einer hohen Morbiditäts- und Mortalitätsrate assoziiert. Weitere Fortschritte auf diesem Gebiet hängen wesentlich von einem tieferen Verständnis der zellulären und molekularen Mechanismen ab, welche den Krankheitsverlauf nach Herzinfarkt (MI) oder akutem Nierenversagen (AKI) bestimmen. Ein Schlüsselereignis in der frühen Phase nach I/R, ist die Freisetzung von ATP durch nekrotische/ apoptotische Zellen, welches typischerweise zu einer pro-inflammatorischen Antwort führt, wohingegen das ATP-Abbauprodukt Adenosin, welches durch die Ektoenzyme CD39 und CD73 gebildet wird, über Adenosinrezeptoren (A_{1R} , A_{2AR} , A_{2BR} oder A_{3R}) anti-inflammatorische Effekte vermittelt. In der vorliegenden Studie wurde die Rolle von Adenosin im Rahmen der purinerger Signaltransduktion in zwei experimentellen Modellen untersucht: im Herzen und in der Niere nach MI bzw. AKI unter Verwendung verschiedener Gewebs-spezifischer CD73 Maus-Mutanten.

Im Herzen war bekannt, dass T-Zellen, welche das Herzgewebe nach Infarkt infiltrieren, die Expression von CD73 hochregulieren. Stimulation von T-Zellen resultierte in erhöhter Hydrolyse von ATP und der Bildung von Adenosin, was die Beteiligung von T-Zellen im Abbau von Nukleotiden belegte. Weiterhin konnten wir zeigen, dass beim extrazellulären ATP Abbau neben der CD39 noch Pyrophosphatasen beteiligt sind. Sowohl infiltrierende als auch im Blut-zirkulierende $CD4^+$ T-Zellen exprimierten wesentlich den A_{2AR} , wobei der A_{2BR} interessanterweise nur in Herz-infiltrierenden $CD4^+$ T-Zellen nach Infarkt hochreguliert wurde. In funktionellen Studien konnten wir zeigen, dass eine Stimulation des A_{2AR} s als auch des A_{2BR} s, eine allgemeine Reduktion der Zytokinausschüttung zur Folge hatte (z. B. $IFN-\gamma$ und IL-17). In der Niere fanden wir, dass ein Verlust von CD73 auf Fibroblasten/ Perizyten der Niere zu einer reduzierten Nierenfunktion, erhöhten Kollagenbildung und Matrixablagerung im Zuge erhöhter Myofibroblasten-Transformation sowie einer gestörten Immunzellinfiltration nach 14 Tagen führt, wobei die initiale Verletzung vergleichbar zu der der Kontrolltier-Gruppe war. Zusätzlich zeigten Fibroblasten, welche aus der Niere von $CD73^{-/-}$ Mäusen isoliert und *in vitro* kultiviert wurden, einen hyperproliferativen Phänotyp. Im Gegensatz dazu führte der Verlust der CD73 auf tubulären Zellen der Niere zu einem erhöhten Gewebsschaden in der initialen Phase der Verletzung, und dies führte langfristig ebenfalls zu gestörter Nierenfunktion und gesteigerten Fibrose.

Insgesamt zeigen unsere Ergebnisse, dass die CD73-Aktivität auf T-Zellen eine zentrale Rolle bei der Heilung des Herzens nach Infarkt spielt, was durch eine Adenosin-bedingte Hemmung pro-inflammatorischer Zytokine bedingt ist und über eine Aktivierung von A_{2AR} und A_{2BR} vermittelt wird. In der Niere sind insbesondere CD73 auf Fibroblasten/ Perizyten und tubulären Zellen wichtig, wobei das dort gebildete Adenosin antifibrotisch und entzündungshemmend wirkt. Zusammenfassend konnten wir die Bedeutsamkeit von CD73 und Adenosin in der Orchestrierung von Wundheilung und Immunantwort aufdecken, was die Möglichkeit für die Entwicklung neuer therapeutische Konzepte für die Behandlung von MI oder AKI bietet.

3. Introduction

3.1. Ischemia/ reperfusion injury

Despite the advances in preventive strategies and treatment of ischemia/ reperfusion injury (IRI), IRI continues to be associated with high morbidity and mortality contributing to a wide range of pathologies, including myocardial infarction, acute kidney injury, ischemic stroke trauma, circulatory arrest, sickle cell disease and sleep apnea. IRI is a pathological condition characterized by an abrupt interruption of blood supply causing tissue hypoxia to an organ followed by regeneration of perfusion and reoxygenation [1]. The extent of tissue injury and cell death is determined by the magnitude and duration of blood supply interruption followed by a subsequent damage induced by reperfusion [2]. After injury many pathological processes contribute to the extent of damage associated with IRI (figure 1) [1].

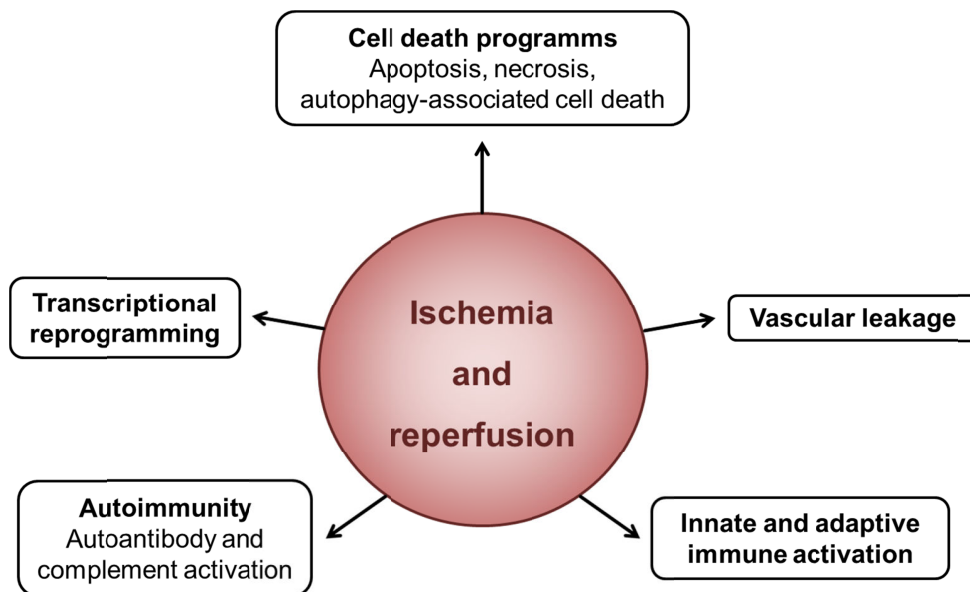


Fig. 1: Pathological processes contributing to ischemia and reperfusion associated tissue injury. Many factors like vascular leakage, innate and adaptive immune activation as well as autoimmunity, transcriptional reprogramming and cell death programmes contribute to tissue injury after IRI [modified;1]. Reprinted from [1] with permission from Springer Nature © 2011.

During ischemia oxygen reserve within the tissue is limited, rapidly leading to hypoxia and dysfunction of endothelial barrier associated with vascular permeability due to a reduction of adenylate cyclase activity and low intracellular cAMP levels [3; 4]. Although IRI typically takes place under sterile conditions, inflammation can occur when hypoxia stimulates the innate and adaptive immune

system including immune cell differentiation and trafficking into the site of injury [5; 6]. In addition reperfusion injury leads to activation of the complement system (autoimmunity) [7]. Moreover, hypoxia is associated with modifications in transcriptional control of gene expression mediated by an inhibition of the oxygen-sensing prolylhydroxylase (PHD), an enzyme, that hydroxylates the alpha subunit of the hypoxia-inducible transcription factor (HIF-1 α or HIF-2 α) [5]. Furthermore, the lack of oxygen supply as well as abrupt reperfusion results in activation of cell death programs, including mainly necrosis but also apoptosis or autophagy-associated cell death [8].

3.1.1. Vascular leakage

The entire circulatory system is constructed by a single layer of cells, the vascular endothelium, which maintains vascular integrity by counteracting leukocyte adhesion and platelet aggregation to prevent inflammation and thrombosis. Moreover, the vascular endothelium is an important regulator of vascular tone by production of vasoactive substances. Ischemia followed by reperfusion disturbs the functional integrity of the endothelium leading to “endothelial dysfunction”, which is associated with increased vascular permeability, endothelial cell inflammation and imbalance between vasodilating and vasoconstricting factors [1; 9]. Loss of endothelial barrier function is caused by reactive oxygen species (ROS) through changes in endothelial cell cytoskeletal proteins leading to intercellular gaps [10]. As a consequence of IRI, infiltrating immune cells play a major role in orchestrating tissue remodeling. Changes in the microenvironment induced by IRI lead to leukocyte activation, chemotaxis, leukocyte-endothelial cell adhesion and transmigration mediated by increased expression of P-selectin inducing leukocyte “rolling” [11]. Once leukocytes transmigrate into the interstitial compartment, toxic ROS, proteases and elastases are released resulting in increased microvascular permeability, oedema, thrombosis and parenchymal cell death [11; 12].

3.1.2. Innate and adaptive immune activation

The immune system is a complex regulatory system of the body for host defense against invasive pathogens. Infection leads to an activation of several signaling cascades resulting in activation and recruitment of immune cells, in particular neutrophils and macrophages, immune cells of the innate immune system. Inflammation, that occurs after injury in the absence of microorganisms, such as in IRI, is called “sterile inflammation”. “Sterile inflammation” is characterized by recruitment of neutrophils and macrophages and production of pro-inflammatory cytokines and chemokines similar to

pathogen-induced inflammation. Damage-associated molecular patterns (DAMPs) are host-derived non-microbial stimuli, that are released from dying cells of injured tissue and trigger pro-inflammatory effects [13]. DAMPs are endogenous factors, such as chromatin-associated protein high-mobility group box 1 (HMGB1), heat shock proteins (HSPs), and purine metabolites, such as ATP and uric acid, which under normal conditions – because of their intracellular location - are hidden from recognition by the immune system [13–17]. Once released into the extracellular microenvironment by necrotic cells, which failed to undergo apoptosis, DAMPs interact with toll-like receptors (TLRs) and other cell surface receptors to initiate sterile inflammation by immune cell recruitment and activation [13].

Beside the activation of the innate immune system, IRI is associated with robust stimulation of T lymphocytes, including CD4⁺ and CD8⁺ T cells as well as regulatory T cells (T_{reg}). T cells are a part of the adaptive immune system activated by antigen specific stimulation in sterile inflammation [6]. Several studies demonstrated the importance of T lymphocytes during ischemia followed by reperfusion, whereas the contributions of T cells to inflammation and healing processes was shown to be dependent on tissue specificity, composition of the innate immune system, infiltration kinetics and developmental states. Depending on their phenotype, activated T cells presented a variety of immune functions. Th1 cells secreting IFN- γ or Th17 cells releasing IL-17 promote inflammatory pathologies. However, IL-4 and IL-13 production by Th2 cells as well as IL-10 secretion by T_{reg} cells are important for resolution of inflammation [18]. Moreover, B cells have been shown to be an important regulator of immune response after IRI by production of antibodies, which bind to ischemic cells contributing to autoimmunity [19].

3.1.3. Autoimmunity

Autoimmunity during IRI is mediated by recognition of natural antibodies against self-proteins leading to activation of the complement system [20]. The complement system acts as an interface between innate and adaptive immune system consisting of several fluid-phase and membrane-bound proteins [21]. In IRI models several studies have shown that inhibition or depletion of the complement components lead to decreased tissue damage [21].

In contrast to T cells, which can be pathological or protective in IRI depending on the type of organ injury or T cell population, B cells have been reported to be predominantly pathogenic in all organs systems including the intestine, heart, kidney and skeletal muscle [22]. For example, B cell deficiency protected mice from injury after IRI in the kidney, whereas serum transfer could partially restore the injury-induced effects [23].

3.1.4. Transcriptional reprogramming

Mammalian organisms are provided with a unique mechanism to adapt to low oxygen levels and oxidative stress (hypoxia). A major mediator in hypoxic conditions is the hypoxia-inducible factor (HIF), a DNA-binding transcription factor, which interacts with specific nuclear cofactors under low oxygen levels to initiate expression of various genes initiating adaptive responses to compromised oxygen tension [24]. HIF is a heterodimer and consists of two subunits, HIF-1 α or HIF-2 α and HIF-1 β . HIF-1 α is ubiquitously expressed, whereas HIF-2 α is restricted to tissue specificity [5; 25]. In further descriptions HIF- α will be used to denote either HIF-1 α or HIF-2 α . Under normal oxygen conditions, the PHD enzyme hydroxylates the proline residues of HIF- α [26]. Because of hydroxylation, HIF- α interacts with the β -domain of the von Hippel-Lindau tumour suppressor protein (pVHL), which leads to subsequent ubiquitylation by the Elongin BC/Cul2/pVHL ubiquitin–ligase complex assembled via the pVHL α domain [27]. Ubiquitinated HIF- α is then recognized by the 26S proteasome and degraded [28]. During normoxia HIF- α is continuously synthesized and degraded, whereas under hypoxic conditions degradation of HIF- α is inhibited [29]. For its catalytic activity the PHD enzyme requires oxygen to hydroxylate proline residues of HIF- α . During hypoxia oxygen levels are decreased and hydroxylation of HIF- α is abrogated resulting in accumulation of the transcription factor and dimerization with the constitutively expressed HIF-1 β subunit [24; 29]. In the nucleus the HIF heterodimer binds to hypoxia-response elements within the DNA and recruits coactivator proteins for increased expression of hypoxia-associated specific target genes [29].

HIF complex-induced gene alterations are a central feature of the cellular stress response to hypoxia, which involves activation of glycolysis, erythropoiesis and angiogenesis for restoration of oxygen homeostasis on systemic, local and cellular levels [30–33]. The primary metabolic pathway of ATP generation is oxidative phosphorylation with the highest intracellular oxygen consumption [32]. During hypoxia, transcription of genes encoding for glucose transporter 1 and enzymes of the glycolytic pathway become activated, whereas expression of genes involved in electron transport chain are downregulated allowing ATP synthesis by an O₂-independent pathway [32; 34; 35].

Several studies have shown that gene expression of erythropoietin (EPO) is initiated by HIF- α , whereas HIF-2 α is the major activator of gene transcription in kidney and liver [36; 37]. In response to hypoxia renal EPO concentrations are controlled by the number of renal EPO-producing cells (REPCs), which increase proportionally to the grade of systemic hypoxia [38; 39]. REPCs are located in the interstitium between tubules and nutritive peritubular capillaries of the deep cortex and outer medulla. They are part of the peritubular interstitial/perivascular fibroblast population characterized by fibroblast/pericyte markers (PDGFR- β polypeptide and ecto-5'-nucleotidase/CD73) and neuronal markers

(microtubule-associated protein 2 (MAP2) and neurofilament protein light polypeptide (NFL)) [39–43]. Beside its role in regulating erythropoiesis, EPO was shown to be an important mediator in anti-apoptotic, anti-oxidative and anti-inflammatory properties after IRI [44].

Moreover, HIF complex-induced transcriptional modulation controls sprouting angiogenesis by activation of vascular endothelial growth factor (VEGF) expression [45]. During the first step of angiogenesis some endothelial cells transform to "tip cells" inside the capillary and start angiogenic expansion according to VEGF stimulation. In the next steps migration and proliferation of endothelial cells as well as tube formation are also regulated by interaction of VEGF and its receptors VEGFR [46].

3.1.5. Cell death programs

After ischemia and reperfusion different cell death programs become activated, which can be categorized in three groups: necrosis, apoptosis and autophagy-associated cell death. Necrosis, usually considered as an “accidental”, non-programmed cell death, is characterized by cell and organelle swelling as well as surface membrane rupture with spillage of intracellular contents as a result from a metabolic failure associated with ATP depletion [8]. Early stages of necrosis are marked by loss of plasma membrane and organelle integrity, which was shown to be related to osmotic forces resulting from opening of non-specific, glycine-inhibitable anion channels (death channels) [47]. Reviewing the literature of the last decades, several studies come to the conclusion that classification of necrosis as uncontrolled cell death is no longer tenable. Necrosis, a controlled and programmed cell death, is not the result of one well-studied signaling pathway, but rather a cause of extensive interaction between several biochemical and molecular events at different cellular levels [48]. Mediators for necrosis are ROS, which are generated as a result of reperfusion after ischemia and activation of aerobic energy synthesis promoting damage to proteins, lipids and DNA using direct or indirect pathways [49]. Moreover, cells undergoing necrotic cell death release their whole cell content including DAMPs (3.1.2), which act like danger signals entering the circulation and activating innate immune cells to induce sterile inflammation [8; 50; 13].

In contrast to necrosis, apoptosis is defined by cell shrinkage, condensed and fragmented nuclei as well as formation of apoptotic bodies leading to the loss of plasma membrane integrity [51]. A characteristic of apoptosis is the cleavage of cytoskeletal proteins by pro-apoptotic aspartate-specific proteases (caspases) resulting in the breakdown of subcellular components [8]. Apoptotic cell death can be activated by two different mechanisms termed the extrinsic and intrinsic pathways. The extrinsic

signaling cascade is mediated by activation of cell-surface death receptors (Fas (CD95) and TRAIL (tumor necrosis factor-related apoptosis-inducing ligand) receptor), which regulate the activation of caspase 8 and thereby mediate cell destruction [8; 52]. The intrinsic pathway is triggered by intracellular stress such as DNA damage, increased ROS formation or changes in the metabolic status of the cell, events that occur after IRI. These triggers affect the permeabilization of the mitochondrial membrane mediated by Bax (or Bak) and a BH3-only protein, such as Bid, leading to release of cytochrome *c* from mitochondria. In the cytoplasm cytochrome *c* forms a multi-protein complex by assembling with APAF1 and recruitment of caspase 9 termed the apoptosome, which activates effector caspases such as caspase 3 leading to dismantling of the cell and the formation of apoptotic bodies [53–55].

The self-digestive process of autophagy is an important regulator for long-lived or excessive proteins and aged organelles under normal conditions to maintain protein and organelle quality [56]. Several studies have shown that autophagic flux during the reperfusion phase is markedly increased in IRI mediated by oxidative stress of the cell [57; 58]. However, the contribution of autophagy to the extent of injury after IRI is controversially discussed in the literature as to whether autophagy will be protective or detrimental. One possibility of its protective effect could be the removal of damaged mitochondria and thereby inhibition of cytochrome *c* release and induction of apoptosis. Moreover, recycling of proteins and organelles by the autophagic-lysosomal pathway provides free amino acids and fatty acids, which are used for mitochondrial ATP production and protein synthesis. In contrast, long-term upregulation of autophagy can trigger cell death by excessive degradation of essential proteins and organelles [59].

3.2. Myocardial Infarction

The heart is a hollow muscular organ, that supplies all other organs and tissues with oxygen and nutrients by rhythmic contractions. To accomplish this enormous functional performance, it is important that the heart muscle itself is provided with blood. This occurs by the coronary arteries, which originate above the aortic valve. Coronary arteries build a coronoid structure all over the heart and branch out in the periphery. Accordingly, the myocardium is well capillarized, which results in short diffusion distances and allows supply of oxygen and nutrients for heart muscle cells (cardiomyocytes) [60]. A narrowing or an occlusion of the coronary arteries leads to ischemia and a lack of nourishment of the surrounding tissue. Acute oxygen deficiency by flow obstruction leads to myocardial infarction (MI) [61]. The leading cause for occlusion of coronary arteries is atherosclerosis

associated with chronic inflammation of the vessel wall. Accumulation of lipids, immune cells, smooth muscle cells as well as extracellular matrix as a cause of endothelial dysfunction results in a critical narrowing of the blood vessel and limits blood flow [62]. Inflammatory processes and biomechanical forces lead to destabilization of the plaque ending in a rupture of the thin fibrous cap and allowing the pro-coagulant lesion center to interact with the flowing blood resulting in initiation of acute thrombosis [62; 63]. As a result, the formation of a thrombus causes an occlusion of the coronary artery leading to MI (figure 2) [62].

3.2.1. Wound healing after myocardial infarction

Wound healing of the heart after MI can be categorized into three phases. During the first 2 days cardiomyocytes undergo cell death due to ischemia (3.2.1.1) followed by an inflammatory response (3.2.1.2). The blood supply is restored and the damaged tissue become remodeled by scar formation (3.2.1.3) (figure 2) [64].

3.2.1.1. Ischemia-induced cell death of cardiomyocytes

Consistent oxygen supply is needed by cardiomyocytes for cellular homeostasis, which is provided by oxidative phosphorylation of mitochondria for generating energy in the form of adenosine triphosphate (ATP) [65]. An occlusion of a coronary artery leads to a lack of oxygen supply for cardiomyocytes resulting in an interruption of the respiratory chain and ATP generation by mitochondria [66]. To compensate for low ATP levels, the cell reacts via activation of another metabolic pathway, termed anaerobic glycolysis, including HIF complex-induced upregulation of enzymes involved in the glycolytic pathway [32; 35; 67; 68]. However, energy production by anaerobic glycolysis is less efficacious than oxidative phosphorylation by mitochondria and is associated with less ATP generation and inhibition of enzymes involved in glycolysis by its accumulating metabolic products [69–71]. As a result, reduced energy supply as well as accumulation of anaerobic metabolic products lead to induction of cell death (3.1.5) [55; 72].

Oxygen levels, which are needed for oxidative phosphorylation, can be restored by opening of the coronary artery and recovery of blood flow in the ischemic heart area. Moreover, after reperfusion metabolic waste products can be removed from the tissue [2]. Early reperfusion of ischemic heart tissue is associated with reduced tissue damage and leads to protection of viable myocardium thereby limiting the infarct area [73]. Although reperfusion mediates tissue protection by restoration of oxygen

and nutrients, its by-products including ROS formation contribute to initiation of cell death programs, such as apoptosis and necrosis, and thereby increasing tissue damage (3.1.5) [49; 74].

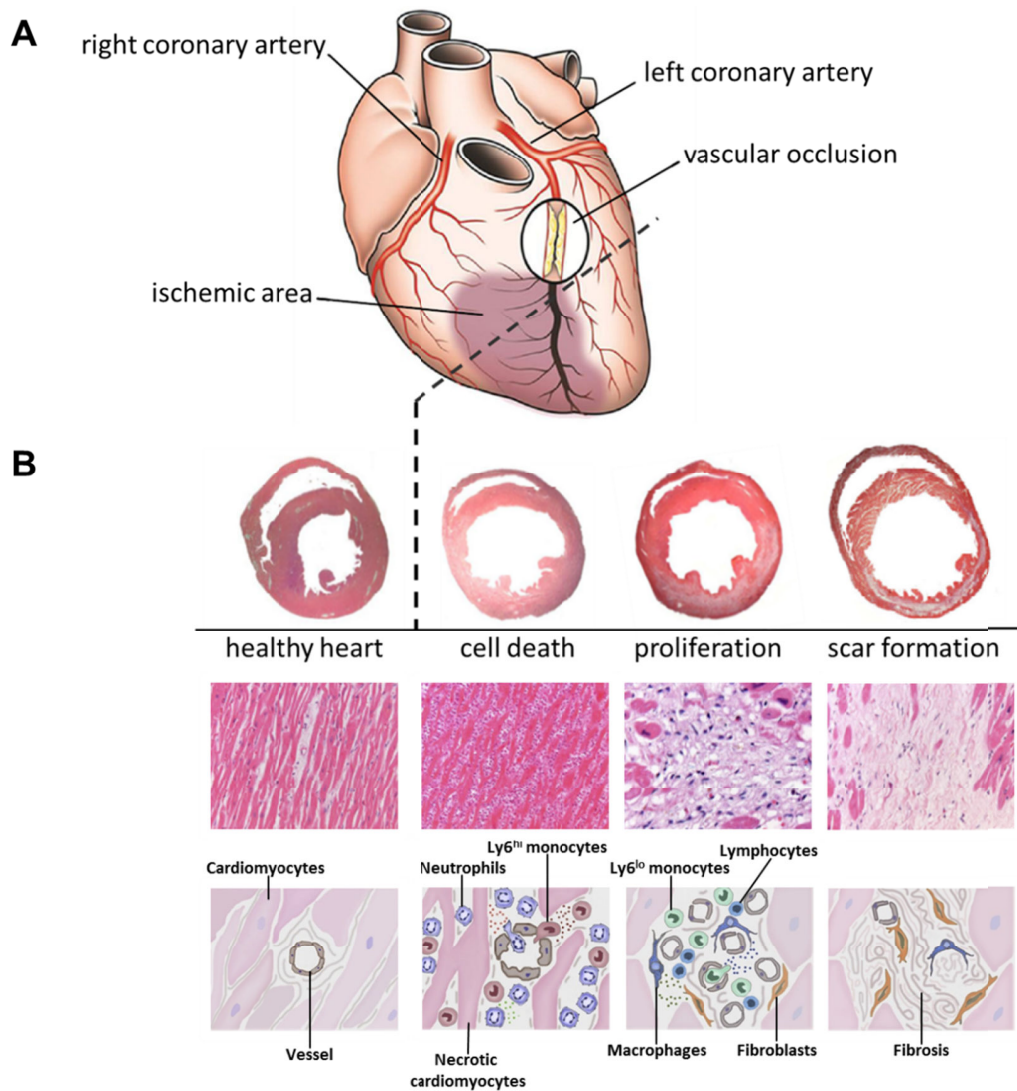


Fig. 2: Healing processes of the heart after MI. A) Schematic picture of the heart with occluded left anterior descending artery (LAD). The gray area indicates the area at risk after MI. B) Histological and schematic pictures of a healthy heart as well as of hearts after MI during different phases in the healing processes. Upper row: Cross-sections of murine hearts. Middle row: Histology of normal myocardium and different phases of infarcted myocardium. Lower row: Schematic representations of healthy heart tissue and alterations, that occur after IRI. An occlusion of the coronary artery leads to a lack of oxygen supply for cardiomyocytes resulting in initiation of cell death (3.2.1.1), which is associated with recruitment and activation of immune cells, such as macrophages and Ly-6C^{hi} monocytes, due to pro-inflammatory signals (3.2.1.2). Pro-inflammatory responses are followed by anti-inflammatory processes mediated by Ly-6C^{lo} monocytes, M2 macrophages and lymphocytes followed by fibroblast activation and scar formation (3.2.1.2 and 3.2.1.3) [modified; 75–78]. Reprinted from [75-78] with permission from BioMed Central Ltd © 2013 (CC BY 2.0)/ Springer Nature © 2018/ Elsevier © 2018 / BMJ Publishing Group Ltd. © 2012.

3.2.1.2. Activation of the inflammatory system

The inflammatory response after MI is initiated by several events including the release of DAMPS, which stimulate the complement system and TLRs [13]. Both processes mediate the activation of the transcription factor NF- κ B contributing to the expression of chemokines, cytokines and cellular adhesion molecules promoting the inflammatory response [79; 80]. Some activated factors of the complement system function as chemoattractants [81]. Moreover, ROS lead to NF- κ B activation and thereby contribute to the release of chemokines and cytokines via inflammasome formation in cardiac fibroblasts [82; 83]. The inflammasome consists of a large multiprotein complex, that processes pro-IL-1 β and secretes mature IL-1 β leading to an initial pro-inflammatory response [84]. Furthermore, P-selectin, which is continuously expressed by endothelial cells and stored in cytosolic bodies, is presented to the cell surface within minutes of reperfusion mediating initial leukocyte binding [85]. Expression of immunoglobulin cell adhesion molecules (CAM), such as ICAM-1, by endothelial cells is increased four to six hours after reperfusion, which regulates immune cell activation and tissue infiltration [86]. Endothelial cells thereby control the recruitment and activation of immune cells circulating in the blood and initiate their infiltration into the damaged tissue starting with neutrophils followed by monocytes/ macrophages and leukocytes [87; 88]. Migration of immune cells occurs along a chemoattractant gradient guiding the way to cells undergoing necrosis [89; 90].

The first immune cell subset infiltrating the infarcted myocardium within one hour after IRI is neutrophils [91]. At the site of injury neutrophils take up denatured matrix proteins and also secrete matrix degrading enzymes, such as matrix metalloproteinases-9 (MMP-9), which are important for tissue repair [92]. On the contrary, neutrophils have been shown to release toxic agents, such as oxidants and proteases, causing harm to the surrounding cardiomyocytes and vascular endothelial cells [93]. Moreover, secretion of chemokines by neutrophils maintains recruitment of inflammatory monocytes and their activation, thereby further promoting inflammation [94].

Monocytes are forming the second wave of immune cells infiltrating the tissue after IRI [87]. In the early phase of monocyte infiltration, Ly-6C^{hi} monocytes migrate to the site of injury mediated by CCR2, a receptor for the chemokine monocyte chemoattractant protein-1 (MCP-1), promoting phagocytic, proteolytic, and inflammatory functions [88]. The inflammatory stimulus influences macrophage differentiation leading to Ly-6C^{hi} monocyte-derived M1 macrophages, that remain inflammatory by expressing IL-1 β and TNF α and by contributing to oxidative stress [95; 96]. The later phase of monocyte infiltration is associated with a decrease in the number of Ly-6C^{hi} monocytes combined with increased accumulation of Ly-6C^{lo} monocytes by CX(3)CR1, which supports healing processes via myofibroblast accumulation, angiogenesis, and deposition of collagen [88]. Moreover, M1

macrophages become replaced by M2 macrophages contributing to tissue healing processes. Due to the fact that macrophage turnover in the infarcted zone is remarkably fast, M2 macrophages are assumed to derive from less inflammatory Ly-6C^{lo} monocytes or from Ly-6C^{hi} monocytes in a microenvironment that promotes resolution [95].

Whereas the innate immune system is rapidly activated in early stages of MI as described above, cells of the adaptive immune system infiltrate the damaged tissue in later stages [87]. Infiltrating T lymphocytes can be categorized into two groups, CD4⁺ and CD8⁺ T cells. Both T cell subsets become activated by interaction with antigen presenting cells (APCs), such as dendritic cells and macrophages. Antigens are internalized by APCs followed by degradation in lysosomes and presentation of antigen-derived peptides on histocompatibility complex (MHC) class I or MHC class II molecules [97; 98]. It has been shown that CD4⁺ T cells are important mediators of wound healing after MI. Deficiency of CD4⁺ T cells in mice resulted in increased left ventricular dilation, higher total numbers of leukocytes and pro-inflammatory monocytes and disturbed collagen matrix formation [99]. Moreover, regulatory T cells (T_{reg}), which are directly derived from CD4⁺ T cells, show protective effects against adverse ventricular remodeling and contribute to improved cardiac function by inhibition of inflammation [100]. On the other hand, it has been shown that CD8⁺ T cells can recognize cardiomyocytes *in vitro* triggering cytotoxic effects [101]. Recent literature suggests an important role of T cells in modifying the response during cardiac IRI. However, the underlying molecular mechanisms by which T cells control cardiac remodeling remain unclear.

3.2.1.3. Proliferation of fibroblasts and endothelial cells

Phagocytosis and clearance of cell debris and necrotic cardiomyocytes by neutrophils, monocytes and macrophage mediate resolution of inflammation and transition into the reparative phase [77]. IL-10, a cytokine secreted by Ly-6C^{lo} monocytes, macrophages and Th2 lymphocytes inhibit the production of pro-inflammatory cytokines and activate the expression of TIMP-1 (tissue inhibitor of metalloproteinases-1) promoting extracellular matrix remodeling [95; 77; 102].

Upregulation of TGF- β suppresses chemokine and cytokine expression and modulates fibroblast phenotype and function by stimulating the synthesis of various extracellular matrix proteins including collagens, fibronectin, tenascin-C and proteoglycans [77; 103]. TGF- β stimulation of fibroblasts leads to activation of α -smooth muscle actin (α -SMA) expression and myofibroblast trans-differentiation and thereby increasing extracellular matrix protein synthesis [104; 105]. Myofibroblast synthesis of collagen III is already starting on day 2 after MI [106]. Collagen III fibers form an elastic network,

which is less stable, but ideal for maintaining structural integrity of the network [107]. During the processes of wound healing and scar formation, collagen III is replaced by stable and dense collagen I fibers creating a mechanical stable infarct area of the heart [106; 107]. During maturation processes the number of cells in between the forming scar decreases due to apoptosis, which includes the elimination of inflammatory cells and the reduction of the number of myofibroblasts [108]. Cross-linking of collagen fibers stabilizes the tissue of the infarcted area and is important in the remodeling phase. On the other hand it has been shown that cross-linking leads to chamber stiffness and is associated with left ventricular dilatation and systolic dysfunction [109–111].

Finally, revascularization is induced by the generation of new blood vessels (angiogenesis), a process, that is mediated by angiogenic growth factors, such as vascular endothelial growth factor A (VEGF-A), angiopoietins and fibroblast growth factor (FGF) [112]. VEGF-A is an important regulator of endothelial proliferation and migration to promote blood vessel formation and cardiac remodeling [112; 113].

3.3. Acute kidney injury

The kidneys are a pair of organs, that are part of the excretory system. Beside the function of blood filtration in order to generate urine for regulation of water balance and excretion of waste products, the kidneys are an important mediator of electrolyte balance and metabolism, blood pressure regulation, and hormone production [114]. The human renal parenchyma is divided into outer cortex and inner medulla forming several conical lobes. Each lobe is based onto the papilla, a region where the urine is directed from the collecting ducts to the ureter. Although rat and mice have unipapillar kidneys, the basic structure is similar to humans and can also be divided into cortex and medulla [115]. Unfiltered blood containing waste products flows via the renal artery to the capillary network of the glomerulus, where the blood is filtered by passive diffusion across the glomerular basement membrane and the glomerular slit diaphragm. The majority of biomolecules, electrolytes and water of the primary filtrate is reabsorbed by a variety of channels and transporters present on the cell surface of the renal epithelium in the proximal tubule. Increase of the surface area by formation of microvilli, finger-like cytoplasmic protrusions, termed the apical brush border, increases uptake efficiency [114; 116]. The urine becomes more concentrated in the Loop of Henle as well as in the distal tubule by reabsorption of water ending up in the collecting duct. Filtered blood free of waste products leaves the kidney via the renal vein (figure 3) [114].

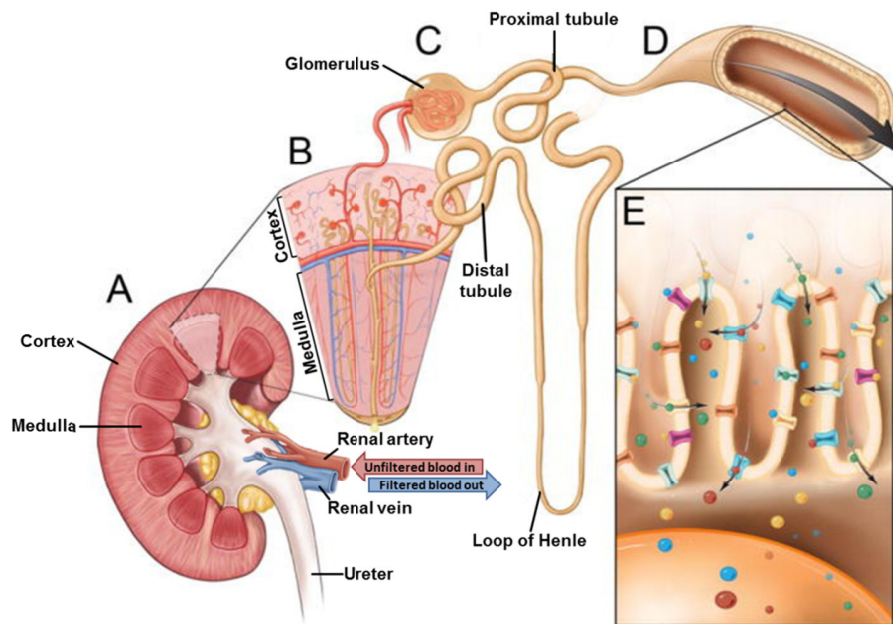


Fig. 3: Anatomic scheme of human kidney. The human kidney parenchyma can be divided into cortex and medulla forming several conical lobes. Unfiltered blood containing waste products enters the kidney via the renal artery and is filtered in the capillary network of the glomerulus. Primary filtrate enters the proximal tubule containing a variety of channels and transporters present on the cell surface of the renal epithelial cells mediating reabsorption of biomolecules, electrolytes and water. Urine becomes more concentrated by passing through the Loop of Henle and distal tubule ending up in the collecting duct, which directs the urine to the ureter. Filtered blood without waste products leaves the kidney via the renal vein [modified; 116]. Reprinted from [116] with permission from Springer Nature © 2018.

A decrease of the arterial blood pressure as a result of acute heart failure is known to be an important cause of acute kidney injury (AKI). AKI is associated with the decrease in renal excretory function leading to accumulation of nitrogen-metabolism products, such as creatinine and urea, as well as accumulation of metabolic acids, and increased potassium and phosphate concentrations in the urine [114; 117]. In response to decreased arterial blood pressure the body reacts with shock-dependent centralization of the circulatory system by adrenergic “emergency” vasoconstriction leading to reduced blood supply for the kidneys (ischemia). Moreover, AKI can be a result of renal events, such as inflammation of glomeruli (glomerulonephritis), poisoning (e. g. heavy metals or fungi) or medications with nephrotoxic effects (e. g. antibiotics, cytostatics or immunosuppressors) [114].

3.3.1. Wound healing after acute kidney injury

AKI displays many common features compared to MI for biological and molecular mechanism, which occur after ischemia. After IRI tissue damage leads to tubular cell necrosis and apoptosis (3.3.1.1) resulting in immune cell infiltration promoting pro-inflammatory responses (3.3.1.2) followed by resolution of inflammation and scar formation (3.3.1.3).

3.3.1.1. Ischemia-induced alterations in tubule cell metabolism and structure

Directly after ischemia ATP depletion initiates a cascade of metabolic changes within tubule cells [118]. A lack of ATP leads to impaired calcium uptake by the endoplasmic reticulum as well as diminished extrusion of cytosolic calcium into the extracellular space resulting in increased free intracellular calcium after injury, which mediates necrosis or apoptosis of the cell [118–121]. Moreover, ischemia activates NO synthesis in tubular cells with the consequence of cell damage induced by oxidant injury as well as protein nitrosylation, which is mediated by NO interaction with superoxide to form peroxynitrate [118; 119]. Collectively, ROS formation leads to increased renal tubule cell injury by oxidation of proteins, peroxidation of lipids, damage to DNA and thereby activation of necrosis or apoptosis [122].

Another phenomenon of IRI is the structural changes of tubular cells. As a result of ischemia tubular cells lose their cell polarity and brush borders, undergo cell death followed by dedifferentiation of viable cells, proliferation, and restitution of a normal epithelium [119]. Depletion of ATP is associated with rapid destruction of the apical actin cytoskeleton and rearrangement of actin from the apical domain and microvilli into the cytoplasm [123]. Because of changes in the structure of microvilli, membrane-bound, free-floating extracellular vesicles, or “blebs,” are formed and either internalized or lost into the tubular lumen contributing to cast formation and obstruction [119; 123]. Polarization of tubular cells is lost by early disruption of basolaterally polarized proteins, such as Na,K-ATPase and integrins. Under normal conditions the Na,K-ATPase is bound to the spectrin-based cytoskeleton at the basolateral domain via the adapter protein ankyrin. After ischemia the Na,K-ATPase, ankyrin, and spectrin accumulate in the cytoplasm of viable cells leading to impaired proximal tubular sodium reabsorption and a consequent increase in fractional excretion of sodium, which is a marker for AKI used in diagnostics [119; 124]. β 1 integrin is normally fixed to the basal domain mediating adhesion, which becomes rearranged to the apical membrane after ischemia leading to detachment of viable cells from the basement membrane [119].

3.3.1.2. Initiation of the cellular immune response

AKI is associated with a rapid immune response, which is initiated directly after injury, similar to those in the heart after MI. In the early phase of IRI, rapid immune cell activation promotes pro-inflammatory events and potentiates early injury, whereas in the later phase immune cells are required for the subsequent successful resolution of damage contributing to anti-inflammatory effects [125; 126].

Initial immune response is mediated by neutrophils, which accumulate at the site of injury 30 min after IRI secreting IL-17 to promote further downstream immune cell activation [127; 128]. The second wave of infiltrating immune cells consists of monocytes/ macrophages starting with Ly6C^{hi} monocytes [129]. Exposure of Ly6C^{hi} monocytes to granulocyte-macrophage colony-stimulating factor (GM-CSF) induces differentiation to M1 macrophages promoting inflammation [130; 131]. First infiltration of Ly6C^{hi} monocytes is followed by increased accumulation of Ly6C^{lo} monocytes and M2 macrophages promoting tissue remodeling, while the number of Ly6C^{hi} monocytes is decreasing [130; 132]. Decrease of Ly6C^{hi} monocytes is mediated by the colony stimulating factor-1 (CSF-1), which induces Ly6C^{hi} monocyte polarization to M2 macrophages [131].

Neither B cells nor T lymphocytes are present in large numbers in the uninjured kidney and after AKI [125; 129]. Because of the small T cell numbers in the kidney, researchers have been skeptical for a long time on their contribution to tissue remodeling. Findings of the last two decades, however, now suggest an important role for T cells in tissue healing after AKI presenting either pathogenic or protective contributions depending on the subtype. Mice lacking CD4⁺ T cells were relatively protected from IRI, whereas adoptive transfer of T cells restored injury [133]. Another study demonstrated that T_{reg} cells infiltrating the injured tissue after IRI promoted healing processes by modulating pro-inflammatory cytokine production of other T cell subsets [134].

3.3.1.3. Fibrosis formation and tissue recovery

The tubular epithelium of mammalian kidney has a unique capacity for repair and regeneration to restore normal epithelial integrity after AKI [135; 136]. To maintain tissue homeostasis, proximal tubular cells have a slow turnover rate under normal conditions, which changes after injury to fast proliferation processes [137]. The origin of proliferating tubular epithelial cells is controversially discussed in the literature. Recent studies support the findings that terminally differentiated epithelial

cells can dedifferentiate after injury, migrate along the basement membrane regaining stem-cell characteristics, proliferate and expand in size to repair the tissue damage [137; 138].

In addition, tubule degeneration and inflammation results in massive accumulation of myofibroblasts. Myofibroblasts are derived from resident interstitial cells, such as fibroblasts or pericytes stimulated by Notch and TGF- β stimulating pathways initiated by tubular epithelial cells [139–141]. Myofibroblast transformation is associated with robust upregulation of α SMA, a hallmark for myofibroblasts, as well as increased collagen I and collagen III secretion leading to organization of interstitial fibrosis and scar formation [139; 142].

3.4. Regulation of tissue healing processes and maladaptive repair mechanism

After IRI inflammatory responses and immune cell activation are necessary for proper tissue remodeling by elimination of cell debris and apoptotic or necrotic cells to initiate scar formation for stability of the tissue. As illustrated in figure 4, the orchestrated interplay of immune cells mediates acute and chronic inflammation in the heart after MI. Inhibition and resolution of inflammation after MI is an active process regulated by recruitment, differentiation and activation of reparative immune cells secreting anti-inflammatory mediators [143]. On a cellular basis macrophage polarization and the balance between M1 and M2 macrophages is an important contributor to tissue healing associated with reduced ventricular dysfunction and lower rate of heart failure [144]. Moreover, T_{reg} cells derived from CD4⁺ T cells have been shown to mediate protective effects against adverse ventricular remodeling and contributed to improved cardiac function by inhibition of inflammation [100].

Excessive or prolonged inflammation is a risk factor promoting additional tissue damage, which is associated with impaired heart function leading to heart failure [143]. For example, excessive immune cell infiltration leads to increased destruction of extracellular matrix, which is a risk factor for disruption of the heart wall [145]. Moreover, prolonged immune cell infiltration disrupts the formation of a stable scar leading to dilatation of the ventricle [143; 146; 147]. Furthermore, no resolution of immune cell response leads to expansion of immune cell infiltration in healthy, not infarcted tissue resulting in fibrosis and reduced pump function of the heart [148–150].

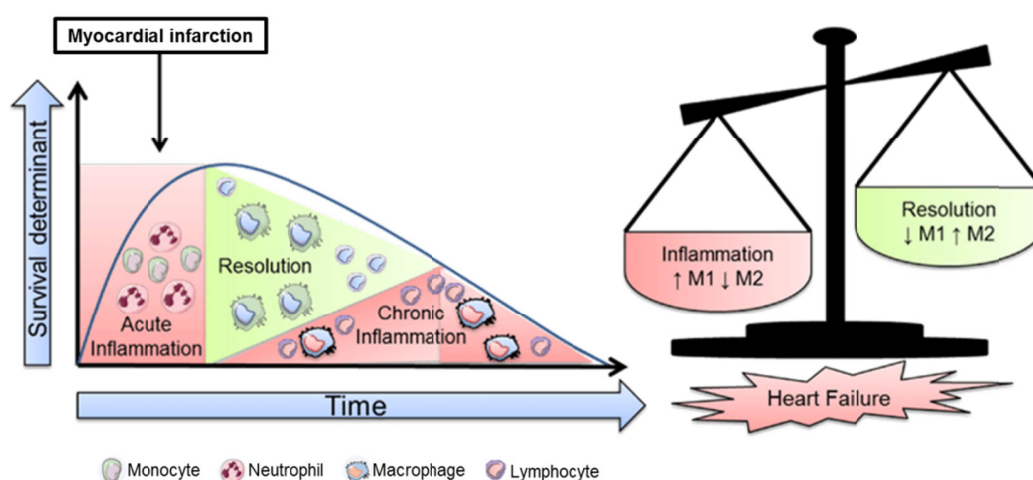


Fig. 4: Orchestrated interplay of pro- and anti-inflammatory immune cells after MI. Limitation of acute inflammation and improved resolution of immune cells by balancing pro- and anti-inflammatory contributors of tissue recovery might lead to reduced ventricular dysfunction and lower rate of heart failure [modified; 144]. Adopted from [144] with permission from Halade © 2013.

Similarly, persistent parenchymal inflammation as a result of AKI is associated with maladaptive repair including increased numbers of myofibroblasts and accumulation of extracellular matrix leading to chronic kidney disease (CKD) [151]. CKD is marked by inflammatory infiltration, tubular atrophy, capillary rarefaction, podocyte depletion, mesangial expansion, thickening of the glomerulus basal membrane (GBM) and fibrosis resulting in irreversible organ scarring (figure 5) [152–155]. Inflammation is triggered by pro-inflammatory cytokines and chemokines, such as TNF- α , IL1- β or MCP-1, mediating increased infiltration of leukocytes [152; 156; 157]. Secretion of TGF- β 1 by infiltrating immune cells and epithelial cells initiates myofibroblast transformation in detached pericytes and fibroblasts after injury [158; 155].

Several studies have shown that TGF- β 1 is a key regulator of fibrosis after kidney injury, but also a risk factor for developing CKD. In CKD multiple mechanisms controlling TGF- β signaling mediated by SMAD are dysregulated [155]. Recently, Li et al. could show that TGF- β signaling is regulated by a positive auto-regulation mechanism mediated by increased miR433 levels. Blockade of miRNA expression inhibited progression of renal fibrosis in obstructive nephropathy [159]. Moreover, increased expression of α VB1 integrin in the tubular epithelium is mediated by TGF- β signaling leading to subsequent tubulointerstitial fibrosis, which could be dampened by blockade of β 1 integrin signaling [155; 160].

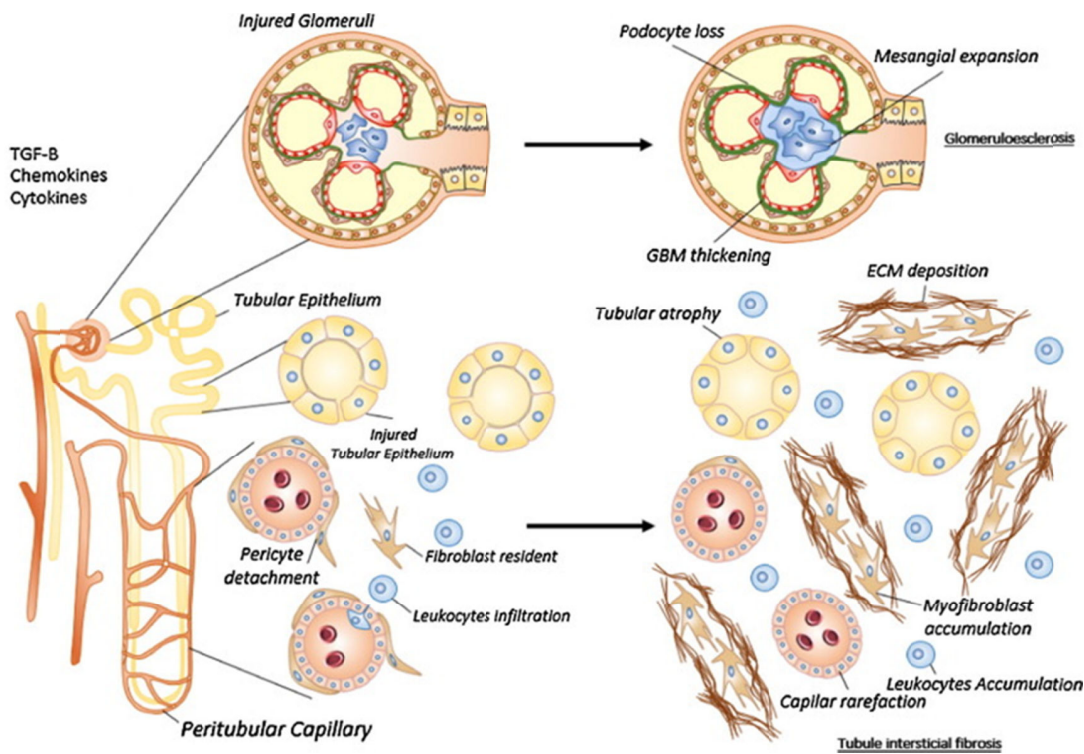


Fig. 5: Scheme of cellular events after AKI leading to maladaptive repair. Ischemia and reperfusion-mediated tissue injury leads to secretion of pro-inflammatory chemokines and cytokines including TGF- β promoting immune cell infiltration, resident fibroblast activation and pericyte detachment. Excessive pro-inflammatory stimuli contribute to podocyte loss, mesangial expansion, GBM thickening and tubular atrophy. Immune cells accumulate at the site of injury driving inflammation. Increased myofibroblast transformation leads to excessive extracellular matrix (EMC) deposition being a risk factor for CKD [modified; 155]. Reprinted from [155] with permission from Elsevier © 2016

In summary, prevention of excessive immune cell infiltration including reduction of pro-inflammatory stimuli as well as intervention in myofibroblast transformation provides an interesting target for treatment in patients suffering from MI or AKI to avoid or reduce progression to chronic diseases. A group of molecules known to be important mediators for the process of wound healing and modulation of immune responses during IRI consists of extracellular nucleotides and nucleosides, which are part of purinergic signaling [161]. In particular, adenosine is known to be an important modulator in this process mediating anti-inflammatory processes [162; 163]. The mechanism of adenosine in promoting healing processes in IRI is still poorly understood. The next chapter briefly introduces synthesis, breakdown, uptake and function of the purinergic mediators as well as ectoenzymes and relevant receptors.

3.5. Purinergic signaling

Within the cell, nucleotides (e.g., ATP, ADP, AMP and NAD) and nucleosides (e.g., adenosine) are building blocks of nucleic acid but also have central functions in cell metabolism and signal transduction [164]. During IRI nucleotides and nucleosides are involved in mediating inflammation as well as fibrosis through interactions with a variety of membrane channels, enzymes and receptors. Release of ATP and NAD occurs after cell lysis being either a passive process or controlled by active mechanisms (3.5.1). Extracellular nucleotides signal via P2 receptors mediating predominantly pro-inflammatory events (3.5.2) or become converted by ectoenzymes to adenosine (3.5.3), which in turn signals via P1 receptors (3.5.4). Additionally, adenosine becomes degraded or taken up again by cells (3.5.5).

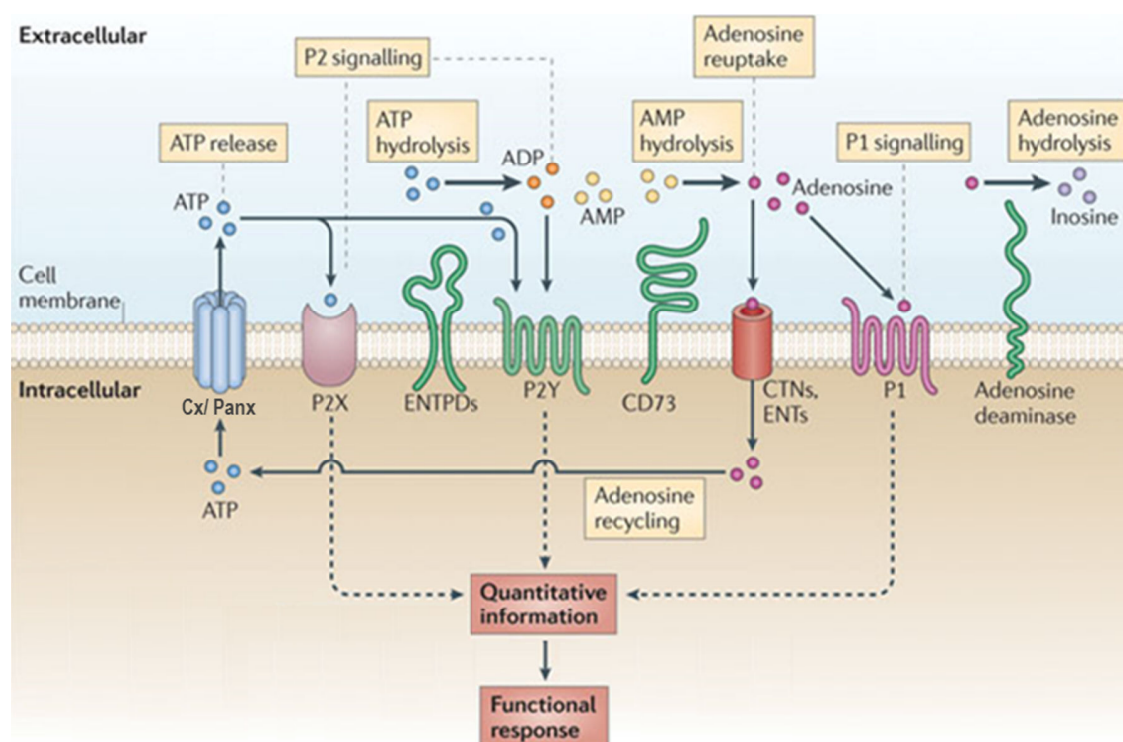


Fig. 6: Schematic overview of the purinergic signaling. ATP is released by connexin (Cx) or pannexin (Panx) channels into the extracellular space. Once released ATP signals via P2X receptors (P2 signalling) or becomes hydrolysed for example by ectonucleoside triphosphate diphosphohydrolases (ENTPDs) to ADP, which signals for example via P2Y receptors (P2 signalling), and further to AMP. In a second step AMP is degraded by CD73 to adenosine, which signals via its specific adenosine receptors (AdoR) (P1 signalling). Moreover, adenosine is taken up by concentrative nucleoside transporters (CNTs) and equilibrative nucleoside transporters (ENTs) or further hydrolyzed by adenosine deaminase (ADA) to inosine [modified; 165]. Reprinted from [165] with permission from Springer Nature © 2011.

3.5.1. Release of nucleotides

Intracellular ATP is needed for energy-requiring processes including active transport, cell motility and biosynthesis, whereas extracellular ATP is considered to be a powerful signaling molecule [166]. Under normal physiological conditions extracellular ATP and NAD concentrations are very low. In the plasma NAD concentrations range from 0.1 to 0.3 μM and are thereby 1000 fold lower compared to respective intracellular concentrations of $\sim 0.3 \text{ mM}$ [167–169]. Extracellular ATP concentrations are only about 1 – 10 nM, whereas respective intracellular concentrations are $\sim 1 – 10 \text{ mM}$ [1; 170–175]. Under basal conditions efflux of ATP out of the cell is rather low (about 20 – 200 $\text{fmol} \times \text{min}^{-1}$ per 10^6 cell) when measured *in vitro* [176]. In contrast to normal conditions, under pathological conditions, such as ischemia following by inflammation, high amounts of nucleotides are released into the extracellular microenvironment mediated by two processes. On the one hand necrotic cells release their entire cell contents due to loss of membrane integrity, while apoptotic or activated cells release nucleotides by controlled mechanisms [1; 13; 177]. Transport of nucleotides is regulated by connexin (Cx) or pannexin (Panx) hemichannels, and additional mechanisms are believed to be involved in this process, such as release by anion channels or vesicles [178–181]. A hemichannel consists of six connexin resp. pannexin subunits forming a central pore in the cell membrane [182; 183]. Depolarization of the membrane, changes in intra- and extracellular ion concentrations, mechanical stress and posttranslational modifications lead to opening of the channels and release of ions or small molecules of about 1 – 2 kDa in size [184]. ATP release is mediated by several Cx and Panx hemichannels, namely Cx26, Cx30, Cx36, Cx37, Cx43 and Panx1, whereas NAD is released only by Cx43 hemichannels [184; 185]. Activated immune cells, such as granulocytes and T cells, release ATP into the microenvironment via Panx1 or Cx43 hemichannels [178; 186]. Extracellular ATP concentrations are elevated by monocytes and macrophages via Cx37 [185].

3.5.2. Signaling via P2 receptors

In the extracellular space nucleotides signal via P2 receptors, which are expressed by nearly every cell population [171]. P2 receptors are divided into two subtypes, namely P2X (ligand-activated ion-channels) and P2Y receptors (G-protein coupled receptors) [187]. The seven P2X receptor subtypes, that are expressed in human and mouse (P2X₁ - P2X₇), are activated by ATP but have differing ligand binding affinities [188]. Binding of ATP results in changes of the receptor conformation leading to opening of an intrinsic pore and thereby to ion exchange; intracellular Ca²⁺ and Na⁺ concentrations increase and K⁺ is released from the cell [189; 190]. As a result the plasma membrane becomes

depolarized and increasing cytosolic Ca^{2+} concentrations lead to activation of several signaling cascades [191]. Immune cells predominantly express P2X₁, P2X₄, P2X₅ and P2X₇ receptor subtypes known to be important contributors to pro-inflammatory effects [16; 171]. For example, stimulation of the P2X₇ receptor on macrophages activates the formation of the inflammasome resulting in secretion of pro-inflammatory cytokines, such as IL-1 β and IL-18 [192; 193]. Moreover, activation of P2X₁, P2X₄, and P2X₇ receptors initiate the activation of T cells, whereas the P2X₁ receptor on neutrophils mediates chemotaxis [194–196].

For the P2Y receptors eight different subtypes have been identified in mammals (P2Y₁, P2Y₂, P2Y₄, P2Y₆, P2Y₁₁ - P2Y₁₄) and they are activated by diverse purine or pyrimidine nucleotides, such as ATP, ADP, ADP-ribose, UTP, UDP and NAD depending on the receptor subtype [191; 165; 197]. Stimulation of P2Y receptors leads to activation of a coupled heterodimeric G-protein, which disassociates its α -subunit and $\beta\gamma$ -complex resulting in initiation of intracellular signaling cascades; in different immune cell populations these signaling pathways predominantly mediate pro-inflammatory effects [191; 198]. For example, activation of the P2Y₆ receptor on macrophages initiates secretion of MCP-1, thereby recruiting immune cells to the site of injury [199; 200]. Moreover, macrophages express the P2Y₁ and P2Y₄ receptor subtypes, but the functional relevance of both receptors is still unclear [198]. Activation of the P2Y₁ receptor may be involved in increased phagocytic activity, whereas stimulation of the P2Y₄ receptor was associated with secretion of pro-inflammatory cytokines [201; 202]. P2Y₂ receptors contribute to directed chemotaxis of neutrophils [203].

3.5.3. Extracellular degradation of nucleotides by ectoenzymes

Extracellular nucleotides become degraded by membranous ectoenzymes. It is important to recognize that the distribution and activity of these enzymes control duration and intensity of P2 receptor-mediated signaling [204].

Nucleoside triphosphate diphosphohydrolases CD39

The family of nucleoside triphosphate diphosphohydrolases (NTPDases) consists of eight members (NTPDase1 – NTPDase8), that differ from each other in their preferences for catalytic hydrolysis of nucleoside tri- (ATP and UTP) or diphosphates (ADP and UDP) [205; 206]. NTPDases 1 – 3 and 8 are located on the cell surface, whereas NTPDases 4 – 7 share an intracellular organellar organization [207]. Moreover, NTPDases 5 and 6 can be secreted by cells [208; 209].

In contrast to other membranous NTPDases, NTPDase 1, also termed CD39, hydrolyses extracellular ATP directly to AMP without accumulation of the intermediate product ADP [205; 207]. Interestingly, membranous CD39 localization is closely related to P2Y receptors assuming that CD39 is an important regulator of P2Y receptor activity by degradation of the substrate ATP [210]. Several studies have underlined the importance of CD39 in modulating purinergic signaling transduction and co-ordination of immunoregulatory functions [211]. Lack of CD39 in diseases of chronic inflammation, such as chronic intestinal inflammation (colitis) or IRI in the liver, led to more pronounced inflammatory reaction compared to the disease response in wildtype mice [161; 212; 213].

Ectonucleotide pyrophosphatases/ phosphodiesterases

The ectonucleotide pyrophosphatase/ phosphodiesterase (ENPP) family consists of seven members (ENPP1 – ENPP7). ENPP1 – 3 are known to hydrolyze extracellular nucleotides [204]. ENPP1 (CD203a or PC-1) is positioned on the outside of the cell membrane and catalyzes 1) ATP to AMP and pyrophosphate or 2) ATP to ADP and phosphate depending on the binding position at the catalytic center of ATP [204; 214]. ENPP1 (CD203c), also localized on the cell surface, hydrolyzes ATP to AMP but with lower efficiency [204; 207]. In addition, breakdown of pyrophosphates or other phosphodiester bonds, such as in NAD and ADP-ribose, is also mediated by these ectoenzymes [215–218].

CD38 and CD157

Extracellular NAD can also be degraded by the multifunctional enzymes CD38 and CD157 (bone marrow stromal cell antigen-1 (BST-1)) [219]. On the one hand both enzymes function as ADP-ribosyl cyclases catalyzing NAD to cyclic ADP-ribose (cADPR), while on the other hand these enzymes can mediate hydrolysis of cADPR to ADP-ribose (ADPR) [219–221]. Beyond that, CD38 catalyzes metabolism of NAD directly to ADPR [219]. ADPR can be degraded by ENPPs or signal via P2Y₁ receptors [222]. In contrast, cADPR is internalized by cells and binds to calcium channels leading to Ca²⁺ release from the endoplasmic reticulum [223].

ADP-ribosyltransferases

ADP-ribosyltransferases (ART) are another class of ectoenzymes, that mediate NAD catalysis [219]. Four members of the ART family have been found in humans (ART1, ART3 – ART5), whereas six subtypes have been found in mice (ART1, ART2a, ART2b, ART3 – ART5) [224]. The two ART2-isoforms are expressed by different leukocyte populations mediating the ADP-ribosylation of the P2X₇ receptor, which initiates apoptosis of the cell [219; 225; 226].

3.5.4. CD73 – a key enzyme for generating extracellular adenosine

The degradation of both extracellular ATP and NAD to AMP is mediated by several ectoenzymes as described above leading to increased AMP levels in the microenvironment. In a second step AMP becomes dephosphorylated mainly by ecto-5'-nucleotidase (CD73) to adenosine [207; 227]. CD73 is a dimeric glycoprotein, that is attached via a glycosyl phosphatidylinositol (GPI)-linked anchor to the extracellular membrane [228; 229]. Each monomer consists of two different domains. The N-terminal domain binds two catalytic divalent metal ions, which are important for the catalytic activity of the enzyme. The C-terminal domain mediates substrate binding and provides the substrate specificity pocket for nucleotides [228; 230]. The substrate with highest affinity for CD73 is AMP (K_m value 1 – 50 μ M), but recently it has been shown that CD73 can convert NAD to adenosine [227; 231; 232]. CD73-mediated NAD hydrolysis is less efficient than AMP hydrolysis, which poses the question whether this pathway has any impact under physiological conditions [232]. Several studies have shown that CD73-dependent adenosine generation is an important mediator in regulation of inflammatory processes. Loss of CD73 in mice led to increased immune cell infiltration and more pronounced tissue damage in different disease models, such as acute lung injury, vascular lesion as well as intestinal IRI compared to wildtype mice [233–236].

Beside CD73, alkaline phosphatases (ALP) can degrade AMP to adenosine. In human and mouse four different subtypes for ALP have been found (ALP - liver/bone/kidney (ALPL), ALP - placental (ALPP), ALP - placental like 2 (ALPP2), ALP – intestinal (ALPI)), whereas the tissue nonspecific ALP (ALPL) showed the widest distribution within several tissues including liver, bones and kidneys [207]. In contrast to CD73, ALPs are less specific resulting in hydrolysis of a broad spectrum of other nucleotides including ATP, ADP and cAMP [204]. Moreover, the substrate affinity of ALPs for AMP is substantially lower compared to CD73 (K_m value 441 μ M) [237]. It was reported that in different organs, such as lung, liver and heart, of CD73 deficient mice extracellular adenosine levels are

significantly decreased suggesting a central role for CD73 in adenosine formation as compared to ALPs [233; 238].

3.5.5. Signaling via P1 receptors (adenosine receptors)

Adenosine signals via its specific adenosine receptors (AdoR), which are located on the outside of the cell surface, resulting in activation of intracellular signal transduction and thereby mediating multiple physiological and pathological processes of the cell [239]. AdoR are G-protein coupled receptors and are divided into four subtypes, namely A₁R, A_{2A}R, A_{2B}R and A₃R [240; 241].

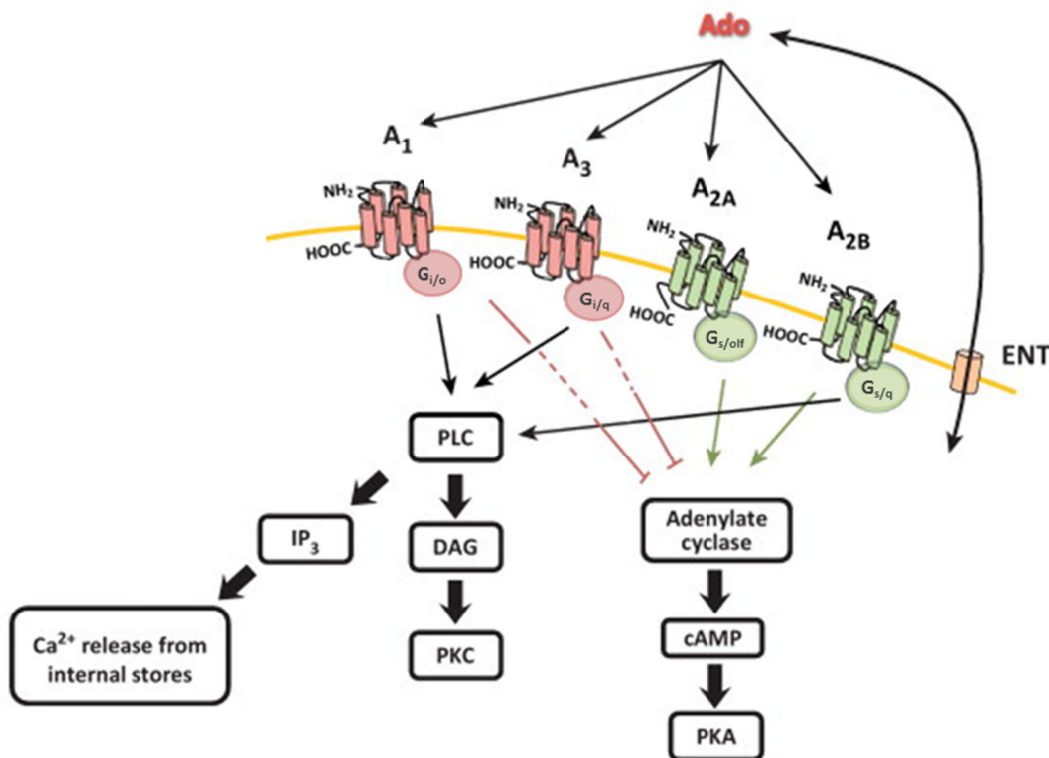


Fig. 7: Schematic overview of signaling via adenosine receptors. In the extracellular space adenosine signals via its specific adenosine receptors, namely A₁R, A_{2A}R, A_{2B}R and A₃R, which are coupled to different G-proteins (A₁R: G_{i/o}, A_{2A}R: G_{i/olf}, A_{2B}R: G_{s/q} and A₃R: G_{i/q}). Activation of A₁R, A_{2B}R and A₃R leads to 1) activation of phospholipase C (PLC), which increases inositol-trisphosphate (IP₃) levels thereby leading to Ca²⁺ release from internal stores or 2) signaling via diacylglycerol (DAG) to activate protein kinase C (PKC). Moreover, A_{2A}R and A_{2B}R signaling results in activation of adenylate cyclase and thereby in increase of intracellular cAMP levels activating protein kinase A (PKA), whereas A₁R and A₃R signaling mediates adenylate cyclase inhibition [modified; 242]. Reprinted from [242] with permission from Elsevier © 2013.

Adenosine A₁ receptor (A₁R)

The A₁R is the most conserved AdoR among different species with a broad expression pattern throughout the body and highest levels in the brain [243; 244]. The A₁R is coupled to a G_{i/o}-protein and its activation leads to inhibition of adenylyl cyclase activity mediating decreased intracellular cAMP concentrations. Moreover, binding by adenosine results in activation of phospholipase C (PLC), which increases intracellular calcium and inositol-trisphosphate (IP₃) levels leading to Ca²⁺ release from internal stores or signaling via diacylglycerol (DAG) to activate protein kinase C (PKC) [239; 245; 246]. In the heart, stimulation of A₁Rs mediates several changes in the cardiovascular system including negative chronotropic and dromotropic effects [162]. Related to the immune response, activation of the A₁R initiates neutrophil and macrophage chemotaxis and adhesion, tumor necrosis factor-alpha (TNF- α) secretion and ROS production [247]. Beside its pro-inflammatory effects, A₁R stimulation using a specific A₁R-agonist in the kidney led to decreased renal tubular necrosis, apoptosis and inflammatory response after IRI, while A₁R deficiency increased renal injury following IR [248; 249].

Adenosine A_{2A} receptor (A_{2A}R)

High levels of A_{2A}R expression were found in the striatum of the brain, immune cells of the spleen and thymus, leukocytes and blood platelets and intermediate levels could be detected in the heart, lung and blood vessels [240; 241]. Stimulation of A_{2A}Rs by adenosine results in activation of the cyclic AMP-protein kinase A (PKA) pathway associated with increased intracellular cAMP levels by coupling to G_s-protein in peripheral tissues or to G_{oif}-protein in the brain [243; 250; 251]. Similar to the A₁R, A_{2A}Rs play an important role in mediating the cardiovascular system resulting in vasodilatation after activation via adenosine [252; 253]. Moreover, it has been shown that A_{2A}R signaling has an important impact on mediating the inflammatory response, because of its expression on a broad range of different immune cells influencing predominantly anti-inflammatory effects [254]. Compared to A₁R stimulation A_{2A}R stimulation functions in opposing ways leading to reduced phagocytosis of neutrophils, production of ROS and endothelial adhesion [247; 255–257]. In addition, several studies have shown that A_{2A}R signaling inhibits expression of pro-inflammatory cytokines, such as IL-12, IFN- γ and TNF- α , in monocytes/ macrophages, dendritic cells and T cells [258–263] The production of the anti-inflammatory cytokine IL-10 was found to be increased in monocytes and macrophages after A_{2A}R activation [264; 265]. Based on these findings a protective role for the A_{2A}R was suggested, as shown by inhibition of inflammatory effects in several disease models [266]. For example, in the heart treatment with A_{2A}R-agonists resulted in decreased infarct size in different species [266–269].

Moreover, in the kidney $A_{2A}R$ stimulation reduces cytokine and chemokine expression in renal tubules cells and leukocytes, including macrophages, lymphocytes and neutrophils [270–272].

Adenosine $A_{2B}R$ receptor ($A_{2B}R$)

The $A_{2B}R$ is widely expressed among different tissues, but mostly in low abundance. In comparison to the other AdoRs ($EC_{50} = 0.3 - 0.7 \mu M$), the $A_{2B}R$ is the most adenosine-insensitive receptor requiring micromolar adenosine concentrations for activation ($EC_{50} = 24 \mu M$), which are rarely achieved under physiological conditions [239; 273]. Because of the high adenosine concentrations required for $A_{2B}R$ activation, the receptor is likely to become stimulated during conditions in which adenosine levels are elevated, such as hypoxia, ischemia or inflammation [239; 274]. $A_{2B}R$ s signals via G_s - or G_{12} -protein coupling leading to adenylate cyclase activation and increased cAMP level as well as in activation of phospholipase C (PLC) resulting in intracellular calcium increase. Several studies have demonstrated both pro- and anti-inflammatory effects for $A_{2B}R$ signaling [266; 275]. For example, in neutrophils and macrophages $A_{2B}R$ activation controls TNF- α secretion [275–277]. Furthermore, $A_{2B}R$ signaling increases production of the anti-inflammatory cytokine IL-10 and contributes to the activation of alternatively activated M2 macrophages [278; 279]. It has been suggested that the observed anti-inflammatory effects are mediated by G_s -mediated increase of intracellular cAMP levels similar to $A_{2A}R$ signaling [266]. In contrast, several studies have demonstrated $A_{2B}R$ contribution to pro-inflammatory effects. In mast cells activation of $A_{2B}R$ s led to secretion of the pro-inflammatory cytokine IL-8 [280]. Moreover, stimulation of the $A_{2B}R$ on an epithelial cell line resulted in increased IL-6 production [281]. Interestingly, in the heart contrary observations have been discussed. In a model of pre-conditioning $A_{2B}R$ expression was induced in cardiac tissue suggesting an important role for the $A_{2B}R$ in tissue remodeling. Treatment with an $A_{2B}R$ -agonist after MI was associated with reduced infarct sizes after ischemia [282]. In contrast, Toldo et al. could show that selective blockade of $A_{2B}R$ s reduces caspase-1 activity in cardiac tissue leading to a more favorable cardiac remodeling after MI in mice [283]. In the kidney $A_{2B}R$ signaling using a $A_{2B}R$ agonist was associated with renal protection after AKI including reduced renal tubular necrosis and inflammation by modulating the neutrophil TNF- α response [163].

Adenosine A₃ receptor (A₃R)

There is substantial variability in A₃R tissue distribution and functionality [239]. Whereas the other P1 receptors conserve high sequence homologies between different families of the mammalian class (86 – 93 %), the A₃R sequence varies highly among species (for example 74% between human and rat) [240]. Signal transduction of the A₃R involves G_i- or G_q-proteins resulting in inhibition of adenylate cyclase, stimulation of PLC and calcium mobilization [241; 284–286]. A₃R activation promoted both pro- and anti-inflammatory stimuli [266]. On the one hand A₃R signaling was associated with mast cell degranulation in mice and stimulated secretion of the inflammatory mediator histamine [287]. On the other hand it was shown that stimulation of A₃Rs on human and murine macrophage cell lines led to inhibition of the lipopolysaccharide (LPS)-associated production of pro-inflammatory cytokines, such as TNF- α [288; 289].

3.5.6. Adenosine degradation and internalization

In the extracellular space, adenosine is degraded to inosine via adenosine deaminase (ADA) [204]. Two isoforms of ADA have been found in humans, namely ADA1 (ADA) and ADA2 (CERC1) [290; 291]. Both enzymes are located in the cytosol, whereas ADA was also found as ectoenzyme on the surface of different cell populations [292]. After deamination, inosine is degraded via the purine-nucleoside-phosphorylase (PNP) to hypoxanthine [204]. PNPs are predominantly localized in the cytoplasm, but are also located on the cell surface [166].

Alternatively, extracellular adenosine can be internalized by nucleoside transporters. Depending on the transport mechanism, nucleoside transporters are grouped into two families including concentrative nucleoside transporters (CNTs) and equilibrative nucleoside transporters (ENTs). In humans three subtypes of CNTs have been found (CNT1 – CNT3), whereas for ENTs four transporters are known (ENT1 – ENT4). CNTs (SLC28) are cation-dependent and internalize nucleosides by coupling transport to the inwardly directed gradient of Na⁺ ions. In contrast, bidirectional transport via ENTs (SLC29) is cation-independent mediating diffusion along the existing concentration gradient [293; 294]. CNT2 is a specific transporter for purines showing a wide-ranging distribution in different tissue including macrophages [295; 296]. ENT1 as well as ENT2 are important mediators for transport of a broad spectrum of purines and pyrimidines, but also of hypoxanthine [294; 297]. Both transporters are important modulators of the extracellular adenosine concentration. Deficiency of ENT1 or ENT2 resulted in increased adenosine levels in plasma and in the bronchoalveolar fluid compared to wildtype mice [298; 299].

Within the cell, incorporated adenosine becomes mainly phosphorylated by adenosine kinases (ADK) to AMP [300]. Subsequently, AMP is converted to higher phosphorylated forms (salvage pathway) by a variety of enzymes serving energy metabolism [301; 302]. Because of the high affinity of ADK (Km value $\sim 2 \mu\text{M}$), there is an efficient recycling of adenosine into the cellular nucleotide pool, so that under physiological condition the flux of adenosine is from extracellular to intracellular. The activity of ADK also assures that intracellular adenosine concentration is normally very low [303; 304]. Under pathological conditions, however, the flux becomes reversed and involves hypoxia-mediated inhibition of ADK [303; 305].

3.6. Aims of the study

The development of novel therapeutic strategies for better prevention or treatment of myocardial infarction (MI) and acute kidney injury (AKI) depend upon a critical understanding of the cellular and molecular mechanisms, which occur after injury and contribute to the formation of fibrosis known to be associated with chronic organ diseases.

Previous studies in the laboratory of Prof. Schrader (Institute of Molecular Cardiology, Düsseldorf, Germany) have underlined the importance of the purinergic signaling in cardiac remodeling after MI. It was shown that CD73 on T cells modulates healing processes of the heart and that lack of CD73 on T cells resulted in impaired cardiac function due to adverse ventricular remodeling comparable to mice globally lacking CD73, but the molecular mechanism how T cells contribute to cardiac remodeling remained still unclear [306–308]. The aim in the first part of this thesis was to study in detail the role of T cells in orchestrating wound healing after MI as well as to investigate the impact of the purinergic signaling not only in acute injury but also in chronic cardiac inflammation. The following leading questions were addressed in this thesis:

- Establishment of a robust cell culture model for T cells to mimic T cell activation after MI
- Functional analysis of the metabolic reprogramming of activated T cells
- Investigation into the role of CD73 on T cells in regulating cytokine secretion after activation
- Examination of the transferability of *in vitro* observations to the whole organ complex
- Identification of AdoRs being involved in controlling T cell function after IRI
- Functional analysis of AdoR stimulation on activated T cells
- Study of the role of the purinergic signaling in a model of myocarditis

The second part of this thesis focuses on AKI. Previous studies of the US host institution in Charlottesville have shown that the major renal CD73-expressing cell populations within the kidney are proximal straight tubules, cortical interstitial fibroblast-like cells and mesangial cells. Lack of CD73 on tubular cells led to impaired renal function after AKI associated with severe proximal tubule injury in the outer medulla and extensive leukocyte infiltration 24h after IRI [309]. Since these observations clearly demonstrated the contribution of CD73 on tubular cells in initial mechanisms, the role of CD73 in orchestrating tissue recovery during healing processes was not examined. Moreover, the impact of CD73 on fibroblasts/ pericytes was fully unknown. I therefore have focused on the role of CD73 on fibroblasts/ pericytes and on tubular cells after AKI in the laboratory of Prof. Okusa (Division of Nephrology, Center for Immunity, Inflammation, and Regenerative Medicine, Department of Medicine, University of Virginia, Charlottesville) using tissue specific mouse mutants. The following questions were addressed:

- Investigation of the role of CD73 on fibroblasts/ pericytes after AKI in
 - Modulating kidney function
 - Controlling matrix deposition and fibrosis formation
 - Influencing myofibroblast transformation
 - Resolution of inflammation and immune cell infiltration
- Establishment of renal fibroblast cell culture to study the role of CD73 on cell proliferation
- Analysis of kidney recovery after reconstitution of CD73 enzymatic activity
- Examination of the role of CD73 on tubular cells after AKI in
 - Modifying kidney function
 - Regulating collagen formation
- Analysis of contribution of CD73 on fibroblasts/ pericytes and tubular cells in initial injury and tissue healing processes

4. Material

4.1. Laboratory equipment

Device	Manufacturer and Type
Analysis scales	Ohaus Europe, PA214
Autoclave machine	F. & M. Lautenschläger, 5169
Bio-Plex Multiplex System	Bio-Rad Laboratories, Bio-Plex 200
Bio-Plex Wash Station	Bio-Rad Laboratories, Pro II Waschstation
Cell Counter	Nexcelom Cellometer Vision
Cell Sorter	Beckman Coulter, MoFlo XDP
Centrifuge	Beckman Coulter, Allegra X-30R Eppendorf, 5415R and 5424R Thermo Scientific, Heraeus Megafuge 16R Beckman, GS-6
Cryostat	Leica, CM1850 UV
Flow Cytometer	BD Biosciences, FACSCanto II
Heat Block	Eppendorf, Thermomixer compact
Incubator	Thermo Fisher Scientific, Heracell 150 i
Langendorff equipment	manufactured at the University of Düsseldorf Data recording: ADInstruments, Powerlab/16SP Pump: Abimed, Minipuls 3
Magnetic stirrer	MP Biomedicals, FastPrep-24
Nano-Drop	Thermo Fisher Scientific, NanoDrop 2000
PCR System	Eppendorf, Mastercycler ep Gradient S
pH Meter	Knick, 766 Calimatic
Pipettes	Eppendorf, Research Gilson, Pipetman
Plate reader	BMG Labtech, FLUOstar Optima
Real Time PCR System	Applied Biosystems, StepOne Plus Real-Time PCR Detection System Bio-Rad, CFX Manager
Shaker	IKA Werke, MTS 2/4

4. Material

Sterile bench	Scanlaf, Mars Pro Cytosafe Class 2 Thermo HERAcell, Vios 160i
Vacuum pump	HLC, AC 04
Vortex Mixer	VWR International
Water Bath	Memmert
Water purification system	Miipore (Milli-Q plus)

Tab. 1: Laboratory equipment

4.2. Chemicals and enzymes

All chemicals were analytically pure purchased from the companies AppliChem, Merck, Carl Roth GmbH and Sigma-Aldrich, if not stated otherwisly in the text.

4.3. Cell culture material, medium, buffer and substances

All expendable material used for cell culture were ordered from Corning, Falcon, Greiner Bio-One and TPP. Medium, buffer and additional cell culture substances were purchased from Gibco.

RPMI-1640

For T cell culture RPMI-1640 was used.

5 ml Minimum essential media (1%)
5 ml Sodium pyruvate (1%)
5 ml GlutaMAX (1%)
50 ml FCS (10 %)
5 ml Penicillin/ Streptomycin (1 %)
0.05 mM β - mercaptoethanol
up to 500 ml RPMI

Dulbecco's Modified Eagle's Medium (DMEM)

For fibroblast cell culture DMEM containing phenol red was used.
For MTT assay analysis DMEM without phenol red was required.

1000 mg/l D-glucose
110mg/l sodium pyruvate
2 mM L-glutamine
50 ml Fetal bovine serum (FBS) (10%)
5 ml Penicillin/ Streptomycin (1%)
5 ml Amphotericin B (1%)
up to 500 ml DMEM

4.4. Buffer and solutions

Langendorff experiments

Wash buffer (pH 7.4)

4 mM NaHCO₃
10 mM HEPES
30 mM 2,3-butanedion-monoxime
11 mM Glucose
0.3 mM EGTA
6.6 mM NaCl
0.22 mM KCl
0.1 mM MgCl₂ x H₂O
Oxygenated wit carbogen (95% O₂ and 5% CO₂)

Bovine serum albumin (BSA) buffer

4 mM NaHCO₃
10 mM HEPES
30 mM 2,3-butanedion-monoxime
11 mM Glucose
0.3 mM EGTA
6.6 mM NaCl
0.22 mM KCl
0.1 mM MgCl₂ x H₂O
2% BSA

HPLC analysis

Buffer A

150 mM potassium dihydrogen orthophosphate
150 mM KCl (pH 6)

Buffer B

15% acetonitrile in buffer A

Flow cytometry analysis

Magnetic-activated cell sorting (MACS) buffer (pH 7.4)

5 mM Ethylenediaminetetraacetic acid (EDTA)
0.5% BSA
in 1% Phosphate-buffered saline (PBS)

Cell proliferation assay

12 mM MTT stock solution

5 mg vial of MTT (Component A)
in 1 ml sterile 1x PBS

Hydroxyproline assay

Chloramine-T solution

1 ml Chloramine-T
4 ml Citrate-Acetate buffer (pH 6.0)

Ehrlich's solution

1 ml Ehrlich's solution
4.3ml Isopropanol

Immunohistochemistry

Blocking solution

0.3 % Triton x-100 solution

0.02 % NaN₃

10 % serum solution (horse/ chicken/ donkey)

in 2.4G2 solution (anti-CD16/ anti-CD32)

4.5. Antibodies

Specificity	Fluorochrome	Clone	Origin	Company
CD3	APC	145-2C11	Hamster	BioLegend Miltenyi Biotec
CD4	PerCP-Cy5.5	RM4-5	Rat	eBiosciences
CD8a	APC-H7	53-6.7	Rat	BD Biosciences
CD11b	FITC	HL3	Hamster	BD Pharmigen
CD11c	PE-Cy7	N418	Hamster	eBiosciences
CD45	PE	30-F11	Rat	BD Biosciences Miltenyi Biotec
CD45R (B220)	APC- eFluor780	RA3-6B2	Rat	eBiosciences
CD69	FITC	H1-2F3	Hamster	BioLegend

Tab. 2: Antibodies for flow cytometry analysis.

4.6. TaqMan assays

Assay-ID	Gene	Gene symbol
Mm00607939_s1	β -actin	<i>Atcb</i>
Mm01308023_m1	Adenosine A ₁ receptor	<i>Adora1</i>
Mm00802075_m1	Adenosine A _{2A} receptor	<i>Adora2a</i>
Mm00839292_m1	Adenosine A _{2B} receptor	<i>Adora2b</i>
Mm01296602_m1	Adenosine A ₃ receptor	<i>Adora3</i>
Mm00446971_m1	TATA-binding protein	<i>Tbp</i>

Tab. 3: TaqMan gene expression assays used for qPCR analysis.

4.7. Gene-specific primers

Gene	Sequence
Arg1_fwd	CAGAAGAATGGAAGAGTCAG
Arg1_rev	CAGATATGCAGGGAGTCACC
Il1b_fwd	AATGACCTGTTCTTTGAAGTTGAC
Il1b_rev	GTGATACTGCCTGCCTGAAG
Mrc1_fwd	CTCTGTTTCAGCTATTGGACGC
Mrc1_rev	CGGAATTTCTGGGATTCAGCTTC
Msr1_fwd	CCAGCAATGACAAAAGAGATGACA
Msr1_rev	CTGAAGGGAGGGGCCATTTT
iNOS(Nos2)_fwd	TCTAGTGAAGCAAAGCCCAACA
iNOS(Nos2)_rev	CCTCACATACTGTGGACGGG
Tnf_fwd	CCCTCACACTCAGATCATCTTCT
Tnf_rev	GCTACGACGTGGGCTACAG
Ym1 (Chil3)_fwd	TGTGGAGAAAGACATTCCAAGG
Ym1 (Chil3)_rev	AAGAGACTGAGACAGTTCAGGG

Tab. 4: Gene-specific primers used for qPCR analysis.

5. Methods

5.1. Mouse models

5.1.1. Mouse studies in the heart including *ex vivo* T cell culture

All animal experiments were performed in accordance with the national guidelines for animal care and were approved by the Landesamt für Natur-, Umwelt- und Verbraucherschutz (LANUV). Animals were housed at 20 – 22 °C room temperature and a 12h light-dark-cycle and fed with a standard chow diet receiving tap water *ad libitum*.

For *ex vivo* T cell cultivation and stimulation female, wildtype C57BL/6J mice (12 weeks of age) were used, which were purchased from Janvier (Saint Berthevin, France).

T cell specific CD73^{-/-} mice (CD4^{Cre/+}/CD73^{fl/fl})

For generation of T cell specific CD73^{-/-} mice (CD4^{Cre/+}/CD73^{fl/fl}), homozygous mice for the CD73 allele floxed in exon 2 (CD73^{fl/fl}) [238] were crossed with mice expressing Cre recombinase under the control of the CD4 promoter (CD4^{Cre/+}) [310; 311]. CD4^{Cre/+} mice were kindly provided by Dr. Jochen Hühn (Experimental Immunology, Helmholtz Centre for Infection Research, Braunschweig, Germany). CD4^{Cre/+}/CD73^{fl/+} progeny of the F1 generation were intercrossed with each other to obtain CD4^{Cre/+}/CD73^{fl/fl} mice. CD4^{Cre/+}/CD73^{fl/fl} mice of the F2 generation were then crossed with CD73^{fl/fl} mice to generate CD4^{Cre/+}/CD73^{fl/fl} and CD73^{fl/fl} control littermates. Female T cell specific CD73^{-/-} (CD4^{Cre/+}/CD73^{fl/fl}) mice (9 – 13 weeks of age) used in this study for *ex vivo* T cell cultivation were bred at the Tierversuchsanlage of the Heinrich-Heine-University (Düsseldorf, Germany). For controls female, wildtype C57BL/6J mice (12 weeks of age) were used, which were purchased from Janvier (Saint Berthevin, France).

CD39^{-/-} mice

In this study female CD39^{-/-} mice (9 – 13 weeks of age) and wildtype littermate controls of the same gender and age were used for *ex vivo* T cell cultivation. CD39^{-/-} mice and wildtype littermate controls were kindly provided by Dr. Verena Jendrossek (Institute for Cell Biology, University Duisburg-Essen, Germany) [312; 313].

Myocarditis mice

Myocarditis mice were kindly provided by Prof. Z. Kaya (Cardiology, Angiology and Pneumology, University Medical Center Heidelberg, Germany). Myocarditis in mice was induced by subcutaneous injection of murine cardiac troponin I (cTnI) solved in Complete Freund's Adjuvant for 3 times (immunization on day 1, 7 and 14) [314]. For immunization female, wildtype A/J mice (6 weeks of age) were used and analysis was done 21d after immunization. For controls A/J mice of the same gender and age were used treated with Complete Freund's Adjuvant only.

5.1.2. Mouse studies in the kidney including *ex vivo* fibroblast culture

All animal experiments were performed in accordance with the National Institutes of Health (NIH) Guide for the Care and Use of Laboratory Animals and all procedures were approved by the University of Virginia, Animal Care and Use Committee. Animals were housed at 20 – 22 °C room temperature and a 12h light-dark-cycle and fed with a standard chow diet receiving tap water *ad libitum*.

Fibroblast/ pericyte specific CD73^{-/-} mice (Foxd1^{Cre/+}/CD73^{fl/fl})

For generation of a fibroblast/ pericyte specific CD73^{-/-} mice (Foxd1^{Cre/+}/CD73^{fl/fl}), CD73^{fl/fl} mice [238] were crossed with mice expressing Cre recombinase under the control of the Foxd1 promoter (Foxd1^{Cre/+}), which already has been described [315]. Foxd1^{Cre/+}/CD73^{fl/+} progeny of the F1 generation were intercrossed with each other to obtain F2 generation Foxd1^{Cre/+}/CD73^{fl/fl} mice, which were then crossed with CD73^{fl/fl} mice to generate Foxd1^{Cre/+}/CD73^{fl/fl} and CD73^{fl/fl} control littermates. In this study, male fibroblast/ pericyte specific CD73^{-/-} mice (Foxd1^{Cre/+}/CD73^{fl/fl}) (12 – 15 weeks of age) and CD73^{fl/fl} control littermates of the same gender and age were used, which were bred at the vivarium of the University of Virginia (Charlottesville, USA).

Tubular cell specific CD73^{-/-} mice (Pepck^{Cre/+}/CD73^{fl/fl})

CD73^{fl/fl} mice [238] were crossed with mice expressing Cre recombinase under the control of the Pepck promoter (Pepck^{Cre/+}) [316] to generate tubular cell specific CD73^{-/-} mice (Pepck^{Cre/+}/CD73^{fl/fl}). Pepck^{Cre/+} mice were kindly provided by Volker Haase (Department of Medicine, Vanderbilt University School of Medicine, Nashville, USA) and backcrossed into C57BL/6NCr for nine

generations. The ninth generation was then crossed with CD73^{fl/fl} mice to generate Pepck^{Cre/+}/CD73^{fl/+}. Pepck^{Cre/+}/CD73^{fl/+} progeny of the F1 generation were intercrossed with each other to obtain F2 generation Pepck^{Cre/+}/CD73^{fl/fl} mice, which were then crossed with CD73^{fl/fl} mice to generate Pepck^{Cre/+}/CD73^{fl/fl} and Pepck^{Cre/+} control littermates. In this study, male tubular cell specific CD73^{-/-} mice (Pepck^{Cre/+}/CD73^{fl/fl}) (12 – 15 weeks of age) and Pepck^{Cre/+} control littermates of the same gender and age were used, which were bred at the vivarium of the University of Virginia (Charlottesville, USA).

CD73^{-/-} mice

For *ex vivo* fibroblast cell culture male global CD73^{-/-} mice (8 – 12 weeks of age) and wildtype C57Bl/6 mice of the same gender and age were used. CD73^{-/-} mice, provided by the National Cancer Institute (USA), and wildtype C57Bl/6 mice, purchased from Jackson Laboratory (Maine, USA), were bred at the vivarium of the University of Virginia (Charlottesville, USA).

5.2. *In vivo* methods

5.2.1. Myocardial infarction in mice

To study the role of cardiac infiltrating T cells in wound healing and organ remodeling after MI, mice were subjected to LAD ligation for induction of ischemia. Surgery was performed by Dr. Zhaoping Ding (Institute of Molecular Cardiology, Düsseldorf, Germany) as described in the following passage. Mice were intubated and anesthetized by mechanical ventilation with isoflurane (1.5%) at a rate of 150 strokes/min and a body weight adapted tidal volume ranging between 225 – 275 μ l. Mice were placed in a supine position on a thermostatic station maintained at a temperature of 37 °C and the chest wall was shaved followed by disinfection using betaisodona. Electrocardiogram (ECG) needles were inserted subcutaneously representing lead II to measure ST-segment elevations during MI surgery, which was performed under an upright dissecting microscope (Leica MS05). After skin incision from the *Processus xiphoideus* to the left armpit, ribs were exposed by blunt preparation of the muscles and the chest was opened by a small lateral incision along the left side of the sternum. Subsequently, the pericardium was gently dissected to allow visualization of coronary artery anatomy. The LAD was ligated using an 8-0 polypropylene suture with a tapered needle passed underneath the vessel 2 mm from the tip of the left auricle. The suture was threaded through a small plastic tube (PE-10 tubing) with blunt ends and two small weights (~1 g) were attached to each end. LAD was occluded by free

hanging of the weights for 50 min. Successfully induction of MI was verified microscopically by paling of the myocardium as well as significant elevations of the ST-segment. After 50 min LAD occlusion was terminated by removal of the weights and reperfusion was controlled by the reddening of the previous pale myocardium and termination of ST-elevation. The chest and skin incisions were closed using a suture and disinfected via betaisodona. For postoperative analgesic mice received buprenorphine (0.15 mg/kg). Mice were kept under animal housing conditions as described before for 3d or 7d.

5.2.2. Acute kidney injury in mice

To study the outcome of AKI depending on CD73 activity, mice were subjected to renal IRI. Surgery was performed by Liping Huang (Division of Nephrology, Center for Immunity, Inflammation, and Regenerative Medicine, Department of Medicine, University of Virginia, Charlottesville) as described in the following passage. Before surgery mice were anesthetized using ketamine (120 mg/kg) and xylazine (12 mg/kg) administered via i.p. injection and the hair was shaved on the side of surgery followed by disinfection using betaisodona. For maintenance of body temperature mice were warmed via a warming pad adjusted at a temperature of 37 °C. Mice were placed on the thermostatic station laying on the left side and unilateral IRI was performed through flank incisions on the right side positioned at 1/3 of the body from the back of the mouse. Then the right kidney was identified and dissected free of the surrounding tissue and renal pedicels (artery and vein) were clamped for 20 min using micro-aneurysm clips. After 20 min clips were removed and the incision sides were sutured after restoration of blood flow, which was visually controlled. For postoperative analgesic mice received buprenorphine (0.15 mg/kg). Mice were kept under animal housing conditions as described before for 14d. To assess kidney function of the injured kidney by measurement of creatinine levels, uninjured left kidneys were removed on day 13. To this end, mice were anesthetized again using ketamine (120 mg/kg) and xylazine (12 mg/kg) administered via i.p. injection and warmed via a warming pad during surgery. Mice were placed on the thermostatic station laying on the right side and nephrectomy was performed through flank incisions of the left side. Kidneys were identified and dissected free of the surrounding tissue and pushed out from the cut to expose the renal pedicles. Renal pedicels were ligated using a suture and kidneys were removed. After Nephrectomy incision sides were closed and mice received postoperative analgesic using buprenorphine (0.15 mg/kg). Uninjured kidneys were collected as controls and treated as described in the following chapters. Finally, mice were euthanized 24h after nephrectomy and injured kidneys were collected as well as blood samples for plasma creatinine analysis.

For drug administration, mini-pumps (micro-osmotic pump Model 1002 - pumping rate: 0.25 $\mu\text{l/hr}$ ($\pm 0.05 \mu\text{l/hr}$); duration: 14d; reservoir volume: 100 μl ($\pm 10 \mu\text{l}$)) purchased from Alzet were used. Mice underwent 20 min unilateral IRI as described before and treatment by administration of 5 U 5'NT per day was started on day 2 resp. day 4. Mini-pumps were prepared 1h before surgery. Therefore mini-pumps were filled either with 5'NT solved in 1x PBS or with 1x PBS only for controls and pre-incubated in sterile saline at 37°C 1h before implantation. Mice were anesthetized again using ketamine (120 mg/kg) and xylazine (12 mg/kg) administrated via i.p. injection and warmed via a warming pad during surgery. A small incision was made in the skin between the scapulae and a small pocket was formed by spreading the subcutaneous connective tissues apart. The pump was inserted into the pocket and the skin incision was closed via sutures. Mice received postoperative analgesic using buprenorphine (0.15 mg/kg) and were kept under animal housing conditions as described before for another 12d resp. 10d. For analysis of kidney function nephrectomy of the uninjured kidney was performed on day 13 as described before and mice were euthanized on day 14 for collection of blood samples and injured kidneys.

To assess initial injury, 20 min unilateral IRI of the right kidney and nephrectomy of the left kidney was performed on the same day as described before. Mice received postoperative analgesic using buprenorphine (0.15 mg/kg) and were euthanized after 24h. Blood samples as well as uninjured and injured kidneys were collected.

5.2.3. Measurement of body and kidney weight

To analyze kidney weight of uninjured and injured kidneys, mice were weighed before nephrectomy or euthanasia. Therefore, a single mouse was removed from the cage, put in a container placed on a scale and the body weight was measured. Mice were anesthetized and kidneys were removed as described before (5.2.2). Isolated kidneys were placed on a small dish and the weight was measured. To exclude size differences of kidneys between mice, a ratio of body to kidney weight was calculated.

5.3. *In vitro* methods

5.3.1. Isolation of cells from different tissues

Since the number of cells, which can be isolated from the heart, is too small for functional studies T cells (CD8^+ and/ or CD4^+ T cells) were isolated from lymph nodes and stimulated *in vitro* to mimic

immune cell activation after IRI (5.3.1.1). Lymphoid T cells were used to study nucleotide metabolism after activation as well as cytokine secretion after AdoR stimulation. To analyze the cytokine profile and expression pattern of cardiac infiltrating T cells, cells were isolated from the heart after MI (5.3.1.2). For characterization of fibroblasts, cells were isolated from kidneys as described in the passage 5.3.1.3.

5.3.1.1. Lymphoid T cell isolation

Mice were euthanized and disinfected using ethanol. Superficial cervical, axillary, brachial, inguinal, lumbar and mesenteric lymph nodes were isolated and transferred to a 70 µm filter fitted into a well of a 6-well plate. Each well of the plate was filled with 3 ml 1x PBS (4 °C) placed on ice. Lymph nodes were mashed using the head of a syringe plunger. The filter was then placed into a 50 ml tube and the cell solution of the well was passed through the filter followed by washing of the filter with 5 ml 1x PBS (4 °C). The cell suspension was centrifuged for 10 min at 300x g and 4 °C. The supernatant was discarded and the pellet was solved in a staining solution prepared for flow cytometry separation of CD8⁺ and/ or CD4⁺ T cells. For cell staining the following panel was used.

Cell subpopulation	Antibody				
CD4 ⁺ and CD8 ⁺ T cells	CD45 PE	CD3 APC	CD4 PerCP5.5	CD8 APC-H7	CD11b FITC

Tab. 5: Antibody labeling of CD4⁺ and CD8⁺ T cells

To prepare the staining solution, 1 µl of each antibody was mixed with 95 µl MACS buffer (4 °C). Each sample was then solved in 100 µl staining solution followed by incubation for 30 min at 4 °C. After incubation cells were washed with 5 ml MACS buffer (4 °C) and transferred through a 30 µm filter fitted into a 10 ml tube. After centrifugation for 10 min at 300x g and 4 °C the supernatant was discarded and the cell pellet was solved in 500 µl MACS buffer (4 °C). To separate dead cells from living cells, 0.1 µg/ml DAPI was added to the cell solution 5 min before cell sorting. Flow cytometry separation was performed by the MoFlo XDP flow cytometer (Beckman - Coulter, Brea CA) at the Core Flow Cytometry Facility in the Institute for Transplantation Diagnostics and Cell Therapeutics (Düsseldorf, Germany) with the help of Katharina Raba. CD4⁺ T cells (CD45⁺, CD3⁺, CD4⁺, CD8⁻, CD11b⁻ and DAPI) and CD8⁺ T cells (CD45⁺, CD3⁺, CD4⁻, CD8⁺, CD11b⁻ and DAPI) were identified and collected to study the role of T cells in nucleotide metabolism (5.3.3.1). CD4⁺ T cell (CD45⁺,

CD3⁺, CD4⁺, CD8⁻, CD11b⁻ and DAPI⁻) alone were collected for functional studies of AdoR signaling (5.3.5).

5.3.1.2. Cardiac T cell isolation

For characterization, infiltrating cardiac T cells were isolated from the infarcted heart by tissue digestion using retrograde perfusion according to the Langendorff procedure [317]. The technique for immune cell isolation is based on the isolation protocol for intact cardiomyocytes and was modified by Bönner and Borg et al. [306; 307; 318; 319]. Mice were anesthetized using pentobarbital (1 mg/kg of body weight) and anticoagulation was inhibited using heparin (100 IE). Hearts were rapidly removed from the thorax and prepared in pre-cooled wash buffer (4 °C) for Langendorff perfusion. Aortas were cannulated and perfused for 5 min with pre-warmed oxygenated wash buffer (37 °C) at a perfusion pressure of 80 mmHg. For tissue digestion collagenase was added to wash puffer (1.32 PZ U/ml (NB 8 Broad Range collagenase, SERVA Electrophoresis GmbH, Germany)) and hearts were perfused for approx. 30 min with pre-warmed oxygenated collagenase solution (37 °C). Tissue digestion was terminated when perfusion pressure decreased to approx. 10 mmHg. After removal of non-ventricular components, heart tissue was transferred into a well of a 6 well plate containing 2 ml 2% bovine serum albumin (BSA) buffer and mechanically chopped using a scalpel. The cell suspension as well as remaining tissue chunks were transferred to a 50 ml tube and suspended in 20 ml 2% bovine serum albumin (BSA) buffer. Heart tissue was gently resuspended by sequent series of several pipetting steps (20x 25 ml pipette - 20x 10 ml pipette - 20x 5 ml pipette). Afterwards, the cell suspension was filtered through a 100 µm cell strainer and centrifuged for 1 min at 55x g and 4 °C to separate cardiomyocytes from non-cardiomyocytes. The supernatant containing the non-cardiomyocyte fraction was passed through a 40 µm cell strainer and centrifuged for 10 min at 300x g and 4 °C. The supernatant was discarded and the pellet was resuspended in 5 ml MACS buffer followed by a second filtration step using a 30 µm cell strainer and centrifugation of the cell suspension for 10 min at 300x g and 4 °C. The pellet was resuspended in 250 µl MACS buffer and 50 µl FcR Blocking Reagent (Miltenyi Biotech) followed by 10 min incubation on ice. Next, a staining solution was prepared for flow cytometry separation of CD3⁺ T cells only or CD4⁺ and CD8⁺ T cells for functional studies or gene expression analysis. For cell staining the following panel was used.

Cell subpopulation	Antibody				
CD3 ⁺ T cells	CD45 PE	CD3 APC	CD11c PE-Cy7		CD11b FITC
CD4 ⁺ and CD8 ⁺ T cells	CD45 PE	CD3 APC		CD4 PerCP5.5	CD8 APC-H7 CD11b FITC

Tab. 6: Antibody labeling of CD3⁺, CD4⁺ and CD8⁺ T cells

To prepare the staining solution, 5 µl of each antibody was added to the sample followed by incubation for 30 min at 4 °C. After incubation cells were washed with 5 ml MACS buffer (4 °C) and transferred through a 30 µm filter fitted into a 10 ml tube. After centrifugation for 10 min at 300x g and 4 °C the supernatant was discarded and the cell pellet was solved in 500 µl MACS buffer (4 °C). To separate dead cells from living cells, 0.1 µg/ml DAPI was added to the cell solution 5 min before cell sorting. Flow cytometry separation was performed by the MoFlo XDP flow cytometer (Beckman - Coulter, Brea CA) at the Core Flow Cytometry Facility in the Institute for Transplantation Diagnostics and Cell Therapeutics (Düsseldorf, Germany) with the help of Katharina Raba. CD3⁺ T cells (CD45⁺, CD3⁺, CD11b⁻, CD11c⁻ and DAPI⁻) were identified and collected to study the role of T cells in nucleotide metabolism (5.3.3.2) and cytokine secretion (5.3.4). CD4⁺ T cells (CD45⁺, CD3⁺, CD4⁺, CD8⁻, CD11b⁻ and DAPI⁻) and CD8⁺ T cell (CD45⁺, CD3⁺, CD4⁻, CD8⁺, CD11b⁻ and DAPI⁻) were collected for gene expression studies of AdoR signaling (5.4.1.1).

5.3.1.3. Renal fibroblast isolation

For fibroblast characterization, cells were isolated from kidneys according to the procedure established by Dr. Amandeep Bajwa (University of Virginia, Charlottesville, USA), which were used in the study of Kharel et al. [320]. The procedure was modified in some steps as described in the following passage. After euthanasia of mice kidneys were rapidly removed and place into a 100 mm dish containing 10 ml 1x PBS. Capsules of kidneys were removed and the tissue was chopped using a scalpel. The cell solution containing tissue pieces was passed via a 40 µm filter fitted in a 50 ml tube. Tissue pieces were mashed using the head of a syringe plunger followed by rinsing of the filter with 5 ml 1x PBS. This process was repeated until the tissue was completely mashed through the filter. To remove glomeruli the cell suspension was pipetted through a second 40 µm filter placed in a new 50 ml tube. After centrifugation of the cell solution for 5 min at 1000 rpm and RT the supernatant was aspirated and the cell pellet was solved in 10 ml DMEM. Cells were plated into a 100 mm dish and cultivated

overnight in a cell culture incubator at 37 °C and 5% CO₂. After 24h the cell solution was carefully resuspended and transferred to a 50 ml tube. The cell culture dish was washed with 10 ml of fresh DMEM, which was also transferred to the tube. The tube was filled up to 25 ml with fresh DMEM and the cell suspension was divided into 10 ml plated on the used 100 mm dish containing already cells, which were settled down. The other 15ml cell suspension were transferred to a T75 cell culture flask. Cells were cultured for another 3d in a cell culture incubator at 37 °C and 5% CO₂. After 3d adherent cells could be detected. The supernatant was removed and cells were washed using 10 ml 1x PBS. Thereafter 10 ml resp. 15 ml fresh DMEM were added to the cells. Cells were placed in the cell culture incubator and incubated at 37 °C and 5% CO₂ until needed for proliferation analysis (5.3.7).

5.3.3. HPLC analysis of T cell nucleotide metabolism

In this thesis, high-performance liquid chromatography (HPLC) was used to separate, identify and quantify several components of the purinergic signaling, which were catalyzed by T cells. The technique is based on pressurized liquid solvent containing the sample mixture, which passes a column filled with a solid adsorbent material. Each component in the sample interacts slightly differently with the adsorbent material causing different flow rates for the components, which leads to separation of the components.

HPLC analysis of lymphoid T cells

To analyze nucleotide metabolism mediated by T cells, CD4⁺ and CD8⁺ T cells were isolated from lymph nodes as described previously (5.3.1.1). After cell sorting T cells were centrifuged for 10 min at 300x g and RT and supernatants were discarded. Next, 20 μM ATP (Sigma-Aldirch), cAMP (BioLog) or etheno-NAD (BioLog) solved in HBSS buffer (165 μl etheno-NAD resp. 245 μl ATP) were added to 240 000 cells per sample and mixed toughly by pipetting. 40 μl resp. 60 μl aliquots of the cell suspension were taken immediately after addition of substrate and cells were then incubated in a cell culture incubator at 37 °C and 5% CO₂. Additional aliquots were taken after 10, 30 and 60 min. Aliquots were immediately centrifuged for 2.5 min at 450x g and 4 °C. After centrifugation 32 μl resp. 50 μl of the supernatant were transferred into glass vials and applied to reverse phase HPLC. Substrates and products were separated by running a linear gradient of buffer A and buffer B using a low-pressure gradient mixing device and a Hypersil BDS C18 column (250 mm x 4.6 mm; particle size 3 μM; Thermo Fisher Scientific). Absorbance was measured at 254 nm and retention times were

assessed using standard samples of nucleotides and nucleosides. cAMP was purchased from BioLog and all other substrates were ordered from Sigma-Aldrich. For fluorescence detection of etheno-derivatives including ϵ -NAD, ϵ -ADPR, ϵ -AMP, ϵ -Ado (BioLog) a Waters Multi λ Fluorescence detector 2475 was used ($\lambda_{EM} = 300$ nm; $\lambda_{EM} = 415$ nm). A linear gradient of buffer A and B was run with a flow profile of 0.8 ml/min (0-5 min 100% A; 5-7.15 min 97% A and 3% B; 7.15-16.5 min 91% A and 9% B; 16.5-24.15 min 0% A and 100% B; 24.1-28.1 min 0% A and 100% B; 28.15-28.35 min 100% A) using a high-pressure gradient mixing device.

To analyze nucleotide metabolism in *ex vivo* stimulated T cells, 96-well plates were prepared 4h before CD4⁺ and CD8⁺ T cell isolation from lymph nodes. Each well of a 96-well plate was coated with 5 μ g/ml anti-CD3- and 8 μ g/ml anti-CD28-antibodies solved in 100 μ l 1x DPBS. Plates were incubated in a cell culture incubator at 37 °C and 5% CO₂ until needed. After cell sorting cells were centrifuged for 10 min at 300x g and 4 °C. The supernatant was discarded and the cell pellet was solved in RPMI up to a cell concentration of 240 000 cells per 100 μ l. The antibody-coating solution was aspirated and wells of the 96-well plate were washed with 100 μ l 1x DPBS. After aspiration of the washing solution each well was filled with 100 μ l of the cell suspension and cells were then incubated for 24h in a cell culture incubator at 37 °C and 5% CO₂. After 48h cells were detached from the wells and transferred into 1.5 ml tubes. Cells were washed with 500 μ l PBS and centrifuged for 10 min at 300x g and RT. Supernatants were discarded and cell pellets were solved in HBSS containing 20 μ M ATP or etheno-NAD. The following procedure was performed as described before. For analysis of HPLC measurements the Empower 2 software was used.

HPLC analysis of cardiac T cells

To study the role of cardiac infiltrating T cells in nucleotide metabolism, cells were isolated 3d after MI as described previously (5.3.1.2). After cell sorting cells were centrifuged for 10 min at 300x g and RT and supernatants were discarded. 20 μ M etheno-AMP (BioLog) solved in 85 μ l HBSS buffer were added to 12 000 cells per sample. 20 μ l aliquots of the cell suspension were taken immediately after addition of substrate and mixed with 50 μ l HBSS buffer (4 °C). Cells were then incubated in a cell culture incubator at 37 °C and 5% CO₂. Additional aliquots were taken after 10, 30 and 60 min. Aliquots were immediately centrifuged for 2.5 min at 450x g and 4 °C. After centrifugation 65 μ l of the supernatant were transferred into glass and applied to reverse phase HPLC. HPLC analysis was performed as described before.

5.3.4. Re-stimulation of cardiac T cells for cytokine secretion

Cardiac infiltrating T cells isolated from the heart 7d after MI (5.3.1.2) were plated in a 96-well plate coated with 5 µg/ml anti-CD3- and 8 µg/ml anti-CD28-antibodies solved in 100 µl 1x DPBS, which had been prepared as described before. Collected cardiac T cells were centrifuged for 10 min at 300x g and RT and the supernatants were discarded. Cell pellets were solved in RPMI up to a cell concentration of approx. 8 000 – 14 000 cells per 100 µl. Wells of the 96-well plate were washed to remove the coating solution and 100 µl of the cell solution was plated in each well. Cells were incubated for 24h in a cell culture incubator at 37 °C and 5% CO₂. After 24h the supernatant of re-stimulated cardiac T cells was collected. Therefore, cells were centrifuged for 5 min at 300x g and RT and 70 µl of the supernatant were transferred to 1,5 ml tubes placed on ice until used for cytokine measurement (5.5.1).

5.3.5. Adenosine receptors activation of stimulated lymphoid T cells

To measure the cytokine secretion of T cells after AdoR stimulation, lymphoid CD4⁺ T cells (5.3.1.1) were plated in 96-well plates coated with 3 µg/ml anti-CD3- and 6 µg/ml anti-CD28-antibodies solved in 100 µl 1x DPBS. 96-well plates were prepared as described before and concentrations were adjusted. Collected lymphoid CD4⁺ T cells were centrifuged for 10 min at 300x g and RT and the supernatants were discarded. Cell pellets were solved in RPMI up to a cell concentration of 200000 cells per 100 µl. After washing of the pre-coated wells, 100 µl of the cell solution was plated in each well. Cells were incubated for 24h in a cell culture incubator at 37 °C and 5% CO₂. After cultivation cells were centrifuged for 5 min at 300x g and RT and the supernatant was carefully removed. Cells were then washed with fresh 100 µl RPMI and centrifuged for 5 min at 300x g and RT. The washing medium was carefully removed and replaced with RPMI containing 1 µM CGS - 21680 (A_{2A}R agonist), 25 µM BAY 60 - 6583 (A_{2B}R agonist) (both purchased from Tocris, Bristol, UK) or an equivalent volume of DMSO only as control (1:200 diluted with medium as control for CGS - 21680 and 1:8 as control for 19 BAY 60 - 6583). Cells were incubated for another 24h in a cell culture incubator at 37 °C and 5% CO₂. Finally, the supernatant of stimulated lymphoid CD4⁺ T cells was collected by centrifugation for 5 min at 300x g and RT and transfer of 70 µl of the supernatant to 1,5 ml tubes, which were placed on ice until used for cytokine measurement (5.5.1).

5.3.6. *Ex vivo* fibroblast cell culture

Fibroblasts were cultured until cells reached a confluence of about 80%. For fresh isolated cells a confluence of 80% was achieved in approx. 1 – 2 weeks with medium changes every 2 – 3d. During this time, heterogeneous cell populations were observed growing out of the isolation. To separate fibroblasts from other cell populations, cells were removed from the plate and cultured in new cell culture flasks with the result that only fibroblasts attached to the new culture ground. To this end, the supernatant was removed and cells were washed using 10 ml 1x PBS. For dissociation of cells 3 – 5 ml 1x trypsin/ EDTA were added followed by incubation in the cell incubator for approx. 2 min. Cells were separated by gently pipetting the solution up and down. Dissociation was interrupted by adding of 10 ml fresh DMEM to the cell solution, which was then transferred to a 50 ml tube. After centrifugation for 5 min at 1000 rpm and RT the supernatant was aspirated, the cell pellet was solved in 30 ml fresh DMEM and separated into two T75 cell culture flasks containing 15 ml each. Cells were incubated at 37 °C and 5% CO₂. Usually fibroblasts were split every 2 – 4d with a confluence about 80% as described above. For the following experiments fibroblasts were used within passages of 3 – 4.

5.3.7. Fibroblast proliferation assay

To study cell proliferation potentials of *ex vivo* fibroblasts, cells were analyzed using the colorimetric MTT (3-(4,5-dimethylthiazol-2-yl)-2,5-diphenyltetrazolium bromide) assay. This assay was developed for assessing cell metabolic transformation rate by NAD(P)H-dependent cellular oxidoreductase enzymes activity reflecting the number of viable cells. Oxidoreductases catalyze the reduction of the tetrazolium dye MTT to insoluble formazan, which can be measured at OD₅₄₀ [321].

For analysis fibroblast were plated in a 96 well plate using various cell concentrations (2500, 5000 or 10000 cell per well) and incubated for different time points (1d, 2d and 4d) at 37 °C and 5% CO₂. After incubation the supernatant of the cells was aspirated and replaced with 100 µl fresh DMEM (without phenol red). Additional wells were filled with 100 µl DMEM only for blank measurements. For each sample and blank 10 µl 12 mM MTT stock solution was added and cells were incubated for 4h at 37°C and 5% CO₂. After 4h the formation of blue crystals could be detected. To resolve crystals all but 25 µl was removed from each well and 50 µl DMSO were added and mixed thoroughly by pipetting. Samples were incubated for 10 min at 37°C and 5% CO₂ and the absorbance of the samples was measured at 540nm.

5.4. Molecular biological methods

5.4.1. RNA isolation

For gene expression analysis, first of all RNA was isolated from cells or tissues of interest. In the next step, isolated RNA became reverse-transcribed to complementary DNA (cDNA) by the reverse transcriptase, a RNA-dependent DNA polymerase. To study gene expression the quantitative polymerase chain reaction (qPCR) was used. Therefore, cDNA was amplified during several polymerase chain reactions (PCR) and monitored using DNA-probes or SYBR Green. In this study, RNA was isolated from CD4⁺ and CD8⁺ T cells infiltrating the heart after MI and from CD4⁺ T cell isolated from lymph nodes and stimulated *in vitro* to analyze AdoR expression. Moreover, RNA was isolated from whole renal tissue to examine myofibroblast transformation, inflammation status and immune cell infiltration.

RNA isolation from cardiac T cells

Since the numbers of cells, which can be isolated from the heart, is very small the TaqMan Gene Expression Cells-to-C_T Kit (Ambion – Life Technologies) was used. RNA extraction was performed according to the manufactory protocol. Briefly, after cell isolation from the heart and cell sorting (5.3.1.2) cardiac T cells (3000 cells per sample) were centrifuged for 10 min at 300x g and 4 °C. The supernatant was discarded and the cell pellet was washed with 50 µl 1x PSB (4°C). The cell suspension was centrifuged again for 10 min at 300x g and 4 °C and the supernatant was aspirated leaving a rest of approx. 5 µl. Cells were lysed by solving in 50 µl prepared lysis solution, which contains 0.5 µl DNase I and 49.5 µl lysis solution. Lysis reaction was mixed by pipetting up and down for 5 times followed by incubation for 5 min at RT. To stop cell lysis, 5 µl stop solution was added to each sample and mixed by pipetting up and down for 5 times. Samples were incubated for 2 min at RT and placed on ice until needed for reverse transcription (5.4.2.1).

RNA isolation from lymphoid T cells

For RNA isolation from *in vitro* stimulated lymphoid CD4⁺ T cells (5.3.1.1), the RNeasy Mini Kit (Qiagen) was used. RNA extraction was performed according to manufacturer's instructions. For unstimulated controls, 200000 cells were collected into a 1.5 ml tube directly after cell sorting and washed using 1x PBS. After centrifugation for 5 min at 300x g and RT the supernatant was removed

and cells were frozen at -80 °C until used. For RNA isolation, cell pellets were defrosted and solved in 350 µl RLT buffer containing 3.5 µl β-mercaptoethanol for cell disruption. Stimulated cells were collected 48h after anti-CD3-/ anti-28-antibody stimulation. First the supernatant was transferred into 1,5 ml tubes for cytokine measurement (5.3.5) and cells were washed using 100 µl 1x PBS. The 96-well plate was centrifuged for 5 min at 300x g and RT and the supernatant was discarded. Cells were solved in 100 µl 1x PBS and transferred into 1.5 ml tubes. After centrifugation for 5 min at 300x g and RT the supernatant was removed and the cells were disrupted by adding 350 µl RLT buffer containing 3.5 µl β-mercaptoethanol. After cell disruption of both, unstimulated and stimulated cells, 350 µl 70 % Ethanol were added to each sample for homogenization and mixed thoroughly by pipetting. Next, 700 µl of each sample were transferred to a RNeasy spin column and columns were centrifuged for 15 sec at maximal speed and RT. The flow-through was discarded. If necessary, this step was repeated until the whole cell lysate was passed by the column. Columns were washed with 350 µl RW1 buffer and samples were centrifuged for 15 sec at maximal speed and RT followed by discard of the flow-through. To eliminate DNA contamination samples were incubated with DNase for 15 min at RT. Therefore 80 µl DNase solution containing 70 µl RDD buffer and 10 µl DNase were added to each sample. After incubation columns were washed first with 350 µl RW1 buffer followed by wash steps of 500 µl RPE buffer and 500 µl 80 % Ethanol. Columns were centrifuged for 15 sec at maximal speed and RT after each wash step and flow-throughs were discarded. After the last wash step, the column was transferred into a new 1,5 ml tube and 30 µl DEPC H₂O was pipetted into the middle of the column. After centrifugation for 1 min at maximal speed and RT samples were placed on ice until needed. RNA concentration and quality was measured using the NanoDrop system. Therefore, 1.5 µl of each sample were loaded onto the pedestal and measured. RNA quality and purity was defined by a ratio of ~ 2.0 at an absorbance of 260 nm to 280 nm.

RNA isolation from whole renal tissue

To study gene expression in uninjured and injured kidneys after IRI, RNA was isolated from whole kidney tissue. To this end, the capsule of the kidney was removed after isolation and the kidney was transversal sliced into six sections. The middle part of the kidney (third section) was used for RNA extraction. The slices were transferred in 2 ml tubes and immediately frozen in liquid nitrogen and stored at -80 °C until RNA isolation. For isolation tissue samples were refrozen and one Dynabead (Invitrogen) was added to each tube. 1 ml TRI Reagent was pipetted to each sample, which were homogenated for 5 min at 50 oscillations per sec and RT. The TRI Reagent contains a mixture of guanidine thiocyanate and phenol in a monophasic solution for effectively solving of DNA, RNA, and

protein on homogenization. Next, 200 μ l chloroform were added to each tube. Samples were mixed vigorously and stored for 2 min at RT followed by centrifugation for 15 min at 12000 rpm and 4°C. After centrifugation samples are separated into 3 phases: an aqueous phase containing RNA, the interphase containing DNA and an organic phase containing proteins. The aqueous phase was transferred to a 1.5 ml tube and 500 μ l isopropanol were added for RNA precipitation. Samples were mixed and stored for 5 min at RT followed by centrifugation for 8 min at 12000 rpm and 4°C. After centrifugation, a small RNA pellet was observed. The supernatant was removed, the RNA pellet was washed with 1 ml 75 % Ethanol and samples were centrifuged again for 5 min at 7500 rpm and 4°C. The supernatant was aspirated and the RNA pellet was air dried. After drying, the pellet was solved in 100 μ l and samples were placed on ice until needed. RNA concentration and quality was measured using the NanoDrop system. Therefore, 1.5 μ l of each sample were loaded onto the pedestal and measured. RNA quality and purity was defined by a ratio of \sim 2.0 at an absorbance of 260 nm to 280 nm.

5.4.2. Reverse transcription

After RNA extraction from cardiac or lymphoid T cells as well as from whole renal tissues Reverse Transcription (RT) was performed for cDNA synthesis. For cardiac T cells a pre-amplification step was integrated since the number of cells is very small. All other cDNA synthetizations were performed without pre-amplification.

cDNA synthesis of RNA isolated from cardiac T cells and pre-amplification

After RNA extraction from cardiac T cells cDNA synthesis was performed using the TaqMan Gene Expression Cells-to-C_T Kit (Ambion – Life Technologies) according to the manufactory protocol. All pipetting steps were performed on ice. First, a RT Master-Mix was prepared for all samples according to the following reaction setup for one sample:

RT Buffer (2x)	25 μ l
RT Enzyme Mix (20x)	2.5 μ l
Nuclease-free H ₂ O	12.5 μ l
<hr/>	
Total	40 μ l

5. Methods

40 μ l of the Master Mix were pipetted into nuclease-free PCR tubes and 10 μ l of the cell lysate were added. RT reactions were mixed by vortexing and centrifuged briefly to collect the contents at the bottom of the tube. Tubes were placed into the PCR machine (Eppendorf Mastercycler ep Gradient S, Eppendorf) and RT reaction was performed according to the following program:

Reverse Transcription	37 °C	60 min
RT Inactivation	95 °C	5 min
Hold	4 °C	∞

After cDNA synthesis, a pre-amplification step was performed to increase the amount of template for qPCR analysis. For amplification, the TaqMan PreAmp Master Mix (Thermo Fisher Scientific) and TaqMan Gene Expression Assays (20x) for the gene of interest were used. TaqMan Gene Expression Assays (20x) were diluted in TE buffer up to 0.2x in a total volume of 100 μ l. For example, a pooled assay mix containing six TaqMan Gene Expression Assays for A₁R, A_{2A}R, A_{2B}R, A₃R, β -actin and TATA-box binding protein (Tbp) 94 μ l TE buffer were pipetted into a 1,5 ml tube and 1 μ l of each TaqMan Gene Expression Assay was added. The pre-amplification Master-Mix was prepared for all samples according to the following reaction setup for one sample:

TaqMan PreAmp Master Mix (2x)	25 μ l
Pooled Assay Mix (0.2x)	12.5 μ l
cDNA	12.5 μ l
<hr/>	
Total	50 μ l

Pre-amplification reactions were pipetted into nuclease-free PCR tubes, mixed thoroughly and centrifuged briefly. Tubes were placed into the PCR machine (Eppendorf Mastercycler ep Gradient S, Eppendorf) and pre-amplification reaction was performed according to the following program:

Enzyme Activation	95 °C	10 min	} 14 Cycles
Denaturation	95 °C	15 sec	
Annealing/ Extension	60 °C	4 min	
Hold	4 °C	∞	

After amplification samples were placed on ice or stored at -20 °C until needed for qPCR analysis.

cDNA synthesis of RNA isolated from lymphoid T cells

For cDNA synthesis after RNA extraction of lymphoid T cells, the QuantiTect Reverse Transcription Kit (Qiagen) was used according to the manufacturer's instructions. All pipetting steps were performed on ice. Briefly, 12 μ l of RNA sample were incubated with 2 μ l gDNA Wipeout buffer (7x) in nuclease-free PCR tubes for 2 min at 42 °C to eliminate genomic DNA from the sample. Next, a RT Master-Mix was prepared for all samples according to the following reaction setup for one sample:

Quantiscript Reverse Transcriptase	1 μ l
Quantiscript RT Buffer (5x)	4 μ l
RT Primer Mix	1 μ l
<hr/>	
Total	6 μ l

6 μ l of the Master Mix were added to each RNA sample. RT reactions were mixed by vortexing and centrifuged briefly to collect the contents at the bottom of the tube. Tubes were placed into the PCR machine (Eppendorf Mastercycler ep Gradient S, Eppendorf) and RT reaction was performed according to the following program:

Reverse Transcription	42 °C	15 min
RT Inactivation	95 °C	3 min
Hold	4 °C	∞

After cDNA synthesis samples were placed on ice or stored at -20 °C until needed for qPCR analysis.

cDNA synthesis of RNA isolated from whole renal tissue

RNA extracted from whole renal tissue was reverse transcribed using the iScript cDNA Synthesis Kit (Bio-Rad). Procedure was performed on ice according to the manufactory protocol. Briefly, a RT Master Mix was prepared for all samples as described in the following reaction setup for one sample:

iScript Reverse Transcriptase	1 μ l
iScript reaction mix (5x)	4 μ l
<hr/>	
Total	5 μ l

800 – 1000 ng RNA was pipetted into nuclease-free PCR tubes and nuclease-free H₂O was added up to a total volume of 15 μ l. 5 μ l of the RT Master Mix were pipetted to the RNA samples and RT reactions were mixed by vortexing and centrifuged. Tubes were placed into the PCR machine (Eppendorf

Mastercycler ep Gradient S, Eppendorf) and RT reaction was performed according to the following program:

Priming	25 °C	5 min
Reverse Transcription	42 °C	30 min
RT Inactivation	85 °C	5 min
Hold	4 °C	∞

After cDNA synthesis samples were placed on ice or stored at -20 °C until needed for qPCR analysis.

5.4.3. qPCR analysis

After cDNA synthesis of RNA isolated from cardiac and lymphoid T cells and whole renal tissue, qPCR analysis was performed. For T cell studies TaqMan Gene Expression Assays (Thermo Fisher Scientific) were used, which contain gene specific primer and a probe coupled with a fluorescence reporter and quencher on its 3'- and 5'-end. When the probe is intact the reporter dye emission is quenched. After binding of the probe to its specific complementary strand the DNA polymerase cleaves the reporter dye from the probe during each extension cycle and once separated from the quencher emission can be measured. For renal tissue studies SYBR Green (Bio-Rad) technique was used. SYBR Green emits fluorescence after binding to double stranded DNA. After annealing of sequence-specific primers and elongation by the DNA polymerase, SYBR Green binds during each extension cycle to the generated double stranded DNA and a signal can be measured.

qPCR analysis of cDNA generated from T cell RNA

After pre-amplification of cDNA generated from cardiac T cells 5 µl of the product were diluted in 95 µl TE buffer (1 : 20). cDNA generated from lymphoid T cells was used without dilution. For qPCR analysis the TaqMan Gene Expression Master Mix and TaqMan Gene Expression Assays purchased from Thermo Fisher Scientific were used. A qPCR Master Mix was prepared for all samples as described in the following reaction setup for one sample:

5. Methods

	Cardiac T cells	Lymphoid T cells
TaqMan Gene Expression Master Mix (2x)	5 μ l	5 μ l
TaqMan Gene Expression Assay (20x)	0.5 μ l	0.5 μ l
Nuclease-free H ₂ O	2 μ l	2.5 μ l
Total	7.5 μ l	8 μ l

7.5 μ l resp. 8 μ l qPCR Master Mix were pipetted into a 96-well plate and 2.5 μ l of the diluted pre-amplified product from cardiac T cells resp. 2 μ l of the cDNA from lymphoid T cell were added. Assay plates were covered with a Microseal 'B' Adhesive Sealing Film (Bio-Rad), mixed by vortexing and briefly centrifuged. All experiments were performed using the StepOne Plus Real-Time PCR Detection System (Applied Biosystems) according to the following program:

Uracil-DNA Glycosylase Incubation	50 °C	2 min	
Enzyme Activation	95 °C	10 min	
Denaturation	95 °C	15 sec] 45 Cycles
Annealing/ Extension	60 °C	4 min	
Hold	4 °C	∞	

Analysis was performed using the StepOne Software v2.3. For calculation the comparative Ct Method, also known as $2^{-\Delta\Delta Ct}$ method, was used to analyze relative changes in gene expression [322]. This method is based on gene expression comparison of a gene of interest (Target) normalized to an endogenous reference gene (Reference) under specified conditions to control conditions:

$$\Delta Ct = Ct_{\text{Target}} - Ct_{\text{Reference}}$$

$$\Delta\Delta Ct = (Ct_{\text{Target}} - Ct_{\text{Reference}})_{\text{Specified condition}} - (Ct_{\text{Target}} - Ct_{\text{Reference}})_{\text{Normal condition}}$$

$$R = 2^{-\Delta\Delta Ct}$$

qPCR analysis of cDNA generated from whole renal tissue

20 μ l cDNA generated from whole renal tissue of the product were diluted in 20 μ l (1 : 2) or 80 μ l (1 : 5) H₂O. For qPCR analysis the iTaq Universal SYBR Green Supermix (Bio-Rad) and primers purchased from Integrated DNA Technologies were used. A qPCR Master Mix was prepared for all samples as described in the following reaction setups for one sample:

iTaq Universal SYBR Green Supermix (2x)	5 μ l
cDNA	1 μ l
<hr/>	
Total	6 μ l
Primer (forward and reverse) (100 μ M)	0.2 μ l
Nuclease-free H ₂ O	3.8 μ l
<hr/>	
Total	4 μ l

4 μ l Primer Master Mix were pipetted into a 96-well plate and 6 μ l of cDNA Master Mix of each sample was added. Assay plates were covered with a Microseal 'B' Adhesive Sealing Film (Bio-Rad), mixed by vortexing and briefly centrifuged. All experiments were performed using the CFX Connect™ Real-Time PCR Detection System (Bio-Rad) according to the following program:

Enzyme Activation	95 °C	20 sec	
Denaturation	95 °C	5 sec	} 45 Cycles
Annealing/ Extension	56 °C	15 sec	
Start Melting Curve	65 °C	5 sec	
Melting Curve Analysis	up to 95 °C in 0.5 °C steps		
Hold	4 °C	∞	

Analysis was performed using the Bio-Rad CFX Manager (Bio-Rad). For calculation the comparative Ct Method was used as described before.

5.5. Biochemical methods

5.5.1. Analysis of T cell cytokine secretion

For analysis of T cell cytokine profiles after stimulation, Mouse Cytokine 23-Plex or Mouse Cytokine Th17 6-Plex assays were used (all purchased from Bio-Rad). Additionally, singleplex assays for IL-2, IL-3, IL-4, IL-5 and IL-13 (all purchased from Bio-Rad) were added to the Mouse Cytokine Th17 6-Plex assay. The principle of the multiplex system is based on fluorescently dyed magnetic beads, each with a specific spectral address to permit discrimination of individual tests within a multiplex suspension. Capture antibodies, which are directed against a specific cytokine, are covalently coupled to the magnetic beads. After reacting of the coupled beads with the sample containing the cytokine of

interest and series of washes all unbound proteins are removed. A biotinylated detection antibody directed against the specific cytokine is added to create a sandwich complex. The final detection complex is formed by addition of streptavidin-phycoerythrin (SA-PE), in which phycoerythrin serves as a fluorescent reporter. The different molecules bound to the surface of the beads are measured by a flow cytometer containing two lasers and associated optics.

Analysis was performed according to the manufactory protocol. Briefly, coupled beads were vortexed thoroughly and diluted up to 1x in Bio-Plex assay buffer. 50 μ l of the coupled bead solution were added to each well of a 96-well plate and beads were washed 2 times with 100 μ l Bio-Plex wash buffer using a magnetic wash station. After washing 50 μ l of each sample including supernatants collected from stimulated T cells resp. effluate of Langendorff hearts, blank (RPMI only resp. Krebs-Henseleit buffer) and standards were added to the wells. Samples were incubated for 30 min on a shaker at 850 rpm and RT protected from light. After incubation samples were washed 3 times with 100 μ l Bio-Plex wash buffer using a magnetic wash station. Detection antibodies were mixed thoroughly and diluted up to 1x in Bio-Plex detection antibody diluent. 25 μ l of the detection antibody solution were added to each sample and the assay plate was incubated for 30 min on a shaker at 850 rpm and RT protected from light followed by washing for 3 times with 100 μ l Bio-Plex wash buffer using a magnetic wash station. SA-PE was mixed thoroughly and diluted up to 1x in Bio-Plex assay buffer. 50 μ l of the SA-PE solution were added to each sample and the assay plate was incubated for 10 min on a shaker at 850 rpm and RT protected from light. After incubation samples were washed 3 times with 100 μ l Bio-Plex wash buffer using a magnetic wash station and 125 μ l Bio-Plex assay buffer was filled in each sample well. The assay plate was placed for 30 sec on a shaker at 850 rpm and RT protected from light and immediately measured by the Bio-Plex system. The red laser (635 nm) illuminates the fluorescent dyes within each bead to provide bead classification and thereby assay identification. At the same time, a green laser (532 nm) excites PE for generating a reporter signal, which is detected by a photomultiplier tube (PMT). For data analysis, the Bio-Plex Manager software was used, which presents data as median fluorescence intensity (MFI) as well as concentration (pg/ml). The concentration of a cytokine bound to each bead is proportional to the MFI of reporter signal. Due to variability of cell numbers isolated from the heart of T cell-specific CD73^{-/-} mice, cytokine concentration was normalized to 1 000 cells.

5.5.2. Flow cytometry analysis of immune cells

In this study flow cytometry was used to analyze changes in CD69 synthesis after AdoR stimulation on CD4⁺ T cells or to identify distribution of CD39 and CD73 on T cells and B cells. The principle of flow cytometry is based on laser detection system used for cell counting, cell sorting, biomarker detection and protein engineering. Physical properties, such as size (represented by forward angle light scatter) and internal complexity (represented by right-angle scatter) were used to resolve certain cell populations. Labeling of cells by specific antibodies coupled to a fluorescence dye allowed identification of specific cell subpopulations and protein distribution. Cells in suspension are drawn into a stream created by a surrounding sheath of isotonic fluid inside of a flow cytometer, which creates a laminar flow allowing cells to pass individually through an interrogation point. At the interrogation point, a beam of monochromatic light, intersects the cells and emitted light, which is given off in all directions, becomes collected via optics directing the light to a series of filters and dichroic mirrors leading to isolation of particular wavelength bands. The light signals become detected by photomultiplier tubes and digitized for computer analysis.

To study changes in CD69 synthesis after AdoR stimulation on CD4⁺ T cells, in a first step the supernatant was transferred into 1,5 ml tubes for cytokine measurement of treated cells (5.3.5) and cells were washed using 100 µl 1x PBS. The 96-well plate was centrifuged for 5 min at 300x g and RT and the supernatant was discarded. Cells were solved in 100 µl 1x PBS and transferred into round-bottom polystyrene tubes placed on ice. Each sample was stained using 1 µl of the CD69 – FITC antibody solution and incubated for 30 min at 4 °C. After incubation cells were washed with 5 ml MACS buffer (4 °C) and centrifuged for 10 min at 300x g and 4 °C. Supernatants were discarded and cell pellets were solved in 100 µl MACS buffer (4 °C). To separate dead cells from living cells, 0.1 µg/ml DAPI was added to cell solutions 5 min before measurement. Cells were analysed using the FACSCanto II system. To define negative and positive signals in multiparameter analysis, Fluorescence-minus-one (FMO) controls were performed. For data analysis, the FACSDiva Software (BD Bioscience) was used.

To analyze CD39 and CD73 distribution, immune cell populations were isolated from hearts of myocarditis mice as described previously (5.3.1.2). For unstimulated controls, immune cell populations were isolated from the blood. To this end, mice were anesthetized using pentobarbital (1 mg/kg of body weight) and anticoagulation was inhibited using heparin (100 IE). Blood was collected from the abdominal vein using a BD Ultra-Fine Needle Insulin syringe and transferred into a 15 ml tube prepared with 100 IE heparin. 5 ml ammonium chloride potassium (ACK) lysis buffer was added to each blood sample, which was then incubated for 10 min on ice. After incubation reaction was stopped

by adding of 10 ml MACS buffer and cells were centrifuged for 10 min at 300x g and 4 °C. The supernatant was discarded and the blood cell pellets as well as the pellet of cells isolated from the heart were solved in 2 ml MACS buffer. 50 µl FcR Blocking Reagent (Miltenyi Biotech) were added to each sample followed by 10 min incubation on ice. Samples were washed with 8 ml MACS buffer and centrifuged for 10 min at 300x g and 4 °C. Supernatants were discarded and the cell pellets were solved in 1 ml MACS buffer. For antibody labelling 100 µl of each sample were pipetted into round-bottom polystyrene tubes placed on ice. For cell staining the following panel was used.

Cell subpopulation	Antibody					
T cells Staining I	CD45 PE	CD3 APC	CD4 PerCP5.5	CD8 APC-H7	CD39 PE-Cy7	CD73 FITC
T cells Staining II	CD45 PE	CD3 APC	CD4 PerCP5.5	CD8 APC-H7	CD25 PE-Cy7	CD73 FITC
B cells	CD45 PE	CD3 APC	CD45R (B220) APC-eFluor780		CD39 PE-Cy7	CD73 FITC

Tab. 7: Antibody labeling of different immune cell subsets.

For identification of the different cell populations, staining panels of 100 µl total were pipetted as shown in table 3. Therefore 1 µl of each antibody was added to 94 µl resp. 95 µl MACS buffer (4 °C). Each sample was solved in 100 µl staining solution and incubated for 30 min at 4 °C. After incubation cells were washed with 5 ml MACS buffer (4 °C) and centrifuged for 10 min at 300x g and 4 °C. Supernatants were discarded and cell pellets were solved in 300 µl MACS buffer (4 °C). To separate dead cells from living cells, 0.1 µg/ml DAPI was added to cell solutions 5 min before measurement. Cells were analysed using the FACSCanto II system. To define negative and positive signals in multiparameter analysis, Fluorescence-minus-one (FMO) controls were performed. For data analysis, the FACSDiva Software (BD Bioscience) was used.

5.5.3. Analysis of kidney function by measurement of plasma creatinine levels

Kidney function was measured by assessment of plasma creatinine levels. Therefore, blood samples were incubated at RT at least for 15 min to allow blood clotting. Samples were then centrifuged for 30 min at 1000x g and RT and plasma was transferred into 1.5 ml tubes. For plasma creatinine

measurements, the Diazyme Creatinine Liquid Reagents Assay (Diazyme Store) was used. The assay principle is based on a series of coupled enzymatic reactions including creatininase enzymatic conversion of creatinine into the product creatine which itself is converted to sarcosine by creatine amidinohydrolase (creatinase) followed by oxidation of sarcosine by sarcosine oxidase (SOD) producing hydrogen peroxide. In the presence of peroxidase (POD) the hydrogen peroxide is quantified at 550 nm by the formation of a colored dye. Analysis was kindly performed by Liping Huang according to the manufactory protocol.

5.5.4. Quantification of renal collagen content by hydroxyproline assay

To quantify the collagen concentration of kidney tissues, the colorimetric hydroxyproline assay was used in this study. The synthetization of the amino acid hydroxyproline is a post-translational modification of proline mediated by the prolyl hydroxylase. Hydroxyproline is a major component of collagen stabilizing the helical structure. Because hydroxyproline is found almost exclusively in collagen, measurement of hydroxyproline levels correlate to the levels of collagen present in the tissue. The principle of this assay is based on the conversion of hydroxyproline to pyrrole in acid hydrolyzed samples through a reaction with Chloramine T. Pyrrole reacts with the Ehrlich's Reagent to form a chromophore, which can be detected at 550 nm [323].

After kidney isolation, the capsule was peeled off and half of the kidney was transferred into a glass tube placed on ice until all samples had been collected. The tissue was dried overnight in a heat block at 110 °C. After 24 h the dried tissue was weighted, transferred into glass ampoules and 1 ml 6 M HCl was added. Glass ampoules were sealed by melting of the glass on the opening side using a Bunsen burner and the tissue was hydrolyzed overnight in a heat block at 110 °C. On the next day 1,5 ml tubes were prepared with 8 mg Amberlite Monobed Resin and the hydrolysate was transferred into the tubes. Samples were rotated for 30 min at RT. After rotation, samples were centrifuged for 30 min at 12000 rpm and RT and the supernatant of each ample was transferred into a new 1,5 ml tube. 25 µl of each sample including hydrolysates, blank (6 M HCl only) and standards were pipetted into 5 ml glass tubes. 500 µl Chloramine-T solution were added and samples were mixed by vortexing followed by incubation of 20 min at RT. After incubation, 500 µl 3.15 M HClO₄ were pipetted to each sample, which was mixed by vortexing and incubated for 5 min at RT. Next, 500 µl Ehrlich's solution was added and samples were mixed by vortexing again. Samples were incubated for 20 min in a water bath at 60 °C sealed with parafilm. Immediately after incubation samples were cooled in an ice bath for

5 min to stop the reaction. After mixing, 200 μ l of each sample were transferred into a well of a 96-well plate and measured at 550 nm.

5.6. Histochemical methods

5.6.1. Detection of renal tissue fibrosis and matrix deposition by Masson's trichrome staining

For detection of fibrosis formation and matrix deposition in renal tissues, the Masson's trichrome staining was used in this thesis. The staining, based on the receipt evolved by Claude L. Pierre Masson, displays tissue integrity. Collagen fibers and dead tubular cells appear in a blue color, nuclei are in black and cytoplasm of intact cells is stained in magenta [324].

After kidney isolation, the capsule was removed and the kidney was transversal sliced into six sections. The middle part of the kidney (fourth section) was used for Masson's trichrome staining. Therefore, kidney section was transferred into histology cassettes and incubated overnight in 10 % formalin at 4 °C. After 24 h cassettes containing tissue sections were washed with 70 % Ethanol and incubated overnight in 70 % Ethanol at 4 °C. Paraffin embedding, cutting of kidney slices and transfer of slices onto cover slides as well as trichrome staining was done by the Research Histology Core at the University of Virginia, School of Medicine (Charlottesville, USA) with the kindly help of Sheri VanHoose.

5.6.2. Immunofluorescence analysis of renal tissue sections and confocal microscopy

Immunofluorescence analysis was performed to study renal cell composition and matrix deposition. To this end, the renal capsule was removed after kidney isolation and the kidney was transversal sliced into six sections. The end parts of the kidney (fifth and sixth sections) were transferred into histology cassettes and incubated in 2% periodate-lysine-paraformaldehyde (PLP) buffer for 2.5h. After incubation, tissue sections were washed with 1x PBS and transferred into a 5% sucrose solution overnight. After 24h renal tissue sections were equilibrated in 15% sucrose solution for 2h followed by 3h in 30% sucrose solution. Then tissue sections were transferred into a well filled with optimum-cutting-temperature (OCT) compound. For tissue equilibration, this process was repeated two times. A mold was prepared with OCT compound and the tissue section was placed in the mold. Tissue sections were frozen placed on dry ice and stored at -80 °C. Before cutting, tissue samples were equilibrated at -20 °C. For immunohistochemistry 5 μ m slices of renal tissue were cut and transferred onto slides

(Thermo Fisher Scientific) For immunohistochemistry staining, slides were warmed up at RT for 15min and washed with 1x PBS for 5 min. Next, slides were submerged in a 0.3% Triton x-100 blocking solution for 1 h. Afterwards slides were washed three times in 1x PBS and incubated in a 2.4G2 serum solution overnight. After 24 h slides were washed three times in 1x PBS and the staining solution was prepared. Because of high background with secondary antibodies, all staining was performed with directly conjugated antibodies. For labeling AlexaFluor Dye Antibody Labeling Kits (Molecular Probes – Life Technologies – Thermo Fischer Scientific) were used and kindly provided by Dr. Sun-sang J. Sung (University of Virginia, Charlottesville, USA). Antibodies were diluted in 50 μ l 2.4G2 solution up to a final concentration of 2.0 – 2.5 μ g/ml. 50 μ l of the staining solution were added onto the tissue sections and slides were incubated for 2 h at RT protected from light in a petri dish prepared with moistened paper towels to avoid drying of samples. After incubation the staining solution was aspirated and slides were washed three times in 1x PBS. Slides were covered using a coverslips (Thermo Fisher Scientific) fixed with Elvanol. For immunofluorescence analysis, a Zeiss LSM700 Confocal Microscope (Carl Zeiss GmbH) was used equipped with 405 nm, 488 nm, 543 nm and 633 nm lasers at the Advanced Microscopy Facility (University of Virginia, Charlottesville, USA). Images were analyzed using the Zeiss program ZEN. Staining and images used in this thesis were done with the kindly help of Dr. Sun-sang J. Sung.

5.7. Statistics

All data is represented as mean \pm standard deviation. For data analysis Microsoft Excel Professional Plus 2010 and Graph Pad Prism 5 was used. Statistical analysis was performed by two way ANOVA followed by Bonferoni post test or student's t-test. In cases where Shapiro Wilk test of normality failed, Mann-Whitney Rank Sum test was used. Differences of $p < 0.05$ were considered statistically significant (* $p \leq 0.05$; ** $p \leq 0.01$; *** $p \leq 0.001$).

6. Results

Aim of this work was to investigate the contribution of the purinergic signaling to tissue recovery processes after ischemia/ reperfusion injury (IRI) in the heart and the kidney. In the first part of this study, metabolic reprogramming of T cells after myocardial infarction (MI) was studied, in particular the impact of CD73-derived adenosine on adenosine receptors (AdoRs) in mediating wound healing and resolution of inflammation. Moreover, the role of the purinergic signaling in chronic diseases, such as myocarditis, was examined. In the second part of this thesis, the function of CD73 in the kidney was investigated, in particular the role of CD73 on tubular cells and fibroblast/ pericytes in modulating tissue healing and inflammation after acute kidney injury (AKI).

6.1. Extracellular nucleotide metabolism after T cell activation

In previous studies we demonstrated that T cells are crucial mediators of healing processes in the heart after MI [306–308]. After invading into the injured cardiac tissue, gene expression analysis of CD4⁺ and CD8⁺ T cells revealed that T cell activation at the site of injury is associated with upregulation of enzymes, channels and transporters, which are involved in nucleotide release and extracellular degradation [308]. Based on these observations we were interested whether increased expression levels of enzymes involved in the degradation of nucleotides, such as ATP and NAD, are associated with accelerated enzymatic function. To address this question, we first established an *in vitro* cell culture model to mimic T cell activation after invasion into the heart, since the number of cells, that can be isolated from the heart, is too small for functional studies. To this end CD4⁺ and CD8⁺ T cells were isolated from lymph nodes and stimulated *in vitro* using anti-CD3-/ anti-28-antibodies. ATP and NAD were added to *in vitro* activated CD4⁺ and CD8⁺ T cells and kinetics of ATP and NAD degradation was measured using HPLC analysis.

From the data summarized in figure 8A, activated CD4⁺ and CD8⁺ T cells degraded ATP more rapidly than unstimulated control cells resulting in increased ADP, AMP and adenosine (ADO) levels. Similarly, NAD was hydrolyzed more efficient by stimulated CD4⁺ and CD8⁺ T cells compared to unstimulated control cells leading to higher AMP, ADP-ribose (ADPR) and adenosine levels (ADO) (figure 8B). In summary, our results indicate that CD4⁺ and CD8⁺ T cells, which infiltrate the heart after MI, upregulate expression levels of enzymes, channels and transporters, that are involved in the degradation of ATP and NAD to adenosine as well as in adenosine metabolism. Moreover, these

findings correspond with accelerated enzymatic activity by *in vitro* activated CD4⁺ and CD8⁺ T cells as shown by increased nucleotide metabolism of ATP and NAD to its breakdown products.

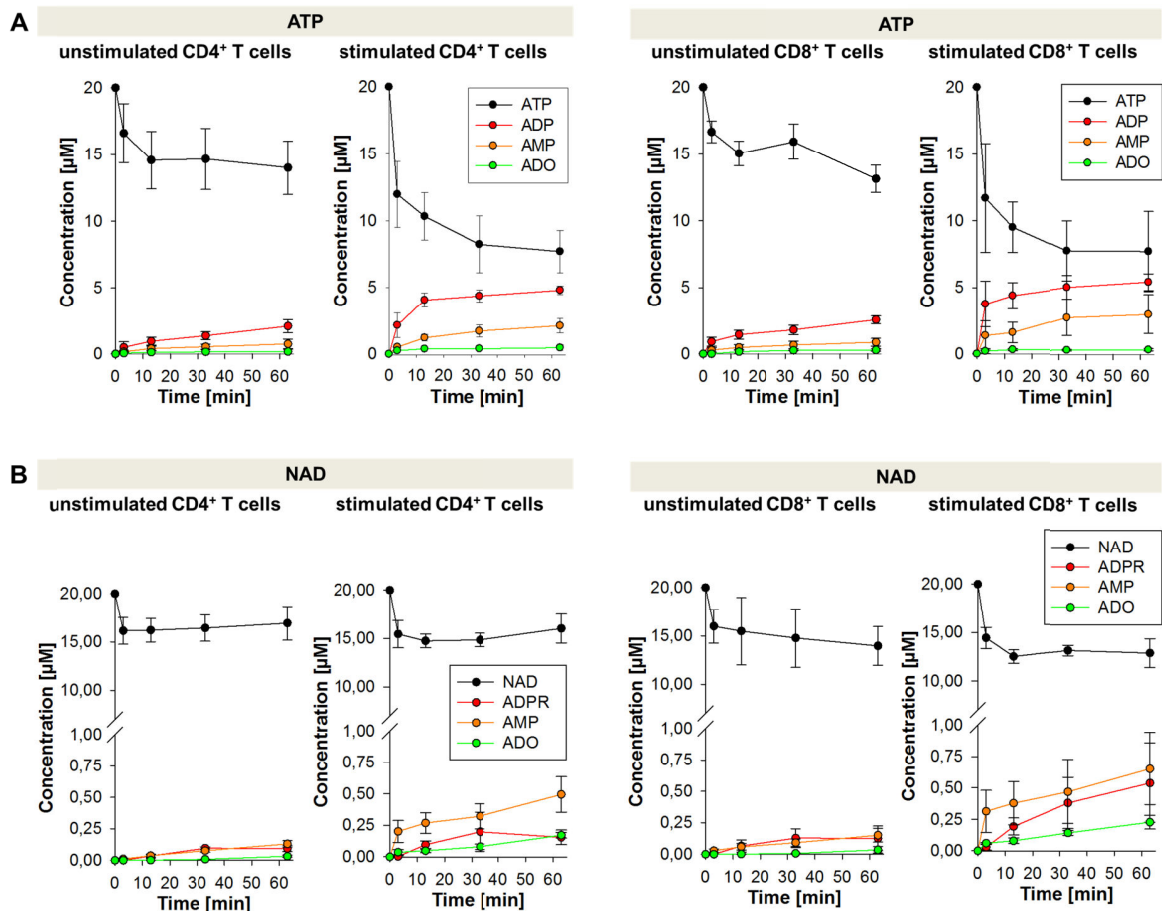


Fig. 8: Kinetics of extracellular degradation of ATP (A) or NAD (B) by activated CD4⁺ and CD8⁺ T cells isolated from wildtype mice. CD4⁺ and CD8⁺ T cells were isolated from lymph nodes of wildtype mice and stimulated *in vitro* using anti-CD3-/ anti-CD28-antibodies for 48h. For measurement of enzyme activity, unstimulated and stimulated CD4⁺ T cells and CD8⁺ T cells were incubated either with ATP or NAD. Supernatants were collected after 10, 30, and 60 min and ATP or NAD degradation was measured using HPLC analysis. Data represent mean \pm SD (n=6-8). ADO: adenosine.

As to the fact, that numerous studies support the concept of CD39 as the rate limiting step in ATP degradation by regulating ATP half-life after IRI, we were interested to what extend CD39 contributes to overall ATPase activity [161]. To assess the contribution of CD39 on overall ATPase activity on activated T cells compared to unstimulated cells, we analyzed ATP hydrolysis of *in vitro* stimulated

CD4⁺ and CD8⁺ T cells isolated from lymph nodes of CD39^{-/-} mice compared to cells isolated from wildtype mice as assessed by HPLC analysis.

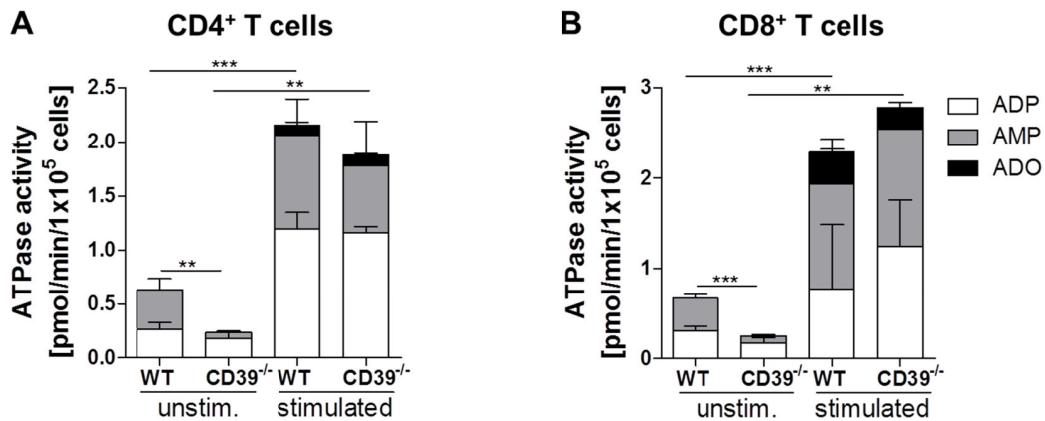


Fig. 9: Kinetics of extracellular degradation of ATP by activated CD4⁺ (A) and CD8⁺ (B) T cells isolated from CD39^{-/-} or wildtype mice. CD4⁺ and CD8⁺ T cells were isolated from lymph nodes of CD39^{-/-} or wildtype mice and stimulated *in vitro* using anti-CD3-/ anti-CD28-antibodies for 48h. To analyze ATPase activity, unstimulated and stimulated CD4⁺ and CD8⁺ T cells were incubated with ATP. Supernatants were collected after 60 min of incubation and ATP degradation was measured using HPLC analysis. Data represent mean \pm SD (n=4-5; ** p \leq 0.01; *** p \leq 0.001). ADO: adenosine.

As shown in figure 9A and B, total ATPase activity was inhibited in unstimulated CD4⁺ and CD8⁺ T cells isolated from mice lacking CD39 compared to wildtype cells. Quite unexpected we made the observation that total ATPase activity in stimulated CD4⁺ and CD8⁺ T cells isolated from CD39^{-/-} and wildtype mice was nearly identical as indicated by similar levels of ADP, AMP and adenosine (ADO) suggesting, that beside CD39 other ATP-degrading enzymes may be involved in the hydrolysis of ATP after T cell stimulation.

Next, we were wondering whether adenosine formation is mainly provided by CD73 on T cells, which becomes upregulated after invading into the infarcted myocardium. To analyze AMPase activity of cardiac T cells after activation following IRI, mice were subjected to 50' of ischemia by occlusion of the left anterior descending (LAD) artery followed by reperfusion. T cells were isolated from the heart of T cell-specific CD73^{-/-} or wildtype control mice by digestion of the tissue using retrograde perfusion according to the Langendorff procedure 3d after MI (figure 10A) [306; 307]. For controls, unstimulated circulating T cells were isolated from the blood of wildtype mice 3d after MI. After isolation, etheno-AMP was added to the cells and AMPase activity was measured by HPLC analysis.

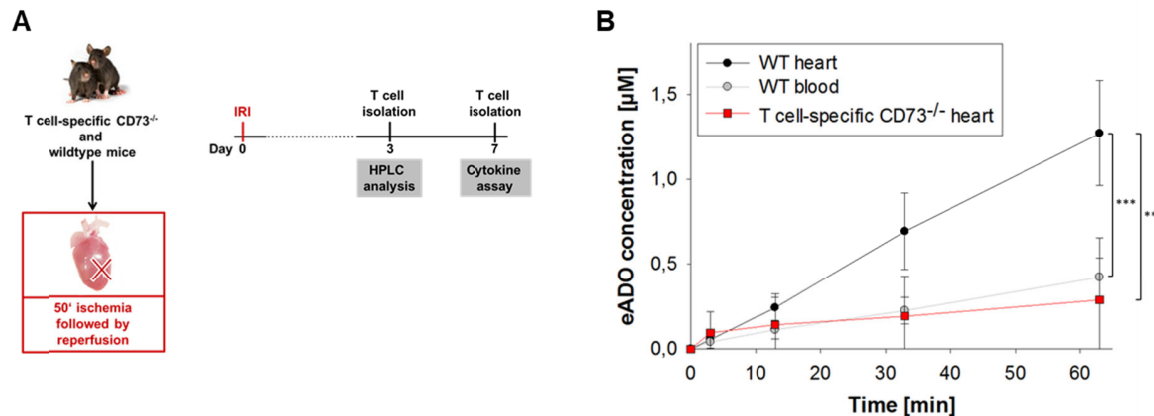


Fig. 10: Scheme of the experimental procedure (A) and kinetics of extracellular degradation of etheno-ATP by activated T cells isolated from the heart and blood of T cell-specific CD73^{-/-} or wildtype mice. A) T cell-specific CD73^{-/-} and wildtype mice were subjected to 50' ischemia by occlusion of the LAD followed by reperfusion. For measurement of AMPase activity, as assessed by HPLC analysis, cardiac T cells were isolated on day 3 after MI by digestion of the tissue using retrograde perfusion according to the Langendorff procedure. For controls, T cells were isolated from the blood. To analyze cytokine production of cardiac T cells, cells were isolated on day 7 after MI, re-stimulated and the cytokine profile was measured using the Bioplex system. B) T cells were isolated from the heart of T cell-specific CD73^{-/-} and wildtype mice 3d after MI by digestion of the tissue using retrograde perfusion according to the Langendorff procedure. Cells were incubated with etheno-AMP and AMPase activity was measured by HPLC analysis. Data represent mean \pm SD (n=5-6; ** p \leq 0.01; *** p \leq 0.001). ADO: adenosine; IRI: ischemia/ reperfusion injury; WT: wildtype. Image by noBacs.com (by: Erma Simon).

As summarized in figure 10B, AMPase activity of cardiac T cells isolated from the heart of wildtype mice was significantly increased due to activation compared to unstimulated cells isolated from the blood as assessed by increased adenosine (ADO) concentrations. Interestingly, AMPase activity of cardiac T cells isolated from T cell specific CD73^{-/-} mice was found to be rather low comparable to AMPase activity of unstimulated T cells isolated from the blood of wildtype mice. In summary, these observations suggest that CD73 on cardiac invading T cells is the major enzyme catalyzing AMP to adenosine after MI suggesting a negligible contribution of alkaline phosphatases or other AMP-degrading enzymes.

6.2. Cytokine profile of isolated cardiac T cells lacking CD73

Previous data clearly demonstrated that CD73 is an important regulator of tissue remodeling after MI, which becomes upregulated on cardiac infiltrating T cells [306; 307]. Since new observation showed that CD73 on T cells is the major source for adenosine and that lack of CD73 on T cells resulted in

adverse cardiac remodeling and an inflammatory phenotype identical to global $CD73^{-/-}$ mice, we were interested whether a lack of CD73 influences the phenotype of T cells and cytokine production [308]. To this end cardiac T cells were isolated from T cell-specific $CD73^{-/-}$ and wildtype mice 7d after MI by digestion of the tissue using the Langendorff procedure as mentioned before and re-stimulated *in vitro* to measure cytokine production using the Bioplex system (figure 10A).

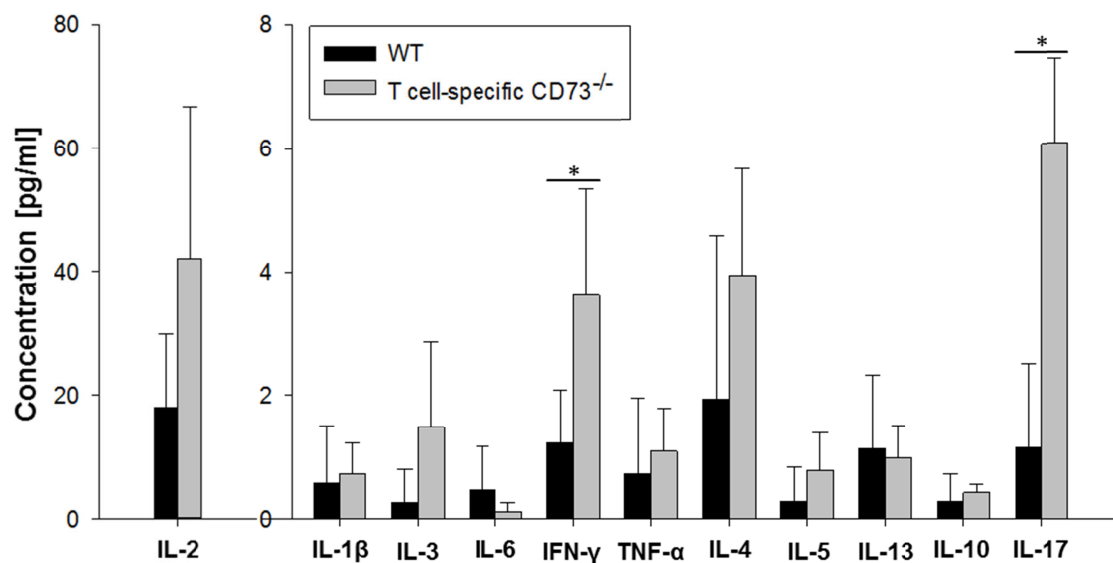


Fig. 11: Cytokine profile of cardiac T cells isolated from the heart of T cell-specific $CD73^{-/-}$ or wildtype mice 7d after MI. T cells were isolated from the heart of T cell-specific $CD73^{-/-}$ and wildtype mice 7d after MI by digestion of the tissue using retrograde perfusion according to the Langendorff procedure. T cells were re-activated *in vitro* for 24h using anti-CD3/ anti-CD28-stimulation. Supernatants were collected and cytokine secretion was measured via Bioplex analysis. Concentrations were normalized to 1 000 T cells. Data represent mean \pm SD (n=4; *p \leq 0.05). WT: wildtype.

As shown in figure 11, cardiac T cells lacking CD73 secreted predominately pro-inflammatory and pro-fibrotic cytokines after *in vitro* re-stimulation in comparison to cardiac T cells isolated from wildtype mice. Cytokine production of IFN- γ and IL-17 was significantly increased in CD73 deficient T cells compared to control cells. Moreover, the secretion of IL-2, IL-3, IL-4 and IL-5 by $CD73^{-/-}$ T cells also tended to be elevated after re-stimulation. In contrast, the release of IL-6 and IL-13 tended to be lower. In summary, deficiency of CD73 changed the cytokine profile of infiltrating T cells 7d after MI and led predominately to increased secretion of pro-inflammatory and pro-fibrotic cytokines, such as IFN- γ and IL-17.

6.3. Expression of the various adenosine receptors in T cells infiltrating the heart after myocardial infarction

As adenosine signals via activation of G protein-coupled AdoR, denoted A₁R, A_{2A}R, A_{2B}R or A₃R, we next investigated whether activation of T cells also results in changes of AdoR expression after IRI. To this end cardiac infiltrating CD4⁺ and CD8⁺ T cells were isolated 3d after MI and expression of all four AdoR was measured using qPCR analysis. CD4⁺ and CD8⁺ T cells were isolated from heart tissue using the Langendorff procedure as mentioned before. For controls, unstimulated circulating CD4⁺ and CD8⁺ T cells were isolated from the blood 3d after IRI.

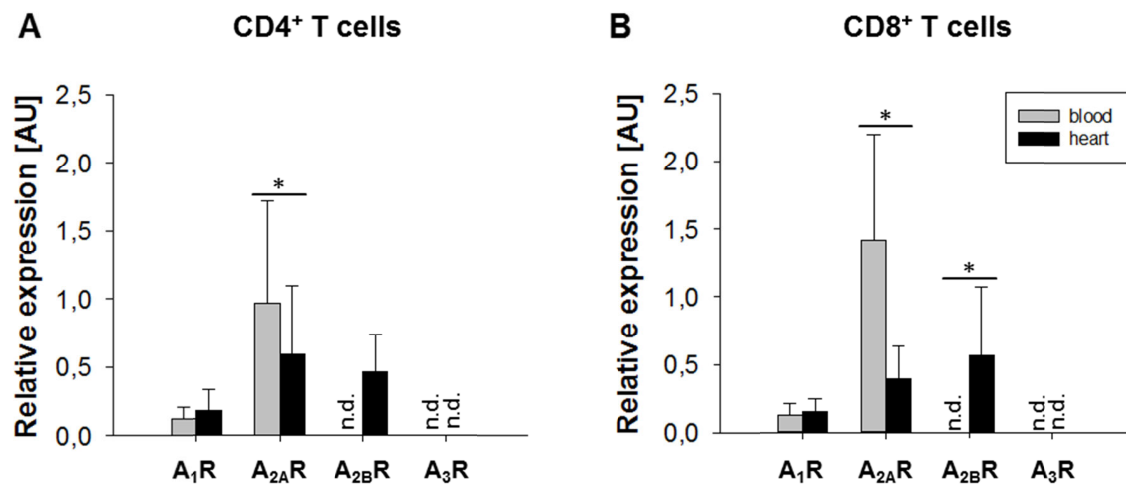


Fig. 12: Gene expression of the various AdoR in CD4⁺ (A) and CD8⁺ (B) T cells infiltrating the heart 3d after MI. CD4⁺ and CD8⁺ T cells were isolated from the heart of wildtype mice 3d after IRI by digestion of the tissue using retrograde perfusion according to the Langendorff procedure. For controls, unstimulated blood circulating CD4⁺ and CD8⁺ T cells were used. Expression levels were quantified by qPCR normalized to β -actin and TATA-box binding protein (Tbp). Data represent mean \pm SD (n=3-5; *p \leq 0.05). n.d. = not detectable.

From the data summarized in figure 12A and B, it can be seen that under unstimulated control conditions the A_{2A}R shows the highest expression values in CD4⁺ or CD8⁺ T cells. Interestingly, no expression of the A_{2B}R and the A₃R was detectable in blood circulating CD4⁺ or CD8⁺ T cells. The A₁R was slightly expressed in unstimulated control CD4⁺ and CD8⁺ T cells. After T cell activation, expression of the A_{2A}R became significantly downregulated in cardiac CD4⁺ and CD8⁺ T cells. Expression levels of the A₁R did not change after T cell activation and the A₃R was still not detectable in cardiac CD4⁺ or CD8⁺ T cells. Most interestingly, expression of the A_{2B}R was increased after infiltration of cardiac CD4⁺ and CD8⁺ T cells into the infarcted myocardium. Taking together, these

results provide first evidence that the $A_{2A}R$ and more interestingly the $A_{2B}R$ may play a role on cardiac infiltrating T cells in tissue healing processes and scar formation. Interestingly, expression of the $A_{2A}R$ became downregulated after T cell activation nearly to the same level of $A_{2B}R$ expression.

6.4. Function of the $A_{2A}R$ and the $A_{2B}R$ on activated $CD4^+$ T cells

Since the $A_{2A}R$ and the $A_{2B}R$ are expressed on cardiac infiltrating T cells, we were interested whether changes in AdoR gene expression are associated with alterations in T cell function. As the number of cells, which can be isolated from the heart, is too small for functional studies, the established cell culture model was used and cells were analyzed for the expression of the $A_{2A}R$ and the $A_{2B}R$. To this end $CD4^+$ T cells were isolated from lymph nodes, stimulated *in vitro* with anti-CD3-/ anti-CD28 antibodies and expression of the $A_{2A}R$ and the $A_{2B}R$ was measured using qPCR analysis.

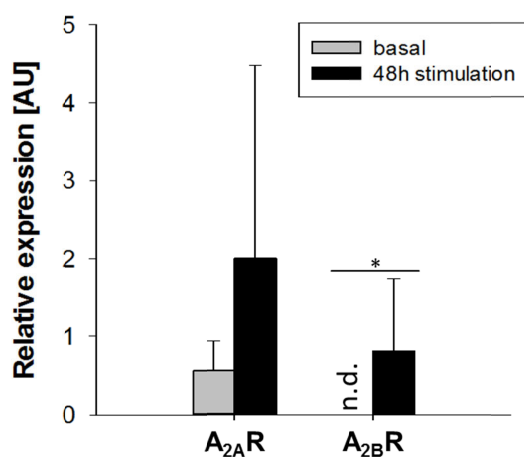


Fig. 13: Gene expression of the $A_{2A}R$ and the $A_{2B}R$ in $CD4^+$ T cells after *in vitro* stimulation. $CD4^+$ T cells were isolated from lymph nodes and stimulated *in vitro* using anti-CD3-/ anti-CD28-antibodies for 48h. For controls, unstimulated cells were used. Expression levels were quantified by qPCR normalized to β -actin. Data represent mean \pm SD (n=7; * $p \leq 0.05$). n.d. = not detectable.

As shown in figure 13, comparable to cardiac infiltrating $CD4^+$ T cells, the $A_{2B}R$ was not detectable on unstimulated $CD4^+$ T cells, but became upregulated after anti-CD3-/ anti-CD28 stimulation. The $A_{2A}R$ was expressed in unstimulated and stimulated $CD4^+$ T cells.

After having established an *in vitro* model for simulating changes in AdoR expression, we next measured whether stimulation of the AdoR influences cytokine formation. To address this question, $CD4^+$ T cells were stimulated for 24h and treated either with an $A_{2A}R$ (CGS-21680) or an $A_{2B}R$ agonist (BAY 60-6583) followed by incubated for 24h and measurement of the cytokine profile using Bioplex analysis.

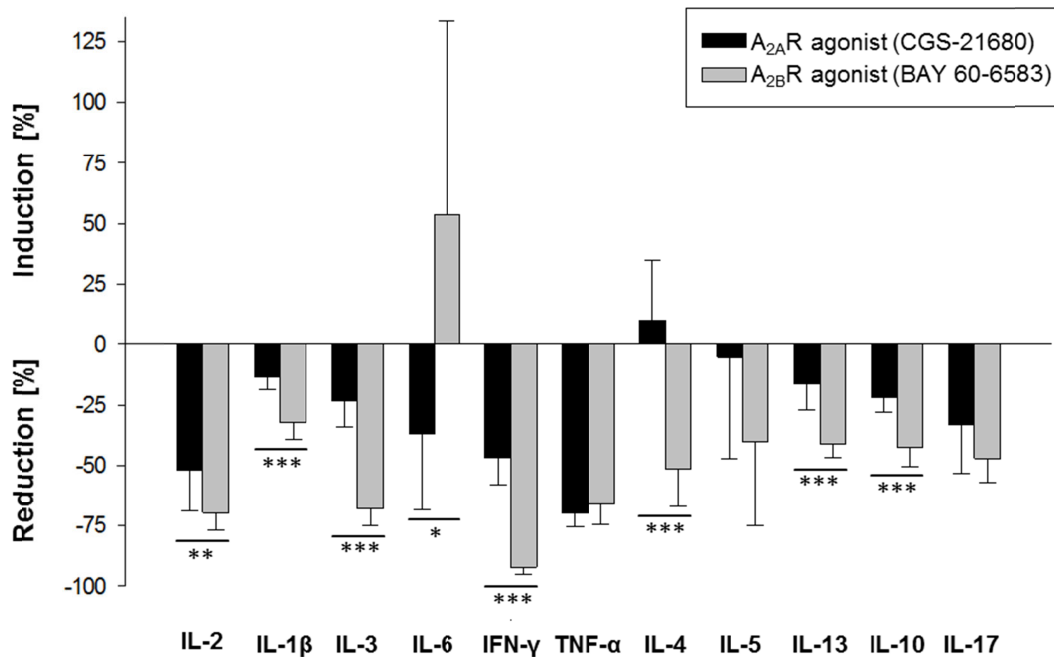


Fig. 14: Induction or reduction of cytokine secretion from *in vitro* activated CD4⁺ T cells after A_{2A}R or A_{2B}R agonist treatment. CD4⁺ T cells were isolated from lymph nodes and stimulated *in vitro* using anti-CD3-/ anti-CD28-antibodies for 24h. Cells were treated either with an A_{2A}R (CGS-21680) or an A_{2B}R agonist (BAY 60-6583) followed by incubation for 24h. Cytokine profile was measured using Bioplex analysis. Data represent mean ± SD (n=6-7; * p ≤ 0.05; ** p ≤ 0.01; *** p ≤ 0.001).

As it can be seen in figure 14, treatment with an A_{2A}R (CGS-21680) or an A_{2B}R agonist (BAY 60-6583) resulted nearly in an overall reduction of cytokine secretion. In general, stimulation of the A_{2B}R seemed to be more efficacious. In cases of IL-1β, IL-2, IL-3, IL-10, IL-13 and IFN-γ activation of the A_{2B}R resulted in a significant stronger reduction of cytokine secretion in comparison to stimulation of the A_{2A}R. Production of IL-5, IL-17 and TNF-α was reduced by activation of the A_{2A}R or the A_{2B}R without any significant differences. Interestingly, secretion of IL-4 was only reduced by treatment with an A_{2B} agonist, whereas treatment with an A_{2A} agonist had negligible effects. IL-6 formation tended to be induced by stimulation of the A_{2B}R, whereas stimulation of the A_{2A}R led to reduction of IL-6 secretion. In summary, cytokines, that were upregulated in the absence of CD73 on T cells (IL1β, IL-2, IL-3, IL-5, IL-10, IL-17, IFN-γ and TNF-α,) (figure11), were downregulated after stimulation of the A_{2A}R or the A_{2B}R.

To investigate, whether the overall reduction of cytokine secretion is related to the activation state of CD4⁺ T cells, cells were isolated from lymph nodes and stimulated *in vitro* as described before. After

treatment with either an $A_{2A}R$ (CGS-21680) or an $A_{2B}R$ agonist (BAY 60-6583) an activation marker for T cells, CD69, was measured using flow cytometry [325].

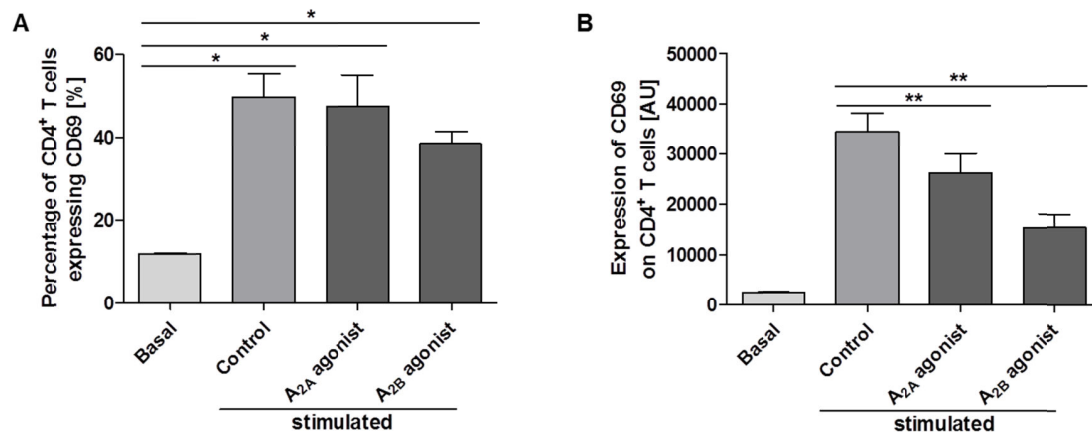


Fig. 15: Percentage of CD4⁺ T cells expressing CD69 (A) and mean fluorescence intensity of CD69 expression on CD4⁺ T cells (B). CD4⁺ T cells were isolated from lymph nodes and stimulated *in vitro* using anti-CD3-/ anti-CD28-antibodies for 24h. Cells were treated either with an $A_{2A}R$ (CGS-21680) or an $A_{2B}R$ agonist (BAY 60-6583) followed by incubation for 24h. The percentage of CD4⁺ T cells expressing CD69 and the mean fluorescence intensity of CD69 expression was determined using flow cytometry analysis. Data represent mean \pm SD (n=3; ** p \leq 0.01).

As shown in figure 15A, *in vitro* stimulation of CD4⁺ T cells led to significant increased numbers of cells expressing CD69, while activation of the $A_{2A}R$ or the $A_{2B}R$ had no effects on the number of CD4⁺ T cells expressing CD69. In contrast, the mean fluorescence intensity of CD69 expression was significantly increased after cell activation and treatment with an $A_{2A}R$ (CGS-21680) or an $A_{2B}R$ agonist (BAY 60-6583) reduced the mean fluorescence intensity of CD69 expression (figure 15B). Interestingly, stimulation of the $A_{2B}R$ was more efficacious. Taking together, these findings provide evidence that stimulation of the $A_{2A}R$ and the $A_{2B}R$ reduces CD4⁺ T cell activity, which finally results in an overall reduction of cytokine secretion.

6.5. Purinergic signaling in a chronic cardiac disease model

Previous work of our laboratory revealed that CD39 becomes upregulated on myeloid cells, whereas CD73 expression is increased on lymphoid cells infiltrating the heart after MI [306; 307]. We therefore hypothesized that extracellular ATP released by apoptotic/ necrotic cardiomyocytes or activated immune cells is mainly degraded by CD39 upregulated on myeloid cells, while the formation of

immunosuppressive adenosine is mainly hydrolyzed by CD73 present on lymphoid cells. This poses the question whether the changes observed in an acute model of cardiac injury, such as MI, can also be observed in a chronic cardiac disease model. In cooperation with Prof. Z. Kaya (Cardiology, Angiology and Pneumology, University Medical Center Heidelberg) we analyzed the expression of CD39 and CD73 on T cells and B cells in a myocarditis model. Myocarditis in mice was induced by subcutaneously injection of murine cardiac troponin I (cTnI) solved in Complete Freund's Adjuvant for 3 times (immunization on day 1, 7 and 14) [314]. Controls were treated with Complete Freund's Adjuvant only. For analysis, cardiac immune cells were isolated from the heart using the Langendorff procedure as mentioned before. Additionally, unstimulated immune cells were isolated from the blood. Immune cell subpopulations and expression of CD39 and CD73 was analyzed using flow cytometry analysis.

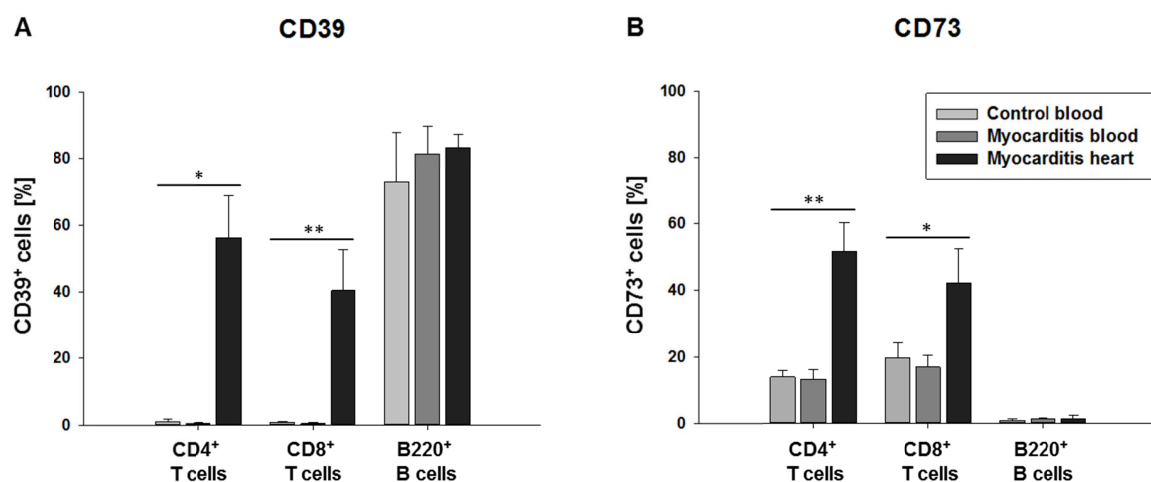


Fig. 16: Expression of CD39 (A) and CD73 (B) on cardiac immune cells in a chronic inflamed heart. Myocarditis in mice was induced by injection of cTnI solved in Complete Freund's Adjuvant for 3 times on day 1, 7 and 14 [314]. Controls were treated with Complete Freund's Adjuvant only. Immune cells were isolated from the heart on day 21 by digestion of the tissue using retrograde perfusion according to the Langendorff procedure. For controls, unstimulated cells were isolated from the blood. Immune cell subpopulations and expression of CD39 and CD73 was examined using flow cytometry analysis. Data represent mean \pm SD (n=3; * $p \leq 0.05$; ** $p \leq 0.01$).

As summarized in figure 16A, the percentage of CD4⁺ CD39⁺ and CD8⁺ CD39⁺ T cells was significantly increased in hearts of mice suffering from myocarditis compared to blood of myocarditis mice or blood of controls. The same phenomenon could be observed for CD4⁺ CD73⁺ and CD8⁺ CD73⁺ T cells (figure 16B). The percentage of CD39⁺ B cells was very high and nearly the same in in the heart and blood of myocarditis mice as well as in blood of control mice (figure 16A). In contrast,

nearly no CD73⁺ B cells could be detected in the heart or blood of mice suffering from myocarditis as well as in blood of control mice (figure 16B). Based on these findings it is evident that upregulation of CD39 and CD73 on T cells infiltrating the heart is not restricted to acute myocardial injury, but can also be observed in a chronic cardiac disease model.

6.6. Characterization of Foxd1^{Cre/+}/CD73^{fl/fl} mice

In the second part of my thesis I focused on the role of CD73 on fibroblasts/ pericytes and on tubular cells in the kidney after IRI. It is well known from the literature, that renal CD73 is expressed by tubular luminal membranes on the brush border line, fibroblasts and mesangial cells, but until now the role of CD73 in AKI and tissue remodeling remains still unclear [326].

6.6.1. Kidney function of Foxd1^{Cre/+}/CD73^{fl/fl} mice after acute kidney injury

To study the function of CD73 on fibroblasts/ pericytes after injury, Foxd1^{Cre/+}/CD73^{fl/fl} mice and CD73^{fl/fl} control littermates were subjected to subthreshold ischemia conditions of 20' unilateral IRI by occlusion of renal pedicels. For quantification of kidney function, contralateral uninjured kidneys were removed on day 13. Mice were euthanized on day 14 and injured kidneys as well as blood were collected. Kidneys were analyzed for size, collagen formation, matrix deposition, myofibroblast transformation and immune cell infiltration. Quantification of plasma creatinine levels was used for measurement of kidney function (figure 17A).

As shown in figure 17B, ratio of kidney to body weight of kidneys isolated from CD73^{fl/fl} control littermates was the same between uninjured (C) and injured (I) kidneys. Interestingly, injured kidneys of mice lacking CD73 on fibroblasts/ pericytes were significantly smaller than uninjured contralateral kidneys. Moreover, kidney function of Foxd1^{Cre/+}/CD73^{fl/fl} mice was impaired 14d after IRI compared to controls as assessed by increased plasma creatinine levels (figure 17C). Taken together, this data gave first evidence that loss of CD73 on fibroblasts/ pericytes is related to shrinking kidney size due to injury and reduced kidney function 14d after IRI.

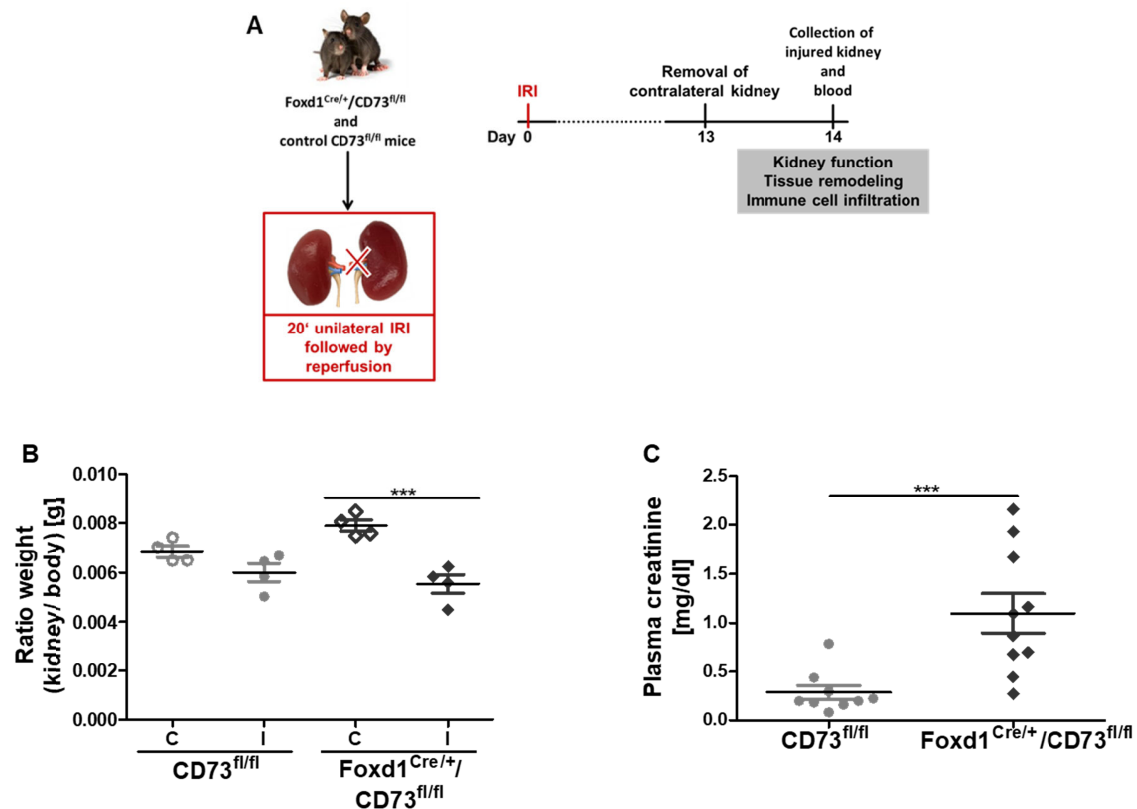


Fig. 17: Scheme of the experimental procedure (A), kidney size (B) and function (C) of Foxd1^{Cre/+}/CD73^{fl/fl} mice and CD73^{fl/fl} control littermates after IRI. A) Mice were subjected to 20' unilateral IRI (day 0). Uninjured contralateral kidneys were removed on day 13 for quantification of kidney function on day 14. Mice were euthanized on day 14d and injured kidneys as well as blood were collected. Kidneys were analyzed for function, tissue remodeling and immune cell infiltration. B) Mice were subjected to AKI as described previously. To measure kidney function, uninjured kidneys were removed on day 13. Mice were euthanized on day 14 and injured kidneys as well as blood were collected. C) Ratio of kidney to body weight of kidneys isolated from Foxd1^{Cre/+}/CD73^{fl/fl} mice and CD73^{fl/fl} control littermates 14d (resp. 13d) after IRI. Data represent mean \pm SD (n = 4; *** p \leq 0.001). C = contralateral; I = injured. C) Plasma creatinine levels of Foxd1^{Cre/+}/CD73^{fl/fl} mice and CD73^{fl/fl} control littermates 14d after IRI. Data represent mean \pm SEM (n=9-10; *** p \leq 0.001). Image by noBacs.com (by: Erma Simon).

6.6.2. Collagen formation and matrix deposition in Foxd1^{Cre/+}/CD73^{fl/fl} mice after acute kidney injury

Next, we were wondering whether reduced kidney size and function in mice lacking CD73 on fibroblasts/ pericytes after AKI is related to increased scar formation and matrix deposition. To this end uninjured and injured kidneys of Foxd1^{Cre/+}/CD73^{fl/fl} mice and CD73^{fl/fl} control littermates were stained using Masson's trichrome staining 14d (resp. 13d) after IRI to display collagen formation and matrix

deposition. In addition, we used the colorimetric hydroxyproline assay to quantify the collagen concentration of kidney tissue since hydroxyproline is a major component of collagen [323].

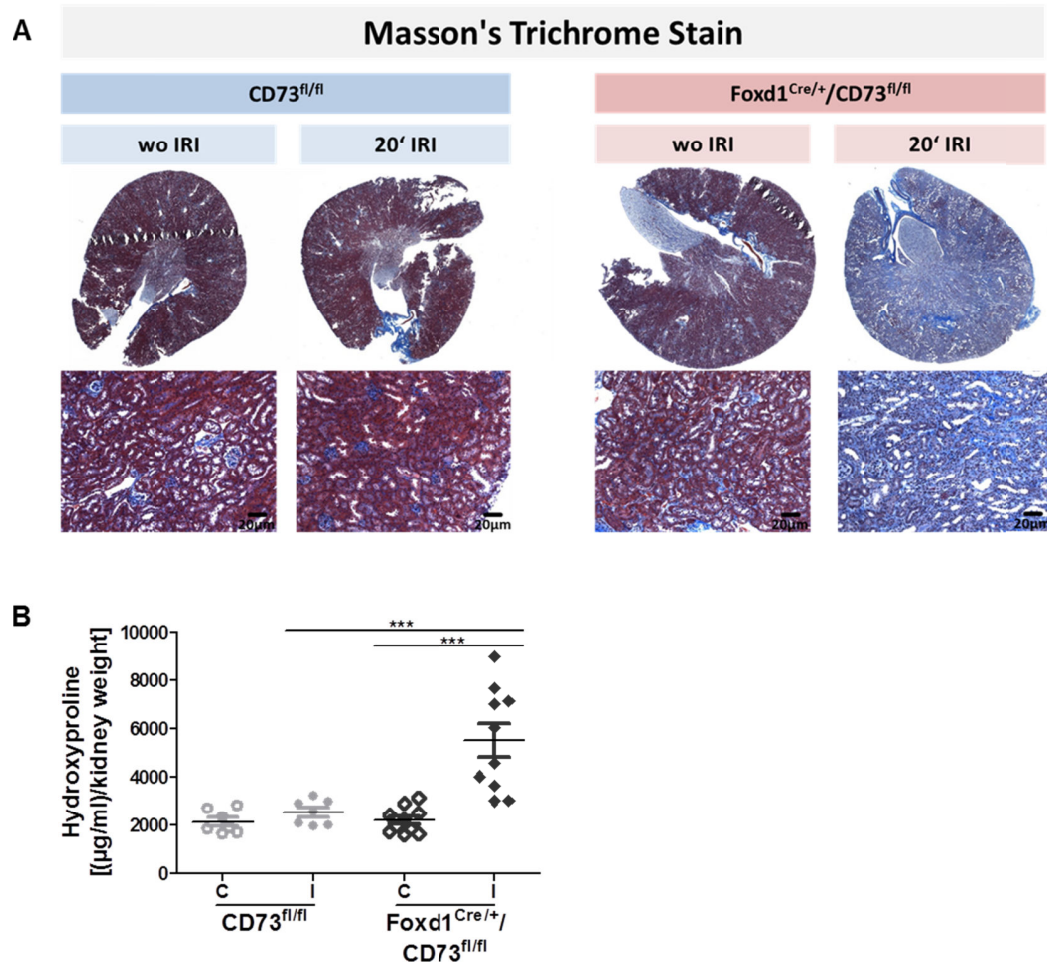


Fig. 18: Masson's trichrome staining of kidneys sections (A) and quantification of the hydroxyproline concentration (B) of Foxd1^{Cre/+}/CD73^{fl/fl} mice and CD73^{fl/fl} control littermates after IRI. For Masson's trichrome staining and quantification of hydroxyproline concentrations kidney sections were used, which were isolated 14d (resp. 13d) after IRI of Foxd1^{Cre/+}/CD73^{fl/fl} mice and CD73^{fl/fl} control littermates. A) Tissue sections of uninjured (wo IRI) and injured (20' IRI) kidneys from Foxd1^{Cre/+}/CD73^{fl/fl} mice and CD73^{fl/fl} control littermates were fixed in 10% formalin. Collagen formation and matrix deposition is shown using Masson's trichrome staining (blue). B) Quantification of collagen concentration of uninjured contralateral (C) and injured (I) kidneys from Foxd1^{Cre/+}/CD73^{fl/fl} mice and CD73^{fl/fl} control littermates using hydroxyproline assay. Data represent mean \pm SEM (n=6-10; *** p \leq 0.001). C: control; I: injured.

In Masson's trichrome staining, collagen and dead tubular cells appear in blue, nuclei are in black and cytoplasm of intact cells is stained in magenta. As shown in figure 18A, in the representative picture of

uninjured contralateral kidneys isolated from $Foxd1^{Cre/+}/CD73^{fl/fl}$ mice and $CD73^{fl/fl}$ control littermate glomeruli are stained in blue and intact tubular cells appear in magenta. The tissue is organized without extensive collagen formation in between the cells. After IRI, structural integrity of kidneys isolated from controls is still intact, whereas kidneys isolated from mice lacking CD73 on fibroblasts/ pericytes were stained predominantly in blue because of cellular destruction and collagen formation. Moreover, the tissue appears unorganized and disrupted. Our findings could be confirmed by quantification of collagen concentration using a hydroxyproline assay (figure 18B). The hydroxyproline formation was unchanged in uninjured contralateral kidneys isolated from $CD73^{fl/fl}$ control littermate compared to kidneys, which were subjected to 20' IRI. As expected, hydroxyproline concentration was the same in uninjured contralateral kidney of mice deficient for CD73 on fibroblasts/ pericytes compared to controls, but became significantly increased after IRI. In summary, these data show that decreased kidney size and function of mice lacking CD73 on fibroblasts/ pericytes 14d after IRI is associated with increased collagen formation and matrix deposition, whereas kidneys of control littermates seems to recover.

6.6.3. Myofibroblast transformation in $Foxd1^{Cre/+}/CD73^{fl/fl}$ mice after acute kidney injury

Next, we tested whether increased collagen expression in $Foxd1^{Cre/+}/CD73^{fl/fl}$ mice after injury is due to uncontrolled fibroblast/ pericyte proliferation and transformation. To examine the role of CD73 in controlling myofibroblast transformation, RNA was isolated from kidneys of $Foxd1^{Cre/+}/CD73^{fl/fl}$ mice and control littermates 14d (resp. 13d) after IRI and tested for myofibroblast marker, *Acta2* (α -SMA) and *Col3a1* (collagen III). Moreover kidney sections were stained for PDGFR- β , collagen III and DAPI using immunofluorescence analysis.

As shown in figure 19A, no differences could be detected in the expression levels of *Acta2* and *Col3a1* in uninjured kidneys of $Foxd1^{Cre/+}/CD73^{fl/fl}$ mice and control littermates. Interestingly, both genes were found to be upregulated only in injured kidneys of mice lacking CD73 on fibroblasts/ pericytes after IRI, whereas no upregulation was detected in kidneys of control littermates. Moreover, the area occupied by PDGFR- β -immunoreactive fibroblasts/ pericytes (red) was increased in the injured kidney of mice deficient for CD73 on fibroblasts/ pericytes compared to controls (figure 19B). Concomitant with these findings collagen III expression (green) was upregulated after IRI in mice lacking CD73 on fibroblasts/pericytes. Taking together, analysis of marker for increased fibroblast/ pericyte activity and myofibroblast transformation gave first evidence that CD73 and the formation of adenosine is important in controlling cell proliferation and matrix deposition.

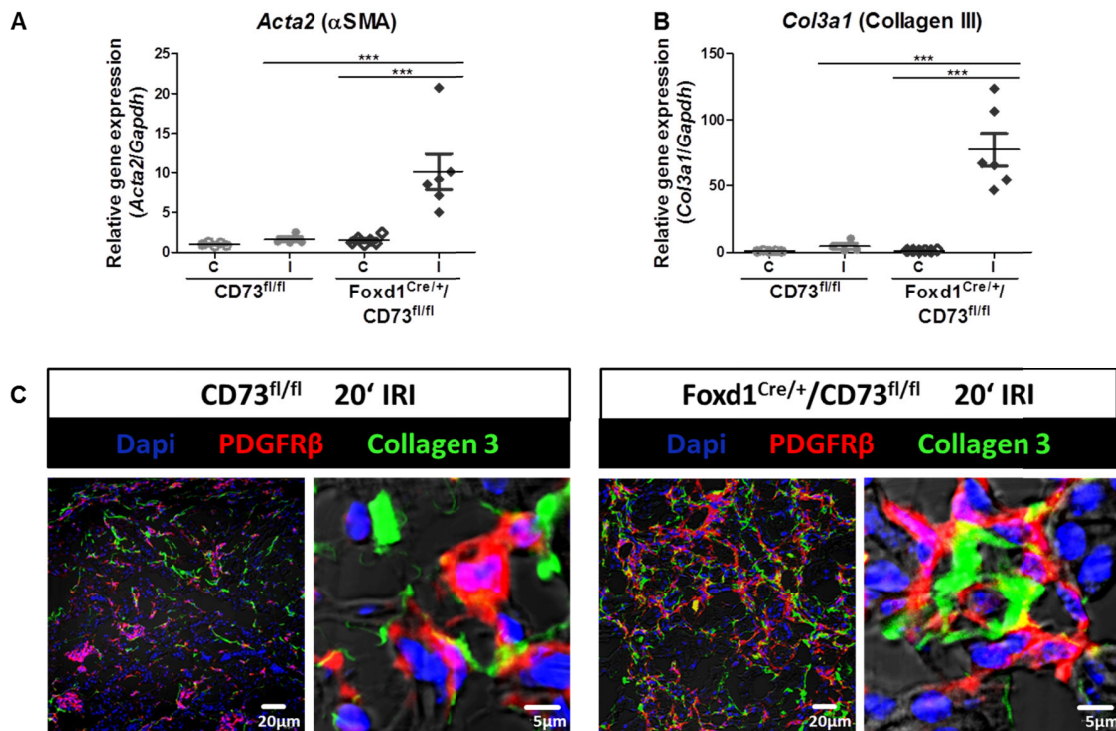


Fig. 19: Gene expression (A and B) and immunofluorescence analysis (B) for myofibroblast marker of kidney sections isolated from Foxd1^{Cre/+}/CD73^{fl/fl} mice and CD73^{fl/fl} control littermates after IRI. For RNA isolation and immunofluorescence analysis kidney sections were used, which were isolated 14d (resp. 13d) after IRI of Foxd1^{Cre/+}CD73^{fl/fl} mice and CD73^{fl/fl} control littermates. A and B) Expression levels of myofibroblast marker (*Acta2* and *Col3a1*) were quantified by qPCR and normalized to *Gapdh*. Data represent mean \pm SEM (n=5-6; *** p \leq 0.001). C: control; I: injured; SMA: smooth muscle actin. B) Fibroblasts/ pericytes and myofibroblasts, marked by PDGFR- β expression, were stained in red. Collagen III deposition is shown in green. Cell nuclei were stained in blue using DAPI. Scale bars: 20 μ m left panel; 5 μ m right panel.

6.6.4. Immune cell infiltration in Foxd1^{Cre/+}/CD73^{fl/fl} mice after acute kidney injury

As a lack of CD73 on fibroblasts/ pericytes led to increased cell proliferation, myofibroblast transformation and enhanced matrix deposition, further analysis of immune cell infiltration should identify a possible role of CD73 in controlling immune cell activation and resolution of inflammation. To this end, kidney sections of Foxd1^{Cre/+}/CD73^{fl/fl} mice and CD73^{fl/fl} control littermates isolated 14d (resp. 13d) after IRI were analyzed for renal immune cells using immunofluorescence. Tissue sections were stained for ER-TR7 to identify fibroblast populations, immune cells were localized using F4/80 antibodies. Moreover, RNA was generated from kidney sections of mice lacking CD73 on fibroblasts/ pericytes and controls isolated 14d (resp. 13d) after IRI to analyze for macrophage marker (*Il-1 β* , *Arg1*, *Chil3*, *Mcr1*, *Msr1*, *Nos2* and *Tnf- α*) [327].

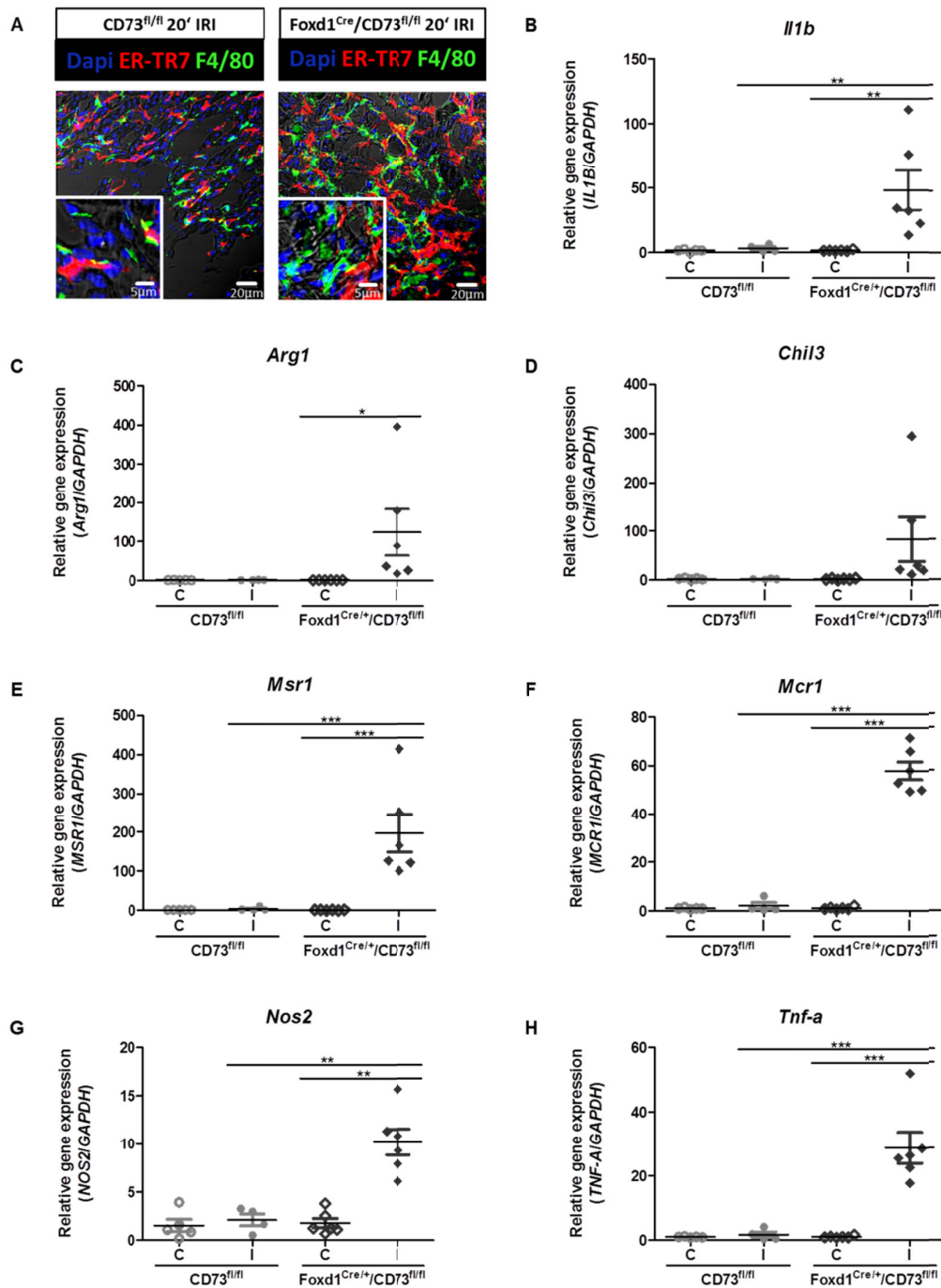


Fig. 20: Immunofluorescence (A) and gene expression analysis (B) for renal immune cells of kidney sections isolated from Foxd1^{Cre/+}/CD73^{fl/fl} mice and CD73^{fl/fl} control littermates after IRI. For RNA isolation and immunofluorescence analysis kidney sections were used, which were isolated 14d (resp. 13d) after IRI of Foxd1^{Cre/+}/CD73^{fl/fl} mice and CD73^{fl/fl} control littermates. A) Fibroblasts, marked by ER-TR7 expression, were stained in red. F4/80⁺ immune cells are shown in green. Cell nuclei were stained in blue using DAPI. Scale bars: 5 μm; 20 μm. B) Gene expression levels of macrophage marker (*Il-1β*, *Arg1*, *Chil3*, *Mcr1*, *Msr1*, *Nos2* and *Tnf-α*) were quantified by qPCR and normalized to *Gapdh*. Data represent mean ± SEM (n=5-6; * p ≤ 0.05; ** p ≤ 0.01; *** p ≤ 0.001). C: control; I: injured.

From the representative immunofluorescence pictures in figure 20A it can be seen that the area occupied by F4/80-immunoreactive immune cells (green) was increased in injured kidneys of mice lacking CD73 on fibroblasts/ pericytes compared to control littermates. As mentioned before, we confirmed our findings (figure 19B) and showed that the area covered by ER-TR7-immunoreactive fibroblasts (red) was increased after IRI in mice deficient for CD73 on fibroblast/ pericytes. Quantitative qPCR analysis for macrophage marker of kidney sections isolated from $Foxd1^{Cre/+}/CD73^{fl/fl}$ mice compared to controls led to the same conclusion (figure 20B – H). The immune cell fraction was increased in injured kidneys of mice lacking CD73 on fibroblasts/ pericytes in comparison to injured kidneys of control littermates after IRI. Expression levels of *Il-1 β* , *Arg1*, *Mcr1*, *Msr1*, *Nos2* and *Tnf- α* were significantly increased in $Foxd1^{Cre/+}/CD73^{fl/fl}$ mice compared to controls (figure 21B, C, E – H). Gene expression of *Chil3* tended to be upregulated (figure 21D). Expression levels of *Il-1 β* , *Arg1*, *Chil3*, *Mcr1*, *Msr1*, *Nos2* and *Tnf- α* were not affected in uninjured kidneys of $Foxd1^{Cre/+}/CD73^{fl/fl}$ mice and controls. In summary, these data show that after injury the fraction of F4/80⁺ immune cells was increased in mice lacking CD73 on fibroblasts/ pericytes. Moreover, markers for macrophages were upregulated on gene expression levels in the injured tissue of $Foxd1^{Cre/+}/CD73^{fl/fl}$ mice.

6.6.5. 5'NT treatment of $Foxd1^{Cre/+}/CD73^{fl/fl}$ mice after acute kidney injury

Since lack of CD73 on fibroblasts/ pericyte influenced healing processes, scar formation and immune cell resolution of the kidney after IRI, we wondered whether substitution of CD73 can rescue kidney function by administration of 5'NT. To this end $Foxd1^{Cre/+}/CD73^{fl/fl}$ mice were treated with soluble CD73 (5' NT) starting at day 2 or day 4 after 20' IRI to ensure that treatment of mice is restricted to tissue healing processes and does not affect initial injury. Soluble 5'NT was administered via mini pumps to allow constant drug infusion. Mini pumps containing 5'NT (5 U/mouse per day) or PBS only (control) were implanted at day 2 or day 4 after 20' of unilateral IRI (day 0) (figure 21). Uninjured contralateral kidneys were removed on day 13. Mice were euthanized after 14d and kidney function as well as hydroxyproline content was measured.

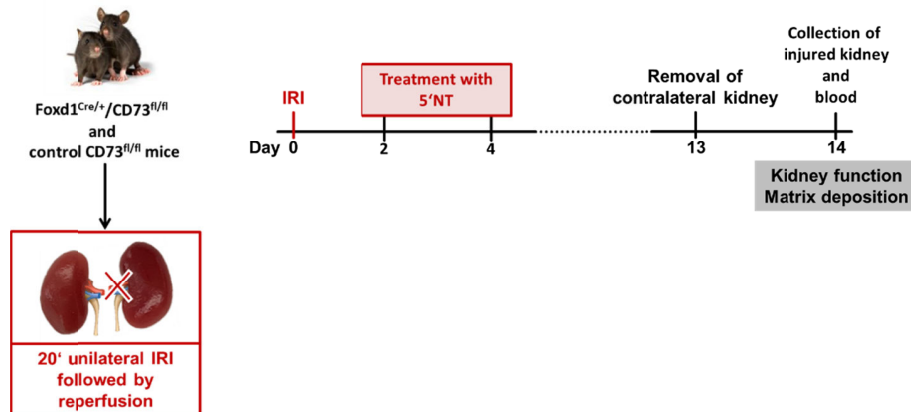


Fig. 21: Scheme of the experimental procedure. Mice were subjected to 20' unilateral IRI (day 0). Mini pumps containing soluble 5'NT or PBS only (control) were implanted at day 2 or day 4 after IRI. Contralateral uninjured kidneys were collected on day 13. Mice were euthanized 14d after IRI and kidney function or hydroxyproline content was measured. Image by noBacks.com (by: Erma Simon).

From data summarized in figure 22A, it can be seen that without treatment plasma creatinine levels were significant higher in Foxd1^{Cre/+}/CD73^{fl/fl} mice compared to CD73^{fl/fl} control littermates 14d after IRI, similar to experimental series performed before (figure 17C). Hydroxyproline concentrations of injured kidneys in mice lacking CD73 on fibroblasts/ pericytes were increased compared to injured kidneys of controls and uninjured contralateral kidney of both groups (figure 22B). Again, the extend of hydroxyproline concentration was similar to data shown before in figure 18B. The hydroxyproline content of uninjured kidneys was similar between all tested groups. Interestingly, treatment of animals with 5' NT starting on day 2 decreased plasma creatinine concentrations to basal levels in mice lacking CD73 on fibroblasts/ pericytes comparable to control littermates (figure 22A). Foxd1^{Cre/+}/CD73^{fl/fl} mice, which were treated starting on day 4, showed a tendency in reduced plasma creatinine levels compared to CD73^{fl/fl} controls. As shown in figure 22B, corresponding to kidney function, hydroxyproline concentrations decreased in injured kidneys of mice lacking CD73 on fibroblasts/ pericytes after treatment with 5'NT starting on day 2 compared to untreated mice. Surprisingly, the hydroxyproline content was elevated in control mice treated with 5'NT starting on day 2. Although we observed decreased plasma creatinine levels in Foxd1^{Cre/+}/CD73^{fl/fl} mice treated with 5'NT starting on day 4, hydroxyproline concentrations seemed unchanged compared to untreated mice. Hydroxyproline concentrations of littermate controls were on basal levels like uninjured kidneys. From the representative pictures of Masson's trichrome staining in figure 22C it can be seen that without infusion of 5'NT kidney sections isolated from injured kidneys of Foxd1^{Cre/+}/CD73^{fl/fl} mice showed increased collagen formation and matrix deposition 14d after IRI compared to injured kidneys of CD73^{fl/fl} control littermates. Corresponding to reduced plasma creatinine levels and hydroxyproline

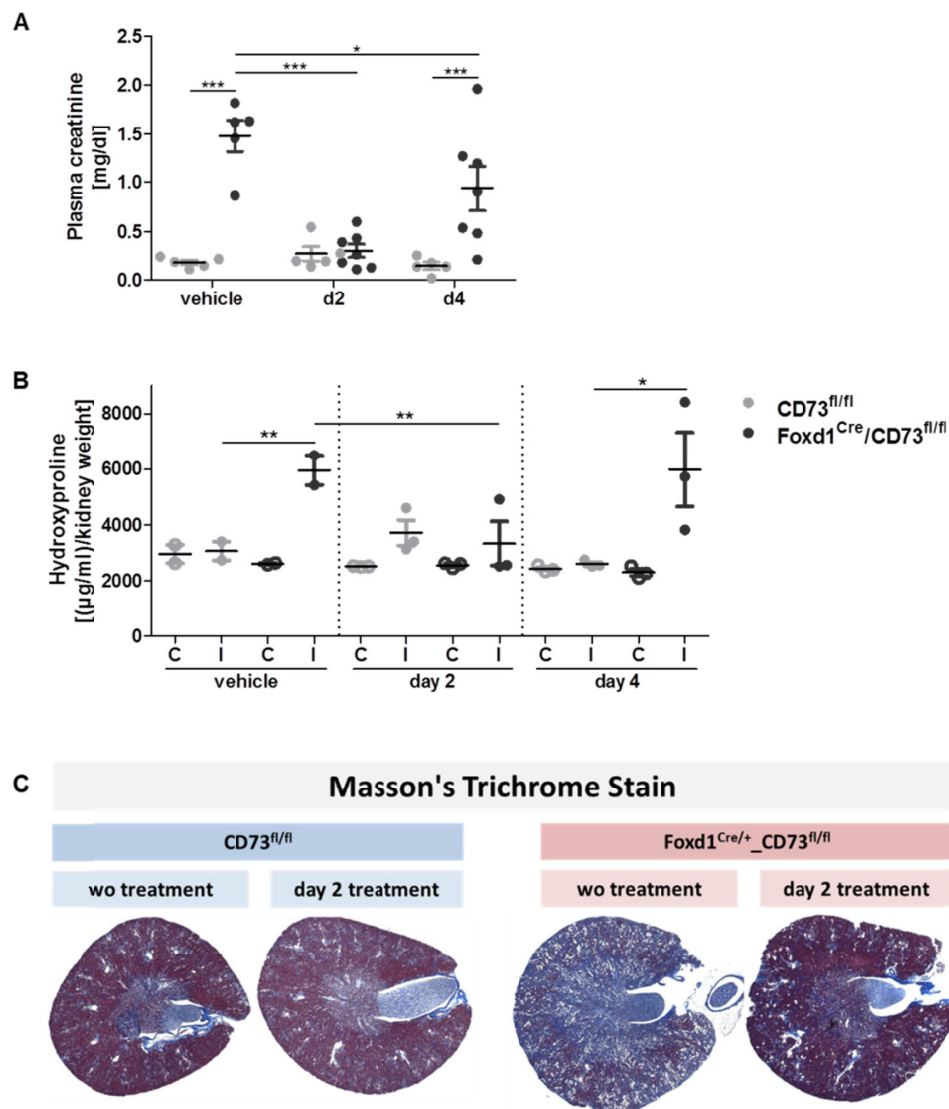


Fig. 22: Kidney function (A), quantification of hydroxyproline concentration (B) and Masson's trichrome staining of kidneys sections (C) isolated from Foxd1^{Cre/+}/CD73^{fl/fl} mice and CD73^{fl/fl} control littermates after IRI. Mice were subjected to 20' unilateral IRI (day 0). Mini pumps containing 5'NT or PBS only (control) were implanted at day 2 or day 4 after IRI. To measure kidney function, uninjured kidneys were removed on day 13 and mice were euthanized on day 14 to isolate injured kidneys and blood. A) Plasma creatinine levels of Foxd1^{Cre/+}/CD73^{fl/fl} mice and CD73^{fl/fl} control littermates 14d after IRI. Treatment with 5'NT started on day 2 or day 4. Vehicles received PBS only. Data represent mean \pm SEM (n=6-10; * $p \leq 0.05$; *** $p \leq 0.001$). B) Quantification of collagen concentration of uninjured contralateral (C) and injured (I) kidneys isolated from Foxd1^{Cre/+}/CD73^{fl/fl} mice and CD73^{fl/fl} control littermates using hydroxyproline assay. Data represent mean \pm SD (n=2-3; * $p \leq 0.05$; ** $p \leq 0.01$). C: control; I: injured. C) Representative pictures of injured kidneys isolated 14d after IRI from Foxd1^{Cre/+}/CD73^{fl/fl} mice and CD73^{fl/fl} control littermates. Both groups were treated either with 5'NT starting on day 2 after IRI (day 2 treatment) or PBS only (wo treatment). Tissue was fixed in 10% formalin. Collagen formation and matrix deposition is shown using Masson's trichrome staining (blue).

concentrations, collagen formation and matrix deposition was reduced by administration of 5'NT in mice lacking CD73 on fibroblasts/ pericytes starting on day 2 as depicted by less blue staining of kidney sections. Littermate controls seemed to be unchanged. In summary, our data show that kidney function in mice lacking CD73 on fibroblast/ pericytes can be rescued by administration of 5'NT starting on day 2 comparable to littermate controls. These findings were associated with reduced collagen formation and matrix deposition.

6.7. *Ex vivo* fibroblast cell culture

Our findings demonstrate the importance of CD73 on fibroblasts/ pericytes in tissue remodeling and wound healing in kidney IRI. Loss of CD73 on fibroblast/ pericytes led to increased cell proliferation, myofibroblast transformation and collagen expression in Foxd1^{Cre/+}/CD73^{fl/fl} mice 14d after tissue injury. Since CD73 seems to control fibroblast/ pericyte proliferation we were wondering if this effect can be observed in *ex vivo* isolated fibroblast cell culture. To this end fibroblasts were isolated from kidneys of wildtype and CD73^{-/-} mice and cultured *in vitro* for further analysis.

6.7.1. Cell proliferation of *ex vivo* wildtype and CD73^{-/-} kidney fibroblasts

To study cell proliferation of *ex vivo* wildtype and CD73^{-/-} fibroblasts, cells were isolated from kidneys, cultured and analyzed using the colorimetric MTT assay.

As summarized in figure 23, after 1 day of cultivation the number of viable cells and metabolic activity was the same between wildtype and CD73^{-/-} fibroblast cells starting cell culture with 2500, 5000 or 10000 cells. Already after 2 days of cultivation, CD73^{-/-} fibroblasts of each starting condition (2500, 5000 and 10000 cells) showed significantly increased oxidoreductase enzymes activity compared to wildtype fibroblasts associated with increased cell numbers. This proliferation difference was maintained also on day 4, although there was a tendency, that the differences starting with 2 500 cells increased over time. Taking together, these findings revealed that CD73 on fibroblasts prevents cell proliferation.

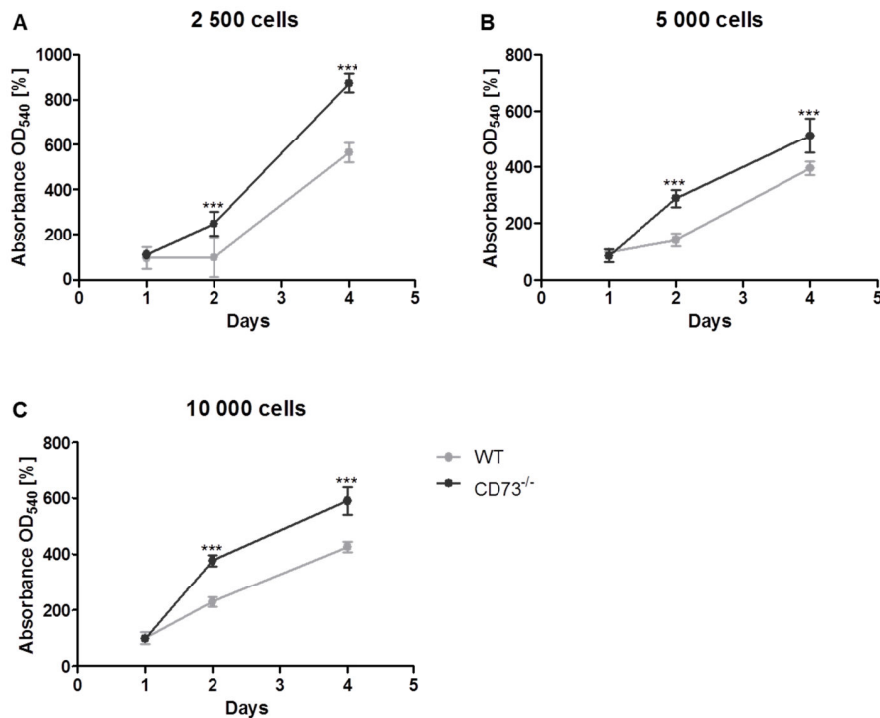


Fig. 23: Cell proliferation of *ex vivo* wildtype and CD73^{-/-} kidney fibroblasts. Fibroblasts were isolated from kidneys of wildtype and CD73^{-/-} mice. Cell proliferation was analyzed using MTT assays. For analysis passage 3 of each cell line was used. Cells were plated in different concentrations of 2 500 (A), 5 000 (B) and 10 000 (C) cells per well for 4 days. Proliferation was measured on day 1, 2 and 4. For each cell concentration the absorbance (OD₅₄₀) of wildtype fibroblast (day 1) was set to 100%. Data represent mean \pm SD (n=5; *** p < 0.001).

6.8. Characterization of Pepck^{Cre/+}/CD73^{fl/fl} mice

Sung et al. already reported that the major renal CD73-expressing cell populations are proximal straight tubules, cortical interstitial fibroblast-like cells and mesangial cells [309]. Since CD73 on tubular cells was shown to be important in mediating initial injury after mild IRI, its role in fibrosis formation remains unclear [309].

6.8.1. Kidney function and collagen formation of Pepck^{Cre/+}/CD73^{fl/fl} mice after acute kidney injury

To analyze the role of CD73 on tubular cells, IRI studies in Pepck^{Cre/+}/CD73^{fl/fl} mice were performed according to the same experimental setup as described before for Foxd1^{Cre/+}/CD73^{fl/fl} mice. Briefly,

Pepck^{Cre/+}/CD73^{fl/fl} mice and Pepck^{Cre/+} control littermates were subjected to subthreshold ischemia conditions of 20' by unilateral occlusion of renal pedicels. Uninjured contralateral kidneys were removed on day 13. Mice were euthanized on day 14 and injured kidneys as well as blood was collected.

As summarized in figure 24A, kidney function was impaired in mice lacking CD73 on tubular cells as shown by significantly increased plasma creatinine concentrations 14d after IRI compared to littermate controls. Hydroxyproline concentration was unchanged in uninjured contralateral kidneys isolated from Pepck^{Cre/+} control littermates compared to kidneys, which were subjected to 20' IRI (figure 24B). Interestingly, the hydroxyproline content was the same in uninjured contralateral kidneys of Pepck^{Cre/+}/CD73^{fl/fl} mice compared to controls, but was significantly increased after IRI. Taken together, loss of CD73 on tubular cells also resulted in reduced kidney function as assessed by increased plasma creatinine concentrations and upregulation of collagen formation. A comparison of kidney function and collagen formation between Foxd1^{Cre/+}/CD73^{fl/fl} and Pepck^{Cre/+}/CD73^{fl/fl} mice shows that both models with either an specific knockout on fibroblast/ pericytes or on tubular cells resulted in increased plasma creatinine levels (Foxd1^{Cre}/CD73^{fl/fl}: mean = 1,1 mg/dl and Pepck^{Cre}/CD73^{fl/fl}: mean = 1,1 mg/dl) and enhanced hydroxyproline concentrations (Foxd1^{Cre}/CD73^{fl/fl}: mean = 5495 µg/ml and Pepck^{Cre}/CD73^{fl/fl}: mean = 4839 µg/ml) to the same extent.

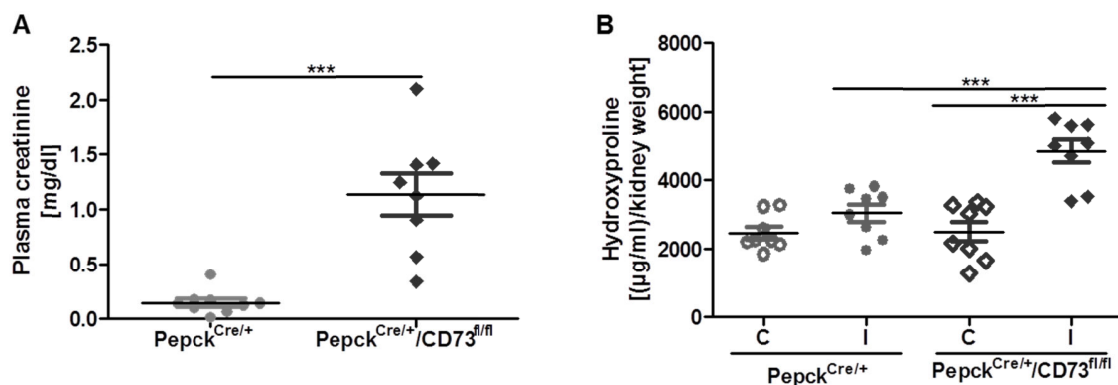


Fig. 24: Kidney function (A) and quantification of hydroxyproline concentration (B) of Pepck^{Cre/+}/CD73^{fl/fl} mice and Pepck^{Cre/+} littermate controls after IRI. To measure kidney function, uninjured kidneys were removed on day 13 and mice were euthanized on day 14 to isolate injured kidneys and blood. A) Plasma creatinine levels of Pepck^{Cre/+}/CD73^{fl/fl} mice and Pepck^{Cre/+} littermate controls 14d after IRI. Data represent mean \pm SD (n = 8; *** p \leq 0.001). B) Quantification of collagen concentration of uninjured contralateral (C) and injured (I) kidneys isolated 14d (resp. 13d) after IRI from Pepck^{Cre/+}/CD73^{fl/fl} mice and Pepck^{Cre/+} littermate controls using hydroxyproline assay. Data represent mean \pm SEM (n = 8; *** p \leq 0.001). C: control; I: injured.

6.9. Initial injury in $Foxd1^{Cre/+}/CD73^{fl/fl}$ and $Pepck^{Cre/+}/CD73^{fl/fl}$ mice after acute kidney injury

As the outcome of kidney remodeling and function after 14d following 20' unilateral IRI was the same between mice lacking CD73 on fibroblast/ pericytes or on tubular cells indicating that CD73 is important in tissue healing processes we investigated whether CD73 function is also a crucial mediator of initial injury after IRI. To analyze initial injury, $Foxd1^{Cre/+}/CD73^{fl/fl}$, $Pepck^{Cre/+}/CD73^{fl/fl}$ mice and control littermates were subjected to 20' unilateral IRI and at the same time point nephrectomy of the contralateral kidney was performed to measure kidney function by plasma creatinine levels. Mice were euthanized after 24h and blood was collected (figure 25A).

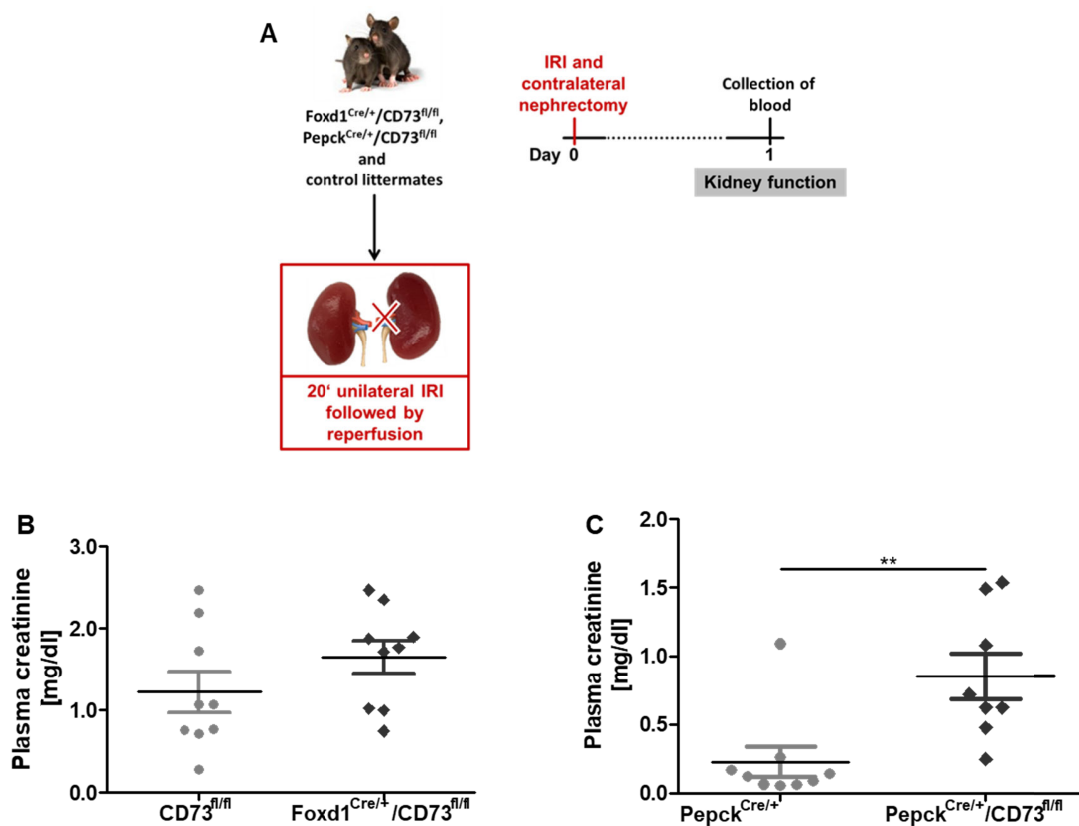


Fig. 25: Scheme of the experimental procedure (A), kidney function of $Foxd1^{Cre/+}/CD73^{fl/fl}$ (B), $Pepck^{Cre/+}/CD73^{fl/fl}$ mice (C) and littermate controls after IRI. A) Mice were subjected to 20' unilateral IRI and at the same time nephrectomy of the contralateral kidney was performed (day 0). Mice were euthanized 1 day after IRI and kidney function was measured. B and C) To analyze kidney function uninjured contralateral kidneys were removed in parallel to 20' unilateral IRI. Mice were euthanized after 1 day and blood was collected for quantification of plasma creatinine concentrations. Data represent mean \pm SEM (n = 9-10; ** p \leq 0.01). Image by noBacs.com (by: Erma Simon).

As it can be seen in figure 25B, no significant differences of plasma creatinine concentrations could be detected between $Foxd1^{Cre/+}/CD73^{fl/fl}$ and $CD73^{fl/fl}$ control littermates 24h after IRI. However, plasma creatinine levels were significantly increased in $Pepck^{Cre/+}/CD73^{fl/fl}$ mice compared to $Pepck^{Cre/+}$ control littermates 24h after IRI (figure 25C). In conclusion, kidney function was only affected in the absence of CD73 on tubular cells, while plasma creatinine concentrations showed no significant differences in mice lacking CD73 on tubular cells 24h after IRI suggesting an important role for CD73 on tubular cells in promoting initial injury.

7. Discussion

The present work addressed the modulatory role of purinergic signaling after IRI in two organs, the heart and the kidney. In the heart, signaling of extracellular adenosine formed by CD73 was investigated on T cells migrating into the infarcted heart using T cell specific CD73^{-/-} mice. In the kidney, the role of CD73-derived adenosine formed by tissue fibroblasts/ pericytes and tubular cells was studied with respect to tissue remodeling using a newly generated fibroblast/ pericyte-specific CD73^{-/-} mouse as well as tubular cell-specific CD73^{-/-} mice.

7.1. Myocardial infarction – the medical dimension

Despite the advances in preventive strategies and treatment of IRI, interruption of blood supply and subsequent damage induced by reperfusion continues to be associated with high morbidity and mortality [2]. Since years ischemic heart disease is the leading course of death in the past decades [328]. Moreover cardiac circulatory disorders – including MI – cause the highest costs for prevention, treatment and care of patients among all other diseases in Germany [329]. The development of novel therapeutic strategies for better prevention or treatment depend upon a critical understanding of the molecular mechanisms, that occur after injury and contribute to the formation of fibrosis known to be associated with chronic organ diseases. In the first part of my thesis I focused on the role of the purinergic signaling on cardiac infiltrating T cells after MI to analyze how T cells contribute to wound healing and organ remodeling by metabolic purinergic reprogramming.

7.2. Purinergic signaling and its contribution to healing processes in the heart

In previous studies we could show that under normal conditions the leukocyte fraction was about 2.3×10^3 resident leukocytes per mg tissue in the unstressed murine heart with the most prominent fraction being APCs (CD11b⁺, CD11c⁺, F4/80⁺, MHCII⁺) followed by B cells, monocytes and T cells. CD73 was highly expressed by circulating and resident cardiac lymphoid cells, whereas CD39 was predominately found on myeloid cells. The total number of immune cells within the heart increased to 9.1×10^3 leukocytes per mg heart tissue 3d after MI, with the main fraction consisting of granulocytes and monocytes followed by CD8⁺ T cells, CD4⁺ T cells, NK cells and APCs. Interestingly, CD73 was significantly upregulated on invading granulocytes and T cells [306]. Studies of the CD73 promoter revealed at least one binding site for HIF-1, the hypoxia regulated transcription factor. Inhibition of

HIF-1 α expression led to significant inhibition of hypoxia-regulated CD73 expression [330]. In view of these findings, the observed MI-induced upregulation of CD73 on infiltrating immune cells can be explained by the ischemia/ hypoxia-induced activation of the transcription factor HIF-1 α . We hypothesized that extracellular ATP released by apoptotic/ necrotic cells or immune cells activated after IRI are preferentially degraded by CD39 present on myeloid cells, while the formation of immunosuppressive adenosine is mainly formed by CD73 present on granulocytes and lymphoid cells, which becomes upregulated due to hypoxia after invading into the injured heart.

Subsequent studies pointed out the critical importance of CD73 in regulating cardiac remodeling after MI. Cardiac function was deteriorated in CD73^{-/-} mice after IRI compared to control littermates. Mice lacking CD73 showed increased myocardial edema formation and persistence of cardiac immune cell subsets within the cardiac tissue. Impaired healing was paralleled by a MI-driven immune response with increased TNF- α and IL-17 levels as well as decreased TGF- β and IL-10 synthesis [307]. Mice lacking CD73 displayed expansion of the infarct area accompanied by an immature scar formation and diffuse ventricular fibrosis. Interestingly, bone marrow transplantation studies showed that transplantation of wildtype bone marrow into CD73^{-/-} mice fully restored ventricular function indicating that CD73 present on immune cells is a major determinant promoting cardiac healing [307].

7.3. The destructive and protective role of T cells in myocardial infarction

The role of T cell in IRI is controversially discussed in the literature and depends on the organ, which is affected, as well on the T cell subtype and on the composition of surrounding immune cells and their inflammatory status. Under normal conditions the number of lymphocytes is less than 10 000 per milligram of tissue, whereas B cells are twice as prevalent as T cells. After MI, induced by permanent coronary artery occlusion, B cell and T cell levels increase 5 – 10-fold with a peak of lymphocytes around day 7, most likely as a result of recruitment because no lymphocyte proliferation has been reported until now [331]. The response of T cells to MI include activation and proliferation in heart-draining lymph nodes of both subtypes, conventional and Foxp3⁺ regulatory CD4⁺ T cells [99]. In the injured myocardium conventional CD4⁺ T cells are mainly Th1 polarized after IRI, as indicated by increased IFN- γ expression, whereas Th17- and Th2-differentiated T cells are barely detectable in infarcted myocardium [331].

First experimental evidence that T cells are involved in tissue remodeling after MI was demonstrated by a study using Rag1^{-/-} mice. Deficiency of lymphocytes in mice led to significantly smaller infarct sizes compared to control mice. Interestingly, depletion of CD4⁺ T cells in mice, but not CD8⁺ T cell-

depleted mice, showed a significantly decreased infarct size. Adoptive transfer of CD4⁺ T cells reversed protection in Rag1^{-/-} mice, whereas reconstitution of Rag1^{-/-} mice by CD4⁺ T cells isolated from IFN- γ ^{-/-} mice did not increase myocardial infarct size, indicating CD4⁺ T cells contribute to IRI by IFN- γ expression [269; 332]. In contrast, CD4⁺ T_{reg} cells, which rapidly accumulated in murine hearts following IRI, have been shown to improve cardiac healing after MI. Adoptive transfer of *in vitro* activated T_{reg} cells decreased myocardial injury, whereas transfer of non-activated T cells had no effect. The protective effect was thought to be related to CD39 expression in T_{reg} cells [333].

7.3.1. Role of T cells in mediating healing processes and tissue recovery after myocardial infarction

In a recently published study we could show that T cells infiltrating the heart after MI play a major role in orchestrating wound healing, tissue recovery and immune cell resolution. In contrast to the debate that T cells play a destructive role in MI we gave evidence that CD73 on T cells is important for cardiac protection following IRI. CD73 deficiency on T cells increased tissue fibrosis and led to deterioration of cardiac function after MI to the same extend compared to global CD73^{-/-} mice [308]. As mentioned previously that the major cell populations expressing CD73 in the injured heart consist of granulocytes and T cells, the present study showed an identical functional response to IRI of global CD73^{-/-} mice and mice lacking CD73 only on T cells, which places T cells in a central metabolic position in adenosine formation [306]. Based on these findings it was hypothesized that T cells infiltrating the heart after IRI upregulate CD73 expression and thereby regulate tissue healing and immune cell responses.

7.3.2. Metabolic reprogramming in T cells after infiltrating into the infarcted heart

Since the number of T cells within the heart after MI is rather small, we assumed that adenosine production by T cells may be accelerated by metabolic reprogramming of extracellular purine catabolism during T cell activation after infiltrating into the heart. We found first evidence that the microenvironment of the injured heart importantly shapes CD4⁺ and CD8⁺ T cell response by accelerating the rate of extracellular nucleotide metabolism. CD4⁺ and CD8⁺ T cells, which were isolated from the heart 3d after MI, upregulated expression of Cx37, Cx43 and Panx1 hemichannels known to be involved in ATP and NAD release compared to CD4⁺ and CD8⁺ T cells, which were isolated from the blood. Interestingly, Cx43 was not detectable in circulating CD4⁺ and CD8⁺ T cells,

but became upregulated after infiltrating into the injured heart [308]. Moreover, ATP-degrading ectoenzymes, such as CD39, ENPP1 and ENPP3, as well as NAD-hydrolyzing enzymes, including CD38, CD157, ENPP1 and ENPP3, were found to be upregulated after CD4⁺ and CD8⁺ T cell activation following IRI compared to unstimulated blood cells [308]. On the one hand expression levels of enzymes, which are involved in the breakdown of nucleotides to adenosine, such as CD73 and ADK, were increased in infiltrating CD4⁺ and CD8⁺ T cells. On the other hand expression of ADA, which catalyzes the breakdown of adenosine to inosine, as well as expression of the adenosine transporter ENT1 became upregulated after CD4⁺ and CD8⁺ T cell stimulation and infiltration into the site of injury [308]. In summary, acceleration of nucleotide metabolism by increased hydrolysis of pro-inflammatory ATP and pro-apoptotic NAD may serve a dual purpose by reducing the biological half live of ATP and thereby attenuating activation of various P2 receptors expressed on cardiac T cells. In the case of NAD, ADP-ribosylation of the P2X7 receptors is reduced, which is likely to preserve T cell function under conditions when more anti-inflammatory adenosine is formed. Moreover, accumulation of adenosine in the microenvironment promotes anti-inflammatory effects via signaling by AdoR.

Next, we were wondering if the observed change in gene expression levels of enzymes, channels and transporter in T cells after infiltrating into the injured heart also result in increased protein synthesis as evidenced by purine nucleotide breakdown. Since the number of cells, which can be isolated from the heart, is too small for functional studies, CD4⁺ and CD8⁺ T cells were isolated from lymph nodes and stimulated *in vitro* to mimic T cell activation after IRI. *In vitro* stimulated CD4⁺ and CD8⁺ T cells were then incubated either with ATP and NAD to study nucleotide metabolism. The results of ATP and NAD hydrolysis were consistent with the observations of gene expression analysis, that showed upregulation of relevant enzymes. Activated CD4⁺ and CD8⁺ T cells hydrolyzed ATP more rapidly than unstimulated cells leading to increased ADP, AMP and slightly elevated adenosine levels (figure 8A). Similar, NAD degradation was accelerated by stimulated CD4⁺ and CD8⁺ T cells compared to unstimulated controls resulting in higher ADP, AMP and adenosine concentrations (figure 8B). Taking together, ATP and NAD released by apoptotic/ necrotic cardiomyocytes and activated immune cells becomes degraded mainly by cardiac infiltrating T cells, which leads to dampening of the danger signal and diminishing of P2 receptor signaling. On the one hand AMP generated by activated T cells is hydrolyzed by CD73, which becomes upregulated after migrating of T cells to the site of injury, leading to increased adenosine concentrations. On the other hand AMP catalyzed by monocytes, invading the heart at early stages after MI, may reach T cells by diffusion, thereby contributing to adenosine accumulation. As a consequence high adenosine concentrations in the cardiac interstitial space promote wound healing and tissue recovery by signaling via AdoR on surrounding cells in a paracrine fashion. It is well known from the literature that signaling via the A_{2A}R stimulates anti-

inflammatory effects in various cellular systems including immune cells [334; 335]. In addition, stimulation of the A_{2B}R was shown to be associated with suppression of pro-inflammatory TNF- α release from neutrophils and macrophages, inhibition of superoxide production in neutrophils, upregulation of anti-inflammatory IL-10 production in macrophages and activation of alternative (M2) macrophages [276; 278; 279; 336]. Under normal conditions activation of the A_{2A}R and the A_{2B}R by accumulation of adenosine in the microenvironment promotes anti-inflammatory effects. Loss of CD73 in mice under conditions of MI increased TNF- α and reduced IL-10 production. In addition there was a reduction in the M1 macrophage-driven phenotype, which can be well explained by impaired A_{2A}R and A_{2B}R signaling [306; 307]. Thus, suppression of immune cell activation and initiation of tissue repair is critically determined by adenosine produced by CD73 in T cells.

The ectoenzyme CD39 is generally considered to be the most prominent ATP-hydrolyzing enzyme and the first important step regulating ATP half-life after IRI and numerous studies support the concept that CD39 is even the rate limiting step in ATP degradation [161]. To assess the contribution of CD39 on overall ATPase activity on activated T cells compared to unstimulated cells, we analyzed ATP hydrolysis of *in vitro* stimulated CD4⁺ and CD8⁺ T cells isolated from lymph nodes of CD39^{-/-} mice compared to cells isolated from wildtype mice. Quite unexpected we made the observation that ATPase activity of activated CD4⁺ and CD8⁺ T cells was nearly the same between cells isolated from wildtype and CD39^{-/-} mice leading to similar levels of ADP, AMP and adenosine, while nearly no enzyme activity was measurable in unstimulated CD4⁺ and CD8⁺ T cells of wildtype and CD39^{-/-} mice (figure 9A and B). Among the various inhibitors tested for NTPDase1 – 3 and ENPP1 (POM1 and POM144), alkaline phosphatases (Lemivasol) and acid prostate phosphatase (BABPA) only POM144 strongly inhibited ATPase activity to the same extent in the presence or absence of CD39 of activated CD4⁺ and CD8⁺ T cells [308]. Gene expression analysis of several ATPases, such as NTPDase1 – 8, ENNP1 – 3, alkaline phosphatases (ALP) 1, 3 and 6, prostatic acid phosphatases (ACPP) and tartrate-resistant acid phosphatase (TRAP) in CD4⁺ and CD8⁺ T cells isolated from lymph nodes of CD39^{-/-} mice showed persistent expression of ENPP1 in unstimulated and activated cells, while there was a downregulation of other ATPases detectable [308]. Flow cytometry analysis of CD39 and ENPP1 on *in vitro* stimulated lymphoid CD4⁺ and CD8⁺ T cells isolated from wildtype mice confirmed that both enzymes were upregulated after T cell activation, which can explain the increased ATPase activity [308]. The same observation was made on CD4⁺ and CD8⁺ T cells, which were isolated from the heart and blood of wildtype mice 7d after MI [308]. In summary, these findings gave first evidence that under normal conditions both enzymes, CD39 and ENPP, contribute to ATP hydrolysis. However, their fractional participation remains unclear. Since in global CD39^{-/-} mice, CD39 activity is fully compensated by ENPP1, this observation points to an important role of ENPP1 on activated T cells. The functional role

of ENPP1 on purine degradation has so far not been systematically explored. In future studies it would be certainly worthwhile to create mice lacking ENPP1 to analyze to what extent activated cells rely on this pathway and what the functional consequences are. It should be noted that in contrast to CD39, which breaks down ATP and ADP to AMP, ENPP1 degrades ATP directly to AMP and pyrophosphate. This may be functionally relevant in platelets, where ADP is known to be an important regulator in platelet aggregation and thrombus formation [337].

In the present study the possible participation of other enzymes aside of CD73 contributing to adenosine formation was investigated by measuring AMPase activity assessed by HPLC techniques. AMPase activity of T cells isolated from T cell specific CD73^{-/-} mice was found to be rather low comparable to AMPase activity of T cells isolated from the blood of wildtype mice (figure 10B). Cardiac infiltrating T cells isolated from wildtype mice showed a significantly increased AMPase activity compared to T cells isolated from the blood or to cardiac T cells lacking CD73. These results indicate that CD73 on T cells migrating to the heart is the major enzyme catalyzing AMP to adenosine suggesting a negligible contribution of alkaline phosphatases or other AMP-degrading enzymes.

7.3.3. Role of CD73 on T cells in mediating cytokine production

Since our data clearly demonstrated that metabolic reprogramming in T cells infiltrating into the heart after MI accelerated extracellular purine catabolism to adenosine, modulating wound healing and scar formation, it was important to answer the question, by which mechanism CD73 contributes to tissue recovery. To this end T cells were isolated 7d after MI from the heart of T cell specific CD73^{-/-} mice and wildtype controls and their cytokine secretion profile was measured. Interestingly, stimulated T cells lacking CD73 secreted predominantly pro-inflammatory and pro-fibrotic cytokines (figure 11). The production of IFN- γ and IL-17 was significantly increased compared to control cells. Moreover, the secretion of IL-2, IL-3 and IL-4 by CD73^{-/-} T cells also tended to be elevated after re-stimulation. In contrast, the release of IL-6 tended to be lower.

Although T cells constitute only a rather small cell population infiltrating the heart mainly during the later phase after MI, T cell-derived signals via macrophages and fibroblasts can importantly regulate inflammatory and reparative responses [87; 306; 338; 339]. The present study demonstrates that T cell-mediated formation of IL-2, IL-3, IL-4, IL-17 and IFN- γ is under the control of CD73-derived adenosine, which places infiltrating T cells in an important strategic position in orchestrating tissue recovery and resolution of inflammation. It was reported that IFN- γ mediates leukocyte attraction, macrophage activation and chemokine secretion, which triggers tissue damage and immune cell

infiltration [340]. As already mentioned above, reconstitution of mice lacking T cells by CD4⁺ T cells isolated from IFN- γ ^{-/-} mice decreased myocardial infarct size [269]. Moreover, IL-2 and IL-17 are known to be crucial mediators for cardiomyocytes promoting toxic effects and deficiency of IL-17 improved cardiac healing [341]. Additionally, IL-4 and IL-17 were found to be associated with activation of pro-fibrotic pathways stimulating fibroblast proliferation and pro-fibrotic gene expression [342]. For IL-2 and IL-3 effects on cardiac rhythm have been documented resulting in a complete cessation of spontaneous contractions of cardiomyocytes and a severe loss of myocyte inotropy [343]. The present study indicates that T cell polarization is imbalanced in T cells lacking CD73 tending to higher levels of Th1 cells secreting IFN- γ and IL-2 as well as of TH17 cells being the predominant source of IL-17 [344]. Imbalance of T cell subsets associated with increased levels of Th1 and Th17 cells are known to be involved in tissue destruction being key mediators of autoimmunity. In particular, IL-17 has been reported to induce a positive feedback loop perpetuating the primary immune response and promoting a pro-inflammatory milieu leading to excessive tissue destruction [345]. Based on these observations our previous results in infarcted hearts of mice lacking CD73, which displayed high numbers of neutrophils, can be explained by Th1/ Th2 cell imbalance and increased Th17 cell distribution resulting in neutrophil recruitment [307; 345].

7.3.4. Contribution of the A_{2A}R and the A_{2B}R to wound healing and immune response

Adenosine as well as specific agonists and antagonists for the four adenosine receptor subtypes (A₁R, A_{2A}R, A_{2B}R and A₃R) play an important role in several key physiological and pathophysiological processes, including the regulation of vascular tone, immune response, inflammation, thrombosis and angiogenesis [346]. In the present study the expression of all four AdoR was measured in CD4⁺ and CD8⁺ T cells isolated from cardiac tissue and blood 3d after MI (figure 12A and B). Interestingly, the A_{2B}R was not expressed in circulating CD4⁺ or CD8⁺ T cells, but became significantly upregulated after infiltrating into the injured myocardium after MI. The A_{2A}R was expressed in CD4⁺ and CD8⁺ T cells isolated from the blood as well as in cardiac cells, while mRNA expression was decreased after migration into the heart resulting in almost equally expression levels for A_{2A}R and A_{2B}R. In further studies we could show that the A_{2B}R also became upregulated in granulocytes and APCs after infiltrating into the injured myocardium compared to cells isolated from the blood [308]. Cardiomyocytes in the unstressed heart expressed mainly the A₁R, followed by A_{2A}R, A_{2B}R and A₃R. A_{2A}R expression was significantly downregulated 3d after MI, whereas the A_{2B}R was upregulated, similarly to what was observed in CD4⁺ and CD8⁺ T cells [308]. Studies of A_{2A}R expression suggested that gene expression is modulated by the receptor itself in hypoxia after receptor activation. During

early events of hypoxia expression of the $A_{2A}R$ became upregulated. Stimulation of the receptor resulted in downregulation of gene expression, suggesting that the receptor modulates its own expression during hypoxia by feedback mechanisms [347]. The promoter sequence of the $A_{2B}R$ contains a functional hypoxia-responsive region including a functional binding site for HIF within the promoter [348]. Moreover, studies in an epithelial cell line gave first evidence that the $A_{2B}R$ is intracellular at rest and stimulation with adenosine induces vesicular trafficking and recruitment of the $A_{2B}R$ to the membrane [349]. It is also conceivable that extracellular adenosine, which is formed by CD73 after IRI, may induce upregulation of the $A_{2B}R$ by stimulating trafficking of intracellular vesicles containing $A_{2B}R$ s to the outer membrane as a quick response immediately after ischemia. Long term exposure of the $A_{2B}R$ to stimuli has been reported to trigger receptor internalization and recycling [350]. To counteract reduced receptor signaling, hypoxia initiates HIF-controlled gene expression and thereby transcriptional upregulation of the $A_{2B}R$ for long term signaling promoting resolution of inflammation.

The number of T cells, which can be isolated from the heart, is very small and too small for more detailed functional studies and a systematic cytokine analysis. We have therefore developed an *in vitro* model mimicking T cell activation after cell infiltration into the heart to further study the function of the $A_{2A}R$ and the $A_{2B}R$. To this end CD4⁺ T cells were isolated from lymph nodes, which showed a basal expression of the $A_{2A}R$, and no $A_{2B}R$ expression (figure 13). However, T cell activation - like in the *in vivo* situation - led to robust upregulation of the $A_{2B}R$, while the $A_{2A}R$ was still expressed. In this experimental model, treatment with either an $A_{2A}R$ (CGS-21680) or an $A_{2B}R$ agonist (BAY 60-6583) resulted nearly in an overall reduction of cytokine secretion, notably of IL-1 β , IL-2, IL-3, IL-5, IL-10, IL-13, IL17 and IFN- γ (figure 14). In general stimulation with the $A_{2B}R$ agonist seemed to be more efficacious than the $A_{2A}R$ agonist. Repression of TNF- α was slightly stronger by activation of the $A_{2A}R$ compared to the $A_{2B}R$. Secretion of IL-4 was only reduced by treatment with the $A_{2B}R$ agonist, while the $A_{2A}R$ agonist had negligible effects. IL-6 formation tended to be induced by $A_{2B}R$ signaling, however, with high standard deviations, whereas the $A_{2A}R$ reduced IL-6 secretion. When comparing our *in vitro* results with those obtained from cardiac T cells lacking CD73 isolated from the injured heart (figure 11), it is obvious that both the $A_{2A}R$ and $A_{2B}R$ contributed to the formation IL-2, IL-3, IL-4, IL17 and IFN- γ by reducing cytokine secretion. Moreover, the observed overall reduction of cytokine secretion was associated with decreased T cell activation as was assessed by CD69 flow cytometry (figure 15) [325]. *In vitro* stimulation of lymphoid T cells resulted in increased synthesis of CD69, which was found to be downregulated after treatment with either an $A_{2A}R$ (CGS-21680) or an $A_{2B}R$ agonist (BAY 60-6583). However, a word of caution is required when interpreting the results for BAY 60-6583, which is known to act as a partial agonist for the $A_{2B}R$ and may have unspecific side

effects [351; 308]. In a recent study we have therefore used NECA, a high affinity general AdoR agonist, which reduced IFN- γ . Reduction of IFN- γ was reversed by a specific A_{2B}R antagonist (PSB-603), indirectly confirming that A_{2B}R activation mediates anti-inflammatory activity on T cells [308]. In summary, our data suggests that cytokine production by activated T cells can be mediated by CD73-derived adenosine in an autocrine fashion signaling via the A_{2A}R and the A_{2B}R.

The interaction between the different AdoR expressed on one cell may be complex. Several studies indicated that AdoRs are able to form homo- or heterodimers thereby importantly influencing the outcome of adenosine signaling. Heterodimerization of the A_{2A}R with the A₁R, which are coupled to opposite signaling pathways, allows adenosine to modulate striatal glutamatergic neurotransmission by providing a concentration dependent switch mechanism to either inhibit or stimulate glutamate release [352]. Fluorescence resonance energy transfer (FRET) studies of the A_{2A}R and the A_{2B}R provided new evidence for A_{2A}R/ A_{2B}R heterodimerization, but the mechanistically relevance remains still unclear [353]. It could be possible that A_{2A}R/ A_{2B}R heterodimerization results in synergetic signaling, whereby the high-affinity A_{2A}R potentiates low-affinity A_{2A}R signaling promoting healing processes in tissue due to stress events like IRI. However, there is clearly a need for more specific A_{2B}R agonist to examine the role of the A_{2B}R in modulating tissue healing after IRI. Additionally, a more specific A_{2B}R agonist could provide a novel tool for therapy of MI. Since the low-affinity A_{2B}R requires high adenosine concentrations for activation, signaling via the A_{2B}R is restricted to tissues offering high adenosine levels, which can be found in the heart after MI. A_{2B}R agonist treatment of patients with MI could address specific A_{2B}Rs, which become upregulated in cardiac infiltrating immune cells promoting anti-inflammatory effects.

7.4. Purinergic signaling in chronic inflammation of the heart

The results presented so far clearly demonstrate the importance of the purinergic signaling, especially of CD73, in acute injury models, such as MI. It was therefore of interest to know whether similar effects can be observed in chronic disease models, such as myocarditis. Flow cytometry of immune cells isolated from hearts of mice suffering from myocarditis again revealed upregulated numbers of cells positive for CD39 and CD73 suggesting that adenosine could play a role in chronic inflammation (figure 16A and B). The percentage of CD4⁺ CD39⁺ and CD8⁺ CD39⁺ T cells was significantly increased in hearts of mice suffering from myocarditis compared to blood of myocarditis mice or blood of controls. The same phenomenon could be observed for CD4⁺ CD73⁺ and CD8⁺ CD73⁺ T cells. The percentage of CD39⁺ B cells was very high and nearly the same in in the heart and blood of

myocarditis mice as well as in blood of control mice. In contrast, nearly no CD73⁺ B cells could be detected in the heart or blood of mice suffering from myocarditis as well as in blood of control mice.

The number of B cells and T cells positive for CD39 was high in myocarditis mice suggesting that the metabolism of ATP is accelerated promoting anti-inflammatory effects. Moreover, the percentage of CD4⁺ CD73⁺ and CD8⁺ CD73⁺ T cells was found to be increased underlining the assumption of accelerated adenosine synthesis to promote healing processes. However, little is known on the role of CD39 and CD73 in myocarditis. ATP signaling via P2Y or P2X receptors has been reported to promote chronic inflammation associated with asthma and atherosclerosis [354]. Upregulation of CD39 could be associated with accelerated ATP signaling in chronic heart diseases leading to increased formation of AMP and thus adenosine. Further studies are needed, however, to substantiate this view, in particular determine the contribution of adenosine in chronic inflammatory heart diseases and the AdoR subtype involved.

7.5. Acute kidney injury – the medical dimension

AKI describes a complex clinical disorder, which is still associated with severe morbidity and mortality leading to approx. 2 million deaths annually worldwide [355–358]. Moreover, those patients with the most severe form of AKI, requiring renal replacement therapy, have a mortality rate of 50 – 80% [358]. However, patients recovering from AKI remain dialysis-dependent or are left with severe renal impairment [359; 360]. A critical understanding of the molecular mechanism contributing to tissue injury and fibrosis formation known to be associated with the development of CKD is needed for development of novel therapeutic strategies. In the second part of my thesis I investigated the role of CD73 on fibroblasts/ pericytes and tubular cells in the kidney after IRI.

7.6. CD73 expression in renal tissue and its contribution to injury

Kidney CD73 is expressed by different cell types within the renal tissue, including tubular luminal membranes on the brush border line, fibroblasts and mesangial cells, but until now the role of CD73 in IRI and tissue remodeling remained unclear [325]. In the literature contribution of CD73 after IRI in the kidney is controversially discussed. Preconditioning comprising short, repeated cycles of ischemia and reperfusion resulted in increased renal CD73 mRNA, CD73 activity and total adenosine formation, which was associated with subsequent protection from IRI [361]. Moreover, CD73-derived adenosine and signaling via the A_{2B}R mediated kidney protection in diabetic nephropathy [362]. Deficiency of

CD73 and lack of adenosine formation led to development of autoimmune renal injury and reduced renal function [363]. In contrast, studies of rats using a specific inhibitor for CD73 (α,β -methyleneadenosine 5'-diphosphate (AMPCP)) demonstrated protection of the kidney after IRI [364]. Additionally, mild ischemia in CD73^{-/-} mice was associated with reduced injury compared to wildtype mice [365]. The contrasting results of adenosine-mediated tissue protection could be depended on the distribution of CD73 in the renal microenvironment, because physical barriers, fluid flows, enzymatic and transporter activities limit the access of adenosine across renal interstitial compartments.

Tissue protection may be dependent on the proximity of CD73 expression in the major site of injury. Indeed, CD73 expression was found to be the highest in proximal tubular epithelial cells and cortical type 1 fibroblast-like cells in the deep cortex outer medulla region where injury due to IRI is the most severe [326]. Sung et al. demonstrated that deletion of CD73 on tubular cells showed exacerbated injury 24h after IRI comparable to global CD73^{-/-} mice. Deficiency of CD73 on other cell types, including fibroblasts/ pericytes, mesangial cells, macrophages and dendritic cells resulted in small or no increases in tissue injury compared to control mice when subjected to mild ischemia [309]. These data indicated that the small differences, which could be observed in the extend of IRI between mice lacking CD73 on tubular cells and global CD73^{-/-} mice, is due to CD73 expression on cortical fibroblasts and/or mesangial cells. Since these observations clearly demonstrated the importance of CD73 in mediating early injury after IRI in renal tissue, its contribution to renal fibrosis in healing processes remained unclear.

7.6.1. Role of CD73 on fibroblasts/ pericytes in promoting matrix deposition due to myofibroblast transformation and immune cell resolution

Since the observations of Sung et al. demonstrated that under mild ischemia conditions CD73 on fibroblasts/ pericytes had only a small impact on tissue injury 24h after IRI, I have addressed the question whether CD73 on fibroblasts/ pericytes may play an important role in promoting wound healing and fibrosis formation after AKI [309]. Therefore, mice lacking CD73 on fibroblasts/ pericytes were subjected to subthreshold ischemia conditions of 20' and kidney function was analyzed after 14d. Quite unexpected we made the observation that lack of CD73 on fibroblasts/ pericytes resulted in reduced kidney function as assessed by plasma creatinine levels compared to control littermates (figure 17B). Reduced kidney function was associated with shrinking of the injured kidney, whereas the size of the contralateral kidney was significantly increased, which could be explained by the attempt of the body to compensate kidney function (figure 17A). Moreover, collagen formation and matrix deposition

was increased in the injured kidney of fibroblast/ pericyte-specific CD73^{-/-} mice compared to uninjured contralateral kidneys or control littermates (figure 18A and B). Interestingly, injured kidneys of controls nearly totally recovered after IRI, which can be explained by the threshold ischemia of 20' used in this study. We found that lack of CD73 on fibroblasts/ pericytes was associated with increased deposition of collagen, which was most likely due to increased myofibroblast transformation. Expression of myofibroblast marker, such as *Acta2* (α -SMA) and *Col3a1* (Collagen III), were upregulated in injured kidneys isolated from fibroblast/ pericyte-specific CD73^{-/-} mice compared to contralateral kidneys or control littermates (figure 19A and B). Increased expression of myofibroblast marker was associated with expansion of the area occupied by PDGFR- β ⁺ and ER-TR7⁺ cells, indicating increased fibroblast proliferation (figure 19C and 20A). In summary these findings indicate that loss of CD73 on fibroblasts/ pericytes leads to increased proliferation of fibroblasts and myofibroblast transformation associated with extensive fibrosis formation and matrix deposition resulting in shrinking of kidney size and functional loss.

These conclusions could be confirmed and extended by *ex vivo* fibroblast cell culture. Renal fibroblasts lacking CD73 showed increased proliferation rates compared to cells, which were isolated from kidneys of wildtype mice (figure 23A – C). Our data suggest that CD73 on fibroblasts/ pericytes are an important mediator after AKI in regulation proliferation of fibroblasts and transformation to myofibroblasts and thereby reducing excessive matrix deposition. Studies in mice globally lacking CD73 spontaneously develop renal fibrosis by 6 months of age as indicated by glomerulitis, tubulitis, and tubulointerstitial fibrosis [363]. Marker for pro-inflammatory macrophages (CD11b⁺ GR1⁺) and CD8⁺ T cells infiltrating into the interstitium were increased as well as serum levels of pro-inflammatory cytokines [366]. These observations clearly demonstrated the impact of fibrosis formation in renal tissue, immune cell infiltration and functional outcome.

Next, we were interested whether CD73 on fibroblasts/ pericytes regulate immune cell resolution after IRI. Gene expression analysis of injured kidneys isolated from fibroblast/ pericyte-specific CD73^{-/-} mice showed that pro-inflammatory marker, such as *Il-1 β* and *Tnf- α* , were upregulated compared to contralateral uninjured kidneys or kidneys of control littermates (figure 20A and H). Moreover, expression of macrophage marker, including *Il-1 β* , *Tnf- α* as well as *Arg1*, *Chil3*, *Mcr1*, *Msr1* and *Nos2*, were also upregulated in kidneys of fibroblast/ pericyte-specific CD73^{-/-} mice, which were subjected to IRI (figure 20B – H). In addition, the area occupied by F4/80⁺ cells was increased after AKI in kidneys lacking CD73 on fibroblasts/ pericytes, indicating extensive macrophage infiltration or proliferation (figure 20A). It has been shown that pro-inflammatory M1 macrophages develop in early events after IRI due to ATP release into the microenvironment [16; 367]. In contrast, CD73-derived adenosine is

known to inhibit M1 macrophage activity by activation of the $A_{2A}R$ reducing pro-inflammatory cytokine release [259; 368; 369]. Moreover, $A_{2B}R$ signaling mediated a phenotype switch of M1 to M2 macrophages, which leads to generation of an anti-inflammatory milieu by producing cytokines, including Il-10 and Il-4 [279; 370]. Interestingly, preliminary data showed that depletion of macrophages in mice lacking CD73 on fibroblasts/ pericytes after IRI recovered kidney function [manuscript in preparation]. In summary, our data suggests that loss of CD73 on fibroblasts/ pericytes enhanced matrix deposition due to fibroblast proliferation and myofibroblast transformation. Moreover, extensive macrophage infiltration and proliferation associated with the generation of a pro-inflammatory milieu, which most likely relates to the lack of CD73-derived adenosine.

7.6.2. Treatment of mice lacking CD73 on fibroblast/ pericytes with soluble CD73 restored kidney function after acute kidney injury

Provided loss of extracellular adenosine is responsible for the increased matrix deposition and impaired resolution of inflammation leading to the assumption that administration of soluble CD73 (5' NT) should restore kidney function. Several publications have already shown that administration of soluble 5'NT is an important mediator for restoration of organ function in different ischemic models. In a mouse model of ischemic preconditioning (IP), Grenz et al. could show that kidney protection by IP could be restored in CD73^{-/-} mice by treatment with soluble 5'-NT [361]. The recent literature is mainly focusing on short term effects and acute injury that occur after IRI, but until now nothing is known whether it could be possible to rescue kidney function in a long term fibrosis model by substitution of soluble CD73 in global or specific CD73 deficient mice. To ensure that treatment of mice is restricted to tissue healing processes and does not affect initial injury, administration of 5'NT was started on day 2 and 4 after IRI. We found that treatment of fibroblast/ pericyte-specific CD73^{-/-} mice with 5'NT starting on day 2 fully recovered kidney function comparable to littermate controls (Figure 22A). Moreover, collagen formation and matrix deposition was decreased in injured kidneys of mice lacking CD73 on fibroblast/ pericytes compared to injured kidneys of fibroblast/ pericyte-specific CD73^{-/-} mice without treatment (Figure 22B and C). Starting treatment on day 4, plasma creatinine levels tended to be reduced in fibroblast/ pericyte-specific CD73^{-/-} mice associated with better kidney function (Figure 22A), while collagen formation was still high (figure 22B). These data clearly show that changes in the local concentration of CD73-derived adenosine mediated the observed pathology. Generally, administration of 5'NT starting on day 4 led to results with high standard deviations, which might be due to the use of mouse strain with a mixed background. Note, that controls used in this study were littermates of the same breeding, thereby including all aspects of strain differences in susceptibility.

The A_{2B}R was shown to be the predominant receptor on isolated renal fibroblasts, which becomes upregulated due to fibrosis. Interestingly, antagonism of the A_{2B}R on renal fibroblasts limited the expression of pro-collagen mRNA. Moreover, A_{2B}R signaling mediated induction of IL-6 contributed to renal fibrogenesis. Mice lacking adenosine deaminase (ADA) exhibit chronically elevated adenosine levels leading to development of glomerulosclerosis, interstitial fibrosis and collagen deposition in renal tissue, which could be attenuated by treatment with a selective A_{2B}R inhibitor (PSB-1115) suggesting that A_{2B}R signaling promotes renal injury via IL-6 secretion [371]. Nevertheless, contrary results have been reported for A_{2B}R contribution in renal tissue fibrosis. Although IL-6 signaling was implicated in A_{2B}R-driven fibrosis, other studies have shown that mice lacking IL-6 were not protected from fibrosis in the same injury model [372]. Negative contribution of A_{2B}R signaling was shown to take place in chronic inflammation, which may actually promote fibrosis [366]. Interestingly, for lung disease the two sides of A_{2B}R signaling could be identified. Whereas A_{2B}R activation revealed anti-inflammatory effects during acute lung injury, pro-fibrotic contributions could be demonstrated during chronic disease stages [373]. These observations highlight that the intensity and duration of A_{2B}R signaling can mediate protective or detrimental influences to tissue recovery. To which extent this applies to acute or chronic kidney diseases is presently unclear. The model used in the present study was designed for acute renal injury, and in this model stimulation of the A_{2B}R may promote tissue healing and recovered kidney function.

7.6.3. Role of CD73 on tubular cells in healing processes of the kidney

Sung et al. already demonstrated the importance of CD73 on tubular cells in mediating initial injury after mild IRI, but its role in fibrosis formation remained unclear [309]. Mice lacking CD73 on tubular cells were subjected to threshold ischemia comparable to the experiments described previously for fibroblast/ pericyte-specific CD73^{-/-} mice. In tubular cell-specific CD73^{-/-} mice we made similar observations as in mice lacking CD73 on fibroblast/pericytes: kidney function in tubular cell-specific CD73^{-/-} mice was decreased compared to control littermates as assessed by plasma creatinine levels (figure 24A). Reduced kidney function was associated with increased collagen formation in the injured kidney of mice lacking CD73 on tubular cells compared to contralateral uninjured kidneys and controls (figure 24B).

Interestingly, CD73 expression levels are the highest in proximal tubule S3 segment epithelial cells, which are located at the primary site of injury in kidney following IRI [309]. CD73 was found to be higher in the outer medulla, an area more susceptible to IRI because of the sustained outer medullary

blood flow impairment after IRI, the energy demand and poor anaerobic respiratory capacity of the S3 segment and the extensive inflammatory cell infiltration at the outer medulla [119; 374–376]. Increased levels of CD73 at the brush border line of proximal tubular cells places the enzyme in a central metabolic position with significant functional consequences. The proximal tubule concentration of ATP ranges physiologically significant concentrations suggesting that the nucleotide is released by epithelial cells themselves [377]. Release of ATP into the lumen and the presence of apical P2 receptors as well as of enzymes involved in controlled nucleotide degradation places extracellular nucleotides in a position acting as important autocrine or paracrine regulators of tubular function by limiting solute transport and reducing proximal tubule energy requirements [377]. After IRI, high ATP concentrations accumulate in the urinary space mediated by apoptotic/ necrotic cells or stress-mediated processes [378; 379]. NTPDase2 (CD39L1) on proximal tubules degrades ATP and thereby provides substrates for other enzymes, including CD73, which further generates adenosine [380]. In the tubular space adenosine acts on A₁Rs and A_{2A}Rs present on proximal tubule cells promoting oxidant injury protection [381]. Moreover, it has been demonstrated that signaling via the A_{2A}R promotes kidney protection after AKI by inhibition of inflammatory cells [309; 382]. These observations go in line with the findings we made in our heart studies, in which A_{2A}R activation controlled T cell activity and cytokine secretion. In addition, transepithelial transport of luminal adenosine into the interstitial space mediated by nucleoside transporter modulates inflammation [294; 383].

In conclusion, lack of CD73 on both cell types, fibroblasts/ pericytes and tubular cells, leads to impaired renal function due to increased collagen formation when kidneys were subjected to subthreshold IRI. These observations provided strong evidence that CD73 in both systems is an important regulator for kidney protection and healing processes of renal tissue after IRI by regulating fibroblast activation as well as immune cell resolution by signaling via AdoRs. Sung et al. could demonstrate that global or tissue-specific loss of CD73 as well as inhibition of CD73 enzymatic activity increased susceptibility to IRI, whereas reconstitution of enzyme activity or upregulation of extracellular adenosine levels by inhibiting its breakdown or membrane transport in mice lacking CD73 provided protection from IRI [309]. In addition, here we found that administration of soluble CD73 rescued kidney function in mice lacking CD73 on fibroblasts/ pericytes. Our findings and the observations of Sung et al. support the hypothesis that CD73 and the formation of adenosine mediates kidney protection.

7.6.4. Potential interaction between fibroblasts/ pericytes and tubular cells in orchestrating cellular processes injury

An intriguing question is how CD73 on fibroblasts/ pericytes and tubular cells may interact with each other to promote proper tissue recovery. To address this question, both mouse models were subjected to the same subthreshold IRI conditions and kidney function was measured 24h thereafter to analyze early injury. Similar to the findings of Sung et al., kidney function of mice lacking CD73 on fibroblast/ pericytes was nearly the same to kidney function of control littermates, while tubular cell-specific CD73^{-/-} mice showed increased plasma creatinine levels (figure 25B and C). These findings are quite surprisingly, because fibroblast/ pericyte-specific CD73^{-/-} mice show nearly no loss of kidney function 24h after IRI, but the severeness of tissue damage after 14d was similar to tubular cell-specific CD73^{-/-} mice, which are more susceptible to IRI immediately after 24h. As described previously, it is known, that tubular cells are more susceptible to IRI, which could explain that mice lacking CD73 on tubular cells showed increased tissue damage resulting in reduced kidney function.

Based on these findings, I propose the following intercellular communication to explain kidney protection mediated via CD73-derived adenosine. It is generally believed that tubular cells are more susceptible to ischemia than fibroblasts. As a consequence, when ischemia hits the kidney, tubular cells are the first to be injured. When CD73 lacks on tubular cells, this leads to excessive tissue damage. Obviously, adenosine derived from fibroblasts/ pericytes is not sufficient to protect tubular cells. On the other hand, when CD73 is lacking on fibroblasts/ pericytes, there are no differences in initial injury. However, over time progressive fibrosis develops leading to severe tissue damage. Thus it appears that under control conditions adenosine derived from tubular cells and fibroblasts/ pericytes synergistically provide protection to tubular cells.

8. Conclusion

8.1. Purinergic signaling in myocardial infarction and acute kidney injury

The first part of this study clearly demonstrated the importance of CD73-derived adenosine formed by cardiac infiltrating T cells after MI in orchestrating wound healing by regulation of fibrosis and resolution of inflammation. T cells invading the injured heart undergo substantial purinergic metabolic reprogramming, that is associated with upregulation of the enzymatic machinery for accelerated hydrolysis of ATP and NAD released by apoptotic/ necrotic cardiomyocytes and by activated immune cells as well. Conversion of ATP and NAD by several enzymes, such as CD39, ENPP1 and 3, CD38 and CD157, results in the accumulation of AMP, the substrate for CD73. In a final step adenosine becomes generated by CD73, while our results clearly place T cells in a central metabolic position for adenosine formation. As summarized in figure 26, CD73-derived adenosine promotes anti-inflammatory effects by an autocrine and paracrine manner via signaling by the $A_{2A}R$ and the $A_{2B}R$.

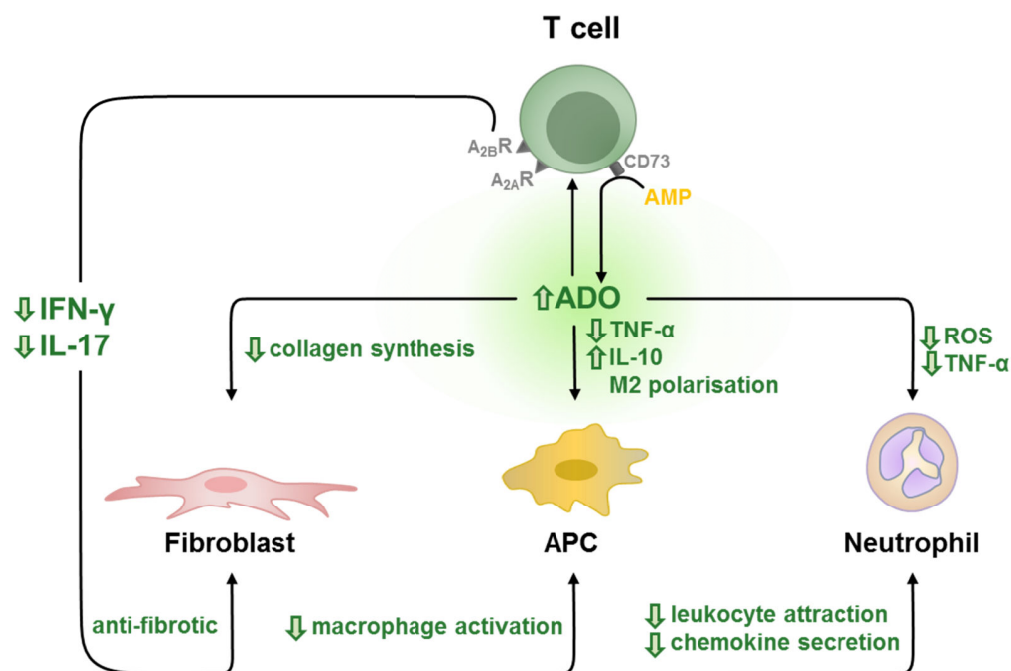


Fig. 26: Adenosine generated by CD73 on T cells orchestrates wound healing after MI through signaling via autocrine and paracrine fashion. Adenosine formed by CD73 on T cells acts in an autocrine fashion on $A_{2A}R$ s and $A_{2B}R$ s regulating secretion of pro-inflammatory cytokines and pro-fibrotic mediators, such as IFN- γ and IL-17, which promotes anti-fibrotic effects and attenuates macrophage activation, chemokine secretion and leukocyte attraction. In a paracrine fashion adenosine reduces collagen synthesis in fibroblasts, inhibits TNF- α secretion of macrophages and initiates M2 macrophage polarization leading to increased IL-10 concentrations. Moreover, adenosine inhibits ROS formation and TNF- α production of neutrophils.

Activation of both the A_{2A}R and the A_{2B}R on T cells inhibits the formation of pro-inflammatory cytokines and pro-fibrotic factors, such as IFN- γ and IL-17. Reduced IL-17 secretion moderates fibroblast proliferation and pro-fibrotic gene expression [341; 342; 384]. Decreased IFN- γ accumulation attenuates leukocyte attraction, macrophage activation and chemokine secretion [340]. Moreover, adenosine promotes anti-inflammatory effects in a paracrine fashion by regulating collagen synthesis in fibroblasts as well as ROS formation and TNF- α secretion of neutrophils [385–387]. In addition, A_{2B}R signaling on neutrophils and macrophages suppresses the release of pro-inflammatory TNF- α , increases anti-inflammatory IL-10 production in macrophages and promotes alternative (M2) macrophage activation [276–279; 336]. In summary, CD73-generated adenosine mediates tissue healing processes after MI by regulating fibroblast activity and by promoting resolution of inflammation preventing adverse ventricular remodeling and development of heart failure (figure 26).

The second part of this thesis reports on the importance of CD73 on tubular cells and on fibroblast/pericytes in regulating healing processes after AKI. Our data gave first evidence that the intercellular interplay between tubular cells and fibroblasts/pericytes in generating adenosine via CD73 is a crucial mediator in kidney protection after IRI. CD73-derived adenosine provided by fibroblast/pericytes surrounding tubular cells is therefore likely to promote tubular cell protection. As summarized in figure 27, tubular cells, the major cell fraction expressing CD73 in the renal compartment, together with fibroblast/pericytes promotes accumulation of adenosine at the site of injury, which again signals in autocrine and paracrine fashions regulating matrix deposition and immune cell resolution. In acute injury events, such as IRI in the kidney, adenosine A_{2B}R signaling on fibroblast may control cell proliferation and activation [366; 373]. On tubular cells adenosine acts on A₁Rs and A_{2A}Rs promoting oxidant injury protection [381]. Moreover, adenosine modulates immune cell resolution via signaling in a paracrine fashion by A_{2A}R activation on macrophages leading to inhibition of M1 macrophage activity and reduction of the release of pro-inflammatory cytokines [259; 368; 369]. Activation of A_{2A}R initiates phenotype switch of M1 to M2 macrophages, that leads to generation of an anti-inflammatory milieu by producing cytokines, including IL-10 and IL-4 [279; 370]. Taking together, CD73-derived adenosine is a crucial mediator for kidney fibrosis due to fibroblast regulation and immune cell resolution after AKI (figure 27).

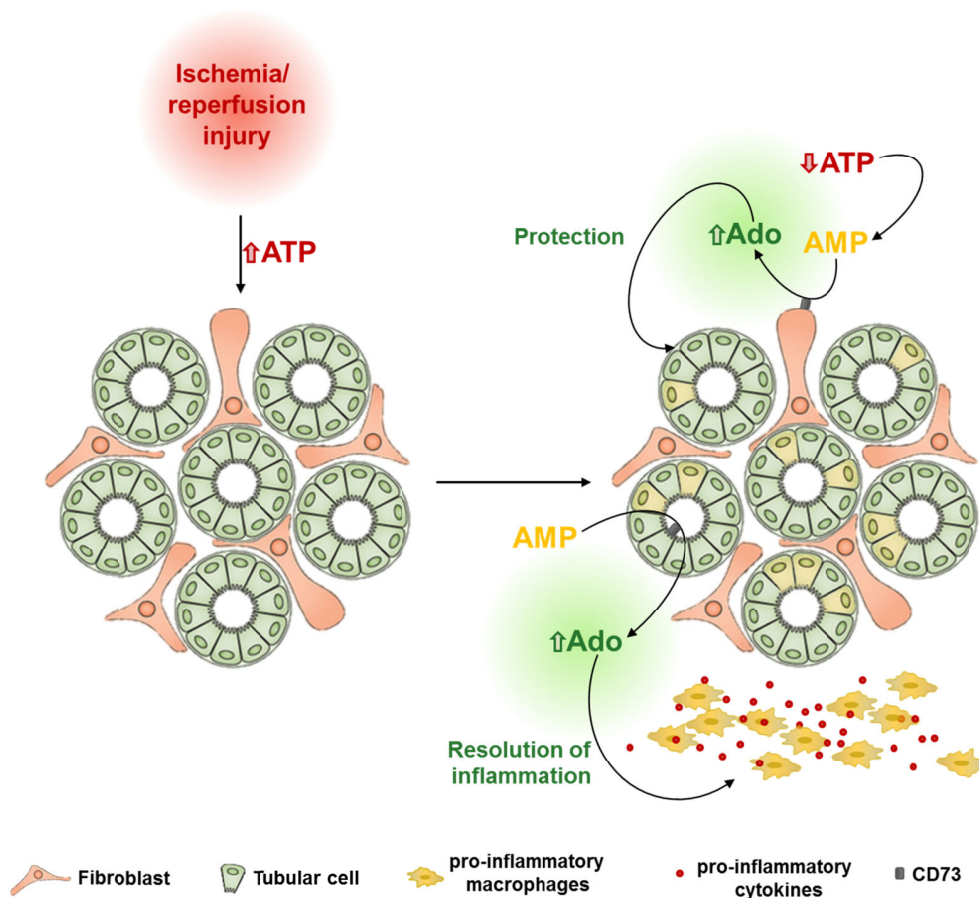


Fig. 27: Adenosine generated by CD73 on tubular cells and fibroblast/ pericytes orchestrates wound healing after AKI through signaling via autocrine and paracrine fashion. After IRI, ATP released into the microenvironment becomes degraded to AMP and in a second step via CD73 to adenosine. Adenosine provided by fibroblast/ pericytes promotes protection of tubular cells. CD73-derived adenosine generated by tubular cells and fibroblast/ pericytes modulates fibroblast phenotype and activation as well resolution of inflammation.

Despite heart and kidney serve obviously different functions in the body, a direct comparison of both disease models reveals a quite similar response to IRI, that can be categorized into several phases. After IRI, tissue undergoes necrosis and apoptosis resulting in immune cell infiltration promoting pro-inflammatory responses followed by resolution of inflammation and scar formation. By this mechanism damaged tissue is removed followed by repair mechanisms including matrix deposition and scar formation. Danger signals due to injury mediate the upregulation of chemokines, cytokines and cellular adhesion molecules promoting inflammatory response. Subsequent infiltration of neutrophils, monocytes and T lymphocytes invade into the injured tissue. Promotion of an anti-inflammatory milieu goes along with activation of fibroblast to initiate tissue healing and scar formation followed by

immune cell resolution. In both organs, CD73 regulates tissue healing processes by orchestrating scar formation and inflammation after IRI. Despite these similarities, there are important differences in the cell type being involved in tissue remodeling. In the injured heart, the majority of CD73 resides mainly in one cell fraction: infiltrating T cells, so that T cells are the major source of adenosine. However, in the kidney, CD73 is expressed on fibroblasts/ pericytes, tubular cells, mesangial cells of glomeruli and immune cells, so that at least four different cellular sites in the kidney contribute to the formation of adenosine. Their individual contribution to the generation of adenosine is difficult to assess, but our results gave first evidence that CD73 on tubular cells and fibroblasts/ pericytes is important in tissue healing. Little is also known on the kinetics of CD73 upregulation in the different cellular compartments after injury. Differences in the time course of CD73 expression in the different cell types may importantly influence signaling and consequently functional outcome. In addition, little is known on the turnover of interstitial adenosine and the diffusion distances adenosine has to travel to reach cellular adenosine receptors. The interplay and contribution of the different CD73 expression cells in the kidney certainly requires future attention. Similar arguments apply to the cellular distribution of the adenosine receptors. In the heart, the $A_{2A}R$ and the $A_{2B}R$ appear to inhibit the inflammatory response on T cells after IRI. In the kidney, activation of $A_{2A}R$ promotes tissue healing and there may be an $A_{2B}R$ -mediated anti-inflammatory response, which needs to be studied more in detail.

The healing processes mediated by adenosine is very likely based on a well-balanced but complicated interaction between channels, enzymes and receptors and a disruption of this fine-tuned interaction can led to maladaptive repair mechanism resulting in chronic diseases in heart and kidney. Our studies uncovered a part of the hidden mechanism behind tissue recovery and offers new insights into the molecular interplay. The observation that the $A_{2B}R$ only becomes upregulated on fibroblast and infiltrating immune cells during stress conditions, such as IRI, may provide specificity for pharmacologic targeting. Reviewing the literature, activation of the $A_{2B}R$ yielded conflicting conclusions in a variety of systems [275; 388]. It has been reported that cardiac remodeling can be significantly attenuated by application of a specific $A_{2B}R$ antagonists [283]. However, the situation is presently unclear since also $A_{2B}R$ agonists have been reported to protect the injured heart. Cardiac healing could be significantly improved by administration of the $A_{2B}R$ agonist (BAY 60-6583), which might include off target effects of the drug. Similarly, treatment of AKI using the $A_{2B}R$ agonist (BAY 60-6583) improved renal function [389]. The reported inconsistencies of $A_{2B}R$ activation and healing processes need to be explored in future studies using inhibitors and activators of the $A_{2B}R$, which are highly selective and show favorable pharmacokinetics.

9. Publications

Parts of this study have been published in:

Borg N, Alter C, Görldt N, Jacoby C, Ding Z, Steckel B, Quast C, Bönner F, Friebe D, Temme S, Flögel U, Schrader J

CD73 on T-Cells Orchestrates Cardiac Wound Healing After Myocardial Infarction by Purinergic Metabolic Reprogramming

Circulation. 2017 Apr 21. pii: CIRCULATIONAHA.116.023365. doi: 10.1161 /CIRCULATION AHA.116.023365

Further publications:

Sung SJ, Li L, Huang L, Lawler J, Ye H, Rosin DL, Vincent IS, Le TH, Yu J, Görldt N, Schrader J, Okusa MD

Proximal Tubule CD73 Is Critical in Renal Ischemia-Reperfusion Injury Protection

J Am Soc Nephrol. 2016 Sep 14. pii: ASN.2016020229

10. References

- 1 Eltzschig HK, Eckle T. Ischemia and reperfusion--from mechanism to translation. *Nat Med.* 2011 Nov 7;17(11):1391-401. doi: 10.1038/nm.2507.
- 2 Kalogeris T, Baines CP, Krenz M, Korthuis RJ. Cell biology of ischemia/reperfusion injury. *Int Rev Cell Mol Biol.* 2012;298:229-317. doi: 10.1016/B978-0-12-394309-5.00006-7.
- 3 Ogawa S, Gerlach H, Esposito C, Pasagian-Macaulay A, Brett J, Stern D. Hypoxia modulates the barrier and coagulant function of cultured bovine endothelium. Increased monolayer permeability and induction of procoagulant properties. *J Clin Invest.* 1990 Apr;85(4):1090-8.
- 4 Ogawa S, Koga S, Kuwabara K, Brett J, Morrow B, Morris SA, Bilezikian JP, Silverstein SC, Stern D. Hypoxia-induced increased permeability of endothelial monolayers occurs through lowering of cellular cAMP levels. *Am J Physiol.* 1992 Mar;262(3 Pt 1):C546-54.
- 5 Eltzschig HK, Carmeliet P. Hypoxia and inflammation. *N Engl J Med.* 2011 Feb 17;364(7):656-65. doi: 10.1056/NEJMra0910283.
- 6 Zuidema MY, Zhang C. Ischemia/reperfusion injury: The role of immune cells. *World J Cardiol.* 2010 Oct 26;2(10):325-32. doi: 10.4330/wjc.v2.i10.325.
- 7 Gorsuch WB, Chrysanthou E, Schwaeble WJ, Stahl GL. The complement system in ischemia-reperfusion injuries. *Immunobiology.* 2012 Nov;217(11):1026-33. doi: 10.1016/j.imbio.2012.07.024. Epub 2012 Aug 7.
- 8 Hotchkiss RS, Strasser A, McDunn JE, Swanson PE. Cell death. *N Engl J Med.* 2009 Oct 15;361(16):1570-83. doi: 10.1056/NEJMra0901217.
- 9 Yang Q, He GW, Underwood MJ, Yu CM. Cellular and molecular mechanisms of endothelial ischemia/reperfusion injury: perspectives and implications for postischemic myocardial protection. *Am J Transl Res.* 2016 Feb 15;8(2):765-77. eCollection 2016.
- 10 Hastie LE, Patton WF, Hechtman HB, Shepro D. Filamin redistribution in an endothelial cell reoxygenation injury model. *Free Radic Biol Med.* 1997;22(6):955-66.
- 11 Eltzschig HK, Collard C. D. Vascular ischaemia and reperfusion injury. *Br Med Bull.* 2004 Oct 19;70:71-86. Print 2004.
- 12 Carden DL, Granger D. N. Pathophysiology of ischaemia-reperfusion injury. *J Pathol.* 2000 Feb;190(3):255-66.
- 13 Chen GY, Nuñez G. Sterile inflammation: sensing and reacting to damage. *Nat Rev Immunol.* 2010 Dec;10(12):826-37. doi: 10.1038/nri2873. Epub 2010 Nov 19.

- 14 Scaffidi P, Misteli T, Bianchi ME. Release of chromatin protein HMGB1 by necrotic cells triggers inflammation. *Nature*. 2002 Jul 11;418(6894):191-5.
- 15 Quintana FJ, Cohen I. R. Heat shock proteins as endogenous adjuvants in sterile and septic inflammation. *J Immunol*. 2005 Sep 1;175(5):2777-82.
- 16 Bours MJ, Swennen EL, Di Virgilio F, Cronstein BN, Dagnelie PC. Adenosine 5'-triphosphate and adenosine as endogenous signaling molecules in immunity and inflammation. *Pharmacol Ther*. 2006 Nov;112(2):358-404. Epub 2006 Jun 19.
- 17 Kono H, Chen CJ, Ontiveros F, Rock KL. Uric acid promotes an acute inflammatory response to sterile cell death in mice. *J Clin Invest*. 2010 Jun;120(6):1939-49. doi: 10.1172/JCI40124. Epub 2010 May 24.
- 18 Rao J, Lu L, Zhai Y. T cells in organ ischemia reperfusion injury. *Curr Opin Organ Transplant*. 2014 Apr;19(2):115-20. doi: 10.1097/MOT.0000000000000064.
- 19 Chen J, Crispín JC, Tedder TF, Dalle Lucca J, Tsokos GC. B cells contribute to ischemia/reperfusion-mediated tissue injury. *J Autoimmun*. 2009 May-Jun;32(3-4):195-200. doi: 10.1016/j.jaut.2009.02.021. Epub 2009 Apr 1.
- 20 Zhang M, Carroll M. C. Natural antibody mediated innate autoimmune response. *Mol Immunol*. 2007 Jan;44(1-3):103-10. Epub 2006 Jul 28.
- 21 Diepenhorst GM, van Gulik TM, Hack CE. Complement-mediated ischemia-reperfusion injury: lessons learned from animal and clinical studies. *Ann Surg*. 2009 Jun;249(6):889-99. doi: 10.1097/SLA.0b013e3181a38f45.
- 22 Linfert D, Chowdhry T, Rabb H. Lymphocytes and ischemia-reperfusion injury. *Transplant Rev (Orlando)*. 2009 Jan;23(1):1-10. doi: 10.1016/j.trre.2008.08.003.
- 23 Burne-Taney MJ, Ascon DB, Daniels F, Racusen L, Baldwin W, Rabb H. B cell deficiency confers protection from renal ischemia reperfusion injury. *J Immunol*. 2003 Sep 15;171(6):3210-5.
- 24 Greer SN, Metcalf JL, Wang Y, Ohh M. The updated biology of hypoxia-inducible factor. *EMBO J*. 2012 May 30;31(11):2448-60. doi: 10.1038/emboj.2012.125. Epub 2012 May 4.
- 25 Zhao J, Du F, Shen G, Zheng F, Xu B. The role of hypoxia-inducible factor-2 in digestive system cancers. *Cell Death Dis*. 2015 Jan 15;6:e1600. doi: 10.1038/cddis.2014.565.
- 26 Epstein AC, Gleadle JM, McNeill LA, Hewitson KS, O'Rourke J, Mole DR, Mukherji M, Metzen E, Wilson MI, Dhanda A, Tian YM, Masson N, Hamilton DL, Jaakkola P, Barstead R, Hodgkin J, Maxwell PH, Pugh CW, Schofield CJ, Ratcliffe PJ. C. elegans EGL-9 and mammalian homologs define a family of dioxygenases that regulate HIF by prolyl hydroxylation. *Cell*. 2001 Oct 5;107(1):43-54.

- 27 Maxwell PH, Wiesener MS, Chang GW, Clifford SC, Vaux EC, Cockman ME, Wykoff CC, Pugh CW, Maher ER, Ratcliffe PJ. The tumour suppressor protein VHL targets hypoxia-inducible factors for oxygen-dependent proteolysis. *Nature*. 1999 May 20;399(6733):271-5.
- 28 Ohh M, Park CW, Ivan M, Hoffman MA, Kim TY, Huang LE, Pavletich N, Chau V, Kaelin WG. Ubiquitination of hypoxia-inducible factor requires direct binding to the beta-domain of the von Hippel-Lindau protein. *Nat Cell Biol*. 2000 Jul;2(7):423-7.
- 29 Semenza GL. Life with oxygen. *Science*. 2007 Oct 5;318(5847):62-4.
- 30 Carmeliet P, Dor Y, Herbert JM, Fukumura D, Brusselmans K, Dewerchin M, Neeman M, Bono F, Abramovitch R, Maxwell P, Koch CJ, Ratcliffe P, Moons L, Jain RK, Collen D, Keshert E. Role of HIF-1alpha in hypoxia-mediated apoptosis, cell proliferation and tumour angiogenesis. *Nature*. 1998 Jul 30;394(6692):485-90.
- 31 Wenger RH, Gassmann M. Oxygen(es) and the hypoxia-inducible factor-1. *Biol Chem*. 1997 Jul;378(7):609-16.
- 32 Semenza GL. Transcriptional regulation by hypoxia-inducible factor 1 molecular mechanisms of oxygen homeostasis. *Trends Cardiovasc Med*. 1996 Jul;6(5):151-7. doi: 10.1016/1050-1738(96)00039-4.
- 33 Dor Y, Keshet E. Ischemia-driven angiogenesis. *Trends Cardiovasc Med*. 1997 Nov;7(8):289-94. doi: 10.1016/S1050-1738(97)00091-1.
- 34 Stein I, Neeman M, Shweiki D, Itin A, Keshet E. Stabilization of vascular endothelial growth factor mRNA by hypoxia and hypoglycemia and coregulation with other ischemia-induced genes. *Mol Cell Biol*. 1995 Oct;15(10):5363-8.
- 35 Webster KA, Gunning P, Hardeman E, Wallace DC, Kedes L. Coordinate reciprocal trends in glycolytic and mitochondrial transcript accumulations during the in vitro differentiation of human myoblasts. *J Cell Physiol*. 1990 Mar;142(3):566-73.
- 36 Kapitsinou PP, Liu Q, Unger TL, Rha J, Davidoff O, Keith B, Epstein JA, Moores SL, Erickson-Miller CL, Haase VH. Hepatic HIF-2 regulates erythropoietic responses to hypoxia in renal anemia. *Blood*. 2010 Oct 21;116(16):3039-48. doi: 10.1182/blood-2010-02-270322. Epub 2010 Jul 13.
- 37 Rankin EB, Biju MP, Liu Q, Unger TL, Rha J, Johnson RS, Simon MC, Keith B, Haase VH. Hypoxia-inducible factor-2 (HIF-2) regulates hepatic erythropoietin in vivo. *J Clin Invest*. 2007 Apr;117(4):1068-77.
- 38 Koury ST, Koury MJ, Bondurant MC, Caro J, Graber SE. Quantitation of erythropoietin-producing cells in kidneys of mice by in situ hybridization: correlation with hematocrit, renal erythropoietin mRNA, and serum erythropoietin concentration. *Blood*. 1989 Aug 1;74(2):645-51.

- 39 Obara N, Suzuki N, Kim K, Nagasawa T, Imagawa S, Yamamoto M. Repression via the GATA box is essential for tissue-specific erythropoietin gene expression. *Blood*. 2008 May 15;111(10):5223-32. doi: 10.1182/blood-2007-10-115857. Epub 2008 Jan 17.
- 40 Asada N, Takase M, Nakamura J, Oguchi A, Asada M, Suzuki N, Yamamura K, Nagoshi N, Shibata S, Rao TN, Fehling HJ, Fukatsu A, Minegishi N, Kita T, Kimura T, Okano H, Yamamoto M, Yanagita M. Dysfunction of fibroblasts of extrarenal origin underlies renal fibrosis and renal anemia in mice. *J Clin Invest*. 2011 Oct;121(10):3981-90. doi: 10.1172/JCI57301. Epub 2011 Sep 12.
- 41 Bachmann S, Le Hir M, Eckardt KU. Co-localization of erythropoietin mRNA and ecto-5'-nucleotidase immunoreactivity in peritubular cells of rat renal cortex indicates that fibroblasts produce erythropoietin. *J Histochem Cytochem*. 1993 Mar;41(3):335-41.
- 42 Maxwell PH, Osmond MK, Pugh CW, Heryet A, Nicholls LG, Tan CC, Doe BG, Ferguson DJ, Johnson MH, Ratcliffe PJ. Identification of the renal erythropoietin-producing cells using transgenic mice. *Kidney Int*. 1993 Nov;44(5):1149-62.
- 43 Pan X, Suzuki N, Hirano I, Yamazaki S, Minegishi N, Yamamoto M. Isolation and characterization of renal erythropoietin-producing cells from genetically produced anemia mice. *PLoS One*. 2011;6(10):e25839. doi: 10.1371/journal.pone.0025839. Epub 2011 Oct 11.
- 44 Paschos N, Lykissas MG, Beris AE. The role of erythropoietin as an inhibitor of tissue ischemia. *Int J Biol Sci*. 2008 Jun 10;4(3):161-8.
- 45 Forsythe JA, Jiang BH, Iyer NV, Agani F, Leung SW, Koos RD, Semenza GL. Activation of vascular endothelial growth factor gene transcription by hypoxia-inducible factor 1. *Mol Cell Biol*. 1996 Sep;16(9):4604-13.
- 46 Tahergorabi Z, Khazaei M. A review on angiogenesis and its assays. *Iran J Basic Med Sci*. 2012 Nov;15(6):1110-26.
- 47 Nishimura Y, Lemasters J. J. Glycine blocks opening of a death channel in cultured hepatic sinusoidal endothelial cells during chemical hypoxia. *Cell Death Differ*. 2001 Aug;8(8):850-8.
- 48 Festjens N, Vanden Berghe T, Vandenabeele P. Necrosis, a well-orchestrated form of cell demise: signalling cascades, important mediators and concomitant immune response. *Biochim Biophys Acta*. 2006 Sep-Oct;1757(9-10):1371-87. Epub 2006 Jul 8.
- 49 Raedschelders K, Ansley DM, Chen DD. The cellular and molecular origin of reactive oxygen species generation during myocardial ischemia and reperfusion. *Pharmacol Ther*. 2012 Feb;133(2):230-55. doi: 10.1016/j.pharmthera.2011.11.004. Epub 2011 Nov 27.

-
- 50 Lotze MT, Tracey K. J. High-mobility group box 1 protein (HMGB1): nuclear weapon in the immune arsenal. *Nat Rev Immunol.* 2005 Apr;5(4):331-42.
- 51 Kerr JF, Wyllie AH, Currie AR. Apoptosis: a basic biological phenomenon with wide-ranging implications in tissue kinetics. *Br J Cancer.* 1972 Aug;26(4):239-57.
- 52 Lenihan CR, Taylor C. T. The impact of hypoxia on cell death pathways. *Biochem Soc Trans.* 2013 Apr;41(2):657-63. doi: 10.1042/BST20120345.
- 53 Gottlieb RA. Cell death pathways in acute ischemia/reperfusion injury. *J Cardiovasc Pharmacol Ther.* 2011 Sep-Dec;16(3-4):233-8. doi: 10.1177/1074248411409581.
- 54 Porter AG, Jänicke R. U. Emerging roles of caspase-3 in apoptosis. *Cell Death Differ.* 1999 Feb;6(2):99-104.
- 55 Zhao Y, Wieman HL, Jacobs SR, Rathmell JC. Mechanisms and methods in glucose metabolism and cell death. *Methods Enzymol.* 2008;442:439-57. doi: 10.1016/S0076-6879(08)01422-5.
- 56 Ma S, Wang Y, Chen Y, Cao F. The role of the autophagy in myocardial ischemia/reperfusion injury. *Biochim Biophys Acta.* 2015 Feb;1852(2):271-6. doi: 10.1016/j.bbadis.2014.05.010. Epub 2014 May 21.
- 57 Xie M, Morales CR, Lavandero S, Hill JA. Tuning flux: autophagy as a target of heart disease therapy. *Curr Opin Cardiol.* 2011 May;26(3):216-22. doi: 10.1097/HCO.0b013e328345980a.
- 58 Hariharan N, Zhai P, Sadoshima J. Oxidative stress stimulates autophagic flux during ischemia/reperfusion. *Antioxid Redox Signal.* 2011 Jun;14(11):2179-90. doi: 10.1089/ars.2010.3488. Epub 2011 Jan 27.
- 59 Gustafsson AB, Gottlieb R. A. Recycle or die: the role of autophagy in cardioprotection. *J Mol Cell Cardiol.* 2008 Apr;44(4):654-61. doi: 10.1016/j.yjmcc.2008.01.010. Epub 2008 Feb 13.
- 60 Schrader J, Gödecke A, Kelm M. Das Herz. *Physiologie.* 2010. 6. Auflage Thieme Verlagsgruppe, Stuttgart, New York, Delhi, Rio.
- 61 Thygesen K, Alpert JS, Jaffe AS, Simoons ML, Chaitman BR, White HD; Task Force for the Universal Definition of Myocardial Infarction. Third universal definition of myocardial infarction. *Nat Rev Cardiol.* 2012 Nov;9(11):620-33. doi: 10.1038/nrcardio.2012.122. Epub 2012 Aug 25.
- 62 Bui QT, Prempeh M, Wilensky RL. Atherosclerotic plaque development. *Int J Biochem Cell Biol.* 2009 Nov;41(11):2109-13. doi: 10.1016/j.biocel.2009.06.002. Epub 2009 Jun 10.
- 63 Hansson GK, Robertson AK, Söderberg-Nauclér C. Inflammation and atherosclerosis. *Annu Rev Pathol.* 2006;1:297-329.

- 64 Blankesteyn WM, Creemers E, Lutgens E, Cleutjens JP, Daemen MJ, Smits JF. Dynamics of cardiac wound healing following myocardial infarction: observations in genetically altered mice. *Acta Physiol Scand.* 2001 Sep;173(1):75-82.
- 65 Scheuer J. Myocardial metabolism in cardiac hypoxia. *Am J Cardiol.* 1967 Mar;19(3):385-92.
- 66 Jennings RB. Early phase of myocardial ischemic injury and infarction. *Am J Cardiol.* 1969 Dec;24(6):753-65.
- 67 Braasch W, Gudbjarnason S, Puri PS, Ravens KG, Bing RJ. Early changes in energy metabolism in the myocardium following acute coronary artery occlusion in anesthetized dogs. *Circ Res.* 1968 Sep;23(3):429-38.
- 68 Kübler W, Spieckermann P. G. Regulation of glycolysis in the ischemic and the anoxic myocardium. *J Mol Cell Cardiol.* 1970 Dec;1(4):351-77.
- 69 Jennings RB, Reimer KA, Hill ML, Mayer SE. Total ischemia in dog hearts, in vitro. 1. Comparison of high energy phosphate production, utilization, and depletion, and of adenine nucleotide catabolism in total ischemia in vitro vs. severe ischemia in vivo. *Circ Res.* 1981 Oct;49(4):892-900.
- 70 Mochizuki S, Neely, JR. Control of glyceraldehyde-3-phosphate dehydrogenase in cardiac muscle. *J Mol Cell Cardiol.* 1979 Mar;11(3):221-36.
- 71 Rovetto MJ, Lamberton WF, Neely JR. Mechanisms of glycolytic inhibition in ischemic rat hearts. *Circ Res.* 1975 Dec;37(6):742-51.
- 72 Jennings RB, Reimer K. A. Lethal myocardial ischemic injury. *Am J Pathol.* 1981 Feb;102(2):241-55.
- 73 Reimer KA, Lowe JE, Rasmussen MM, Jennings RB. The wavefront phenomenon of ischemic cell death. 1. Myocardial infarct size vs duration of coronary occlusion in dogs. *Circulation.* 1977 Nov;56(5):786-94.
- 74 Hausenloy DJ, Yellon D. M. Myocardial ischemia-reperfusion injury: a neglected therapeutic target. *J Clin Invest.* 2013 Jan;123(1):92-100. doi: 10.1172/JCI62874. Epub 2013 Jan 2.
- 75 Meier P, Schirmer SH, Lansky AJ, Timmis A, Pitt B, Seiler C. The collateral circulation of the heart. *BMC Med.* 2013 Jun 4;11:143. doi: 10.1186/1741-7015-11-143.
- 76 Xia Y, Lee K, Li N, Corbett D, Mendoza L, Frangogiannis NG. Characterization of the inflammatory and fibrotic response in a mouse model of cardiac pressure overload. *Histochem Cell Biol.* 2009 Apr;131(4):471-81. doi: 10.1007/s00418-008-0541-5. Epub 2008 Nov 22.

- 77 Frangogiannis NG. The immune system and cardiac repair. *Pharmacol Res.* 2008 Aug;58(2):88-111. doi: 10.1016/j.phrs.2008.06.007. Epub 2008 Jun 24.
- 78 van der Laan AM, Nahrendorf M, Piek JJ. Healing and adverse remodelling after acute myocardial infarction: role of the cellular immune response. *Heart.* 2012 Sep;98(18):1384-90. doi: 10.1136/heartjnl-2012-301623.
- 79 Baeuerle PA, Henkel T. Function and activation of NF-kappa B in the immune system. *Annu Rev Immunol.* 1994;12:141-79.
- 80 Kilgore KS, Schmid E, Shanley TP, Flory CM, Maheswari V, Tramontini NL, Cohen H, Ward PA, Friedl HP, Warren JS. Sublytic concentrations of the membrane attack complex of complement induce endothelial interleukin-8 and monocyte chemoattractant protein-1 through nuclear factor-kappa B activation. *Am J Pathol.* 1997 Jun;150(6):2019-31.
- 81 Birdsall HH, Green DM, Trial J, Youker KA, Burns AR, MacKay CR, LaRosa GJ, Hawkins HK, Smith CW, Michael LH, Entman ML, Rossen RD. Complement C5a, TGF-beta 1, and MCP-1, in sequence, induce migration of monocytes into ischemic canine myocardium within the first one to five hours after reperfusion. *Circulation.* 1997 Feb 4;95(3):684-92.
- 82 Sen CK, Packer L. Antioxidant and redox regulation of gene transcription. *FASEB J.* 1996 May;10(7):709-20.
- 83 Kawaguchi M, Takahashi M, Hata T, Kashima Y, Usui F, Morimoto H, Izawa A, Takahashi Y, Masumoto J, Koyama J, Hongo M, Noda T, Nakayama J, Sagara J, Taniguchi S, Ikeda U. Inflammasome activation of cardiac fibroblasts is essential for myocardial ischemia/reperfusion injury. *Circulation.* 2011 Feb 15;123(6):594-604. doi: 10.1161/CIRCULATIONAHA.110.982777. Epub 2011 Jan 31.
- 84 Takahashi M. Role of the inflammasome in myocardial infarction. *Trends Cardiovasc Med.* 2011 Feb;21(2):37-41. doi: 10.1016/j.tcm.2012.02.002.
- 85 Vinten-Johansen J, Zhao ZQ, Nakamura M, Jordan JE, Ronson RS, Thourani VH, Guyton RA. Nitric oxide and the vascular endothelium in myocardial ischemia-reperfusion injury. *Ann N Y Acad Sci.* 1999 Jun 30;874:354-70.
- 86 Singhal AK, Symons JD, Boudina S, Jaishy B, Shiu YT. Role of Endothelial Cells in Myocardial Ischemia-Reperfusion Injury. *Vasc Dis Prev.* 2010;7:1-14.
- 87 Yang F, Liu YH, Yang XP, Xu J, Kapke A, Carretero OA. Myocardial infarction and cardiac remodelling in mice. *Exp Physiol.* 2002 Sep;87(5):547-55.
- 88 Nahrendorf M, Swirski FK, Aikawa E, Stangenberg L, Wurdinger T, Figueiredo JL, Libby P, Weissleder R, Pittet MJ. The healing myocardium sequentially mobilizes two monocyte subsets with divergent and complementary functions. *J Exp Med.* 2007 Nov 26;204(12):3037-47. Epub 2007 Nov 19.

- 89 Li W, Goldstein DR, Kreisel D. Intravital 2-photon imaging, leukocyte trafficking, and the beating heart. *Trends Cardiovasc Med.* 2013 Nov;23(8):287-93. doi: 10.1016/j.tcm.2013.04.002. Epub 2013 May 22.
- 90 McDonald B, Pittman K, Menezes GB, Hirota SA, Slaba I, Waterhouse CC, Beck PL, Muruve DA, Kubes P. Intravascular danger signals guide neutrophils to sites of sterile inflammation. *Science.* 2010 Oct 15;330(6002):362-6. doi: 10.1126/science.1195491.
- 91 Dreyer WJ, Michael LH, West MS, Smith CW, Rothlein R, Rossen RD, Anderson DC, Entman ML. Neutrophil accumulation in ischemic canine myocardium. Insights into time course, distribution, and mechanism of localization during early reperfusion. *Circulation.* 1991 Jul;84(1):400-11.
- 92 Lindsey M, Wedin K, Brown MD, Keller C, Evans AJ, Smolen J, Burns AR, Rossen RD, Michael L, Entman M. Matrix-dependent mechanism of neutrophil-mediated release and activation of matrix metalloproteinase 9 in myocardial ischemia/reperfusion. *Circulation.* 2001 May 1;103(17):2181-7.
- 93 Vinten-Johansen J. Involvement of neutrophils in the pathogenesis of lethal myocardial reperfusion injury. *Cardiovasc Res.* 2004 Feb 15;61(3):481-97.
- 94 Soehnlein O, Zernecke A, Eriksson EE, Rothfuchs AG, Pham CT, Herwald H, Bidzhekov K, Rottenberg ME, Weber C, Lindbom L. Neutrophil secretion products pave the way for inflammatory monocytes. *Blood.* 2008 Aug 15;112(4):1461-71. doi: 10.1182/blood-2008-02-139634. Epub 2008 May 19.
- 95 Nahrendorf M, Swirski F. K. Monocyte and macrophage heterogeneity in the heart. *Circ Res.* 2013 Jun 7;112(12):1624-33. doi: 10.1161/CIRCRESAHA.113.300890.
- 96 Robbins CS, Chudnovskiy A, Rauch PJ, Figueiredo JL, Iwamoto Y, Gorbатов R, Etzrodt M, Weber GF, Ueno T, van Rooijen N, Mulligan-Kehoe MJ, Libby P, Nahrendorf M, Pittet MJ, Weissleder R, Swirski FK. Extramedullary hematopoiesis generates Ly-6C(high) monocytes that infiltrate atherosclerotic lesions. *Circulation.* 2012 Jan 17;125(2):364-74. doi: 10.1161/CIRCULATIONAHA.111.061986. Epub 2011 Dec 5.
- 97 Macpherson G & Austyn J. *Exploring Immunology: Concepts and Evidence.* April 2012. Wiley-Blackwell.
- 98 Serhan CN, Ward PA, & Gilroy DW. *Fundamentals of inflammation.* 2010. Cambridge University Press.
- 99 Hofmann U, Beyersdorf N, Weirather J, Podolskaya A, Bauersachs J, Ertl G, Kerkau T, Frantz S. Activation of CD4+ T lymphocytes improves wound healing and survival after experimental myocardial infarction in mice. *Circulation.* 2012 Apr 3;125(13):1652-63. doi: 10.1161/CIRCULATIONAHA.111.044164. Epub 2012 Mar 2.

- 100 Tang TT, Yuan J, Zhu ZF, Zhang WC, Xiao H, Xia N, Yan XX, Nie SF, Liu J, Zhou SF, Li JJ, Yao R, Liao MY, Tu X, Liao YH, Cheng X. Regulatory T cells ameliorate cardiac remodeling after myocardial infarction. *Basic Res Cardiol.* 2012 Jan;107(1):232. doi: 10.1007/s00395-011-0232-6. Epub 2011 Dec 22.
- 101 Varda-Bloom N, Leor J, Ohad DG, Hasin Y, Amar M, Fixler R, Battler A, Eldar M, Hasin D. Cytotoxic T lymphocytes are activated following myocardial infarction and can recognize and kill healthy myocytes in vitro. *J Mol Cell Cardiol.* 2000 Dec;32(12):2141-9.
- 102 Frangogiannis NG, Mendoza LH, Lindsey ML, Ballantyne CM, Michael LH, Smith CW, Entman ML. IL-10 is induced in the reperfused myocardium and may modulate the reaction to injury. *J Immunol.* 2000 Sep 1;165(5):2798-808.
- 103 Bassols A, Massagué J. Transforming growth factor beta regulates the expression and structure of extracellular matrix chondroitin/dermatan sulfate proteoglycans. *J Biol Chem.* 1988 Feb 25;263(6):3039-45.
- 104 Dobaczewski M, Chen W, Frangogiannis NG. Transforming growth factor (TGF)- β signaling in cardiac remodeling. *J Mol Cell Cardiol.* 2011 Oct;51(4):600-6. doi: 10.1016/j.yjmcc.2010.10.033. Epub 2010 Nov 6.
- 105 Desmoulière A, Geinoz A, Gabbiani F, Gabbiani G. Transforming growth factor-beta 1 induces alpha-smooth muscle actin expression in granulation tissue myofibroblasts and in quiescent and growing cultured fibroblasts. *J Cell Biol.* 1993 Jul;122(1):103-11.
- 106 Cleutjens JP, Verluyten MJ, Smiths JF, Daemen MJ. Collagen remodeling after myocardial infarction in the rat heart. *Am J Pathol.* 1995 Aug;147(2):325-38.
- 107 Weber KT. Cardiac interstitium in health and disease: the fibrillar collagen network. *J Am Coll Cardiol.* 1989 Jun;13(7):1637-52.
- 108 Zhao W, Lu L, Chen SS, Sun Y. Temporal and spatial characteristics of apoptosis in the infarcted rat heart. *Biochem Biophys Res Commun.* 2004 Dec 10;325(2):605-11.
- 109 Holmes JW, Borg TK, Covell JW. Structure and mechanics of healing myocardial infarcts. *Annu Rev Biomed Eng.* 2005;7:223-53.
- 110 Koshy SK, Reddy HK, Shukla HH. Collagen cross-linking: new dimension to cardiac remodeling. *Cardiovasc Res.* 2003 Mar;57(3):594-8.
- 111 Badenhorst D1, Maseko M, Tsotetsi OJ, Naidoo A, Brooksbank R, Norton GR, Woodiwiss AJ. Cross-linking influences the impact of quantitative changes in myocardial collagen on cardiac stiffness and remodelling in hypertension in rats. *Cardiovasc Res.* 2003 Mar;57(3):632-41.

- 112 van der Laan AM, Piek JJ, van Royen N. Targeting angiogenesis to restore the microcirculation after reperfused MI. *Nat Rev Cardiol.* 2009 Aug;6(8):515-23. doi: 10.1038/nrcardio.2009.103. Epub 2009 Jun 16.
- 113 Zhao T, Zhao W, Chen Y, Ahokas RA, Sun Y. Vascular endothelial growth factor (VEGF)-A: role on cardiac angiogenesis following myocardial infarction. *Microvasc Res.* 2010 Sep;80(2):188-94. doi: 10.1016/j.mvr.2010.03.014. Epub 2010 Apr 1.
- 114 Silbernagl S. Die Funktion der Nieren. *Physiologie.* 2010. 6. Auflage Thieme Verlagsgruppe, Stuttgart, New York, Delhi, Rio.
- 115 Cullen-McEwen L, Sutherland MR, Black MJ. Chapter 3 - The Human Kidney: Parallels in Structure, Spatial Development, and Timing of Nephrogenesis. *Kidney Development, Disease, Repair and Regeneration.* 2016. Elsevier Inc.
- 116 Wessely O, Cerqueira DM, Tran U, Kumar V, Hassey JM, Romaker D. The bigger the better: determining nephron size in kidney. *Pediatr Nephrol.* 2014 Apr;29(4):525-30. doi: 10.1007/s00467-013-2581-x. Epub 2013 Aug 22.
- 117 Bellomo R, Kellum JA, Ronco C. Acute kidney injury. *Lancet.* 2012 Aug 25;380(9843):756-66. doi: 10.1016/S0140-6736(11)61454-2. Epub 2012 May 21.
- 118 Devarajan P. Cellular and molecular derangements in acute tubular necrosis. *Curr Opin Pediatr.* 2005 Apr;17(2):193-9.
- 119 Devarajan P. Update on mechanisms of ischemic acute kidney injury. *J Am Soc Nephrol.* 2006 Jun;17(6):1503-20. Epub 2006 May 17.
- 120 Yang D, Yang D. Role of intracellular Ca²⁺ and Na⁺/Ca²⁺ exchanger in the pathogenesis of contrast-induced acute kidney injury. *Biomed Res Int.* 2013;2013:678456. doi: 10.1155/2013/678456. Epub 2013 Nov 18.
- 121 Wilson DR, Arnold PE, Burke TJ, Schrier RW. Mitochondrial calcium accumulation and respiration in ischemic acute renal failure in the rat. *Kidney Int.* 1984 Mar;25(3):519-26.
- 122 Himmelfarb J, McMonagle E, Freedman S, Klenzak J, McMenamin E, Le P, Pupim LB, Ikizler TA, The PICARD Group. Oxidative stress is increased in critically ill patients with acute renal failure. *J Am Soc Nephrol.* 2004 Sep;15(9):2449-56.
- 123 Molitoris BA. Actin cytoskeleton in ischemic acute renal failure. *Kidney Int.* 2004 Aug;66(2):871-83.
- 124 Woroniecki R, Ferdinand JR, Morrow JS, Devarajan P. Dissociation of spectrin-ankyrin complex as a basis for loss of Na-K-ATPase polarity after ischemia. *Am J Physiol Renal Physiol.* 2003 Feb;284(2):F358-64. Epub 2002 Oct 29.

- 125 Ferenbach DA, Bonventre J. V. Mechanisms of maladaptive repair after AKI leading to accelerated kidney ageing and CKD. *Nat Rev Nephrol.* 2015 May;11(5):264-76. doi: 10.1038/nrneph.2015.3. Epub 2015 Feb 3.
- 126 Lee S, Huen S, Nishio H, Nishio S, Lee HK, Choi BS, Ruhrberg C, Cantley LG. Distinct macrophage phenotypes contribute to kidney injury and repair. *J Am Soc Nephrol.* 2011 Feb;22(2):317-26. doi: 10.1681/ASN.2009060615.
- 127 Bolisetty S, Agarwal A. Neutrophils in acute kidney injury: not neutral any more. *Kidney Int.* 2009 Apr;75(7):674-6. doi: 10.1038/ki.2008.689.
- 128 Li L, Huang L, Vergis AL, Ye H, Bajwa A, Narayan V, Strieter RM, Rosin DL, Okusa MD. IL-17 produced by neutrophils regulates IFN-gamma-mediated neutrophil migration in mouse kidney ischemia-reperfusion injury. *J Clin Invest.* 2010 Jan;120(1):331-42. doi: 10.1172/JCI38702. Epub 2009 Dec 14.
- 129 Ysebaert DK, De Greef KE, Vercauteren SR, Ghielli M, Verpooten GA, Eyskens EJ, De Broe ME. Identification and kinetics of leukocytes after severe ischaemia/reperfusion renal injury. *Nephrol Dial Transplant.* 2000 Oct;15(10):1562-74.
- 130 Wermuth PJ, Jimenez S. A. The significance of macrophage polarization subtypes for animal models of tissue fibrosis and human fibrotic diseases. *Clin Transl Med.* 2015 Feb 7;4:2. doi: 10.1186/s40169-015-0047-4. eCollection 2015.
- 131 Lenzo JC, Turner AL, Cook AD, Vlahos R, Anderson GP, Reynolds EC, Hamilton JA. Control of macrophage lineage populations by CSF-1 receptor and GM-CSF in homeostasis and inflammation. *Immunol Cell Biol.* 2012 Apr;90(4):429-40. doi: 10.1038/icb.2011.58. Epub 2011 Jul 5.
- 132 Lin SL, Castaño AP, Nowlin BT, Lupper ML Jr, Duffield JS. Bone marrow Ly6Chigh monocytes are selectively recruited to injured kidney and differentiate into functionally distinct populations. *J Immunol.* 2009 Nov 15;183(10):6733-43. doi: 10.4049/jimmunol.0901473. Epub 2009 Oct 28.
- 133 Burne MJ, Daniels F, El Ghandour A, Mauiyyedi S, Colvin RB, O'Donnell MP, Rabb H. Identification of the CD4(+) T cell as a major pathogenic factor in ischemic acute renal failure. *J Clin Invest.* 2001 Nov;108(9):1283-90.
- 134 Gandolfo MT, Jang HR, Bagnasco SM, Ko GJ, Agreda P, Satpute SR, Crow MT, King LS, Rabb H. Foxp3+ regulatory T cells participate in repair of ischemic acute kidney injury. *Kidney Int.* 2009 Oct;76(7):717-29. doi: 10.1038/ki.2009.259. Epub 2009 Jul 22.
- 135 Bonventre JV, Yang L. Cellular pathophysiology of ischemic acute kidney injury. *J Clin Invest.* 2011 Nov;121(11):4210-21. doi: 10.1172/JCI45161. Epub 2011 Nov 1.

- 136 Yoshida M, Honma S. Regeneration of injured renal tubules. *J Pharmacol Sci.* 2014;124(2):117-22. Epub 2014 Jan 25.
- 137 Duann P, Lianos EA, Ma J, Lin PH. Autophagy, Innate Immunity and Tissue Repair in Acute Kidney Injury. *Int J Mol Sci.* 2016 May 3;17(5). pii: E662. doi: 10.3390/ijms17050662.
- 138 Kusaba T, Humphreys B. D. Controversies on the origin of proliferating epithelial cells after kidney injury. *Pediatr Nephrol.* 2014 Apr;29(4):673-9. doi: 10.1007/s00467-013-2669-3. Epub 2013 Dec 10.
- 139 Kaissling B, Lehir M, Kriz W. Renal epithelial injury and fibrosis. *Biochim Biophys Acta.* 2013 Jul;1832(7):931-9. doi: 10.1016/j.bbadis.2013.02.010. Epub 2013 Mar 1.
- 140 Picard N, Baum O, Vogetseder A, Kaissling B, Le Hir M. Origin of renal myofibroblasts in the model of unilateral ureter obstruction in the rat. *Histochem Cell Biol.* 2008 Jul;130(1):141-55. doi: 10.1007/s00418-008-0433-8. Epub 2008 May 1.
- 141 Kramann R, DiRocco DP, Humphreys BD. Understanding the origin, activation and regulation of matrix-producing myofibroblasts for treatment of fibrotic disease. *J Pathol.* 2013 Nov;231(3):273-89. doi: 10.1002/path.4253.
- 142 Forbes JM, Hewitson TD, Becker GJ, Jones CL. Ischemic acute renal failure: long-term histology of cell and matrix changes in the rat. *Kidney Int.* 2000 Jun;57(6):2375-85.
- 143 Frangogiannis NG. Regulation of the inflammatory response in cardiac repair. *Circ Res.* 2012 Jan 6;110(1):159-73. doi: 10.1161/CIRCRESAHA.111.243162.
- 144 Halade GV. Targeting Resolution of Inflammation Following Myocardial Infarction. *J Cardiol Clin Res.* 2013;1(2): 1008.
- 145 van den Borne SW, Cleutjens JP, Hanemaaijer R, Creemers EE, Smits JF, Daemen MJ, Blankesteijn WM. Increased matrix metalloproteinase-8 and -9 activity in patients with infarct rupture after myocardial infarction. *Cardiovasc Pathol.* 2009 Jan-Feb;18(1):37-43. doi: 10.1016/j.carpath.2007.12.012. Epub 2008 Mar 4.
- 146 Huebener P, Abou-Khamis T, Zymek P, Bujak M, Ying X, Chatila K, Haudek S, Thakker G, Frangogiannis NG. CD44 is critically involved in infarct healing by regulating the inflammatory and fibrotic response. *J Immunol.* 2008 Feb 15;180(4):2625-33.
- 147 Panizzi P, Swirski FK, Figueiredo JL, Waterman P, Sosnovik DE, Aikawa E, Libby P, Pittet M, Weissleder R, Nahrendorf M. Impaired infarct healing in atherosclerotic mice with Ly-6C(hi) monocytosis. *J Am Coll Cardiol.* 2010 Apr 13;55(15):1629-38. doi: 10.1016/j.jacc.2009.08.089.

- 148 Abbate A, Bonanno E, Mauriello A, Bussani R, Biondi-Zoccai GG, Liuzzo G, Leone AM, Silvestri F, Dobrina A, Baldi F, Pandolfi F, Biasucci LM, Baldi A, Spagnoli LG, Crea F. Widespread myocardial inflammation and infarct-related artery patency. *Circulation*. 2004 Jul 6;110(1):46-50. Epub 2004 Jun 21.
- 149 Frangogiannis NG, Ren G, Dewald O, Zymek P, Haudek S, Koerting A, Winkelmann K, Michael LH, Lawler J, Entman ML. Critical role of endogenous thrombospondin-1 in preventing expansion of healing myocardial infarcts. *Circulation*. 2005 Jun 7;111(22):2935-42. Epub 2005 May 31.
- 150 Sun M, Dawood F, Wen WH, Chen M, Dixon I, Kirshenbaum LA, Liu PP. Excessive tumor necrosis factor activation after infarction contributes to susceptibility of myocardial rupture and left ventricular dysfunction. *Circulation*. 2004 Nov 16;110(20):3221-8. Epub 2004 Nov 8.
- 151 Grgic I, Campanholle G, Bijol V, Wang C, Sabbisetti VS, Ichimura T, Humphreys BD, Bonventre JV. Targeted proximal tubule injury triggers interstitial fibrosis and glomerulosclerosis. *Kidney Int*. 2012 Jul;82(2):172-83. doi: 10.1038/ki.2012.20. Epub 2012 Mar 21.
- 152 Duffield JS, Luper M, Thannickal VJ, Wynn TA. Host responses in tissue repair and fibrosis. *Annu Rev Pathol*. 2013 Jan 24;8:241-76. doi: 10.1146/annurev-pathol-020712-163930. Epub 2012 Oct 22.
- 153 Campanholle G, Ligresti G, Gharib SA, Duffield JS. Cellular mechanisms of tissue fibrosis. 3. Novel mechanisms of kidney fibrosis. *Am J Physiol Cell Physiol*. 2013 Apr 1;304(7):C591-603. doi: 10.1152/ajpcell.00414.2012. Epub 2013 Jan 16.
- 154 Duffield JS. Cellular and molecular mechanisms in kidney fibrosis. *J Clin Invest*. 2014 Jun;124(6):2299-306. doi: 10.1172/JCI72267. Epub 2014 Jun 2.
- 155 Vega G, Alarcón S, San Martín R. The cellular and signalling alterations conducted by TGF- β contributing to renal fibrosis. *Cytokine*. 2016 Dec;88:115-125. doi: 10.1016/j.cyto.2016.08.019. Epub 2016 Sep 4.
- 156 Hirschberg R. Wound healing in the kidney: complex interactions in renal interstitial fibrogenesis. *J Am Soc Nephrol*. 2005 Jan;16(1):9-11. Epub 2004 Dec 1.
- 157 Meng XM, Nikolic-Paterson DJ, Lan HY. Inflammatory processes in renal fibrosis. *Nat Rev Nephrol*. 2014 Sep;10(9):493-503. doi: 10.1038/nrneph.2014.114. Epub 2014 Jul 1.
- 158 Wu CF, Chiang WC, Lai CF, Chang FC, Chen YT, Chou YH, Wu TH, Linn GR, Ling H, Wu KD, Tsai TJ, Chen YM, Duffield JS, Lin SL. Transforming growth factor β -1 stimulates profibrotic epithelial signaling to activate pericyte-myofibroblast transition in obstructive kidney fibrosis. *Am J Pathol*. 2013 Jan;182(1):118-31. doi: 10.1016/j.ajpath.2012.09.009. Epub 2012 Nov 9.

- 159 Li R, Chung AC, Dong Y, Yang W, Zhong X, Lan HY. The microRNA miR-433 promotes renal fibrosis by amplifying the TGF- β /Smad3-Azin1 pathway. *Kidney Int.* 2013 Dec;84(6):1129-44. doi: 10.1038/ki.2013.272. Epub 2013 Jul 17.
- 160 Yeh YC, Wei WC, Wang YK, Lin SC, Sung JM, Tang MJ. Transforming growth factor- β 1 induces Smad3-dependent β 1 integrin gene expression in epithelial-to-mesenchymal transition during chronic tubulointerstitial fibrosis. *Am J Pathol.* 2010 Oct;177(4):1743-54. doi: 10.2353/ajpath.2010.091183. Epub 2010 Aug 13.
- 161 Eltzschig HK, Sitkovsky MV, Robson SC. Purinergic signaling during inflammation. *N Engl J Med.* 2013 Mar 28;368(13):1260. doi: 10.1056/NEJMc1300259.
- 162 Boros D, Thompson J, Larson DF. Adenosine regulation of the immune response initiated by ischemia reperfusion injury. *Perfusion.* 2016 Mar;31(2):103-10. doi: 10.1177/0267659115586579. Epub 2015 May 18.
- 163 Rabadi MM, Lee H. T. Adenosine receptors and renal ischaemia reperfusion injury. *Acta Physiol (Oxf).* 2015 Jan;213(1):222-31. doi: 10.1111/apha.12402. Epub 2014 Oct 27.
- 164 Berg JM, Tymoczko JL, & Stryer L. *Biochemie.* 2003. 5. Auflage. Spektrum Akademischer.
- 165 Junger WG. Immune cell regulation by autocrine purinergic signalling. *Nat Rev Immunol.* 2011 Mar;11(3):201-12. doi: 10.1038/nri2938. Epub 2011 Feb 18.
- 166 Yegutkin GG. Nucleotide- and nucleoside-converting ectoenzymes: Important modulators of purinergic signalling cascade. *Biochim Biophys Acta.* 2008 May;1783(5):673-94. doi: 10.1016/j.bbamcr.2008.01.024. Epub 2008 Feb 12.
- 167 Kim UH, Kim MK, Kim JS, Han MK, Park BH, Kim HR. Purification and characterization of NAD glycohydrolase from rabbit erythrocytes. *Arch Biochem Biophys.* 1993 Aug 15;305(1):147-52.
- 168 Terada M, Fujiki H, Marks PA, Sugimura T. Induction of erythroid differentiation of murine erythroleukemia cells by nicotinamide and related compounds. *Proc Natl Acad Sci U S A.* 1979 Dec;76(12):6411-4.
- 169 Yang H, Yang T, Baur JA, Perez E, Matsui T, Carmona JJ, Lamming DW, Souza-Pinto NC, Bohr VA, Rosenzweig A, de Cabo R, Sauve AA, Sinclair DA. Nutrient-sensitive mitochondrial NAD⁺ levels dictate cell survival. *Cell.* 2007 Sep 21;130(6):1095-107.
- 170 Karczewska J, Martyniec L, Dzierzko G, Stepiński J, Angielski S. The relationship between constitutive ATP release and its extracellular metabolism in isolated rat kidney glomeruli. *J Physiol Pharmacol.* 2007 Jun;58(2):321-33.

- 171 Vitiello L, Gorini S, Rosano G, la Sala A. Immunoregulation through extracellular nucleotides. *Blood*. 2012 Jul 19;120(3):511-8. doi: 10.1182/blood-2012-01-406496. Epub 2012 Jun 1.
- 172 Yin J, Xu K, Zhang J, Kumar A, Yu FS. Wound-induced ATP release and EGF receptor activation in epithelial cells. *J Cell Sci*. 2007 Mar 1;120(Pt 5):815-25. Epub 2007 Feb 6.
- 173 Gribble FM, Loussouarn G, Tucker SJ, Zhao C, Nichols CG, Ashcroft FM. A novel method for measurement of submembrane ATP concentration. *J Biol Chem*. 2000 Sep 29;275(39):30046-9.
- 174 Miller DS, Horowitz S. B. Intracellular compartmentalization of adenosine triphosphate. *J Biol Chem*. 1986 Oct 25;261(30):13911-5.
- 175 Allen DG, Morris PG, Orchard CH, Pirolo JS. A nuclear magnetic resonance study of metabolism in the ferret heart during hypoxia and inhibition of glycolysis. *J Physiol*. 1985 Apr;361:185-204.
- 176 Lazarowski ER, Boucher RC, Harden TK. Constitutive release of ATP and evidence for major contribution of ecto-nucleotide pyrophosphatase and nucleoside diphosphokinase to extracellular nucleotide concentrations. *J Biol Chem*. 2000 Oct 6;275(40):31061-8.
- 177 Lazarowski ER. Vesicular and conductive mechanisms of nucleotide release. *Purinergic Signal*. 2012 Sep;8(3):359-73. doi: 10.1007/s11302-012-9304-9. Epub 2012 Apr 12.
- 178 Eltzschig HK, Eckle T, Mager A, Küper N, Karcher C, Weissmüller T, Boengler K, Schulz R, Robson SC, Colgan SP. ATP release from activated neutrophils occurs via connexin 43 and modulates adenosine-dependent endothelial cell function. *Circ Res*. 2006 Nov 10;99(10):1100-8. Epub 2006 Oct 12.
- 179 Chekeni FB, Elliott MR, Sandilos JK, Walk SF, Kinchen JM, Lazarowski ER, Armstrong AJ, Penuela S, Laird DW, Salvesen GS, Isakson BE, Bayliss DA, Ravichandran KS. Pannexin 1 channels mediate 'find-me' signal release and membrane permeability during apoptosis. *Nature*. 2010 Oct 14;467(7317):863-7. doi: 10.1038/nature09413.
- 180 Sabirov RZ, Okada Y. The maxi-anion channel: a classical channel playing novel roles through an unidentified molecular entity. *J Physiol Sci*. 2009 Jan;59(1):3-21. doi: 10.1007/s12576-008-0008-4. Epub 2008 Dec 9.
- 181 Tokunaga A, Tsukimoto M, Harada H, Moriyama Y, Kojima S. Involvement of SLC17A9-dependent vesicular exocytosis in the mechanism of ATP release during T cell activation. *J Biol Chem*. 2010 Jun 4;285(23):17406-16. doi: 10.1074/jbc.M110.112417. Epub 2010 Apr 9.

- 182 Söhl G, Willecke K. Gap junctions and the connexin protein family. *Cardiovasc Res.* 2004 May 1;62(2):228-32.
- 183 Boassa D, Ambrosi C, Qiu F, Dahl G, Gaietta G, Sosinsky G. Pannexin1 channels contain a glycosylation site that targets the hexamer to the plasma membrane. *J Biol Chem.* 2007 Oct 26;282(43):31733-43. Epub 2007 Aug 22.
- 184 Wang N, De Bock M, Decrock E, Bol M, Gadicherla A, Vinken M, Rogiers V, Bukauskas FF, Bultynck G, Leybaert L. Paracrine signaling through plasma membrane hemichannels. *Biochim Biophys Acta.* 2013 Jan;1828(1):35-50. doi: 10.1016/j.bbame.2012.07.002. Epub 2012 Jul 13.
- 185 Wong CW, Christen T, Roth I, Chadjichristos CE, Derouette JP, Foglia BF, Chanson M, Goodenough DA, Kwak BR. Connexin37 protects against atherosclerosis by regulating monocyte adhesion. *Nat Med.* 2006 Aug;12(8):950-4. Epub 2006 Jul 23.
- 186 Schenk U, Westendorf AM, Radaelli E, Casati A, Ferro M, Fumagalli M, Verderio C, Buer J, Scanziani E, Grassi F. Purinergic control of T cell activation by ATP released through pannexin-1 hemichannels. *Sci Signal.* 2008 Sep 30;1(39):ra6. doi: 10.1126/scisignal.1160583.
- 187 Burnstock G. Introduction: P2 receptors. *Curr Top Med Chem.* 2004;4(8):793-803.
- 188 Jarvis MF, Khakh B. S. ATP-gated P2X cation-channels. *Neuropharmacology.* 2009 Jan;56(1):208-15. doi: 10.1016/j.neuropharm.2008.06.067. Epub 2008 Jul 9.
- 189 Hattori M, Gouaux E. Molecular mechanism of ATP binding and ion channel activation in P2X receptors. *Nature.* 2012 May 10;485(7397):207-12. doi: 10.1038/nature11010.
- 190 Di Virgilio F, Chiozzi P, Ferrari D, Falzoni S, Sanz JM, Morelli A, Torboli M, Bolognesi G, Baricordi OR. Nucleotide receptors: an emerging family of regulatory molecules in blood cells. *Blood.* 2001 Feb 1;97(3):587-600.
- 191 Erb L, Liao Z, Seye CI, Weisman GA. P2 receptors: intracellular signaling. *Pflugers Arch.* 2006 Aug;452(5):552-62. Epub 2006 Apr 4.
- 192 Ferrari D, Chiozzi P, Falzoni S, Dal Susino M, Melchiorri L, Baricordi OR, Di Virgilio F. Extracellular ATP triggers IL-1 beta release by activating the purinergic P2Z receptor of human macrophages. *J Immunol.* 1997 Aug 1;159(3):1451-8.
- 193 Mariathasan S, Weiss DS, Newton K, McBride J, O'Rourke K, Roose-Girma M, Lee WP, Weinrauch Y, Monack DM, Dixit VM. Cryopyrin activates the inflammasome in response to toxins and ATP. *Nature.* 2006 Mar 9;440(7081):228-32. Epub 2006 Jan 11.

- 194 Woehrle T, Yip L, Elkhali A, Sumi Y, Chen Y, Yao Y, Insel PA, Junger WG. Pannexin-1 hemichannel-mediated ATP release together with P2X1 and P2X4 receptors regulate T-cell activation at the immune synapse. *Blood*. 2010 Nov 4;116(18):3475-84. doi: 10.1182/blood-2010-04-277707. Epub 2010 Jul 21.
- 195 Yip L, Woehrle T, Corriden R, Hirsh M, Chen Y, Inoue Y, Ferrari V, Insel PA, Junger WG. Autocrine regulation of T-cell activation by ATP release and P2X7 receptors. *FASEB J*. 2009 Jun;23(6):1685-93. doi: 10.1096/fj.08-126458. Epub 2009 Feb 11.
- 196 Lecut C, Frederix K, Johnson DM, Deroanne C, Thiry M, Faccinnetto C, Marée R, Evans RJ, Volders PG, Bours V, Oury C. P2X1 ion channels promote neutrophil chemotaxis through Rho kinase activation. *J Immunol*. 2009 Aug 15;183(4):2801-9. doi: 10.4049/jimmunol.0804007. Epub 2009 Jul 27.
- 197 Fruscione F, Scarfi S, Ferraris C, Bruzzone S, Benvenuto F, Guida L, Uccelli A, Salis A, Usai C, Jacchetti E, Ilengo C, Scaglione S, Quarto R, Zocchi E, De Flora A. Regulation of human mesenchymal stem cell functions by an autocrine loop involving NAD⁺ release and P2Y11-mediated signaling. *Stem Cells Dev*. 2011 Jul;20(7):1183-98. doi: 10.1089/scd.2010.0295. Epub 2010 Dec 22.
- 198 Jacob F, Pérez Novo C, Bachert C, Van Crombruggen K. Purinergic signaling in inflammatory cells: P2 receptor expression, functional effects, and modulation of inflammatory responses. *Purinergic Signal*. 2013 Sep;9(3):285-306. doi: 10.1007/s11302-013-9357-4. Epub 2013 Feb 13.
- 199 Yadav A, Saini V, Arora S. MCP-1: chemoattractant with a role beyond immunity: a review. *Clin Chim Acta*. 2010 Nov 11;411(21-22):1570-9. doi: 10.1016/j.cca.2010.07.006. Epub 2010 Jul 13.
- 200 Zhang Z, Wang Z, Ren H, Yue M, Huang K, Gu H, Liu M, Du B, Qian M. P2Y(6) agonist uridine 5'-diphosphate promotes host defense against bacterial infection via monocyte chemoattractant protein-1-mediated monocytes/macrophages recruitment. *J Immunol*. 2011 May 1;186(9):5376-87. doi: 10.4049/jimmunol.1002946. Epub 2011 Mar 28.
- 201 Marques-da-Silva C, Burnstock G, Ojcius DM, Coutinho-Silva R. Purinergic receptor agonists modulate phagocytosis and clearance of apoptotic cells in macrophages. *Immunobiology*. 2011 Jan-Feb;216(1-2):1-11. doi: 10.1016/j.imbio.2010.03.010. Epub 2010 Apr 9.
- 202 Matsuyama H, Amaya F, Hashimoto S, Ueno H, Beppu S, Mizuta M, Shime N, Ishizaka A, Hashimoto S. Acute lung inflammation and ventilator-induced lung injury caused by ATP via the P2Y receptors: an experimental study. *Respir Res*. 2008 Dec 13;9:79. doi: 10.1186/1465-9921-9-79.

- 203 Chen Y, Corriden R, Inoue Y, Yip L, Hashiguchi N, Zinkernagel A, Nizet V, Insel PA, Junger WG. ATP release guides neutrophil chemotaxis via P2Y2 and A3 receptors. *Science*. 2006 Dec 15;314(5806):1792-5.
- 204 Kukulski F, Lévesque SA, Sévigny J. Impact of ectoenzymes on p2 and p1 receptor signaling. *Adv Pharmacol*. 2011;61:263-99. doi: 10.1016/B978-0-12-385526-8.00009-6.
- 205 Kukulski F, Lévesque SA, Lavoie EG, Lecka J, Bigonnesse F, Knowles AF, Robson SC, Kirley TL, Sévigny J. Comparative hydrolysis of P2 receptor agonists by NTPDases 1, 2, 3 and 8. *Purinergic Signal*. 2005 Jun;1(2):193-204. doi: 10.1007/s11302-005-6217-x. Epub 2005 Mar 17.
- 206 Robson SC, Sévigny J, Zimmermann H. The E-NTPDase family of ectonucleotidases: Structure function relationships and pathophysiological significance. *Purinergic Signal*. 2006 Jun;2(2):409-30. doi: 10.1007/s11302-006-9003-5. Epub 2006 May 30.
- 207 Zimmermann H, Zebisch M, Sträter N. Cellular function and molecular structure of ecto-nucleotidases. *Purinergic Signal*. 2012 Sep;8(3):437-502. doi: 10.1007/s11302-012-9309-4. Epub 2012 May 4.
- 208 Braun N, Fengler S, Ebeling C, Servos J, Zimmermann H. Sequencing, functional expression and characterization of rat NTPDase6, a nucleoside diphosphatase and novel member of the ecto-nucleoside triphosphate diphosphohydrolase family. *Biochem J*. 2000 Nov 1;351 Pt 3:639-47.
- 209 Mulero JJ, Yeung G, Nelken ST, Ford JE. CD39-L4 is a secreted human apyrase, specific for the hydrolysis of nucleoside diphosphates. *J Biol Chem*. 1999 Jul 16;274(29):20064-7.
- 210 Schicker K, Hussl S, Chandaka GK, Kosenburger K, Yang JW, Waldhoer M, Sitte HH, Boehm S. A membrane network of receptors and enzymes for adenine nucleotides and nucleosides. *Biochim Biophys Acta*. 2009 Feb;1793(2):325-34. doi: 10.1016/j.bbamcr.2008.09.014. Epub 2008 Oct 10.
- 211 Dwyer KM, Deaglio S, Gao W, Friedman D, Strom TB, Robson SC. CD39 and control of cellular immune responses. *Purinergic Signal*. 2007 Mar;3(1-2):171-80. doi: 10.1007/s11302-006-9050-y. Epub 2007 Feb 6.
- 212 Friedman DJ, Künzli BM, A-Rahim YI, Sévigny J, Berberat PO, Enjyoji K, Csizmadia E, Friess H, Robson SC. From the Cover: CD39 deletion exacerbates experimental murine colitis and human polymorphisms increase susceptibility to inflammatory bowel disease. *Proc Natl Acad Sci U S A*. 2009 Sep 29;106(39):16788-93. doi: 10.1073/pnas.0902869106. Epub 2009 Sep 28.

- 213 Sun X, Imai M, Nowak-Machen M, Guckelberger O, Enjyoji K, Wu Y, Khalpey Z, Berberat P, Munasinghe J, Robson SC. Liver damage and systemic inflammatory responses are exacerbated by the genetic deletion of CD39 in total hepatic ischemia. *Purinergic Signal*. 2011 Dec;7(4):427-34. doi: 10.1007/s11302-011-9239-6. Epub 2011 Jun 9.
- 214 Bollen M, Gijsbers R, Ceulemans H, Stalmans W, Stefan C. Nucleotide pyrophosphatases/phosphodiesterases on the move. *Crit Rev Biochem Mol Biol*. 2000;35(6):393-432.
- 215 Bachorik PS, Dietrich L. S. The purification and properties of detergent-solubilized rat liver nucleotide pyrophosphatase. *J Biol Chem*. 1972 Aug 25;247(16):5071-8.
- 216 Evans WH, Hood DO, Gurd JW. Purification and properties of a mouse liver plasma-membrane glycoprotein hydrolysing nucleotide pyrophosphate and phosphodiester bonds. *Biochem J*. 1973 Dec;135(4):819-26.
- 217 Horenstein AL, Chillemi A, Zaccarello G, Bruzzone S, Quarona V, Zito A, Serra S, Malavasi F. A CD38/CD203a/CD73 ectoenzymatic pathway independent of CD39 drives a novel adenosinergic loop in human T lymphocytes. *Oncoimmunology*. 2013 Sep 1;2(9):e26246. Epub 2013 Sep 26.
- 218 Stefan C, Jansen S, Bollen M. Modulation of purinergic signaling by NPP-type ectophosphodiesterases. *Purinergic Signal*. 2006 Jun;2(2):361-70. doi: 10.1007/s11302-005-5303-4. Epub 2006 Jun 1.
- 219 Grahnert A, Grahnert A, Klein C, Schilling E, Wehrhahn J, Hauschildt S. Review: NAD⁺: a modulator of immune functions. *Innate Immun*. 2011 Apr;17(2):212-33. doi: 10.1177/1753425910361989. Epub 2010 Apr 13.
- 220 Hirata Y, Kimura N, Sato K, Ohsugi Y, Takasawa S, Okamoto H, Ishikawa J, Kaisho T, Ishihara K, Hirano T. ADP ribosyl cyclase activity of a novel bone marrow stromal cell surface molecule, BST-1. *FEBS Lett*. 1994 Dec 19;356(2-3):244-8.
- 221 Howard M, Grimaldi JC, Bazan JF, Lund FE, Santos-Argumedo L, Parkhouse RM, Walseth TF, Lee HC. Formation and hydrolysis of cyclic ADP-ribose catalyzed by lymphocyte antigen CD38. *Science*. 1993 Nov 12;262(5136):1056-9.
- 222 Gustafsson AJ, Muraro L, Dahlberg C, Migaud M, Chevallier O, Khanh HN, Krishnan K, Li N, Islam MS. ADP ribose is an endogenous ligand for the purinergic P2Y1 receptor. *Mol Cell Endocrinol*. 2011 Feb 10;333(1):8-19. doi: 10.1016/j.mce.2010.11.004. Epub 2010 Nov 19.
- 223 De Flora A, Zocchi E, Guida L, Franco L, Bruzzone S. Autocrine and paracrine calcium signaling by the CD38/NAD⁺/cyclic ADP-ribose system. *Ann N Y Acad Sci*. 2004 Dec;1028:176-91.

- 224 Seman M, Adriouch S, Haag F, Koch-Nolte F. Ecto-ADP-ribosyltransferases (ARTs): emerging actors in cell communication and signaling. *Curr Med Chem*. 2004 Apr;11(7):857-72.
- 225 Hong S, Brass A, Seman M, Haag F, Koch-Nolte F, Dubyak GR. Basal and inducible expression of the thiol-sensitive ART2.1 ecto-ADP-ribosyltransferase in myeloid and lymphoid leukocytes. *Purinergic Signal*. 2009 Sep;5(3):369-83. doi: 10.1007/s11302-009-9162-2. Epub 2009 Apr 30.
- 226 Seman M, Adriouch S, Scheuplein F, Krebs C, Freese D, Glowacki G, Deterre P, Haag F, Koch-Nolte F. NAD-induced T cell death: ADP-ribosylation of cell surface proteins by ART2 activates the cytolytic P2X7 purinoceptor. *Immunity*. 2003 Oct;19(4):571-82.
- 227 Zimmermann H. 5'-Nucleotidase: molecular structure and functional aspects. *Biochem J*. 1992 Jul 15;285 (Pt 2):345-65.
- 228 Sträter N. Ecto-5'-nucleotidase: Structure function relationships. *Purinergic Signal*. 2006 Jun;2(2):343-50. doi: 10.1007/s11302-006-9000-8. Epub 2006 May 16.
- 229 Colgan SP, Eltzschig HK, Eckle T, Thompson LF. Physiological roles for ecto-5'-nucleotidase (CD73). *Purinergic Signal*. 2006 Jun;2(2):351-60. doi: 10.1007/s11302-005-5302-5. Epub 2006 Jun 1.
- 230 Knöfel T, Sträter N. X-ray structure of the Escherichia coli periplasmic 5'-nucleotidase containing a dimetal catalytic site. *Nat Struct Biol*. 1999 May;6(5):448-53.
- 231 Hunsucker SA, Mitchell BS, Sychala J. The 5'-nucleotidases as regulators of nucleotide and drug metabolism. *Pharmacol Ther*. 2005 Jul;107(1):1-30.
- 232 Garavaglia S, Bruzzone S, Cassani C, Canella L, Allegrone G, Sturla L, Mannino E, Millo E, De Flora A, Rizzi M. The high-resolution crystal structure of periplasmic Haemophilus influenzae NAD nucleotidase reveals a novel enzymatic function of human CD73 related to NAD metabolism. *Biochem J*. 2012 Jan 1;441(1):131-41. doi: 10.1042/BJ20111263.
- 233 Eckle T, Füllbier L, Wehrmann M, Khoury J, Mittelbronn M, Ibla J, Rosenberger P, Eltzschig HK. Identification of ectonucleotidases CD39 and CD73 in innate protection during acute lung injury. *J Immunol*. 2007 Jun 15;178(12):8127-37.
- 234 Reutershan J, Vollmer I, Stark S, Wagner R, Ngamsri KC, Eltzschig HK. Adenosine and inflammation: CD39 and CD73 are critical mediators in LPS-induced PMN trafficking into the lungs. *FASEB J*. 2009 Feb;23(2):473-82. doi: 10.1096/fj.08-119701. Epub 2008 Oct 6.
- 235 Zerneck A, Bidzhekov K, Ozüyan B, Fraemohs L, Liehn EA, Lüscher-Firzlauff JM, Lüscher B, Schrader J, Weber C. CD73/ecto-5'-nucleotidase protects against vascular inflammation and neointima formation. *Circulation*. 2006 May 2;113(17):2120-7. Epub 2006 Apr 24.

- 236 Hart ML, Henn M, Köhler D, Kloor D, Mittelbronn M, Gorzolla IC, Stahl GL, Eltzschig HK. Role of extracellular nucleotide phosphohydrolysis in intestinal ischemia-reperfusion injury. *FASEB J*. 2008 Aug;22(8):2784-97. doi: 10.1096/fj.07-103911. Epub 2008 Mar 19.
- 237 Schütz W, Schrader J, Gerlach E. Different sites of adenosine formation in the heart. *Am J Physiol*. 1981 Jun;240(6):H963-70.
- 238 Koszalka P, Ozüyan B, Huo Y, Zerneck A, Flögel U, Braun N, Buchheiser A, Decking UK, Smith ML, Sévigny J, Gear A, Weber AA, Molojavyi A, Ding Z, Weber C, Ley K, Zimmermann H, Gödecke A, Schrader J. Targeted disruption of cd73/ecto-5'-nucleotidase alters thromboregulation and augments vascular inflammatory response. *Circ Res*. 2004 Oct 15;95(8):814-21. Epub 2004 Sep 9.
- 239 Chen JF, Eltzschig HK, Fredholm BB. Adenosine receptors as drug targets--what are the challenges? *Nat Rev Drug Discov*. 2013 Apr;12(4):265-86. doi: 10.1038/nrd3955.
- 240 Fredholm BB, IJerman AP, Jacobson KA, Klotz KN, Linden J. International Union of Pharmacology. XXV. Nomenclature and classification of adenosine receptors. *Pharmacol Rev*. 2001 Dec;53(4):527-52.
- 241 Fredholm BB, IJerman AP, Jacobson KA, Linden J, Müller CE. International Union of Basic and Clinical Pharmacology. LXXXI. Nomenclature and classification of adenosine receptors--an update. *Pharmacol Rev*. 2011 Mar;63(1):1-34. doi: 10.1124/pr.110.003285. Epub 2011 Feb 8.
- 242 Dias RB, Rombo DM, Ribeiro JA, Henley JM, Sebastião AM. Adenosine: setting the stage for plasticity. *Trends Neurosci*. 2013 Apr;36(4):248-57. doi: 10.1016/j.tins.2012.12.003. Epub 2013 Jan 15.
- 243 Fredholm BB, Arslan G, Halldner L, Kull B, Schulte G, Wasserman W. Structure and function of adenosine receptors and their genes. *Naunyn Schmiedebergs Arch Pharmacol*. 2000 Nov;362(4-5):364-74.
- 244 Daly JW, Padgett W. L. Agonist activity of 2- and 5'-substituted adenosine analogs and their N6-cycloalkyl derivatives at A1- and A2-adenosine receptors coupled to adenylate cyclase. *Biochem Pharmacol*. 1992 Mar 3;43(5):1089-93.
- 245 Schütz W, Freissmuth M, Hausleithner V, Tuisl E. Cardiac sarcolemmal purity is essential for the verification of adenylate cyclase inhibition via A1-adenosine receptors. *Naunyn Schmiedebergs Arch Pharmacol*. 1986 Jun;333(2):156-62.
- 246 Jacobson KA, Gao Z. G. Adenosine receptors as therapeutic targets. *Nat Rev Drug Discov*. 2006 Mar;5(3):247-64.

- 247 Cronstein BN, Daguma L, Nichols D, Hutchison AJ, Williams M. The adenosine/neutrophil paradox resolved: human neutrophils possess both A1 and A2 receptors that promote chemotaxis and inhibit O₂ generation, respectively. *J Clin Invest.* 1990 Apr;85(4):1150-7.
- 248 Lee HT, Gallos G, Nasr SH, Emala CW. A1 adenosine receptor activation inhibits inflammation, necrosis, and apoptosis after renal ischemia-reperfusion injury in mice. *J Am Soc Nephrol.* 2004 Jan;15(1):102-11.
- 249 Lee HT, Xu H, Nasr SH, Schnermann J, Emala CW. A1 adenosine receptor knockout mice exhibit increased renal injury following ischemia and reperfusion. *Am J Physiol Renal Physiol.* 2004 Feb;286(2):F298-306. Epub 2003 Nov 4.
- 250 Corvol JC, Studler JM, Schonn JS, Girault JA, Hervé D. Galpha(olf) is necessary for coupling D1 and A2a receptors to adenylyl cyclase in the striatum. *J Neurochem.* 2001 Mar;76(5):1585-8.
- 251 Kull B, Svenningsson P, Fredholm BB. Adenosine A(2A) receptors are colocalized with and activate g(olf) in rat striatum. *Mol Pharmacol.* 2000 Oct;58(4):771-7.
- 252 Belardinelli L, Shryock JC, Snowdy S, Zhang Y, Monopoli A, Lozza G, Ongini E, Olsson RA, Dennis DM. The A2A adenosine receptor mediates coronary vasodilation. *J Pharmacol Exp Ther.* 1998 Mar;284(3):1066-73.
- 253 Ledent C, Vaugeois JM, Schiffmann SN, Pedrazzini T, El Yacoubi M, Vanderhaeghen JJ, Costentin J, Heath JK, Vassart G, Parmentier M. Aggressiveness, hypoalgesia and high blood pressure in mice lacking the adenosine A2a receptor. *Nature.* 1997 Aug 14;388(6643):674-8.
- 254 Milne GR, Palmer T. M. Anti-inflammatory and immunosuppressive effects of the A2A adenosine receptor. *ScientificWorldJournal.* 2011 Feb 3;11:320-39. doi: 10.1100/tsw.2011.22.
- 255 Salmon JI, Cronstein B. N. Fc gamma receptor-mediated functions in neutrophils are modulated by adenosine receptor occupancy. A1 receptors are stimulatory and A2 receptors are inhibitory. *J Immunol.* 1990 Oct 1;145(7):2235-40.
- 256 Cronstein BN, Levin RI, Philips M, Hirschhorn R, Abramson SB, Weissmann G. Neutrophil adherence to endothelium is enhanced via adenosine A1 receptors and inhibited via adenosine A2 receptors. *J Immunol.* 1992 Apr 1;148(7):2201-6.
- 257 Zhao ZQ, Sato H, Williams MW, Fernandez AZ, Vinten-Johansen J. Adenosine A2-receptor activation inhibits neutrophil-mediated injury to coronary endothelium. *Am J Physiol.* 1996 Oct;271(4 Pt 2):H1456-64.
- 258 Haskó G, Kuhel DG, Chen JF, Schwarzschild MA, Deitch EA, Mabley JG, Marton A, Szabó C. Adenosine inhibits IL-12 and TNF-[alpha] production via adenosine A2a receptor-dependent and independent mechanisms. *FASEB J.* 2000 Oct;14(13):2065-74.

- 259 Kreckler LM, Wan TC, Ge ZD, Auchampach JA. Adenosine inhibits tumor necrosis factor-alpha release from mouse peritoneal macrophages via A2A and A2B but not the A3 adenosine receptor. *J Pharmacol Exp Ther.* 2006 Apr;317(1):172-80. Epub 2005 Dec 9.
- 260 Lappas CM, Rieger JM, Linden J. A2A adenosine receptor induction inhibits IFN-gamma production in murine CD4+ T cells. *J Immunol.* 2005 Jan 15;174(2):1073-80.
- 261 Panther E, Idzko M, Herouy Y, Rheinen H, Gebicke-Haerter PJ, Mrowietz U, Dichmann S, Norgauer J. Expression and function of adenosine receptors in human dendritic cells. *FASEB J.* 2001 Sep;15(11):1963-70.
- 262 Panther E, Corinti S, Idzko M, Herouy Y, Napp M, la Sala A, Girolomoni G, Norgauer J. Adenosine affects expression of membrane molecules, cytokine and chemokine release, and the T-cell stimulatory capacity of human dendritic cells. *Blood.* 2003 May 15;101(10):3985-90. Epub 2002 Nov 21.
- 263 Romio M, Reinbeck B, Bongardt S, Hüls S, Burghoff S, Schrader J. Extracellular purine metabolism and signaling of CD73-derived adenosine in murine Treg and Teff cells. *Am J Physiol Cell Physiol.* 2011 Aug;301(2):C530-9. doi: 10.1152/ajpcell.00385.2010. Epub 2011 May 18.
- 264 Csóka B, Németh ZH, Virág L, Gergely P, Leibovich SJ, Pacher P, Sun CX, Blackburn MR, Vizi ES, Deitch EA, Haskó G. A2A adenosine receptors and C/EBPbeta are crucially required for IL-10 production by macrophages exposed to Escherichia coli. *Blood.* 2007 Oct 1;110(7):2685-95. Epub 2007 May 24.
- 265 Link AA, Kino T, Worth JA, McGuire JL, Crane ML, Chrousos GP, Wilder RL, Elenkov IJ. Ligand-activation of the adenosine A2a receptors inhibits IL-12 production by human monocytes. *J Immunol.* 2000 Jan 1;164(1):436-42.
- 266 Blackburn MR, Vance CO, Morschl E, Wilson CN. Adenosine receptors and inflammation. *Handb Exp Pharmacol.* 2009;(193):215-69. doi: 10.1007/978-3-540-89615-9_8.
- 267 Glover DK, Riou LM, Ruiz M, Sullivan GW, Linden J, Rieger JM, Macdonald TL, Watson DD, Beller GA. Reduction of infarct size and postischemic inflammation from ATL-146e, a highly selective adenosine A2A receptor agonist, in reperfused canine myocardium. *Am J Physiol Heart Circ Physiol.* 2005 Apr;288(4):H1851-8. Epub 2004 Dec 9.
- 268 Lasley RD, Jahania MS, Mentzer RM Jr. Beneficial effects of adenosine A(2a) agonist CGS-21680 in infarcted and stunned porcine myocardium. *Am J Physiol Heart Circ Physiol.* 2001 Apr;280(4):H1660-6.

- 269 Yang Z, Day YJ, Toufektsian MC, Xu Y, Ramos SI, Marshall MA, French BA, Linden J. Myocardial infarct-sparing effect of adenosine A2A receptor activation is due to its action on CD4+ T lymphocytes. *Circulation*. 2006 Nov 7;114(19):2056-64. Epub 2006 Oct 23.
- 270 Okusa MD. A(2A) adenosine receptor: a novel therapeutic target in renal disease. *Am J Physiol Renal Physiol*. 2002 Jan;282(1):F10-8.
- 271 Day YJ, Huang L, McDuffie MJ, Rosin DL, Ye H, Chen JF, Schwarzschild MA, Fink JS, Linden J, Okusa MD. Renal protection from ischemia mediated by A2A adenosine receptors on bone marrow-derived cells. *J Clin Invest*. 2003 Sep;112(6):883-91.
- 272 Day YJ, Huang L, Ye H, Linden J, Okusa MD. Renal ischemia-reperfusion injury and adenosine 2A receptor-mediated tissue protection: role of macrophages. *Am J Physiol Renal Physiol*. 2005 Apr;288(4):F722-31. Epub 2004 Nov 23.
- 273 Fredholm BB, Irenius E, Kull B, Schulte G. Comparison of the potency of adenosine as an agonist at human adenosine receptors expressed in Chinese hamster ovary cells. *Biochem Pharmacol*. 2001 Feb 15;61(4):443-8.
- 274 Fredholm BB. Adenosine, an endogenous distress signal, modulates tissue damage and repair. *Cell Death Differ*. 2007 Jul;14(7):1315-23. Epub 2007 Mar 30.
- 275 Feoktistov I, Biaggioni I. Role of adenosine A(2B) receptors in inflammation. *Adv Pharmacol*. 2011;61:115-44. doi: 10.1016/B978-0-12-385526-8.00005-9.
- 276 Koeppen M, Harter PN, Bonney S, Bonney M, Reithel S, Zachskorn C, Mittelbronn M, Eckle T. Adora2b signaling on bone marrow derived cells dampens myocardial ischemia-reperfusion injury. *Anesthesiology*. 2012 Jun;116(6):1245-57. doi: 10.1097/ALN.0b013e318255793c.
- 277 Chen H, Yang D, Carroll SH, Eltzschig HK, Ravid K. Activation of the macrophage A2b adenosine receptor regulates tumor necrosis factor-alpha levels following vascular injury. *Exp Hematol*. 2009 May;37(5):533-8. doi: 10.1016/j.exphem.2009.02.001.
- 278 Németh ZH, Lutz CS, Csóka B, Deitch EA, Leibovich SJ, Gause WC, Tone M, Pacher P, Vizi ES, Haskó G. Adenosine augments IL-10 production by macrophages through an A2B receptor-mediated posttranscriptional mechanism. *J Immunol*. 2005 Dec 15;175(12):8260-70.
- 279 Csóka B, Selmeczy Z, Koscsó B, Németh ZH, Pacher P, Murray PJ, Kepka-Lenhart D, Morris SM Jr, Gause WC, Leibovich SJ, Haskó G. Adenosine promotes alternative macrophage activation via A2A and A2B receptors. *FASEB J*. 2012 Jan;26(1):376-86. doi: 10.1096/fj.11-190934. Epub 2011 Sep 16.

- 280 Feoktistov I, Goldstein AE, Biaggioni I. Role of p38 mitogen-activated protein kinase and extracellular signal-regulated protein kinase kinase in adenosine A2B receptor-mediated interleukin-8 production in human mast cells. *Mol Pharmacol*. 1999 Apr;55(4):726-34.
- 281 Sitaraman SV, Merlin D, Wang L, Wong M, Gewirtz AT, Si-Tahar M, Madara JL. Neutrophil-epithelial crosstalk at the intestinal luminal surface mediated by reciprocal secretion of adenosine and IL-6. *J Clin Invest*. 2001 Apr;107(7):861-9.
- 282 Eckle T, Krahn T, Grenz A, Köhler D, Mittelbronn M, Ledent C, Jacobson MA, Osswald H, Thompson LF, Unertl K, Eltzschig HK. Cardioprotection by ecto-5'-nucleotidase (CD73) and A2B adenosine receptors. *Circulation*. 2007 Mar 27;115(12):1581-90. Epub 2007 Mar 12.
- 283 Toldo S, Zhong H, Mezzaroma E, Van Tassell BW, Kannan H, Zeng D, Belardinelli L, Voelkel NF, Abbate A. GS-6201, a selective blocker of the A2B adenosine receptor, attenuates cardiac remodeling after acute myocardial infarction in the mouse. *J Pharmacol Exp Ther*. 2012 Dec;343(3):587-95. doi: 10.1124/jpet.111.191288. Epub 2012 Aug 24.
- 284 Zhou QY, Li C, Olah ME, Johnson RA, Stiles GL, Civelli O. Molecular cloning and characterization of an adenosine receptor: the A3 adenosine receptor. *Proc Natl Acad Sci U S A*. 1992 Aug 15;89(16):7432-6.
- 285 Abbracchio MP, Brambilla R, Ceruti S, Kim HO, von Lubitz DK, Jacobson KA, Cattabeni F. G protein-dependent activation of phospholipase C by adenosine A3 receptors in rat brain. *Mol Pharmacol*. 1995 Dec;48(6):1038-45.
- 286 Fossetta J, Jackson J, Deno G, Fan X, Du XK, Bober L, Soudé-Bermejo A, de Bouteiller O, Caux C, Lunn C, Lundell D, Palmer RK. Pharmacological analysis of calcium responses mediated by the human A3 adenosine receptor in monocyte-derived dendritic cells and recombinant cells. *Mol Pharmacol*. 2003 Feb;63(2):342-50.
- 287 Zhong H, Shlykov SG, Molina JG, Sanborn BM, Jacobson MA, Tilley SL, Blackburn MR. Activation of murine lung mast cells by the adenosine A3 receptor. *J Immunol*. 2003 Jul 1;171(1):338-45.
- 288 Martin L, Pingle SC, Hallam DM, Rybak LP, Ramkumar V. Activation of the adenosine A3 receptor in RAW 264.7 cells inhibits lipopolysaccharide-stimulated tumor necrosis factor-alpha release by reducing calcium-dependent activation of nuclear factor-kappaB and extracellular signal-regulated kinase 1/2. *J Pharmacol Exp Ther*. 2006 Jan;316(1):71-8. Epub 2005 Sep 27.
- 289 Sajjadi FG, Takabayashi K, Foster AC, Domingo RC, Firestein GS. Inhibition of TNF-alpha expression by adenosine: role of A3 adenosine receptors. *J Immunol*. 1996 May 1;156(9):3435-42.

- 290 Cristalli G, Costanzi S, Lambertucci C, Lupidi G, Vittori S, Volpini R, Camaioni E. Adenosine deaminase: functional implications and different classes of inhibitors. *Med Res Rev.* 2001 Mar;21(2):105-28.
- 291 Zavialov AV, Engström A. Human ADA2 belongs to a new family of growth factors with adenosine deaminase activity. *Biochem J.* 2005 Oct 1;391(Pt 1):51-7.
- 292 Aran JM, Colomer D, Matutes E, Vives-Corrons JL, Franco R. Presence of adenosine deaminase on the surface of mononuclear blood cells: immunochemical localization using light and electron microscopy. *J Histochem Cytochem.* 1991 Aug;39(8):1001-8.
- 293 Li RW, Yang C, Sit AS, Lin SY, Ho EY, Leung GP. Physiological and pharmacological roles of vascular nucleoside transporters. *J Cardiovasc Pharmacol.* 2012 Jan;59(1):10-5. doi: 10.1097/FJC.0b013e31820eb788.
- 294 Young JD, Yao SY, Baldwin JM, Cass CE, Baldwin SA. The human concentrative and equilibrative nucleoside transporter families, SLC28 and SLC29. *Mol Aspects Med.* 2013 Apr-Jun;34(2-3):529-47. doi: 10.1016/j.mam.2012.05.007.
- 295 Gray JH, Owen RP, Giacomini KM. The concentrative nucleoside transporter family, SLC28. *Pflugers Arch.* 2004 Feb;447(5):728-34. Epub 2003 Jul 11.
- 296 Soler C, García-Manteiga J, Valdés R, Xaus J, Comalada M, Casado FJ, Pastor-Anglada M, Celada A, Felipe A. Macrophages require different nucleoside transport systems for proliferation and activation. *FASEB J.* 2001 Sep;15(11):1979-88.
- 297 Yao SY, Ng AM, Cass CE, Baldwin SA, Young JD. Nucleobase transport by human equilibrative nucleoside transporter 1 (hENT1). *J Biol Chem.* 2011 Sep 16;286(37):32552-62. doi: 10.1074/jbc.M111.236117. Epub 2011 Jul 27.
- 298 Rose JB, Naydenova Z, Bang A, Ramadan A, Klawitter J, Schram K, Sweeney G, Grenz A, Eltzschig H, Hammond J, Choi DS, Coe IR. Absence of equilibrative nucleoside transporter 1 in ENT1 knockout mice leads to altered nucleoside levels following hypoxic challenge. *Life Sci.* 2011 Oct 24;89(17-18):621-30. doi: 10.1016/j.lfs.2011.08.007. Epub 2011 Aug 17.
- 299 Eckle T, Hughes K, Ehrentraut H, Brodsky KS, Rosenberger P, Choi DS, Ravid K, Weng T, Xia Y, Blackburn MR, Eltzschig HK. Crosstalk between the equilibrative nucleoside transporter ENT2 and alveolar Adora2b adenosine receptors dampens acute lung injury. *FASEB J.* 2013 Aug;27(8):3078-89. doi: 10.1096/fj.13-228551. Epub 2013 Apr 19.
- 300 Boison D. Adenosine kinase: exploitation for therapeutic gain. *Pharmacol Rev.* 2013 Apr 16;65(3):906-43. doi: 10.1124/pr.112.006361. Print 2013 Jul.
- 301 Jacob MI, Berne R. M. Metabolism of purine derivatives by the isolated cat heart. *Am J Physiol.* 1960 Feb;198:322-6.

- 302 Murray AW. The biological significance of purine salvage. *Annu Rev Biochem.* 1971;40:811-26.
- 303 Deussen A. Metabolic flux rates of adenosine in the heart. *Naunyn Schmiedebergs Arch Pharmacol.* 2000 Nov;362(4-5):351-63.
- 304 Phillips E, Newsholme E. A. Maximum activities, properties and distribution of 5' nucleotidase, adenosine kinase and adenosine deaminase in rat and human brain. *J Neurochem.* 1979 Aug;33(2):553-8.
- 305 Deussen A, Stappert M, Schäfer S, Kelm M. Quantification of extracellular and intracellular adenosine production: understanding the transmembranous concentration gradient. *Circulation.* 1999 Apr 20;99(15):2041-7.
- 306 Bönner F, Borg N, Burghoff S, Schrader J. Resident cardiac immune cells and expression of the ectonucleotidase enzymes CD39 and CD73 after ischemic injury. *PLoS One.* 2012;7(4):e34730. doi: 10.1371/journal.pone.0034730. Epub 2012 Apr 13.
- 307 Bönner F, Borg N, Jacoby C, Temme S, Ding Z, Flögel U, Schrader J. Ecto-5'-nucleotidase on immune cells protects from adverse cardiac remodeling. *Circ Res.* 2013 Jul 19;113(3):301-12. doi: 10.1161/CIRCRESAHA.113.300180. Epub 2013 May 29.
- 308 Borg N, Alter C, Görltdt N, Jacoby C, Ding Z, Steckel B, Quast C, Bönner F, Friebe D, Temme S, Flögel U, Schrader J. CD73 on T-Cells Orchestrates Cardiac Wound Healing After Myocardial Infarction by Purinergic Metabolic Reprogramming. *Circulation.* 2017 Apr 21. pii: CIRCULATIONAHA.116.023365. doi: 10.1161/CIRCULATIONAHA.116.023365. [Epub ahead of print].
- 309 Sung SJ, Li L, Huang L, Lawler J, Ye H, Rosin DL, Vincent IS, Le TH, Yu J, Görltdt N, Schrader J, Okusa MD. Proximal Tubule CD73 Is Critical in Renal Ischemia-Reperfusion Injury Protection. *J Am Soc Nephrol.* 2016 Sep 14. pii: ASN.2016020229. [Epub ahead of print].
- 310 Sawada S, Scarborough JD, Killeen N, Littman DR. A lineage-specific transcriptional silencer regulates CD4 gene expression during T lymphocyte development. *Cell.* 1994 Jun 17;77(6):917-29.
- 311 Lee PP, Fitzpatrick DR, Beard C, Jessup HK, Lehar S, Makar KW, Pérez-Melgosa M, Sweetser MT, Schlissel MS, Nguyen S, Cherry SR, Tsai JH, Tucker SM, Weaver WM, Kelso A, Jaenisch R, Wilson CB. A critical role for Dnmt1 and DNA methylation in T cell development, function, and survival. *Immunity.* 2001 Nov;15(5):763-74.
- 312 Enjyoji K1, Sévigny J, Lin Y, Frenette PS, Christie PD, Esch JS 2nd, Imai M, Edelberg JM, Rayburn H, Lech M, Beeler DL, Csizmadia E, Wagner DD, Robson SC, Rosenberg RD. Targeted disruption of cd39/ATP diphosphohydrolase results in disordered hemostasis and thromboregulation. *Nat Med.* 1999 Sep;5(9):1010-7.

- 313 Enjyoji K, Kotani K, Thukral C, Blumel B, Sun X, Wu Y, Imai M, Friedman D, Csizmadia E, Bleibel W, Kahn BB, Robson SC. Deletion of cd39/entpd1 results in hepatic insulin resistance. *Diabetes*. 2008 Sep;57(9):2311-20. doi: 10.2337/db07-1265. Epub 2008 Jun 20.
- 314 Zimmermann O, Homann JM, Bangert A, Müller AM, Hristov G, Goeser S, Wiehe JM, Zittrich S, Rottbauer W, Torzewski J, Pfitzer G, Katus HA, Kaya Z. Successful use of mRNA-nucleofection for overexpression of interleukin-10 in murine monocytes/macrophages for anti-inflammatory therapy in a murine model of autoimmune myocarditis. *J Am Heart Assoc*. 2012 Dec;1(6):e003293. doi: 10.1161/JAHA.112.003293. Epub 2012 Dec 19.
- 315 Humphreys BD, Lin SL, Kobayashi A, Hudson TE, Nowlin BT, Bonventre JV, Valerius MT, McMahon AP, Duffield JS. Fate tracing reveals the pericyte and not epithelial origin of myofibroblasts in kidney fibrosis. *Am J Pathol*. 2010 Jan;176(1):85-97. doi: 10.2353/ajpath.2010.090517. Epub 2009 Dec 11.
- 316 Kloor D, Kurz J, Fuchs S, Faust B, Osswald H. S-adenosylhomocysteine-hydrolase from bovine kidney: enzymatic and binding properties. *Kidney Blood Press Res*. 1996;19(2):100-8.
- 317 Langendorff O. Untersuchungen am überlebenden Säugethierherzen. *Pflugers Arch*. 1895;61, pp. 291–332.
- 318 Fiset C, Clark RB, Larsen TS, Giles WR. A rapidly activating sustained K⁺ current modulates repolarization and excitation-contraction coupling in adult mouse ventricle. *J Physiol*. 1997 Nov 1;504 (Pt 3):557-63.
- 319 Zhou YY, Wang SQ, Zhu WZ, Chruscinski A, Kobilka BK, Ziman B, Wang S, Lakatta EG, Cheng H, Xiao RP. Culture and adenoviral infection of adult mouse cardiac myocytes: methods for cellular genetic physiology. *Am J Physiol Heart Circ Physiol*. 2000 Jul;279(1):H429-36.
- 320 Kharel Y, Raje M, Gao M, Gellett AM, Tomsig JL, Lynch KR, Santos WL. Sphingosine kinase type 2 inhibition elevates circulating sphingosine 1-phosphate. *Biochem J*. 2012 Oct 1;447(1):149-57. doi: 10.1042/BJ20120609.
- 321 Mosmann T. Rapid colorimetric assay for cellular growth and survival: application to proliferation and cytotoxicity assays. *J Immunol Methods*. 1983 Dec 16;65(1-2):55-63.
- 322 Livak KJ, Schmittgen T. D. Analysis of relative gene expression data using real-time quantitative PCR and the 2^{(-Delta Delta C(T))} Method. *Methods*. 2001 Dec;25(4):402-8.
- 323 Reddy GK, Enwemeka C. S. A simplified method for the analysis of hydroxyproline in biological tissues. *Clin Biochem*. 1996 Jun;29(3):225-9.

- 324 Masson PJ. Some histological methods: trichrome stainings and their preliminary technique. *Tech Methods* 1929; 12:75 - 90.
- 325 Ziegler SF, Ramsdell F, Alderson MR. The activation antigen CD69. *Stem Cells*. 1994 Sep;12(5):456-65.
- 326 Le Hir M, Kaissling B. Distribution and regulation of renal ecto-5'-nucleotidase: implications for physiological functions of adenosine. *Am J Physiol*. 1993 Mar;264(3 Pt 2):F377-87.
- 327 Inoue T, Abe C, Sung SS, Moscalu S, Jankowski J, Huang L, Ye H, Rosin DL, Guyenet PG, Okusa MD. Vagus nerve stimulation mediates protection from kidney ischemia-reperfusion injury through $\alpha 7nAChR+$ splenocytes. *J Clin Invest*. 2016 May 2;126(5):1939-52. doi: 10.1172/JCI83658. Epub 2016 Apr 18.
- 328 World Health Organisation (WHO). The top 10 causes of death. *Fact sheet N°310; Updated May 2014*.
- 329 Statistisches Bundesamt. Gesundheit - Krankheitskosten. *Wiesbaden*. 2015.
- 330 Synnestvedt K, Furuta GT, Comerford KM, Louis N, Karhausen J, Eltzschig HK, Hansen KR, Thompson LF, Colgan SP. Ecto-5'-nucleotidase (CD73) regulation by hypoxia-inducible factor-1 mediates permeability changes in intestinal epithelia. *J Clin Invest*. 2002 Oct;110(7):993-1002.
- 331 Yan X, Anzai A, Katsumata Y, Matsuhashi T, Ito K, Endo J, Yamamoto T, Takeshima A, Shinmura K, Shen W, Fukuda K, Sano M. Temporal dynamics of cardiac immune cell accumulation following acute myocardial infarction. *J Mol Cell Cardiol*. 2013 Sep;62:24-35. doi: 10.1016/j.yjmcc.2013.04.023. Epub 2013 May 2.
- 332 Hofmann U, Frantz S. Role of T-cells in myocardial infarction. *Eur Heart J*. 2016 Mar 14;37(11):873-9. doi: 10.1093/eurheartj/ehv639. Epub 2015 Dec 8.
- 333 Xia N, Jiao J, Tang TT, Lv BJ, Lu YZ, Wang KJ, Zhu ZF, Mao XB, Nie SF, Wang Q, Tu X, Xiao H, Liao YH, Shi GP, Cheng X. Activated regulatory T-cells attenuate myocardial ischaemia/reperfusion injury through a CD39-dependent mechanism. *Clin Sci (Lond)*. 2015 May 1;128(10):679-93. doi: 10.1042/CS20140672.
- 334 Haskó G, Linden J, Cronstein B, Pacher P. Adenosine receptors: therapeutic aspects for inflammatory and immune diseases. *Nat Rev Drug Discov*. 2008 Sep;7(9):759-70. doi: 10.1038/nrd2638.
- 335 Linden J. Regulation of leukocyte function by adenosine receptors. *Adv Pharmacol*. 2011;61:95-114. doi: 10.1016/B978-0-12-385526-8.00004-7.

- 336 Auchampach JA, Kreckler LM, Wan TC, Maas JE, van der Hoeven D, Gizewski E, Narayanan J, Maas GE. Characterization of the A2B adenosine receptor from mouse, rabbit, and dog. *J Pharmacol Exp Ther.* 2009 Apr;329(1):2-13. doi: 10.1124/jpet.108.148270. Epub 2009 Jan 13.
- 337 Dwyer KM, Robson SC, Nandurkar HH, Campbell DJ, Gock H, Murray-Segal LJ, Fiscicaro N, Mysore TB, Kaczmarek E, Cowan PJ, d'Apice AJ. Thromboregulatory manifestations in human CD39 transgenic mice and the implications for thrombotic disease and transplantation. *J Clin Invest.* 2004 May;113(10):1440-6.
- 338 Hofmann U, Frantz S. Role of lymphocytes in myocardial injury, healing, and remodeling after myocardial infarction. *Circ Res.* 2015 Jan 16;116(2):354-67. doi: 10.1161/CIRCRESAHA.116.304072.
- 339 Saxena A, Dobaczewski M, Rai V, Haque Z, Chen W, Li N, Frangogiannis NG. Regulatory T cells are recruited in the infarcted mouse myocardium and may modulate fibroblast phenotype and function. *Am J Physiol Heart Circ Physiol.* 2014 Oct 15;307(8):H1233-42. doi: 10.1152/ajpheart.00328.2014. Epub 2014 Aug 15.
- 340 Schroder K, Hertzog PJ, Ravasi T, Hume DA. Interferon-gamma: an overview of signals, mechanisms and functions. *J Leukoc Biol.* 2004 Feb;75(2):163-89. Epub 2003 Oct 2.
- 341 Yan X, Shichita T, Katsumata Y, Matsushashi T, Ito H, Ito K, Anzai A, Endo J, Tamura Y, Kimura K, Fujita J, Shinmura K, Shen W, Yoshimura A, Fukuda K, Sano M. Deleterious effect of the IL-23/IL-17A axis and $\gamma\delta$ T cells on left ventricular remodeling after myocardial infarction. *J Am Heart Assoc.* 2012 Oct;1(5):e004408. doi: 10.1161/JAHA.112.004408. Epub 2012 Oct 25.
- 342 Kanellakis P, Ditiatkovski M, Kostolias G, Bobik A. A pro-fibrotic role for interleukin-4 in cardiac pressure overload. *Cardiovasc Res.* 2012 Jul 1;95(1):77-85. doi: 10.1093/cvr/cvs142. Epub 2012 Apr 5.
- 343 Weisensee D, Bereiter-Hahn J, Schoeppe W, Löw-Friedrich I. Effects of cytokines on the contractility of cultured cardiac myocytes. *Int J Immunopharmacol.* 1993 Jul;15(5):581-7.
- 344 Mesquita Jr D, Cruvinel WM, Câmara NO, Kállas EG, Andrade LE. Autoimmune diseases in the TH17 era. *Braz J Med Biol Res.* 2009 Jun;42(6):476-86.
- 345 Raphael I, Nalawade S, Eagar TN, Forsthuber TG. T cell subsets and their signature cytokines in autoimmune and inflammatory diseases. *Cytokine.* 2015 Jul;74(1):5-17. doi: 10.1016/j.cyto.2014.09.011. Epub 2014 Oct 30.

- 346 Leiva A, Guzmán-Gutiérrez E, Contreras-Duarte S, Fuenzalida B, Cantin C, Carvajal L, Salsoso R, Gutiérrez J, Pardo F, Sobrevia L. Adenosine receptors: Modulators of lipid availability that are controlled by lipid levels. *Mol Aspects Med.* 2017 Jan 31. pii: S0098-2997(16)30087-5. doi: 10.1016/j.mam.2017.01.007. [Epub ahead of print].
- 347 Kobayashi S, Millhorn D. E. Stimulation of expression for the adenosine A2A receptor gene by hypoxia in PC12 cells. A potential role in cell protection. *J Biol Chem.* 1999 Jul 16;274(29):20358-65.
- 348 Kong T, Westerman KA, Faigle M, Eltzhig HK, Colgan SP. HIF-dependent induction of adenosine A2B receptor in hypoxia. *FASEB J.* 2006 Nov;20(13):2242-50.
- 349 Wang L, Kolachala V, Walia B, Balasubramanian S, Hall RA, Merlin D, Sitaraman SV. Agonist-induced polarized trafficking and surface expression of the adenosine 2b receptor in intestinal epithelial cells: role of SNARE proteins. *Am J Physiol Gastrointest Liver Physiol.* 2004 Nov;287(5):G1100-7. Epub 2004 Jul 15.
- 350 Klaasse EC, Ijzerman AP, de Grip WJ, Beukers MW. Internalization and desensitization of adenosine receptors. *Purinergic Signal.* 2008 Mar;4(1):21-37. doi: 10.1007/s11302-007-9086-7. Epub 2007 Nov 13.
- 351 Hinz S, Lacher SK, Seibt BF, Müller CE. BAY60-6583 acts as a partial agonist at adenosine A2B receptors. *J Pharmacol Exp Ther.* 2014 Jun;349(3):427-36. doi: 10.1124/jpet.113.210849. Epub 2014 Mar 14.
- 352 Ciruela F, Ferré S, Casadó V, Cortés A, Cunha RA, Lluís C, Franco R. Heterodimeric adenosine receptors: a device to regulate neurotransmitter release. *Cell Mol Life Sci.* 2006 Nov;63(21):2427-31.
- 353 Seibt BF. A2B-Adenosin-Rezeptor-Homo- und Heterodimere Biolumineszenz-Resonanz-Energie-Transfer-Studien und pharmakologische Charakterisierung. *Dissertation.* 2012.
- 354 Idzko M, Ferrari D, Eltzhig HK. Nucleotide signalling during inflammation. *Nature.* 2014 May 15;509(7500):310-7. doi: 10.1038/nature13085.
- 355 Koza Y. Acute kidney injury: current concepts and new insights. *J Inj Violence Res.* 2016 Jan;8(1):58-62. doi: 10.5249/jivr.v8i1.610.
- 356 Ali T, Khan I, Simpson W, Prescott G, Townend J, Smith W, Macleod A. Incidence and outcomes in acute kidney injury: a comprehensive population-based study. *J Am Soc Nephrol.* 2007 Apr;18(4):1292-8. Epub 2007 Feb 21.
- 357 Murugan R, Kellum J. A. Acute kidney injury: what's the prognosis? *Nat Rev Nephrol.* 2011 Apr;7(4):209-17. doi: 10.1038/nrneph.2011.13. Epub 2011 Feb 22.

- 358 Uchino S, Kellum JA, Bellomo R, Doig GS, Morimatsu H, Morgera S, Schetz M, Tan I, Bouman C, Macedo E, Gibney N, Tolwani A, Ronco C; Beginning and Ending Supportive Therapy for the Kidney (BEST Kidney) Investigators. Acute renal failure in critically ill patients: a multinational, multicenter study. *JAMA*. 2005 Aug 17;294(7):813-8.
- 359 Lameire N, Van Biesen W, Vanholder R. Acute kidney injury. *Lancet*. 2008 Nov 29;372(9653):1863-5. doi: 10.1016/S0140-6736(08)61794-8.
- 360 Kliger AS, Foley RN, Goldfarb DS, Goldstein SL, Johansen K, Singh A, Szczech L. KDOQI US commentary on the 2012 KDIGO Clinical Practice Guideline for Anemia in CKD. *Am J Kidney Dis*. 2013 Nov;62(5):849-59. doi: 10.1053/j.ajkd.2013.06.008. Epub 2013 Jul 25.
- 361 Grenz A, Zhang H, Eckle T, Mittelbronn M, Wehrmann M, Köhle C, Kloor D, Thompson LF, Osswald H, Eltzschig HK. Protective role of ecto-5'-nucleotidase (CD73) in renal ischemia. *J Am Soc Nephrol*. 2007 Mar;18(3):833-45. Epub 2007 Jan 31.
- 362 Tak E, Ridyard D, Kim JH, Zimmerman M, Werner T, Wang XX, Shabeka U, Seo SW, Christians U, Klawitter J, Moldovan R, Garcia G, Levi M, Haase V, Ravid K, Eltzschig HK, Grenz A. CD73-dependent generation of adenosine and endothelial Adora2b signaling attenuate diabetic nephropathy. *J Am Soc Nephrol*. 2014 Mar;25(3):547-63. doi: 10.1681/ASN.2012101014. Epub 2013 Nov 21.
- 363 Blume C, Felix A, Shushakova N, Gueler F, Falk CS, Haller H, Schrader J. Autoimmunity in CD73/Ecto-5'-nucleotidase deficient mice induces renal injury. *PLoS One*. 2012;7(5):e37100. doi: 10.1371/journal.pone.0037100. Epub 2012 May 29.
- 364 Van Waarde A, Stromski ME, Thulin G, Gaudio KM, Kashgarian M, Shulman RG, Siegel NJ. Protection of the kidney against ischemic injury by inhibition of 5'-nucleotidase. *Am J Physiol*. 1989 Feb;256(2 Pt 2):F298-305.
- 365 Rajakumar SV, Lu B, Crikis S, Robson SC, d'Apice AJ, Cowan PJ, Dwyer KM. Deficiency or inhibition of CD73 protects in mild kidney ischemia-reperfusion injury. *Transplantation*. 2010 Dec 27;90(12):1260-4. doi: 10.1097/TP.0b013e3182003d9b.
- 366 Roberts VS, Cowan PJ, Alexander SI, Robson SC, Dwyer KM. The role of adenosine receptors A2A and A2B signaling in renal fibrosis. *Kidney Int*. 2014 Oct;86(4):685-92. doi: 10.1038/ki.2014.244. Epub 2014 Jul 23.
- 367 Sakaki H, Tsukimoto M, Harada H, Moriyama Y, Kojima S. Autocrine regulation of macrophage activation via exocytosis of ATP and activation of P2Y11 receptor. *PLoS One*. 2013;8(4):e59778. doi: 10.1371/journal.pone.0059778. Epub 2013 Apr 5.
- 368 Haskó G, Pacher P. Regulation of macrophage function by adenosine. *Arterioscler Thromb Vasc Biol*. 2012 Apr;32(4):865-9. doi: 10.1161/ATVBAHA.111.226852.

- 369 Haskó G, Pacher P, Deitch EA, Vizi ES. Shaping of monocyte and macrophage function by adenosine receptors. *Pharmacol Ther.* 2007 Feb;113(2):264-75. Epub 2006 Sep 14.
- 370 Cohen HB, Briggs KT, Marino JP, Ravid K, Robson SC, Mosser DM. TLR stimulation initiates a CD39-based autoregulatory mechanism that limits macrophage inflammatory responses. *Blood.* 2013 Sep 12;122(11):1935-45. doi: 10.1182/blood-2013-04-496216. Epub 2013 Aug 1.
- 371 Dai Y, Zhang W, Wen J, Zhang Y, Kellems RE, Xia Y. A2B adenosine receptor-mediated induction of IL-6 promotes CKD. *J Am Soc Nephrol.* 2011 May;22(5):890-901. doi: 10.1681/ASN.2010080890. Epub 2011 Apr 21.
- 372 Yang J, Chen J, Yan J, Zhang L, Chen G, He L, Wang Y. Effect of interleukin 6 deficiency on renal interstitial fibrosis. *PLoS One.* 2012;7(12):e52415. doi: 10.1371/journal.pone.0052415. Epub 2012 Dec 18.
- 373 Zhou Y, Schneider DJ, Morschl E, Song L, Pedroza M, Karmouty-Quintana H, Le T, Sun CX, Blackburn MR. Distinct roles for the A2B adenosine receptor in acute and chronic stages of bleomycin-induced lung injury. *J Immunol.* 2011 Jan 15;186(2):1097-106. doi: 10.4049/jimmunol.1002907. Epub 2010 Dec 13.
- 374 Regner KR, Roman R. J. Role of medullary blood flow in the pathogenesis of renal ischemia-reperfusion injury. *Curr Opin Nephrol Hypertens.* 2012 Jan;21(1):33-8. doi: 10.1097/MNH.0b013e32834d085a.
- 375 Padanilam BJ. Cell death induced by acute renal injury: a perspective on the contributions of apoptosis and necrosis. *Am J Physiol Renal Physiol.* 2003 Apr;284(4):F608-27.
- 376 Okusa MD, Linden J, Huang L, Rieger JM, Macdonald TL, Huynh LP. A(2A) adenosine receptor-mediated inhibition of renal injury and neutrophil adhesion. *Am J Physiol Renal Physiol.* 2000 Nov;279(5):F809-18.
- 377 Vekaria RM, Unwin RJ, Shirley DG. Intraluminal ATP concentrations in rat renal tubules. *J Am Soc Nephrol.* 2006 Jul;17(7):1841-7. Epub 2006 Jun 21.
- 378 Bauerle JD, Grenz A, Kim JH, Lee HT, Eltzschig HK. Adenosine generation and signaling during acute kidney injury. *J Am Soc Nephrol.* 2011 Jan;22(1):14-20. doi: 10.1681/ASN.2009121217.
- 379 Schwiebert EM. ATP release mechanisms, ATP receptors and purinergic signalling along the nephron. *Clin Exp Pharmacol Physiol.* 2001 Apr;28(4):340-50.
- 380 Kishore BK, Isaac J, Fausther M, Tripp SR, Shi H, Gill PS, Braun N, Zimmermann H, Sévigny J, Robson SC. Expression of NTPDase1 and NTPDase2 in murine kidney: relevance to regulation of P2 receptor signaling. *Am J Physiol Renal Physiol.* 2005 May;288(5):F1032-43. Epub 2005 Jan 4.

- 381 Lee HT, Emala C. W. Adenosine attenuates oxidant injury in human proximal tubular cells via A(1) and A(2a) adenosine receptors. *Am J Physiol Renal Physiol.* 2002 May;282(5):F844-52.
- 382 Li L, Okusa M. D. Macrophages, dendritic cells, and kidney ischemia-reperfusion injury. *Semin Nephrol.* 2010 May;30(3):268-77. doi: 10.1016/j.semnephrol.2010.03.005.
- 383 Grenz A, Bauerle JD, Dalton JH, Ridyard D, Badulak A, Tak E, McNamee EN, Clambey E, Moldovan R, Reyes G, Klawitter J, Ambler K, Magee K, Christians U, Brodsky KS, Ravid K, Choi DS, Wen J, Lukashev D, Blackburn MR, Osswald H, Coe IR, Nürnberg B, Haase VH, Xia Y, Sitkovsky M, Eltzschig HK. Equilibrative nucleoside transporter 1 (ENT1) regulates postischemic blood flow during acute kidney injury in mice. *J Clin Invest.* 2012 Feb;122(2):693-710. doi: 10.1172/JCI60214. Epub 2012 Jan 24.
- 384 Sempowski GD, Beckmann MP, Derdak S, Phipps RP. Subsets of murine lung fibroblasts express membrane-bound and soluble IL-4 receptors. Role of IL-4 in enhancing fibroblast proliferation and collagen synthesis. *J Immunol.* 1994 Apr 1;152(7):3606-14.
- 385 Villarreal F, Epperson SA, Ramirez-Sanchez I, Yamazaki KG, Brunton LL. Regulation of cardiac fibroblast collagen synthesis by adenosine: roles for Epac and PI3K. *Am J Physiol Cell Physiol.* 2009 May;296(5):C1178-84. doi: 10.1152/ajpcell.00291.2008. Epub 2009 Mar 11.
- 386 Säve S, Mohlin C, Vumma R, Persson K. Activation of adenosine A2A receptors inhibits neutrophil transuroepithelial migration. *Infect Immun.* 2011 Aug;79(8):3431-7. doi: 10.1128/IAI.05005-11. Epub 2011 Jun 6.
- 387 Barletta KE, Ley K, Mehrad B. Regulation of neutrophil function by adenosine. *Arterioscler Thromb Vasc Biol.* 2012 Apr;32(4):856-64. doi: 10.1161/ATVBAHA.111.226845.
- 388 Sun Y, Huang P. Adenosine A2B Receptor: From Cell Biology to Human Diseases. *Front Chem.* 2016 Aug 24;4:37. doi: 10.3389/fchem.2016.00037. eCollection 2016.
- 389 Grenz A, Osswald H, Eckle T, Yang D, Zhang H, Tran ZV, Klingel K, Ravid K, Eltzschig HK. The reno-vascular A2B adenosine receptor protects the kidney from ischemia. *PLoS Med.* 2008 Jun 24;5(6):e137. doi: 10.1371/journal.pmed.0050137.

Statutory declaration

Statutory declaration

I hereby declare that I wrote the dissertation “Role of the Purinergic Signaling in Healing Processes of the Heart and the Kidney after Ischemia/ Reperfusion Injury” independently and without other resources as indicated in compliance with “Grundsätze zur Sicherung guter wissenschaftlicher Praxis an der Heinrich-Heine Universität Düsseldorf”.

Furthermore, I declare that I did not submit this dissertation, either in full or in part, to any other academic institution and did not absolve any promotion trials before.

Düsseldorf,

Nicole Gördlt

Eidesstattliche Erklärung

Ich versichere an Eides Statt, dass die Dissertation „Rolle des purinergen Signalsystems in Heilungsprozessen des Herzens und der Niere nach Ischämie/ Reperfusionsschaden“ von mir selbstständig und ohne unzulässige fremde Hilfe unter Beachtung der „Grundsätze zur Sicherung guter wissenschaftlicher Praxis an der Heinrich-Heine Universität Düsseldorf“ erstellt worden ist.

Darüber hinaus versichere ich, dass ich die Dissertation weder in der hier vorgelegten noch in einer ähnlichen Form bei einem anderen Institut eingereicht habe und bisher keine Promotionsversuche unternommen habe.

Düsseldorf,

Nicole Gördlt

Danksagung

Abschließend möchte ich mich recht herzlich bei Herrn Dr. Jürgen Schrader bedanken, der mir die Möglichkeit gegeben hat, an diesem spannenden Thema zu arbeiten. Vielen Dank für die Unterstützung und fachlichen Anregungen sowie die Gelegenheit, meinen Horizont auf zahlreichen Kongressen zu erweitern und meine Ergebnisse vorstellen zu können.

Vielen Dank, dass ich ein Teil des Teams sein durfte!

Prof. Dr. Thomas Klein danke ich für die freundliche Übernahme des Zweitgutachtens meiner Dissertation.

Außerdem möchte ich allen aktuellen und ehemaligen Mitgliedern des Instituts der Molekularen Kardiologie danken, die mir stets mit Rat und Tat zur Seite standen. Es hat sehr viel Spaß gemacht mit euch zusammen zu arbeiten! Vielen Dank an Nadine, Daniela und Julia, die mich auf dem Weg meiner Doktorarbeit begleitet stets unterstützt haben.

Furthermore, I would like to thank Dr. Mark Okusa and the Department for Nephrology for supporting me and for making me feel being a part of the lab. Especially, I would like to thank Diane, Heather and Tsuyoshi. I enjoyed our critical discussions!

Ich bedanke mich beim gesamten IRTG1902 für die Möglichkeit ein Teil dieses großartigen Austauschprogramms zu sein. Mein besonderer Dank gilt Sandra, die immer ein offenes Ohr hatte.

Ich möchte mich auch aus tiefsten Herzen bei Lucia und Sofia bedanken, die über die Forschung hinaus ein wichtiger Bestandteil meines Lebens geworden sind.

Vielen Dank für die tolle Zeit und jegliche Unterstützung!

Ich möchte mich auch herzlich bei allen meinen Freunden und Mario bedanken, die mir während dieser Zeit viel Kraft gespendet haben.

Ein besonderer Dank geht an meine Eltern, die mich auf meinem Weg immer unterstützt haben, die mir in jeglicher Lebensphase zur Seite standen und mich immer wieder aufgefangen haben.